

Biobarrier Formation For Hydraulic Control In Groundwater Remediation In South Africa

By

A van Wyk

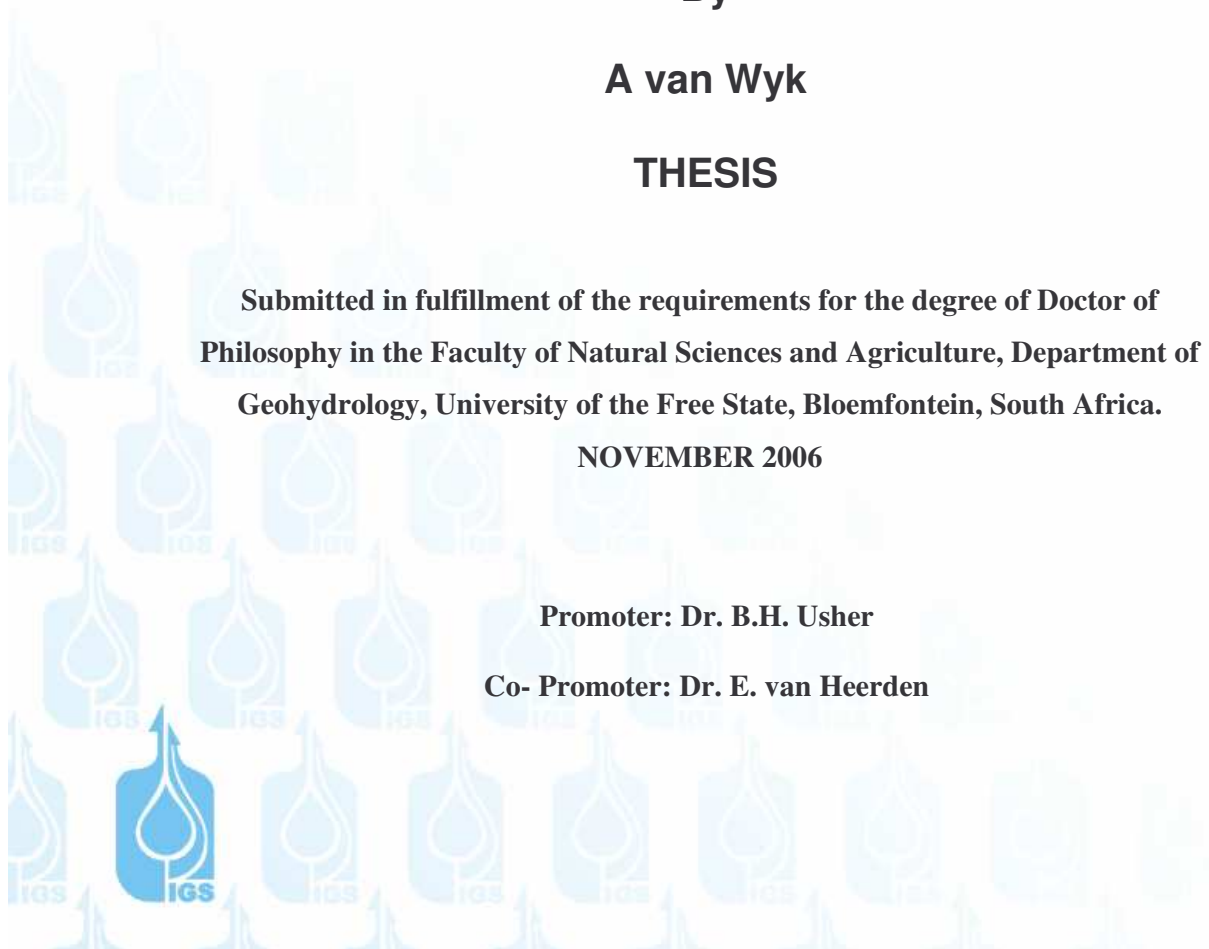
THESIS

Submitted in fulfillment of the requirements for the degree of Doctor of Philosophy in the Faculty of Natural Sciences and Agriculture, Department of Geohydrology, University of the Free State, Bloemfontein, South Africa.

NOVEMBER 2006

Promoter: Dr. B.H. Usher

Co- Promoter: Dr. E. van Heerden



Acknowledgements

I hereby wish to express my sincere thanks to a large number of people who have helped me to complete this thesis:

I gratefully express appreciation to the Director, and all my colleagues at the Institute for Groundwater Studies for assistance in matters ranging from proof-reading, technical expertise, administration, laboratory analyses and field work.

To my promoter, Dr. Brent Usher, a special thank you for your guidance, advice and support.

The research discussed in this thesis emanates from a four-year project funded by BHP Billiton, entitled “Biobarrier formation for hydraulic control in groundwater remediation in South Africa”. The financing of the project by BHP Billiton is gratefully acknowledged.

There are many experts in Hydrology and Microbiology that contributed to the ideas and understanding in this thesis. These include Brent Usher, Gerrit van Tonder, Michael du Preez, Elna de Necker, Michelle Pienaar, Willem Lebogang, John Mpondo, Sakhile Mndaweni, Robel Gebrekristos, Mahari Menghistu, Esta van Heerden, Mariana Erasmus, Christell Moller, Michael Henn and countless others.

Thanks are due to the people at Instrumentation and Electronics for building all the apparatus used during this study.

Thanks are due to Catherine Bitzer for proof-reading.

A special word of thanks to my parents for all their support and for the opportunities provided to further my education.

To my in-laws and the rest of my family, I am grateful for your support, encouragement and understanding throughout the project.

To my husband, Bennie, special thanks for all your love, encouragement and endless patience. I am very grateful for the hours you have sacrificed for me to complete the thesis.

Last but not least to the Light, who gave me strength and hope.

Keywords

Groundwater, biobarrier, bioremediation, bacterial transport, aquifer characterisation, tracer tests, hydraulic conductivity, fracture, porous media.

TABLE OF CONTENTS

1	INTRODUCTION TO BIOBARRIERS.....	1
1.1	BIOBARRIER FORMATION DEVELOPMENT FOR SOUTH AFRICAN AQUIFERS	2
1.2	BACTERIA TRANSPORT IN AQUIFERS	3
1.3	ADVANTAGES OF BIOBARRIER TECHNOLOGY	3
1.4	OBJECTIVES	4
1.5	METHOD OF INVESTIGATION	5
1.6	THESIS STRUCTURE	5
2	SOUTH AFRICAN AQUIFERS AND IMPLICATIONS FOR BIOBARRIERS	7
2.1	INTRODUCTION.....	7
2.2	KAROO AQUIFERS	9
2.3	SEDIMENTATION GROUPS IN THE KAROO SUPERGROUP	10
2.4	MASS TRANSPORT OF DISSOLVED CONTAMINANTS	12
2.4.1	<i>Transport by advection.....</i>	<i>13</i>
2.4.2	<i>Influence of dispersion.....</i>	<i>14</i>
2.4.3	<i>Transport by diffusion</i>	<i>15</i>
2.4.4	<i>Matrix diffusion</i>	<i>16</i>
2.4.5	<i>Sorption in fractured aquifers</i>	<i>17</i>
2.5	TRANSPORT IN FRACTURED AQUIFERS	18
2.6	BIOBARRIERS FOR SOUTH AFRICAN AQUIFERS.....	18
2.7	BIOBARRIERS IN KAROO AQUIFERS	19
3	SITE CHARACTERISATION FOR BIOBARRIER APPLICATION	20
3.1	INTRODUCTION.....	21
3.1.1	<i>Borehole information.....</i>	<i>23</i>
3.2	AQUIFER TESTS – HYDRAULIC TESTS.....	24
3.2.1	<i>Estimation of aquifer parameters</i>	<i>24</i>
3.2.2	<i>Constant rate test.....</i>	<i>24</i>
3.2.3	<i>Recovery test.....</i>	<i>25</i>
3.3	PERFORMING AQUIFER TESTS IN UO7, UO20 AND UO14.....	25
3.3.1	<i>Methods of analysis</i>	<i>26</i>
3.3.2	<i>Diagnostic plots.....</i>	<i>26</i>
3.3.3	<i>Determination of fracture position by FC method.....</i>	<i>28</i>
3.3.4	<i>Summary.....</i>	<i>29</i>
3.4	BOREHOLE VIDEO CAMERA OBSERVATIONS.....	30
3.4.1	<i>Discussion.....</i>	<i>33</i>
3.5	GEOPHYSICAL BOREHOLE LOGGING	33
3.6	MULTIPLE-PARAMETER LOGGING (PH, EC, REDOX POTENTIAL AND TEMPERATURE).....	34
3.7	FRACTURE POSITION DETERMINATION - EC LOGGING.....	35
3.8	TRACER TESTS.....	36
3.8.1	<i>Point dilution tests in UO20, UO7 and UO14.....</i>	<i>36</i>
3.8.2	<i>Conclusion and discussion for the three methods to determine the fracture position</i>	<i>42</i>
3.9	TRACER TESTS.....	43
3.9.1	<i>Types of tracer tests.....</i>	<i>43</i>
3.9.2	<i>Types of tracers</i>	<i>44</i>
3.9.3	<i>Set-up in injection borehole.....</i>	<i>45</i>

3.10	RADIAL CONVERGENT TRACER TESTS	47
3.10.1	Results.....	51
3.10.2	Radial convergent test – UO14-UO7.....	51
3.10.3	Radial convergent test – UO7-UO14.....	53
3.10.4	Discussion of results.....	58
3.11	CONCLUSIONS.....	59
4	LABORATORY TESTING OF DIFFERENT BACTERIA FOR SUITABILITY OF BIOBARRIER PROPERTIES	62
4.1	BACTERIA TRANSPORT.....	62
4.2	PREPARATION OF INOCULUM FOR BACTERIUM RAOULTELLA PLANTICOLA.....	63
4.3	CULTIVATION OF RAOULTELLA PLANTICOLA.....	64
4.4	ANALYSES.....	64
4.4.1	Optical density.....	64
4.5	GROWTH CONDITIONS.....	65
4.6	ADHESION ABILITY OF BACTERIUM.....	65
4.6.1	Adhesion assay methodology.....	65
4.6.2	Results.....	66
4.7	TRACER TRANSPORT IN POROUS MEDIA.....	66
4.8	POROUS MEDIA COLUMN EXPERIMENT.....	67
4.8.1	Test column design.....	67
4.8.2	Packing materials.....	68
4.8.3	Determination of the hydraulic conductivity of the fine and coarse sand.....	69
4.8.4	Pore volume determination.....	70
4.8.5	Porosity determination (Total porosity).....	71
4.8.6	Set-up and operation of the columns.....	71
4.9	LABORATORY TRACER TESTS.....	72
4.9.1	Tracer test methodology.....	72
4.9.2	Tracer test interpretation and results.....	73
4.9.3	Bacteria transport test.....	75
4.9.4	Bacteria transport data interpretation.....	77
4.9.5	Bacteria transport results and discussion.....	79
4.10	IN-SITU REDUCTION OF SATURATED HYDRAULIC CONDUCTIVITY (BACTERIA CLOGGING).....	81
4.10.1	Hydraulic conductivity (K) reduction test.....	81
4.10.2	Hydraulic conductivity (K) reduction test results.....	82
4.11	CONCLUSIONS.....	84
4.12	LABORATORY TESTING OF BACTERIUM BURKHOLDERIA VIETNAMENSIS.....	87
4.12.1	Burkholderia vietnamensis.....	87
4.12.2	Preparations and bacteria growth.....	87
4.12.3	Inoculum preparation.....	87
4.12.4	Adhesion tests.....	88
4.12.5	Packing of columns.....	88
4.12.6	Bacterial transport test methodology.....	88
4.12.7	Bacterial transport discussion.....	89
4.12.8	Continuous injection of columns.....	90
4.12.9	Results from the EC, pH and cell distribution.....	91
4.12.10	Hydraulic conductivity (K) reduction test.....	94
4.12.11	Results from the hydraulic conductivity reduction test - Fine sand column.....	95
4.12.12	Results from the hydraulic conductivity reduction test – Coarse sand column.....	96
4.12.13	Conclusions.....	98
4.13	LABORATORY-SCALE EXPERIMENTS ON BACTERIUM – SERRATIA MARCESCENS	100
4.13.1	Serratia marcescens.....	100
4.13.2	Source of bacteria.....	101

4.13.3	<i>Preparations and growth of bacteria</i>	101
4.13.4	<i>Adhesion tests</i>	101
4.13.5	<i>In-situ hydraulic conductivity reduction test</i>	102
4.13.6	<i>Cell distribution in columns</i>	104
4.13.7	<i>Discussion of results</i>	107
4.13.8	<i>Hydraulic conductivity (K) reduction test</i>	107
4.13.9	<i>Summary of the results and discussion</i>	109
4.14	REPETITION OF COLUMNS INJECTED WITH 10^6 AND 10^8 CELLS/ML.....	110
4.14.1	<i>Cell distribution in Column A and Column B</i>	111
4.14.2	<i>Hydraulic conductivity (K) reduction test – Column A and Column B</i>	112
4.14.3	<i>Results and discussion</i>	112
5 TESTING AND APPLICATION OF BIOBARRIERS IN FRACTURED MEDIA		114
5.1	TESTING BIOBARRIER FORMATION IN SMALL DIAMETER PIPES	114
5.1.1	<i>Set-up of pipe experiments</i>	114
5.1.2	<i>Continuous bacteria and media injection into pipes</i>	116
5.1.3	<i>Results and discussion</i>	120
5.1.4	<i>Conclusions for the pipe experiments</i>	122
5.2	TESTING BIOBARRIER IN A SANDSTONE PARALLEL PLATE FRACTURE.....	123
5.2.1	<i>Experiment 1 – 1.3 mm aperture</i>	123
5.2.2	<i>Methodology</i>	126
5.2.3	<i>Experimental approach</i>	127
5.2.4	<i>Procedure</i>	128
5.2.5	<i>Conservative and bacteria transport tests</i>	129
5.2.6	<i>Results from the EC, pH, OD, mass outflow and DO measurements</i>	132
5.2.7	<i>Hydraulic conductivity (K) reduction test</i>	136
5.2.8	<i>Light sensors</i>	136
5.2.9	<i>Visible bacteria growth</i>	137
5.2.10	<i>Summary and conclusions of the parallel plate fracture – Experiment 1</i>	139
5.3	EXPERIMENT 2 – 0.8 MM APERTURE	140
5.3.1	<i>Experimental approach</i>	140
5.3.2	<i>Procedure</i>	141
5.3.3	<i>Conservative and bacteria transport tests</i>	141
5.3.4	<i>Results from the EC, pH, OD and DO measurements</i>	144
5.3.5	<i>Bacteria breakthrough – Real-Time PCR</i>	147
5.3.6	<i>Calculation of the hydraulic conductivity</i>	149
5.3.7	<i>Hydraulic conductivity (K) reduction test</i>	150
5.3.8	<i>Effect of increasing gradient on bio barrier stability</i>	152
5.3.9	<i>Self potential techniques (SP)</i>	155
5.3.10	<i>Flushing with NaCl</i>	163
5.3.11	<i>Flushing with sodium hypochlorite</i>	164
5.4	DISCUSSION	167
6 FIELD APPLICATION OF BIOBARRIER TECHNOLOGY		172
6.1	SET-UP OF FIELD EXPERIMENT	172
6.1.1	<i>Methodology</i>	172
6.2	PREPARATION OF BACTERIA AND MEDIA USED FOR THE FIELD EXPERIMENT..	174
6.2.1	<i>Media preparation</i>	174
6.2.2	<i>Bacteria preparation</i>	175
6.3	TESTING THE EFFECTIVENESS OF A BIOBARRIER IN FRACTURED ROCK AQUIFERS	175
6.3.1	<i>Methodology for daily injection</i>	175
6.3.2	<i>Sampling</i>	177
6.4	DATA ANALYSES	177

6.4.1	<i>Media breakthrough</i>	177
6.4.2	<i>Bacteria breakthrough – Real-Time PCR</i>	179
6.4.3	<i>Water level measurements</i>	182
6.4.4	<i>Testing the effect on aquifer properties</i>	185
6.4.5	<i>Flowmeter measurements</i>	191
6.4.6	<i>Borehole video camera</i>	194
6.4.7	<i>Rehabilitation of the aquifer</i>	199
6.5	CONCLUSIONS	199
6.6	RECOMMENDATIONS	203
7 APPLICATION OF BIOBARRIER TECHNOLOGY TO SOUTH AFRICAN AQUIFERS		204
7.1	INTRODUCTION.....	204
7.2	TYPES OF GROUNDWATER CONTAMINANTS	204
7.3	GROUNDWATER REMEDIATION TECHNOLOGIES	204
7.4	ADVANTAGES OF BIOBARRIER TECHNOLOGY OVER SOME REMEDIATION TECHNOLOGIES	205
7.4.1	<i>Physical barriers and biobarriers</i>	206
7.4.2	<i>Pump-and-treat systems and biobarriers</i>	207
7.5	BIOREMEDIATION TECHNOLOGIES	211
7.5.1	<i>Bioremediation technologies for remediation of polluted sites</i>	213
7.5.2	<i>Serratia marcescens applied for biobarrier formation as well as bioremediation</i>	214
7.6	IMPLEMENTATION OF BIOBARRIERS IN SOUTH AFRICAN AQUIFERS	215
7.6.1	<i>Practical implementation of biobarrier techniques in South African aquifers</i>	217
7.6.2	<i>Site characterisation</i>	218
7.6.3	<i>Laboratory-scale experiments</i>	220
7.6.4	<i>Column experiments</i>	222
7.7	APPLICATION OF BIOBARRIER TECHNOLOGY TO FIELD SITUATIONS IN SOUTH AFRICA	223
7.7.1	<i>Injection of bacteria and media</i>	224
7.7.2	<i>Intergranular aquifers</i>	225
7.7.3	<i>Dual porosity aquifers and fractured aquifers</i>	226
7.7.4	<i>Set-up of a field site</i>	226
7.8	SUMMARY	226
8 CONCLUSIONS AND RECOMMENDATIONS		229
8.1	CONCLUSIONS	229
8.1.1	<i>Biobarrier formation in porous media</i>	229
8.1.2	<i>Biobarrier formation in fractured media</i>	230
8.1.3	<i>Application of biobarrier formation in a dual porosity fractured rock aquifer</i>	230
8.1.4	<i>Advantage of biobarriers over current remediation technologies</i>	231
8.1.5	<i>Implementation of biobarrier formation in South African aquifers</i>	231
8.2	RECOMMENDATIONS	231
REFERENCES.....		233
8.3	WEB ARTICLES	240
APPENDIX A, B, C AND D.....		242-262
ABSTRACT.....		263-264
OPSOMMING.....		265-266
LIST OF ABBREVIATIONS.....		267-268

LIST OF FIGURES

FIGURE 2-1 GEOLOGICAL MAP OF SOUTH AFRICA WITH THE MAIN KAROO FORMATION (AFTER BOTHA <i>ET AL.</i> , 1998).	9
FIGURE 2-2 THE KAROO SUPERGROUP LITHOLOGY (AFTER TANKARD <i>ET AL.</i> , 1982).	12
FIGURE 3-1 LOCATION OF SOME OF THE BOREHOLES AT THE CAMPUS TEST SITE.	22
FIGURE 3-2 POSITION OF THE SELECTED BOREHOLES.	23
FIGURE 3-3 CONSTANT DISCHARGE TEST ON UO7. WATER LEVEL DATA FOR UO7 AND OBSERVATION BOREHOLES.	26
FIGURE 3-4 LOG-LOG PLOT AND SQUARE ROOT OF TIME PLOT OF THE AQUIFER TEST CONDUCTED ON UO7.	27
FIGURE 3-5 LOG-LOG PLOT AND FOURTH ROOT PLOT OF THE AQUIFER TEST CONDUCTED ON UO14.	27
FIGURE 3-6 LOG-LOG PLOT AND FOURTH ROOT PLOT OF THE AQUIFER TEST CONDUCTED ON UO20.	28
FIGURE 3-7 FRACTURE DETERMINATION FOR UO7, WITH THE USE OF AQUIFER TEST DATA.	28
FIGURE 3-8 FRACTURE DETERMINATION FOR UO14 WITH THE USE OF AQUIFER TEST DATA.	29
FIGURE 3-9 FRACTURE DETERMINATION FOR UO20, WITH THE USE OF AQUIFER TEST DATA.	29
FIGURE 3-10 BOREHOLE VIDEO CAMERA OBSERVATIONS IN UO7. (FRACTURE ZONE).	31
FIGURE 3-11 BOREHOLE VIDEO CAMERA OBSERVATIONS IN UO20. (FRACTURE ZONE).	32
FIGURE 3-12 BOREHOLE VIDEO CAMERA OBSERVATIONS IN UO14. (FRACTURE ZONE).	32
FIGURE 3-13 RESULTS FROM GEOPHYSICAL LOGGING IN UO20 BY THE CALIPER PROBE, THE FWS AND THE NEUTRON-NEUTRON PROBE.	34
FIGURE 3-14 MULTI-PARAMETER LOGGING IN UO23.	35
FIGURE 3-15 FRACTURE DETERMINATION GRAPH FOR UO20 – 18 M INTERVAL (T1-T4).	38
FIGURE 3-16 CUMULATIVE CHANGE OVER TIME GRAPH. FRACTURE DETERMINATION FOR UO20 – 18 M INTERVAL.	38
FIGURE 3-17 CUMULATIVE CHANGE OVER TIME GRAPH. FRACTURE DETERMINATION FOR UO20 – 4 M INTERVAL.	39
FIGURE 3-18 CUMULATIVE CHANGE OVER TIME GRAPH. FRACTURE DETERMINATION FOR UO7 – 14 M INTERVAL.	40
FIGURE 3-19 CUMULATIVE CHANGE OVER TIME GRAPH. FRACTURE DETERMINATION FOR UO14 – 14 M INTERVAL.	41
FIGURE 3-20 SET-UP OF TRACER TEST IN THE INJECTION BOREHOLE.	46
FIGURE 3-21 SET-UP AROUND THE BOREHOLE AND THE FLOWCELL.	46
FIGURE 3-22 SET-UP OF A RADIAL CONVERGENT TEST ON THE CAMPUS TEST SITE.	48
FIGURE 3-23 THE GGUN-FLO2 FILTER FLUOROMETER.	50
FIGURE 3-24 SET-UP OF A RADIAL CONVERGENT TEST IN THE FIELD.	51
FIGURE 3-25 SPACIAL MAXIMA OF THE TRACER PLUME (AFTER VAN WYK. 1998).	53
FIGURE 3-26 RADIAL CONVERGENT TESTS - NaCl BREAKTHROUGH CURVES. UO14 - UO7 vs. UO7-UO14.	54
FIGURE 3-27 RADIAL CONVERGENT TESTS - NaBr BREAKTHROUGH CURVES. UO14 - UO7 vs. UO7-UO14.	55
FIGURE 3-28 RADIAL CONVERGENT TESTS - URANINE BREAKTHROUGH CURVES. UO14 - UO7 vs. UO7-UO14.	55
FIGURE 3-29 TRACER FITS OF THE THREE TRACERS FOR THE RADIAL CONVERGENT TEST BETWEEN UO14-UO7.	57
FIGURE 3-30 TRACER FITS OF THE THREE TRACERS FOR THE RADIAL CONVERGENT TEST BETWEEN UO14-UO7.	57
FIGURE 3-31 CUMULATIVE CHANGE OVER TIME IN UO20 DURING RADIAL CONVERGENT TESTS (UO14-UO7 vs. UO7-UO14).	58
FIGURE 4-1 SCHEMATIC OF THE TEST COLUMN WITH DIMENSIONS.	67
FIGURE 4-2 SAMPLING PORTS.	68
FIGURE 4-3 PACKING MATERIAL - FINE SAND, COARSE SAND, AND GLASS BEADS.	69
FIGURE 4-4 SET-UP OF THE DARCY APPARATUS – CALCULATION OF THE HYDRAULIC CONDUCTIVITY OF THE FINE AND COARSE SAND.	70
FIGURE 4-5 SET-UP OF THE COLUMNS.	71
FIGURE 4-6 TRACER AND BACTERIA TEST SET-UP.	73
FIGURE 4-7 CONSERVATIVE BREAKTHROUGH CURVE FIT WITH THE PULSE SOFTWARE.	75
FIGURE 4-8 TRACER (EC) AND BACTERIA TEST (OD) RESULTS – FINE SAND. C/C_0 VS. PORE VOLUME.	78
FIGURE 4-9 TRACER (EC) AND BACTERIA TEST (OD) RESULTS – COARSE SAND. C/C_0 VS. PORE VOLUME.	79

FIGURE 4-10 CURVE FIT WITH THE USE OF PULSE TO DETERMINE TRANSPORT PARAMETERS FOR THE FINE SAND..... 80

FIGURE 4-11 CURVE FIT WITH THE USE OF PULSE TO DETERMINE TRANSPORT PARAMETERS FOR THE COARSE SAND..... 81

FIGURE 4-12 PERCENTAGE REDUCTION IN HYDRAULIC CONDUCTIVITY FOR THE FINE SAND COLUMN..... 83

FIGURE 4-13 PERCENTAGE REDUCTION IN HYDRAULIC CONDUCTIVITY FOR THE COARSE SAND COLUMN. 84

FIGURE 4-14 C/C_0 VS. PORE VOLUME - BACTERIA TRANSPORT RESULTS. 90

FIGURE 4-15 BACTERIA BREAKTHROUGH CURVE FITTED WITH THE PULSE SOFTWARE. 90

FIGURE 4-16 CELL CONCENTRATION VS. TIME – FINE SAND COLUMN..... 92

FIGURE 4-17 CELL CONCENTRATION VS. TIME – COARSE SAND COLUMN. 94

FIGURE 4-18 RESULTS FROM THE % REDUCTION IN FLOW FOR THE FINE SAND COLUMN. 95

FIGURE 4-19 RESULTS FROM THE HYDRAULIC CONDUCTIVITY VS. TIME FOR THE FINE SAND COLUMN..... 96

FIGURE 4-20 RESULTS FROM THE HYDRAULIC CONDUCTIVITY REDUCTION TEST FOR THE COARSE SAND COLUMN..... 97

FIGURE 4-21 RESULTS FROM THE HYDRAULIC CONDUCTIVITY VS. TIME FOR THE COARSE SAND COLUMN. ... 97

FIGURE 4-22 PLATE WITH *S. MARCESCENS*, SHOWING THE CHARACTERISTIC RED PIGMENT OF THE COLONIES. 100

FIGURE 4-23 SET-UP FOR THE SIMULTANEOUS INJECTION OF BACTERIA AND MEDIA..... 103

FIGURE 4-24 OPTICAL DENSITY VS. TIME GRAPH FOR THE FOUR COARSE SAND COLUMNS. 24-HOUR OUTFLOW. 104

FIGURE 4-25 CELL CONCENTRATION VS. TIME – COLUMN 1. (10^2 CELLS/ML)..... 105

FIGURE 4-26 CELL CONCENTRATION VS. TIME – COLUMN 2. (10^4 CELLS/ML)..... 106

FIGURE 4-27 CELL CONCENTRATION VS. TIME – COLUMN 3. (10^6 CELLS/ML)..... 106

FIGURE 4-28 CELL CONCENTRATION VS. TIME – COLUMN 4. (10^8 CELLS/ML)..... 107

FIGURE 4-29 % REDUCTION IN THE FLOW FOR COLUMN 1, 2 AND COLUMN 4. 109

FIGURE 4-30 DISSOLVED OXYGEN VS. TIME GRAPH FOR COLUMN A (10^6 CELLS/ML)..... 111

FIGURE 4-31 CELL CONCENTRATION VS. TIME – COLUMN A (10^6). 112

FIGURE 5-1 PIPE 1 AND PIPE 2- TRACER BREAKTHROUGH CURVE. 115

FIGURE 5-2 PIPE 1 AND PIPE 2- TRACER BREAKTHROUGH FITTED BY TRACER. 116

FIGURE 5-3 SET-UP OF PIPE EXPERIMENTS..... 117

FIGURE 5-4 STEPS TO DETERMINE THE FREE-FLOW AND ADHESIVE MASS BACTERIA IN PIPE 1 AND PIPE 2. . 119

FIGURE 5-5 RESULTS FROM THE ADHESION MASS IN PIPE 1 AND PIPE 2..... 121

FIGURE 5-6 RESULTS FROM THE FREE-FLOW MASS IN PIPE 1 AND PIPE 2..... 121

FIGURE 5-7 SET-UP OF THE SANDSTONE PARALLEL PLATE EXPERIMENT APPARATUS. 125

FIGURE 5-8 HORIZONTAL PARALLEL PLATE FRACTURE APPARATUS SHOWING THE THREE SECTIONS..... 126

FIGURE 5-9 SET-UP OF THE PARALLEL PLATE FRACTURE APPARATUS – WATER LEVEL CONTROLLERS AND LIGHT SENSORS. 128

FIGURE 5-10 SANDSTONE PARALLEL PLATE NaCl AND BACTERIA BREAKTHROUGH CURVE..... 130

FIGURE 5-11 RESULTS FROM THE TRACER FIT FOR NaCl BREAKTHROUGH CURVE IN EXPERIMENT 1 OF THE HORIZONTAL PARALLEL PLATE FRACTURE..... 131

FIGURE 5-12 RESULTS FROM THE TRACER FIT FOR BACTERIA BREAKTHROUGH CURVE IN EXPERIMENT 1 OF THE HORIZONTAL PARALLEL PLATE FRACTURE. 131

FIGURE 5-13 PARALLEL PLATE FRACTURE EXPERIMENT - OD VS. TIME GRAPH. 133

FIGURE 5-14 PARALLEL PLATE FRACTURE EXPERIMENT – MASS OUTFLOW VS. TIME GRAPH. 134

FIGURE 5-15 PARALLEL PLATE FRACTURE EXPERIMENT - DO VS. TIME GRAPH. 135

FIGURE 5-16 PARALLEL PLATE FRACTURE EXPERIMENT - EC VARIATION DURING THROUGHFLOW OF 2 PORE VOLUMES. 135

FIGURE 5-17 PARALLEL PLATE FRACTURE EXPERIMENT – PERCENTAGE FLOW REDUCTION OVER TWO PORE VOLUMES. 136

FIGURE 5-18 PARALLEL PLATE FRACTURE EXPERIMENT – LIGHT SENSOR DATA. 137

FIGURE 5-19 BACTERIA GROWTH AT INLET AND OUTLET SIDES..... 138

FIGURE 5-20 PARALLEL PLATE FRACTURE EXPERIMENT APPARATUS. 140

FIGURE 5-21 PARALLEL PLATE FRACTURE - NaBr AND BACTERIA BREAKTHROUGH CURVE..... 143

FIGURE 5-22 RESULTS FROM THE TRACER FIT FOR NaBr BREAKTHROUGH CURVE IN EXPERIMENT 2 OF THE HORIZONTAL PARALLEL PLATE FRACTURE..... 143

FIGURE 5-23 RESULTS FROM THE TRACER FIT FOR NaCl BREAKTHROUGH CURVE IN EXPERIMENT 2 OF THE HORIZONTAL PARALLEL PLATE FRACTURE. 144

FIGURE 5-24 PARALLEL PLATE FRACTURE EXPERIMENT - EC VS. TIME GRAPH. 145

FIGURE 5-25 PARALLEL PLATE FRACTURE EXPERIMENT - EC VS. TIME GRAPH. 146

FIGURE 5-26 PARALLEL PLATE FRACTURE EXPERIMENT - DO VS. TIME GRAPH FOR IN-BOX AND OUTFLOW SAMPLES. 147

FIGURE 5-27 PARALLEL PLATE FRACTURE EXPERIMENT – R-T PCR VS. TIME GRAPH FOR SAMPLES. 148

FIGURE 5-28 PARALLEL PLATE FRACTURE EXPERIMENT – R-T PCR VS. TIME GRAPH FOR SAMPLES. 149

FIGURE 5-29 PARALLEL PLATE FRACTURE EXPERIMENT – % REDUCTION IN FLOW VS. TIME GRAPH. 152

FIGURE 5-30 PARALLEL PLATE EXPERIMENT –% INCREASE IN FLOW WITH DIFFERENT GRADIENTS. 154

FIGURE 5-31 PARALLEL PLATE FRACTURE EXPERIMENT – CHANGE IN EC WITH TIME DURING FLUSHING OF THE FRACTURE. 155

FIGURE 5-32 SELF POTENTIAL MEASUREMENTS. (A) GRID WITH 80 PINS. (B) PINS SPACED ON TOP OF THE FRACTURE, (C) VOLTMETER USED FOR TAKING SELF POTENTIAL READINGS. 157

FIGURE 5-33 COMPARISON BETWEEN THE REDUCTION IN FLOW AND THE DAILY AVERAGE SELF POTENTIAL READINGS OVER TIME. 159

FIGURE 5-34 SELF POTENTIAL MEASUREMENTS – FLOW PATTERN DATA (DAY 3 TO DAY 15). 160

FIGURE 5-35 SELF POTENTIAL MEASUREMENTS – FLOW PATTERN DATA (DAY 17 TO DAY 24). 161

FIGURE 5-36 SELF POTENTIAL MEASUREMENTS – FLOW PATTERN DATA (DAY 26 TO DAY 28). 162

FIGURE 5-37 COMPARISON BETWEEN THE % OF THE ORIGINAL FLOW AND THE SELF POTENTIAL READINGS OVER TIME. 163

FIGURE 5-38 PARALLEL PLATE EXPERIMENT –REDUCTION IN FLOW DURING NaCl INJECTION. 164

FIGURE 5-39 BACTERIA MASS AT THE INFLOW SIDE OF THE FRACTURE BEGINS TO DISINTEGRATE. 166

FIGURE 5-40 BACTERIA MASS FLUSHING FROM THE FRACTURE – OUTFLOW SIDE OF THE FRACTURE. 166

FIGURE 6-1 SET-UP OF THE THREE BOREHOLES: UO7 (INJECTION BOREHOLE), UO20 (OBSERVATION BOREHOLE) AND UO14 (ABSTRACTION BOREHOLE). 173

FIGURE 6-2 SET-UP OF THE BIOBARRIER TEST AT THE CAMPUS TEST SITE. 174

FIGURE 6-3 SET-UP AT THE INJECTION POINT. 176

FIGURE 6-4 MEDIA (C/C₀) BREAKTHROUGH CURVES VS. TIME – DAY 1. 178

FIGURE 6-5 MEDIA (C/C₀) BREAKTHROUGH CURVES VS. TIME. 179

FIGURE 6-6 BACTERIA BREAKTHROUGH CURVES DETERMINED BY REAL-TIME PCR – SAMPLES TAKEN FROM UO14. 180

FIGURE 6-7 BACTERIA BREAKTHROUGH CURVE – FIELD EXPERIMENT. – DAY 2 181

FIGURE 6-8 RESULTS FROM THE TRACER FIT FOR THE BACTERIA BREAKTHROUGH CURVE – FIELD EXPERIMENT. 182

FIGURE 6-9 VARIATION IN THE STATIC WATER LEVELS VS. TIME (DAYS). 184

FIGURE 6-10 INCREASE IN THE WATER LEVELS VS. INJECTION TIMES MEASURED AT THE END OF EACH INJECTION DAY (DAYS). 184

FIGURE 6-11 SET-UP FOR A SLUG TEST BY MEANS OF TRANSDUCERS. 186

FIGURE 6-12 VARIATION IN THE HYDRAULIC CONDUCTIVITY OVER TIME IN UO7. 189

FIGURE 6-13 VARIATION IN THE HYDRAULIC CONDUCTIVITY OVER TIME IN UO20. 190

FIGURE 6-14 VARIATION IN THE HYDRAULIC CONDUCTIVITY OVER TIME IN UO14. 190

FIGURE 6-15 REDUCTION IN HYDRAULIC CONDUCTIVITY IN UO7, UO20 AND UO14 (%). 191

FIGURE 6-16 SET-UP OF THE FLOWMETER (UO20 AND UO14). 192

FIGURE 6-17 FLOW RATE VS. DEPTH (UO14). 193

FIGURE 6-18 FLOW RATES VS. DEPTH (UO20). 193

FIGURE 6-19 SET-UP OF THE BOREHOLE VIDEO CAMERA (UO20 AND UO14). 195

FIGURE 6-20 BOREHOLE VIDEO CAMERA OBSERVATIONS (DAY 16, UO7, 16- 21. M) (WHITE MATERIAL IS BIOMASS). 196

FIGURE 6-21 BOREHOLE VIDEO CAMERA OBSERVATIONS (DAY 16, UO7, 22.8. M). (WHITE MATERIAL IS BIOMASS). 197

FIGURE 6-22 BOREHOLE VIDEO CAMERA OBSERVATIONS (DAY 16, U20, 21.3 M). 198

FIGURE 6-23 BOREHOLE VIDEO CAMERA OBSERVATIONS (DAY 16, UO14, 22.7 M). 198

FIGURE 7-1 EXAMPLE OF A FUNNEL AND GATE SYSTEM. 207

LIST OF TABLES

TABLE 2-1 MATRIX DIFFUSION COEFFICIENTS. (AFTER VAN DER VOORT, 2001). 17

TABLE 3-1 BOREHOLE INFORMATION - DISTANCE BETWEEN BOREHOLES..... 24

TABLE 3-2 SUMMARY OF THE FRACTURE POSITIONS (DEPTH IN MBGL AND MAMSL) DETERMINED BY AQUIFER TESTS IN UO7, UO14 AND UO20..... 30

TABLE 3-3 FRACTURE POSITIONS MEASURED BY BOREHOLE CAMERA OBSERVATIONS..... 31

TABLE 3-4 RESULTS FROM GEOPHYSICAL LOGGING IN UO20 (MBGL)..... 34

TABLE 3-5 SUMMARY OF THE THREE METHODS TO DETERMINE THE FRACTURE POSITIONS. 43

TABLE 3-6 SUMMARY OF THE TRANSPORT PARAMETERS FOR THE THREE TRACERS. 56

TABLE 3-7 COMPARISON BETWEEN BREAKTHROUGH TIME AND MASS MIDPOINT. (UO14-UO7) AND (UO7-UO14). 56

TABLE 4-1 RESULTS FROM THE FINE AND COARSE SAND - PULSE CALCULATIONS FOR THE VELOCITY AND DISPERSIVITY OF THE SAND..... 75

TABLE 4-2 RESULTS OF THE BACTERIA TRANSPORT IN THE FINE AND COARSE SAND - PULSE CALCULATIONS FOR THE VELOCITY AND DISPERSIVITY OF THE SAND. 81

TABLE 4-3 RESULTS OF THE BACTERIUM (*B. VIETNAMENSIS*) TRANSPORT IN THE COARSE SAND - CALCULATIONS FOR THE VELOCITY AND DISPERSIVITY OF THE SAND. 90

TABLE 4-4 DATA – CELL/ML, PH AND EC DATA FOR THE FINE SAND COLUMN. 93

TABLE 4-5 DATA – COARSE SAND COLUMN..... 94

TABLE 5-1 SUMMARY OF THE TRANSPORT PARAMETERS CALCULATED BY TRACER FOR EXPERIMENT 1.. 132

TABLE 5-2 SUMMARY OF THE TRANSPORT PARAMETERS CALCULATED BY TRACER FOR EXPERIMENT 2.. 144

TABLE 5-3 INITIAL FLOW UNDER WITH CHANGING HYDRAULIC GRADIENTS..... 149

TABLE 5-4 CHEMICAL ANALYSES OF THE COMPOSITION OF THE MEDIA. 150

TABLE 5-5 % OF THE ORIGINAL FLOW WITH DIFFERENT GRADIENTS 153

TABLE 6-1 VOLUMES OF BACTERIA AND MEDIA INJECTED OVER TIME. BACTERIA CONCENTRATIONS WERE MEASURED IN CELLS/ML). 177

TABLE 6-2 SUMMARY OF THE TRANSPORT PARAMETERS CALCULATED BY TRACER FOR THE FIELD EXPERIMENT. 182

TABLE 7-1 SUMMARY OF REMEDIATION TECHNOLOGIES CURRENTLY USED. 209

TABLE 7-2 SUMMARY OF THE COMPARISON BETWEEN BIOBARRIER TECHNOLOGY AND CURRENTLY USED REMEDIATION TECHNOLOGIES. 210

TABLE 7-3 SUMMARY OF THE MAIN AQUIFER TYPES AND FLOW MECHANISMS IN SOUTH AFRICA..... 216

1 INTRODUCTION TO BIOBARRIERS

One of the major environmental problems facing society today is the pollution of groundwater resources by toxic chemicals from industrial, mining and agricultural wastes (James *et al.*, 1995). Bacterial processes play an extremely important role in *in-situ* groundwater treatment technologies. *In-situ* biological remediation technologies are a promising approach to the successful clean-up of contaminated aquifers, although considerable development is still necessary. One example of such technology is the formation of bacterial biobarriers to manipulate the permeability and mass transport properties of aquifer media (James *et al.*, 2000). The idea that bacterial exopolymers can block, or at least hinder, water flow in natural porous media was suggested as early as in the 1950's (Vandevivere and Baveye, 1992) but never tested or implemented.

Biobarrier technology involves the use of bacterial biomass produced *in situ* to manipulate groundwater flow (James *et al.*, 2000). Biobarrier formation is an innovative approach to controlling pollution plumes in aquifers. The process of clogging the pores of an aquifer with the accumulation of bacterial cell bodies to form extra-cellular polymers (ECP) can be referred to as biobarrier formation. EPS can be defined as sticky polymers (slime formation) that bacteria excrete to adhere to solid surfaces and trap nutrients.

The production of exopolysaccharides (EPS) forming the glycocalyx is also an important factor in reducing the permeability of porous media (Cunningham and Hiebert, 2000) by several mechanisms, such as enhanced cell retention (i.e. biofilm stability) and the enhanced accumulation of organic and inorganic matter by filtration (James *et al.*, 1995). Glycocalyx is the general term for polysaccharide components outside the bacterial cell wall (Madigan *et al.*, 1997).

Selective plugging of permeable strata as a means of preventing the migration of groundwater contaminants from hazardous waste sites was explored by Komlos *et al.* (1998). The penetration of bacteria into porous media, and the subsequent resuscitation by nutrient addition was investigated as a conceivable method for subsurface plugging.

The successful containment of groundwater contaminants is essential to protect downstream resources. The uniform distribution of bacteria in porous media, necessary

to prevent contaminant migration, is dependent on the successful transport of bacteria and nutrients through the subsurface (Komlos *et al.*, 1998).

1.1 BIOBARRIER FORMATION DEVELOPMENT FOR SOUTH AFRICAN AQUIFERS

The biobarrier concept typically involves the construction of a wall of porous carbon-based material (Strietelmeier *et al.*, 2001) placed in a line perpendicular to the direction of groundwater flow that at least extends to the width and depth of a contaminant plume. Biobarrier technology also involves the use of bacterial biomass produced *in situ* to manipulate groundwater flow

Strietelmeier *et al.* (2001) show that the biobarrier can be used as a stand-alone system when biodegradable materials are the only contaminants, or used along with other barriers. Biobarriers can also be combined with bioremediation technologies to simultaneously degrade a contaminant while hindering its migration (Komlos *et al.*, 1998).

Biobarriers were developed by Cunningham and Hiebert, (2000) through injecting large numbers of mucoid bacteria into permeable strata formations. The bacteria were mixed with water and pumped into a series of injection boreholes. A suitable growth substrate and additional nutrients were injected to stimulate bacterial growth. These mucoid bacteria were capable of forming large quantities of extracellular polymer material during their growth phase. The bacterial growth and extracellular polymer production formed a bacterial biomass, which substantially reduced the free pore space in the formation and consequently reduced the hydraulic conductivity. This zone of reduced hydraulic conductivity serves as a novel barrier technology for controlling off-site migration, funneling contaminated groundwater through subsurface treatment systems (Cunningham and Hiebert, 2000)

To date, no biobarrier technology testing has been performed in South African aquifers.

For the successful implementation of biobarriers at a site, the groundwater system must first be well characterised (Strietelmeier *et al.*, 2001). Such characterisation includes hydraulic tests, tracer tests, fracture determination etc, as will be shown later in this thesis.

1.2 BACTERIA TRANSPORT IN AQUIFERS

Bacteria transport in the subsurface is a subject of increasing interest, given the recognition of subsurface delivery of bacteria as an attractive and viable remediation option to degrade or transform contaminants as well as biobarrier formation, to hinder the migration of water.

Processes influencing the transport of bacteria through the subsurface can be divided into two groups: physicochemical and biological (Jordan *et al.*, 2004). Physicochemical processes are governed by water flow and porous media structures and properties. The major physicochemical factors observed to exert control on the movement of cells are grain size, flow velocity, and mineral surface charges (Fuller *et al.*, 2000). Biological processes are governed by properties inherent in the bacterial component of the system (Jordan *et al.*, 2004). Cell size and cell surface properties (charge and hydrophobicity) are the most important biological factors that contribute to the transport and retention of injected organisms (Fuller *et al.*, 2000). In many bacterial transport studies in the past, the biological components were intentionally simplified so that the physicochemical parameters could be better isolated.

The use of homogeneous porous media, usually sand, generally promotes bacterial transport, because physical straining and adsorption is minimised. It is more difficult to generalise the impact of the use of a single bacterium, since depending on the choice and even on how the system is inoculated, transport can either be enhanced or retarded. Jordan *et al.* (2004) also found that there is a significant difference in bacterial transport behaviour in experiments conducted under growth and no-growth conditions.

1.3 ADVANTAGES OF BIOBARRIER TECHNOLOGY

Biobarriers can be maintained through a series of vertical or horizontal injection boreholes that feed the bacteria to maintain the biological barrier. Contaminants trapped in the biobarrier can be contained by maintaining the biobarrier. Once the objectives are reached, the subsurface can be returned to a more normal habitat by lowering the nutrient concentration to the subsurface community and allowing the organisms and biobarrier to die back and return to a bacterial community more consistent with the area and groundwater (www.srs.gov).

Biobarrier technology is believed to be very cost effective to implement, maintain and remove (Komlos *et al.*, 1998), and causes less surface disruption than conventional barrier technologies. Examples include funnel and gate technology, where strings of biobarriers are used to funnel a contaminant into a gate area. Contaminant remediation can be performed on a localised scale.

The main advantages of biobarrier technology are:

1. Biobarrier construction is achieved without excavation and therefore will be economically attractive at many pollution sites.
2. There is no obvious depth limitation for biobarrier technology. Traditional subsurface barrier technologies such as slurry walls and grout curtains are not usually cost effective at depths of more than 50 feet (15 m) (Cunningham and Hiebert, 2000).
3. Biobarrier technology can also be combined with bioremediation technologies to simultaneously degrade a contaminant and hinder its migration (Komlos *et al.*, 1998).

1.4 OBJECTIVES

This thesis outlines the research on bacterial barrier technology for the reduction of the hydraulic conductivity of porous media and of a horizontal fracture in a dual porosity fractured rock aquifer.

To date, no formal field test of bacteria transport and reactive biobarrier technology to reduce the hydraulic conductivity of a dual porosity fractured rock aquifer had been performed on South African aquifers.

The aim of this thesis was therefore to determine the transport properties of bacteria through coarse porous media and fractured rock aquifers and to test the effectiveness of biobarrier formation for reducing the hydraulic conductivity of a dual porosity fractured rock aquifer in order to determine if biobarrier formation is a viable method for subsurface plugging in local aquifers.

The aims of the thesis therefore include:

- To provide an introduction to biobarrier technology.

- To provide an introduction to South African aquifers with reference to biobarriers.
- To give a detailed description of techniques to determine the hydraulic transport of bacteria through porous sand and fractured aquifers.
- To evaluate the results from tracer and bacterial transport tests in the laboratory and the field.
- To investigate the effectiveness of biobarrier formation in decreasing the hydraulic conductivity of sand in laboratory-scale columns.
- To evaluate the efficiency of bacteria in decreasing the hydraulic conductivity of a man-made horizontal fracture on a laboratory-scale.
- To evaluate the efficiency of bacteria in successfully decreasing the hydraulic conductivity of a horizontal fracture in a fractured rock aquifer.
- To investigate the applicability of biobarrier formation to polluted sites in South Africa.

1.5 METHOD OF INVESTIGATION

The research for this thesis includes the following:

- Literature review of relevant documents, journal articles, web sites and MS.c and Ph.D thesis's.
- Selection of appropriate testing methods.
- Laboratory testing with several methodologies, for example fine and coarse sand columns, pipe experiments, and parallel plate fracture experiments.
- Aquifer testing with several methodologies, for example hydraulic tests including aquifer tests, slug tests, fractured determination tests, tracer tests, borehole camera observations, etc.
- Application of biobarrier technology in field situations.

1.6 THESIS STRUCTURE

The thesis is structured as follows:

- Chapter 1 is an introduction to biobarrier technology and the structure of the thesis.
- Chapter 2 focuses on South African aquifers and biobarriers in general.

- The purpose of the research was to test the applicability of biobarriers in South African aquifers. Since 90% of local aquifers are fractured, Chapter 3 concentrates on the characterisation of a target aquifer for biobarrier application. Prior to the injection of the biobarrier into a dual porosity fractured rock aquifer, a detailed characterisation was performed at the UFS campus test site to determine the aquifer hydraulics and fracture positions. These tests include aquifer tests, fracture determination tests, down hole geophysics, tracer tests and borehole video camera observations.
- A first step towards efficient biobarrier application is the use of the correct bacterial species. Chapter 4 provides detailed information on the evaluation and testing of *Raoultella planticola*, *Burkholderia vietnamensis* and *Serratia marcescens* as viable bacteria for sustainable biobarrier formation in porous sand under laboratory conditions. These tests include adhesion tests, conservative tracer transport tests, bacteria transport tests, and hydraulic reduction tests.
- Chapter 5 examines the laboratory testing used to obtain the required parameters for upscaling to the field. This includes testing the effectiveness of *S. marcescens* in clogging 11 m silicone pipes with an internal diameter of 3 mm. Results were also upscaled to a parallel plate fracture with a variable aperture (0.13 mm and 0.08 mm). Hydraulic reduction tests were conducted to determine the effectiveness of *S. marcescens* to reduce and clog a horizontal fracture with these apertures.
- Chapter 6 discusses field application of biobarrier technology in a dual porosity fractured rock aquifer.
- Chapter 7 provides suggested guidelines for the application of biobarrier technology to South African aquifers.
- Chapter 8 provides a discussion of the results obtained during biobarrier testing in the laboratory and field testing. It also provides recommendations on the application and implementation of biobarriers for South African aquifers.
- References.

2 SOUTH AFRICAN AQUIFERS AND IMPLICATIONS FOR BIOBARRIERS

2.1 INTRODUCTION

Approximately 90% of groundwater resources in South Africa are located in fractured-rock aquifer systems (Pietersen, 2004). In such aquifers, groundwater is contained in fractures (hard rocks), fissures and dissolution cavities (dolomite and limestone) and to some lesser extent, also in pores in weathered rock (Vegter, 1995).

In South Africa aquifers consist of four main aquifer types, namely the unconsolidated aquifers, the dual porosity aquifers, the fractured aquifers, and the karstic aquifers (Pietersen, 2004). (See Figure 2-1 for geological map of South Africa with the main Karoo formations).

Unconsolidated (eg. silt, sand and gravel) aquifers:

In unconsolidated sediments, groundwater is stored in the pore spaces between loose grains of sediment. These are typically thin aquifers, with shallow water tables, high organic and clay content, variable lithology and permeability, and are high in porosity. Examples of intergranular aquifers are alluvium, the Cape Flats.

Dual porosity (eg. sandstone, shale and arenite) aquifers:

The main storage of water occurs in the intergranular pore spaces, and the main groundwater transmission system is the fracture system in the rock. Some of the main characteristics of these aquifers are intergranular flow, high fracture hydraulic conductivity (K), low matrix K, fracture/pore water interaction and multi-layered aquifers due to the presence of hydraulic variations. Examples are the Table Mountain Group (TMG) and the Karoo Supergroup.

Fractured (eg. granite) aquifers:

In fractured rock aquifers, groundwater is stored in the fractures, joints, bedding planes and cavities of the rock matrix. Water availability is largely dependent on the nature of the fractures and their interconnection. The dominant flow is in the fractures. Because of the solid structure of the granite, the matrix hydraulic conductivity is low. These aquifers

include the West Rand Group and igneous/metamorphic rocks typically make up the basement.

Karst (eg. dolomite and limestone) aquifers:

Karst aquifers are a special type of fractured rock aquifer (limestone, dolomite or magnesite) in which the water in the fractures dissolves the relatively soft rock, thereby significantly increasing the size of the fractures. In some places, these solution cavities can be tens of meters wide and form underground cave systems. Groundwater flow in karst aquifers are more rapid than in the other aquifer types. The main characteristics of karst aquifers are: preferred pathways, rapid flow, low matrix hydraulic conductivity, fracture/pore water interaction and large seasonal water table variations. These aquifers are mainly found in the Karst belt and the Ghaap Plateau.

For the purpose of this research, the focus is mainly on the dual porosity aquifers (Karoo aquifers).

Characterisation of South African aquifers will be examined more fully in Chapter 7.

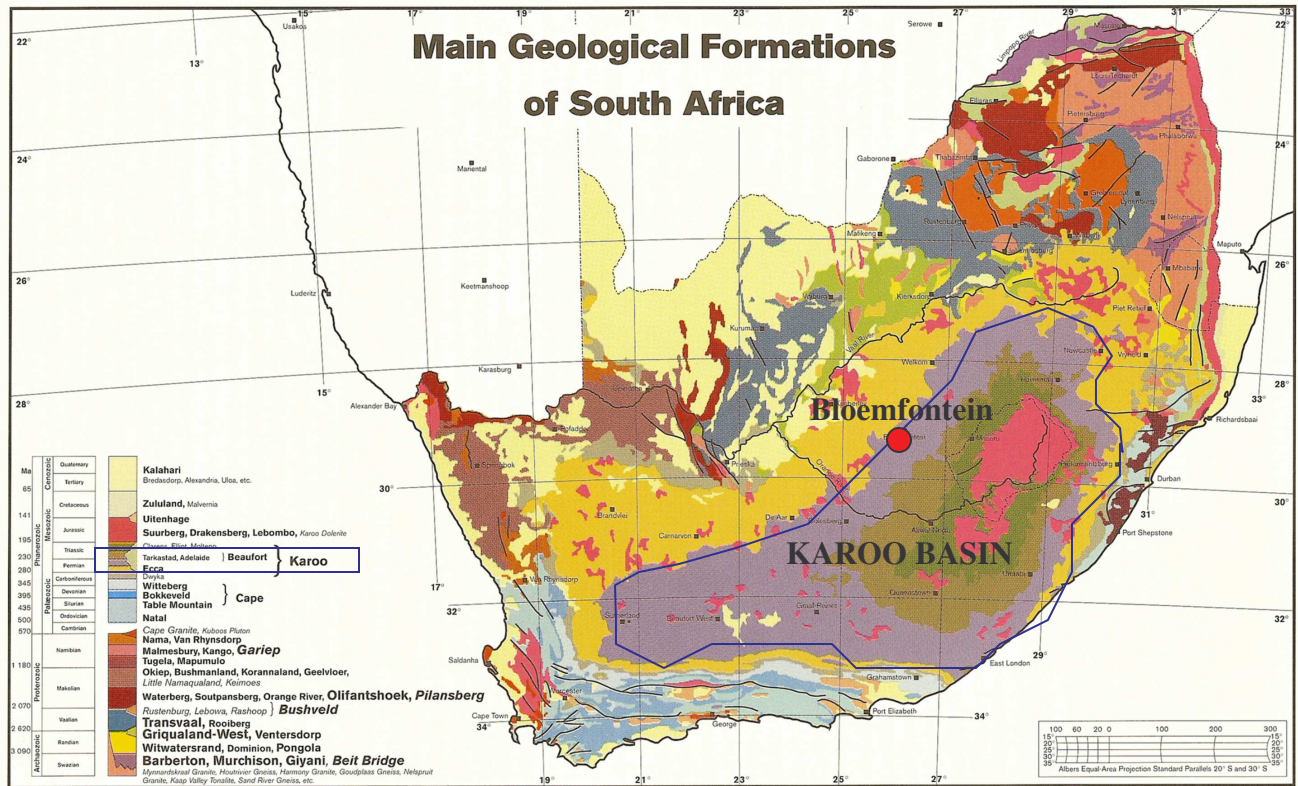


Figure 2-1 Geological map of South Africa with the main Karoo formation and the location of Bloemfontein (after Botha *et al.*, 1998).

2.2 KAROO AQUIFERS

In terms of South African aquifers, approximately 50% of the country is underlain by the so-called Karoo Supergroup geological formation (Botha *et al.*, 1998) (Figure 2-1). The Karoo Supergroup mainly consists of sandstone, mudstone, shale and siltstone. A major characteristic of the Karoo Supergroup is its low permeability (Botha *et al.*, 1998). Karoo aquifers are classified as multi-layered, multi-porous aquifers, in which bedding-parallel plate fractures form the main conduits of water (Botha *et al.*, 1998). The aperture and aerial extent of the fractures, however, are limited. These aquifers cannot transmit large quantities of water, with the result that their piezometric pressure drops rapidly when an intersecting borehole is pumped. The drop in piezometric pressure will cause water to leak from the matrix to the fracture. There are thus two types of flow in a Karoo aquifer: bedding-parallel plate fracture flow and matrix flow. Karoo aquifers can be regarded as dual porosity aquifers. These aquifers behave as if they were homogeneous, even though it is certain that the aquifer properties must be non-uniform.

2.3 SEDIMENTATION GROUPS IN THE KAROO SUPERGROUP

The Karoo Supergroup was formed when sediments filled an intra-cratonic, foreland basin on Gondwanaland, during the Carboniferous, Permian, Triassic and early Jurassic ages, 300 to 160 million years ago (Truswell, 1970 and Botha *et al.*, 1998).

Sedimentation in the Karoo formation occurred under different depositional environments (Tankard *et al.*, 1982). The result is that different groups of sediments can be distinguished, each with its own properties (Botha *et al.*, 1998).

The structure of the different groups in the main basin has an influence on the hydrological properties of the aquifers in the Karoo Supergroup.

The Karoo Supergroup can be divided into five groups, namely the Dwyka Group, the Eccca Group, the Beaufort Group (Adelaide and Tarkastad Subgroup), Stormberg Group (Molteno, Elliot, Clarens formation) and the Drakensberg volcanics (see Figure 2-2).

The Dwyka sediments are situated at the base of the Karoo Supergroup. The Dwyka diamictite, shales and tillites have very low hydraulic conductivities, and virtually no primary voids (Botha *et al.*, 1998). They tend to form more aquitards than aquifers (Freeze and Cherry, 1979).

Due to the fact that the Dwyka sediments were deposited under marine conditions, the water in these aquifers tends to be saline. Exploitable aquifers exist in places where the Dwyka formation is significantly fractured. The Dwyka formation is therefore not ideal for the development of aquifers (Botha *et al.*, 1998).

The Eccca Group consists mainly of shales. The thickness of this formation varies from 1500 m in the south to 600 m in the north. Since the shales are very dense, they were neglected as sources of groundwater in the past (Botha *et al.*, 1998).

Previous researchers (Rowell and De Swardt, 1976) found that porosities tend to decrease from 0.1 (10%) north of latitude 28°S, to < 0.02 (2%) in the southern and south-eastern parts. Thus Eccca shales are possible sources of groundwater. Rowell and De Swardt (1976) found that the permeability of the Eccca sandstones is usually very low. The reason for this is that the sandstones are usually poorly sorted, and that their primary porosities were considerably lowered by diagenesis. In consolidated and hard

rock, primary porosity is present when the rock is formed. The primary porosity of a dense solid rock may be zero and the rock matrix will be impermeable (single porosity system) (Kruseman and de Ridder, 1991).

The Beaufort Group can be stratigraphically divided into two major units, namely the upper Tarkastad Subgroup and the lower Adelaide Subgroup (Botha *et al.*, 1998). The Tarkastad Subgroup can be divided into the upper Burgersdorp formation, consisting of brightly coloured red, blue and green mudstone, and the lower Katberg formation, which contains brightly coloured shales, mudstones and thick layers of coarse-grained sandstone. The Beaufort Group was deposited in a fluvial environment. Aquifers in the Beaufort Group are multi-layered and multi-porous, with variable thicknesses (Botha *et al.*, 1998). The contact plane between two different sedimentary layers will cause a discontinuity in the hydraulic properties of an aquifer. Pumping of multi-layered aquifers cause the piezometric pressure in the more permeable layers to drop faster than that in the less permeable layers. This will mine the more permeable layers of the multi-layered Beaufort aquifers, without affecting the piezometric pressure in the less permeable layers (Botha *et al.*, 1998).

Deposits in the Stormberg Group form part of the upper formations in the Karoo Supergroup. These include the Molteno formation, the Elliott formation and the Clarens formation. The characteristics and depositional history of the Molteno formation indicate that it could form an ideal aquifer. The formation consists of pebble conglomerates and coarse grained sandstone at its base, as well as other sedimentary bodies. Unfortunately the formation does not occur over a large area. It is thus difficult to site high-yielding boreholes in the Molteno formation

The Elliott formation is characterised by a succession of alternating sandstone, siltstone and mudstone layers, but it mostly consists of red mudstone. Thus the formation represents more of an aquitard than an aquifer. This formation has a relatively high and uniform porosity, but it is poorly fractured and has a very low permeability. It is thus able to store large volumes of water, but is unable to release it quickly (Botha *et al.*, 1998).

The Clarens formation consists almost entirely of well sorted, medium- to fine grained sandstone, deposited as thick consistent blankets (Visser, 1984 and Botha *et al.*, 1998). The Clarens formation is more homogeneous than any of the other Karoo formations. This formation has a relatively high and uniform porosity. Unfortunately it is poorly

fractured and has a very low permeability. This formation is also able to store large volumes of water, but are unable to release it quickly (Botha *et al.*, 1998).





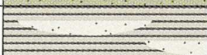

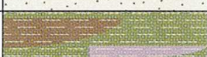

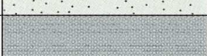

Drakensberg Volcanics			Basalt	Jurassic
Stormberg Group	Clarens		Cross-bedded sandstone	Triassic
	Elliott		Red mudstone and sandstone	
	Molteno		Sandstone, conglomerate and mudstone	
Beaufort Group	Tarkastad Subgroup		Burgersdorp Formation	Permian
			Katberg Sandstone	
	Adelaide Subgroup		Green, grey and purple mudstones	
Ecca Group			Sandstone	
Ecca Group			Shale and sandstone	
Dwyka Group			Tillite and diamictite	Carboniferous

Figure 2-2 The Karoo Supergroup lithology (after Tankard *et al.*, 1982).

2.4 MASS TRANSPORT OF DISSOLVED CONTAMINANTS

In this section, the most important mass transport parameters will be considered in detail. This will enable the reader to understand the effect of these parameters on the transport of conservative tracers and bacteria through porous or fractured materials, as discussed in Chapter 3, 4, 5 and Chapter 6.

Solutes/suspended particles in the groundwater will move in the direction of groundwater flow. (Note: A suspension includes solid plus liquid). In the case of NAPLs, it will not always move in the direction of groundwater flow.

The velocity and concentration of solutes/suspensions are governed by the following parameters: advection, dispersion, and concentration gradient (Fetter, 1999).

Advection is by far the dominant mass transport process in shaping the mass transport plume in a porous, permeable formation. (At low permeability, diffusion is dominant). (Riemann, 2002). Hydrodynamic dispersion is usually a second-order process, except in cases involving fractured rock.

2.4.1 Transport by advection

Advection plays an important role in porous and fracture transport. Advective transport (convection) occurs when dissolved solids (e.g. conservative tracers) are carried along with the flowing groundwater. The amount of transported solute is a function of its concentration in the groundwater and the quantity of the groundwater that flows (Fetter, 1999).

The magnitude and direction of advective transport is controlled by the following:

- The hydraulic conductivity distribution within the flow field
- The configuration of the water table
- The presence of sources or sinks
- The shape of the flow domain

All these parameters are important in controlling groundwater velocity, which drives advective transport.

For one-dimensional flow that is normal to a unit cross-sectional area of the porous medium, the quantity of water flow is equal to the average linear velocity times the effective porosity. Effective porosity (n_e) is the porosity through which flow can occur. Average linear velocity is the rate at which the water flux across the unit cross-sectional area of pore space occurs. The one-dimensional mass flux (F_x), resulting from advection, is equal to the quantity of water flow times the concentration of dissolved solids, and is given by (Fetter, 1999):

$$F_x = v_x n_e C \quad \text{(Equation 2-1)}$$

Where

- v_x = average linear velocity
 n_e = effective porosity
 c = concentration of dissolved solids

Due to the fact that advection will transport solutes at different rates in each stratum, the composite sample from a borehole would be a mixture of water containing the transported solute from the stratum, and also uncontaminated groundwater from a

different stratum, where the average linear velocity is lower. The concentration of the contaminant in the composite sample would thus be less than in the source (Fetter, 1999).

2.4.2 Influence of dispersion

Groundwater moves at rates both greater and smaller than the average linear velocity (Fetter, 1999). When fluid moves through pores, it will move faster in the centre of the pores than along the edges. Some of the fluid particles will travel along longer flow paths in the porous media than other particles that travel the same linear distance. Some pores are larger than others, which allows the fluid to move faster. Due to the fact that the invading solute-containing water is not travelling at a consistent velocity, mixing occurs along the flow path (Fetter, 1999) which is called mechanical dispersion. This results in a dilution of the solute at the advancing edge of flow.

Mixing that occurs along the direction of the flow path is called longitudinal dispersion. Mixing in directions normal to the flow path due to diverging flow paths is called transverse dispersion. For porous media, the concepts of average linear velocity and longitudinal dispersion are closely related. Longitudinal dispersion is the process whereby some of the water molecules and solute molecules travel more rapidly, and others more slowly, than the average linear velocity. The solute therefore spreads out in the direction of flow and decreases in concentration (Fetter, 1999).

Since the effects of molecular diffusion and mechanical dispersion in flowing groundwater cannot be separated, a parameter called hydrodynamic dispersion D combines both processes. This is represented by:

$$D_L = \alpha_L v_i + D^* \quad \text{(Equation 2-2)}$$

And

$$D_T = \alpha_T v_i + D^* \quad \text{(Equation 2-3)}$$

where

- D_L = longitudinal hydrodynamic dispersion coefficient
- D_T = transversal hydrodynamic dispersion coefficient
- D^* = effective molecular diffusion coefficient

- α_L = dispersivity in direction of flow (longitudinal)
 α_T = dispersivity normal to direction of flow (transverse)
 v_i = averaged linear velocity

During conservative tracer transport in fractures under laminar flow conditions, the tracer will disperse both by molecular diffusion perpendicular to flow and by variation in the velocity profile across the fracture in the direction of flow. Fluid closer to the walls flows more slowly than fluid in the aperture centre, so that mass advected with the fluid spreads longitudinally (Zimmerman *et al.*, 2002). This can create a concentration gradient in the transverse direction that, in turn, causes diffusion towards fracture walls. Thus, longitudinal dispersion and transverse molecular diffusion are in competition. Higher velocities and lower diffusion result in significant longitudinal dispersion and a nearly parabolic concentration profile across the aperture (Zimmerman *et al.*, 2002).

Lower velocities and higher diffusion, in contrast, result in mass flux in the transverse direction that tends to equalise concentrations across the fracture aperture, competing with the effects of longitudinal dispersion (Becker, 1996). The latter is typical in small aperture fractures in the field.

2.4.3 Transport by diffusion

Diffusion occurs in the absence of any bulk hydraulic movement of the solution. If the solution is flowing, diffusion is a mechanism which, along with mechanical dispersion, causes mixing of ionic or molecular constituents (Fetter, 1999). Diffusion will occur as long as a concentration gradient exists, even if the fluid is not moving.

The mass of fluid diffusing is then proportional to the concentration gradient, which can be expressed as Fick's first law:

$$F = - D_d (dC/dx) \quad (\text{Equation 2-4})$$

Where

- F = mass flux of solute per unit area per unit time
 D_d = diffusion coefficient
 C = solute concentration
 dC/dx = concentration gradient

In porous media, diffusion cannot proceed as rapidly as in water, because the ions must follow longer pathways, as they travel around mineral grains, or because of adsorption on the solids.

It is sometimes easier to understand diffusion coefficients when expressed in terms of mass of contaminant that passes from the fracture into the matrix.

Ficks law is not valid for bacterial transport. Bacteria cannot dissolve and will remain in suspension. Bacteria will not diffuse along the flow path (under a concentration gradient), but will only be transported by advection.

2.4.4 Matrix diffusion

Matrix diffusion can be defined as solute diffusing from the flowing fluid into zones of immobile water, and solute diffusing into the fluid that fills the small pores and micro-fissures in the rock matrix. This effect causes a delay in the transport process and a loss of solute. Field experiments by Novakowski *et al.* (1995) show that the effect of matrix diffusion cannot be neglected in fractured rock aquifers. In tracer test studies at the UFS campus test site, the loss of tracer mass due to matrix diffusion was approximately 30% (Riemann, 2002).

Matrix diffusion is dominated by the physical properties of the aquifer (i.e. velocity in the fracture, porosity of the matrix, diffusivity of the matrix), rather than the physical properties of the tracer. In smaller fractures, the effect of matrix diffusion can be lower, but could still play a major role in the total mass flux. Due to the much higher velocity in the smaller aperture fracture, dispersivity is lower and diffusion minimal.

Van der Voort (2001) measured matrix diffusion coefficients for different rock types of South Africa by means of laboratory experiments. The difference between the coefficient values for different solutes is small compared with the effect of the variation in rock types.

Table 2-1 Matrix diffusion coefficients. (After Van der Voort, 2001).

Formation	Porosity (%)	D (m ² h) NaCl	D (m ² h) Na ₂ SO ₄
Sandstone (coarse grain)	10.90	2.28*10 ⁻⁷	1.87*10 ⁻⁷
Sandstone (medium grain)	7.10	8.02*10 ⁻⁷	2.68*10 ⁻⁸
Sandstone (medium grain)	6.10	6.82*10 ⁻⁸	2.41*10 ⁻⁸
Sandstone (fine grain)	4.40	3.34*10 ⁻⁹	2.41*10 ⁻⁸
Shale	1.12	1.88*10 ⁻⁷	1.87*10 ⁻⁸
Shale	0.92	1.78*10 ⁻⁷	2.19*10 ⁻⁸
Shale	0.83	7.59*10 ⁻⁷	
Quartzite	0.19	1.80*10 ⁻⁷	

Diffusion of a conservative tracer in the matrix is typically modelled as a function of Fick's law, where the concentration gradient controls the mass transport. However, when a solute is moving between a fracture and matrix, a sharp gradient is encountered in both porosity and diffusion, which are controlled parameters for the mass transport rate (Riemann, 2002).

Bacteria cannot undergo matrix diffusion due to the fact that bacteria do not dissolve. In cases where the matrix contains smaller fractures, some of the bacteria passing through the major fractures will move into these smaller fractures, giving the appearance of matrix diffusion.

2.4.5 Sorption in fractured aquifers

Sorption reactions in fractured aquifers occur by surface sorption at the fracture walls, and by diffusion into the rock matrix followed by particle-surface sorption (Neretnieks *et al.*, 1982 and Zimmerman *et al.*, 2002).

As a result of sorption processes, some solutes will move more slowly through the fracture than the groundwater that transports them, which decreases the maximum concentration of the plume. This effect is called retardation. Biodegradation, radioactive decay and precipitation will decrease the concentration of solute in the plume, but may not necessarily slow the rate of movement.

2.5 TRANSPORT IN FRACTURED AQUIFERS

Fractures are not smooth channels or parallel plates. They have irregular walls that promote zone formation along the length of the fracture. Fractures also contain dead-end passages with non-moving water. The fluid moves through the mobile zone, but the solute can diffuse into the immobile zone. The solute is stored in the immobile fluid during the early part of solute transport and would be released from storage if the solute concentration in the mobile fluid decreases sufficiently (Raven *et al.*, 1998).

Three main effects must be considered when analysing solute transport in fractured aquifers: (1) The geometry of a single fracture; (2) The geometry of the fracture network; (3) The interaction between matrix and fracture flow (Riemann, 2002).

Assuming that the fractures can be simulated with a parallel plate model, transport within the fractures is mainly due to advection, which occurs at different rates, depending on the fracture aperture.

Single fractures and fracture networks cannot be described sufficiently with a parallel plate model of a single fracture. Flow in a fracture normally occurs in a fracture zone consisting of several interconnected fractures. Single fractures have variable apertures, resulting in channels of higher velocity and dead-end zones. The geometry of single fractures and fracture networks is mostly unknown, but has an influence on the flow geometry.

In the past, different conceptual and numerical models have been developed to account for flow geometry, but are based on assumptions about the fracture network and geometry, which might be inconsistent with reality, because the flow geometry is unknown.

2.6 BIOBARRIERS FOR SOUTH AFRICAN AQUIFERS

There are many factors that will influence the effectiveness of biobarriers in South African aquifers. Bacteria used for the building of biobarriers must have the following properties:

- Size is very important in bacteria transport. In porous sands, bacteria must be able to move throughout the surrounding unconsolidated materials rather than collect at the injection site. The transport of bacteria can be prevented by filtration

by pores and fractures that are smaller than the bacteria, as well as bacteria binding to particle surfaces, which prevents movement (DeFlaun *et al.*, 1998). In the case of unconsolidated aquifers, bacteria starvation might be an option for reducing the size of the bacterial cells. Starvation results in changes in cell morphology and physiology (James *et al.*, 1995). Changes in bacterial morphology during starvation often include a reduction in cell size, which may enhance bacteria transport through the porous media. In fractured rock aquifers, bacteria starvation is not required, due to the fact that the fracture allows distribution of bacteria through the system.

- Bacteria injected into an aquifer must be able to advect in the direction of the withdrawal borehole. Bacteria distribution is very important for biobarrier formation. For effective biobarrier formation, bacteria must be equally distributed throughout the area. Cell size and adhesion will have an effect on advection.
- The bacteria must have some adhesion abilities. Due to adhesion, bacteria can accumulate and start to form biomass. Bacteria must be capable of forming large quantities of extracellular polymer material during their growth phase to reduce the free pore space in the formation and consequently reduce the hydraulic conductivity.

2.7 BIOBARRIERS IN KAROO AQUIFERS

In the Karoo aquifers (dual porosity aquifers), the preferred pathway for groundwater and pollution transport is the fracture zones. For the purpose of implementing biobarriers, the fracture areas are therefore targeted. In the Karoo aquifers the matrix porosity is too low and bacteria transport will not be effective in these areas.

Bacteria and media injection can also occur simultaneously, because the fractures are large enough to prevent bacteria from clogging at the injection point in the fracture. Bacteria must also have good adhesion abilities to ensure the formation of biomass throughout the aquifer system.

For the successful implementation of biobarriers at a site, the groundwater system must first be well characterised, aquifer testing done in detail, including hydraulic tests (aquifer tests, slug tests), tracer tests (point dilution and radial convergent tracer tests), fracture determination (large and small interval characterisation), borehole camera observations, etc. (Refer to Chapter 3).

3 SITE CHARACTERISATION FOR BIOBARRIER APPLICATION

The purpose of the research was to test the applicability of biobarriers in South African fractured rock aquifers. Chapter 3 will concentrate on the characterisation of a target aquifer for biobarrier application. Prior to biobarrier injection into the dual porosity fracture rock aquifer, a detailed characterisation was performed on the UFS campus test site to determine aquifer hydraulics and fracture positions. This included aquifer tests, fracture determination tests, tracer tests and borehole camera observations.

The campus test site at the University of the Free State (UFS) is located in Bloemfontein in South Africa (refer to Figure 2-1 for location of Bloemfontein). The site was chosen to test the effectiveness of biobarrier for application on a field scale. The campus test site is set aside for postgraduate students to conduct field experiments. The site covers an area of $180 \times 192 \text{ m}^2$. To date, 41 percussion and seven core boreholes have been drilled. See Figure 3-1 for location of the boreholes at UFS. The yellow dots indicate boreholes no. UO7, UO14 and UO20. The red dots indicate the two observation boreholes and the blue dots indicate the rest of the boreholes at the test site.

The campus test site is underlain by mudstones and sandstones from the Adelaide Subgroup of the Beaufort Group formation. Geological mapping of the outcrops around the site reveals the existence of extensional fractures (Mode I) and shearing fractures (Mode II). The dominant types of fractures identified in the sediments include sub-horizontal, bedding-parallel plate fractures and orthogonal and diagonal fractures (Botha *et al.*, 1998). The Mode I fracture is the most significant on the campus site, and all boreholes with high yields intersect this bedding-plane fracture.

Prior to testing the effectiveness of biobarriers in the field, very intensive field characterisation tests were conducted on the campus test site. For biobarrier research on the field scale, three boreholes, namely UO7, UO14 and UO20, were selected for aquifer tests. (Refer to Figure 3-2).

3.1 INTRODUCTION

The effectiveness of biobarrier technology relies on the successful injection and movement of bacteria through the aquifer, and in this case, movement in the fractures.

The determination of the exact position of main fractures in boreholes is always problematic. In the past, researchers relied on aquifer test data, borehole cameras, acoustic scans, etc. As part of this research, different types of tests were used to determine the position of the Mode I fracture in three boreholes.

The main aim of the research was to clog the fractures in the aquifer in order to decrease the flow in fracture areas. Because the main movement of water is in the fracture area, the position of the fractured zone in the boreholes is very important.

The three boreholes selected for testing are indicated in yellow in Figure 3-1.

During the project, several methods were used to determine the position of the major and minor fractures in the three boreholes on the campus test site. The results were correlated to determine the best method for future tests.

The methods include:

1. Hydraulic tests (aquifer tests).
2. Borehole video camera observations.
3. Down-the-hole geophysics.
4. Multiple-parameter logging (electrical conductivity (EC), pH, Redox potential and temperature).
5. Fracture determination tests - EC logging of boreholes.

Transport in dual porosity aquifers principally occurs in the fracture zones; therefore transport tests were conducted to determine the properties of the fractures. These transport properties were determined by means of tracer tests. Two types of tracer tests were conducted for the above-mentioned boreholes, namely:

- Point dilution tracer tests and
- Radial convergent tracer tests.

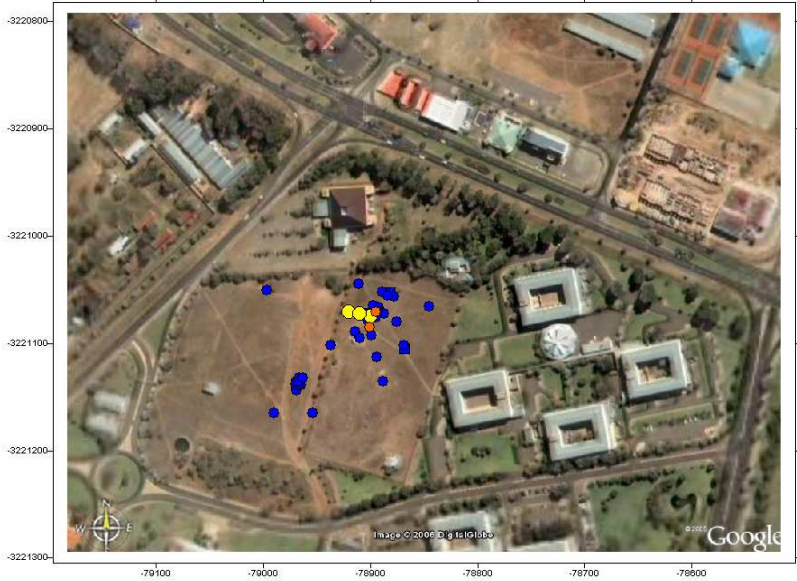
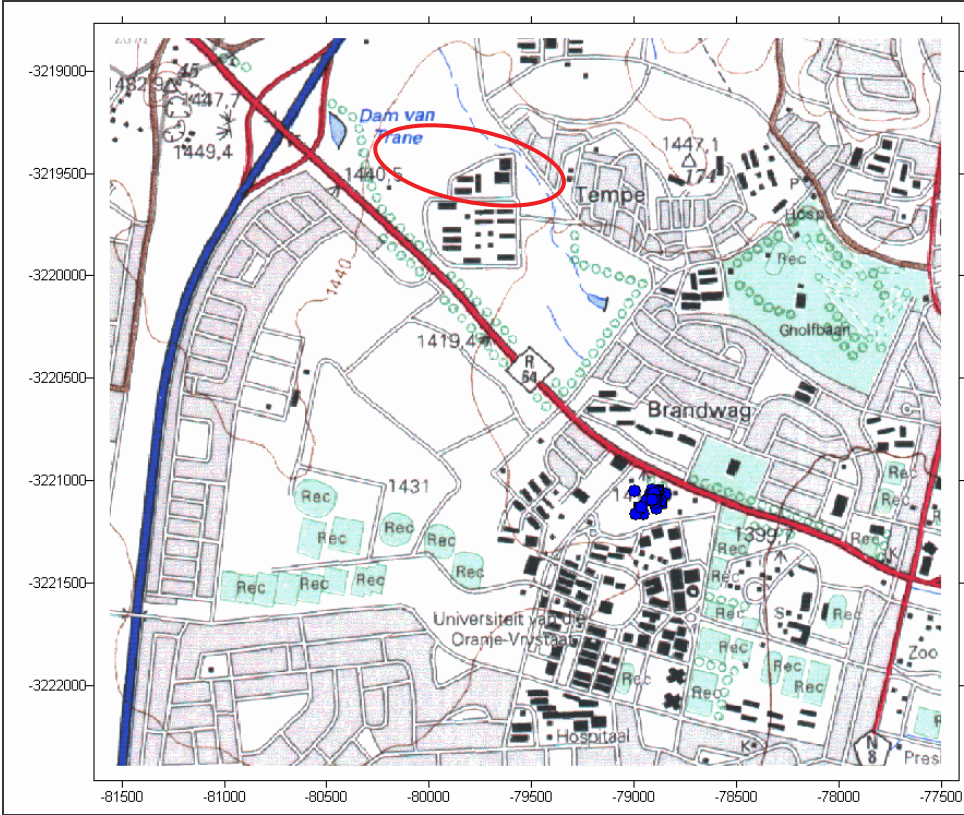


Figure 3-1 Location of some of the boreholes at the campus test site.

3.1.1 Borehole information

The three boreholes selected for the tests, namely UO7, UO14 and UO20, are located on the active part of the Mode I water-bearing fracture. During some of the aquifer tests, UO5 and UO26 were used as observation boreholes to monitor water level reactions (see Figure 3-2 for the positions of boreholes (red) - observation boreholes are marked in black).

See Table 3-1 for the distance between selected and observation boreholes.

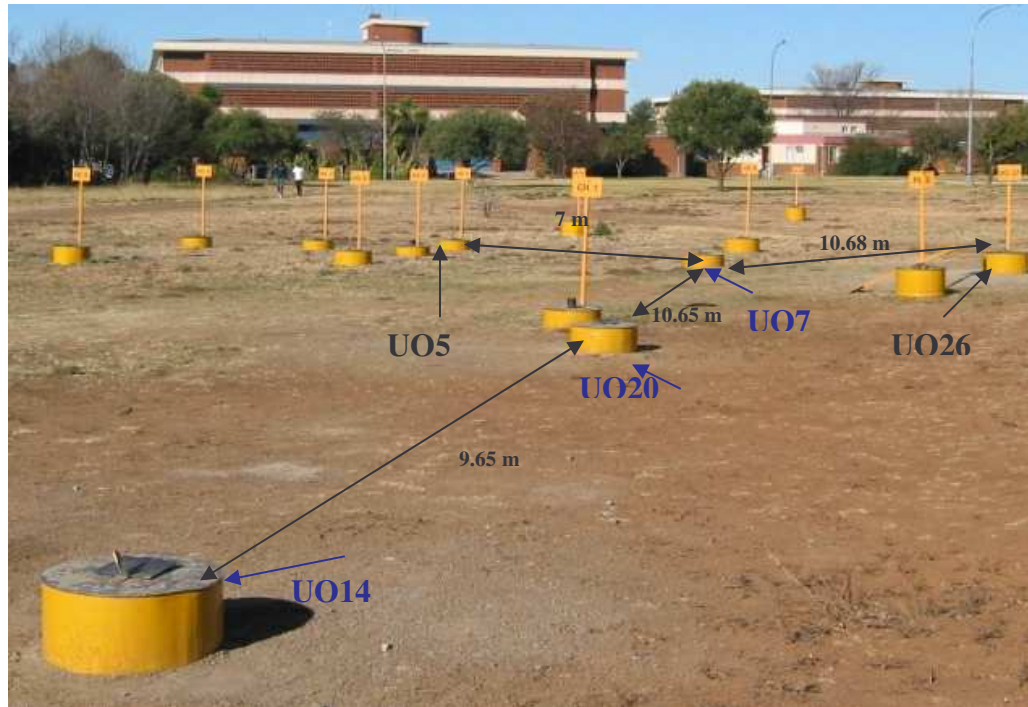


Figure 3-2 Position of the selected boreholes.

Table 3-1 Borehole information - distance between boreholes.

BOREHOLE INFORMATION	
Borehole no.	Distance (m)
UO7-UO14	20.3
UO7-UO20	10.65
UO7-UO26	10.48
UO5-UO7	7
UO5-UO14	25.9
UO5-UO20	16.5
UO5-UO26	15.82
UO14-UO20	9.65
UO14-UO26	23.7
UO20-UO26	15.5

3.2 AQUIFER TESTS – HYDRAULIC TESTS

Aquifer tests are the most important experiments for aquifer investigation in the groundwater industry. This is the only method that provides simultaneous information on the hydraulic behavior of wells (boreholes), the aquifer and the aquifer boundaries, which is essential for efficient aquifer and well-field management (Van Tonder *et al.*, 2002). The complex situation in fractured aquifers requires an adequate understanding of drawdown behaviour if reliable reservoir information is desired. This can be achieved with a detailed diagnosis of drawdown and recovery data in combination with a conceptual model of the geological set-up.

3.2.1 Estimation of aquifer parameters

The aquifer parameters are important for management purposes (yield and pollution management). In the case of contaminated groundwater, the aquifer parameters are important for risk assessments and planning groundwater remediation.

The following tests were performed to determine aquifer parameters:

- Constant rate abstraction test
- Recovery tests

3.2.2 Constant rate test

The constant abstraction rate or constant discharge test is the most common hydraulic test, and also the most common for aquifer parameter estimation. During this test, water

is abstracted from the borehole at a constant rate. The change in the drawdown and pressure in the borehole or observation boreholes are measured and can be related to aquifer properties.

Several hydraulic tests, including constant rate tests, were performed on the campus test site in the past. The tests described and analysed here were conducted on Boreholes UO7, UO14 and UO20 during July 2005. Boreholes UO5, UO26, UO27 were observation boreholes. See Figure 3-2 for borehole positions.

3.2.3 Recovery test

This test provides an indication of the ability of a borehole and groundwater system to recover from the stress of abstraction. This ability can be analysed to provide information with regard to the hydraulic properties of the groundwater system and arrive at an optimum yield for the medium- to long-term utilisation of the borehole. Although referred to as a test, it represents a period of monitoring activity following a period of pumping. The rate at which the water level in the tested borehole (or any other borehole affected by the abstraction) recovers towards its starting level (the groundwater rest level before pumping started), is monitored during this period. The duration of monitoring the recovery in the abstraction borehole is generally until the water level has recovered to 95 % of the original static water level (Van Tonder *et al.*, 2002).

3.3 PERFORMING AQUIFER TESTS IN UO7, UO20 AND UO14

Aquifer tests were conducted on all three boreholes. The drawdown in the pump borehole, as well as that of five observation boreholes (UO5, UO14, UO20, UO26 and UO27), was measured.

The duration of the aquifer tests was 480 min. Recovery tests were also conducted. See Figure 3-3 for the drawdown results during a aquifer test on UO7. From the results, it can be seen that all the observation boreholes, except UO14, react in the same manner. Drawdown is identical in boreholes UO5, UO20 and UO26. UO14 reacts differently from the rest, but similarly to the abstraction borehole.

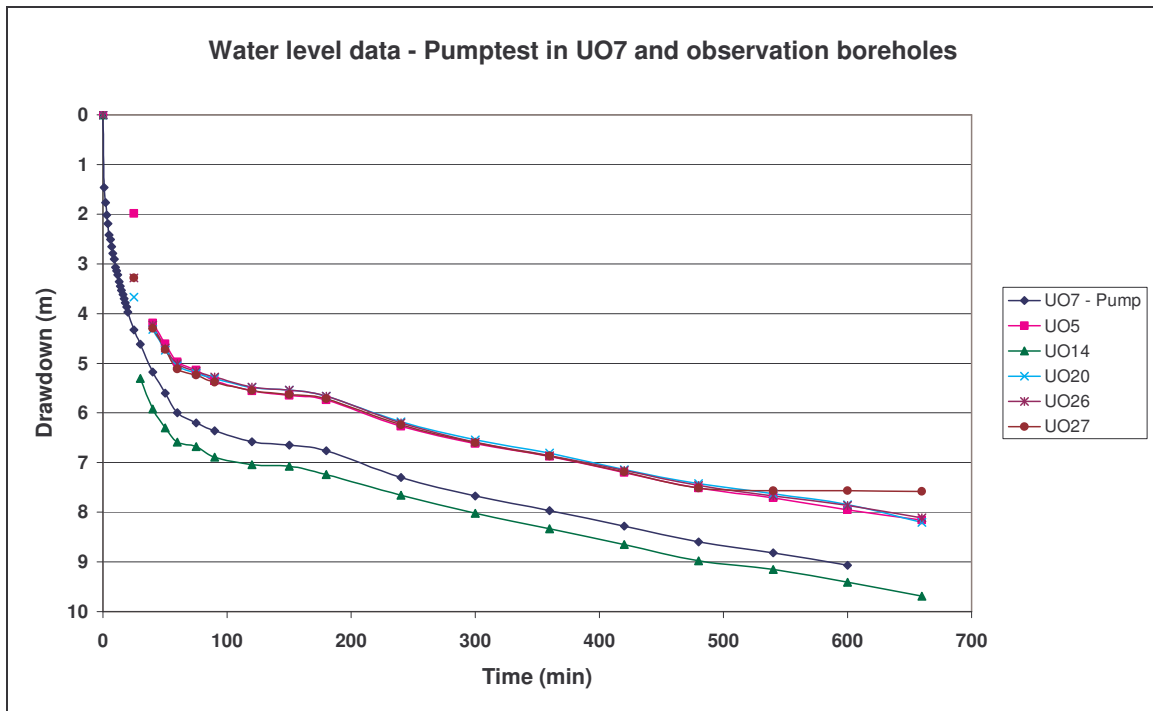


Figure 3-3 Constant discharge test on UO7. Water level data for UO7 and observation boreholes.

3.3.1 Methods of analysis

The aquifer test data were analysed by means of the “FC method“ (flow characteristic method) to evaluate the aquifer parameter (Riemann, 2002)). The flow phases that appear during a aquifer test in a fractured aquifer show characteristic patterns like straight lines, either in a double logarithm or in a linear logarithm plot. Using the concept of derivatives, additional information on the flow regimes can be gathered.

3.3.2 Diagnostic plots

3.3.2.1 UO7

Log-log diagnostic plots show that the early time curve has a slope of 0.5 (Figure 3-4). This indicates linear flow.

The linear flow of the aquifer system is also proved by the square root of time curve. For a square root of time plot, the drawdown data will plot on a straight line that starts at the origin of the diagram.

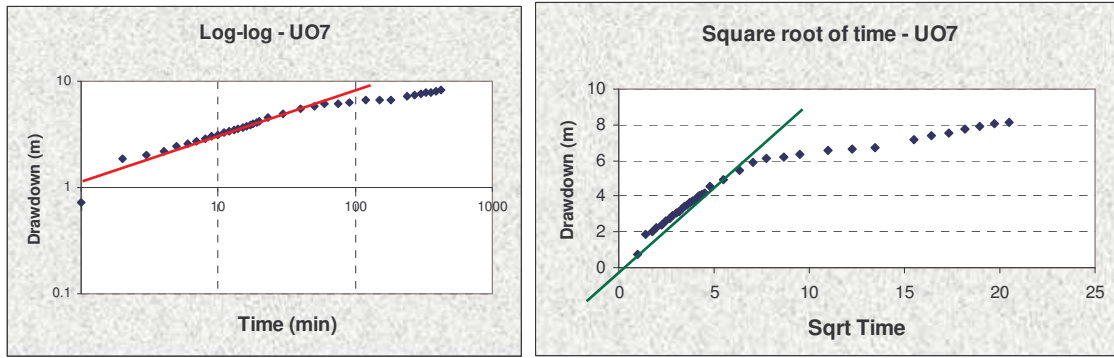


Figure 3-4 Log-log plot and square root of time plot of the aquifer test conducted on UO7.

3.3.2.2 UO14

For UO14, log-log diagnostic plots show that the early time curve has a slope of 0.25 (Figure 3-5). This indicates bilinear flow (flow from the fracture and formation) with little or no well bore storage effect. The bilinear flow of the aquifer system can also be seen by means of the fourth root of time curve. The drawdown data of the bilinear flow phase plot on a straight line, starting at the origin.

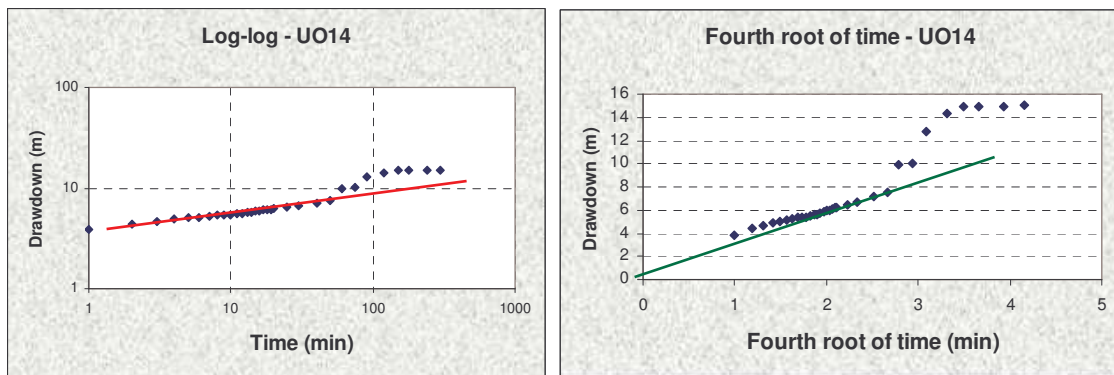


Figure 3-5 Log-log plot and fourth root plot of the aquifer test conducted on UO14.

3.3.2.3 UO20

Log-log diagnostic plots show that the early time curve has a slope of between 0.25 and 0.5 (Figure 3-6). This indicates bilinear flow (flow from the fracture and formation). The bilinear flow of the aquifer system can also be seen in the fourth root of time curves. Here the drawdown data of the bilinear flow phase plot on a straight line, starting at the origin.

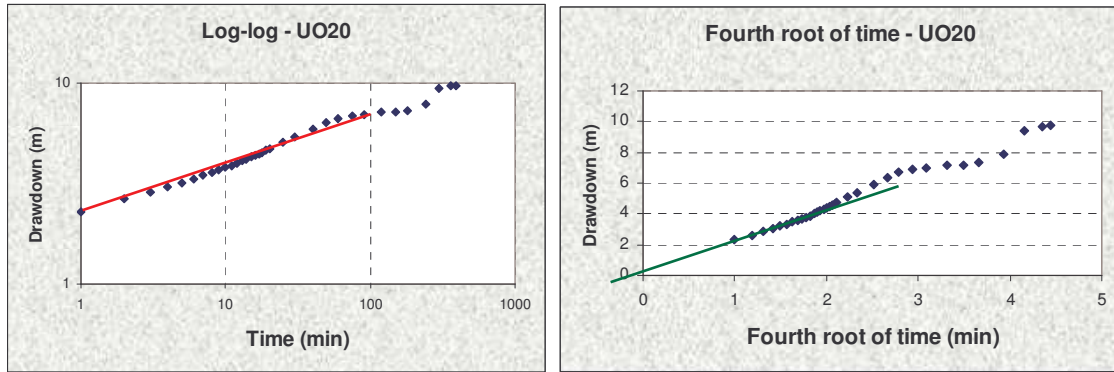


Figure 3-6 Log-log plot and fourth root plot of the aquifer test conducted on UO20.

3.3.3 Determination of fracture position by FC method

3.3.3.1 Aquifer test data

The aquifer test data were used to identify possible fracture zones. The semi-log graph of the FC method was used to identify areas where there is a change in flow regime. The flattening of the curve shows a possible fracture zone. The drawdown in the borehole stabilises due to the fact that the fracture will supply water more rapidly than the matrix. When the fracture zone is dewatered, the drawdown will continue. In UO7, a possible fracture zone is identified between 21.1 and 21.5 m. See Figure 3-7.

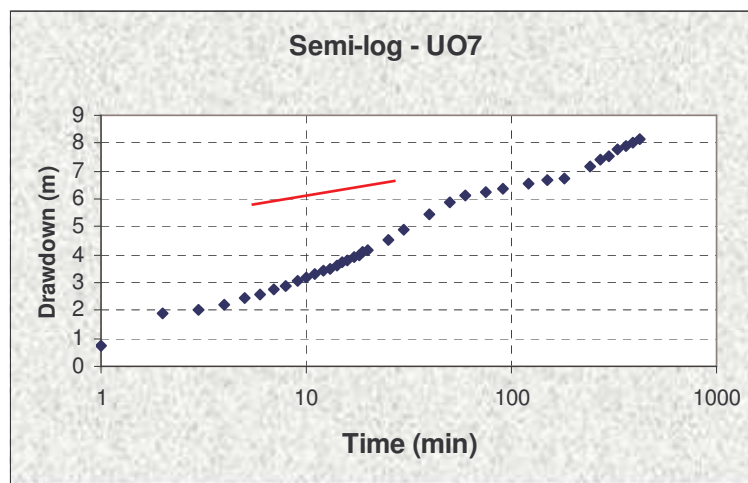


Figure 3-7 Fracture determination for UO7, with the use of aquifer test data.

In UO14, a slight change is detected between 21.95 and 22.3 m, and then again between 29.1 and 29.6 m. See Figure 3-8.

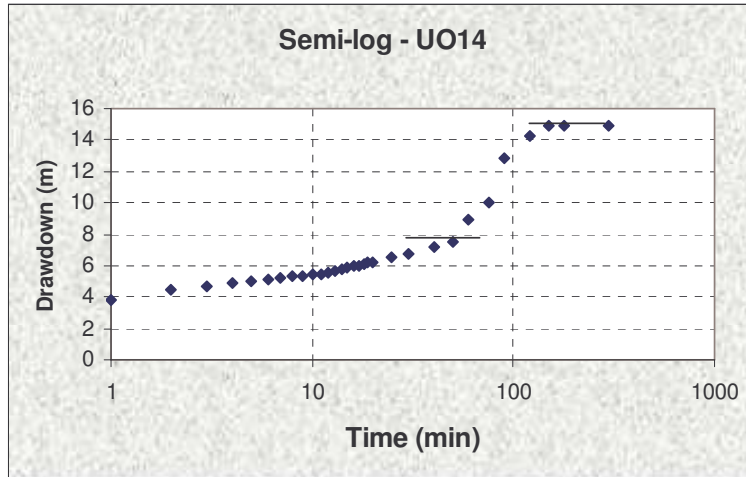


Figure 3-8 Fracture determination for UO14 with the use of aquifer test data.

In UO20, a possible fracture zone can be identified between 20.9 and 21.2 m and again between 23.67 and 23.70 m. See Figure 3-9.

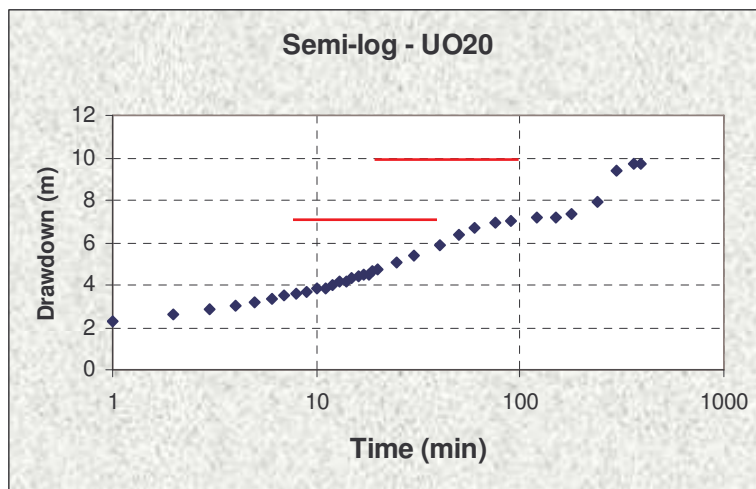


Figure 3-9 Fracture determination for UO20, with the use of aquifer test data.

3.3.4 Summary

The diagnostics for each borehole were obtained from the aquifer test data.

For UO7, the log-log diagnostic plots show that the early time curve has a slope of 0.5, which is an indication of linear flow.

For UO14, log-log diagnostic plots show that the early time curve has a slope of 0.25 (Figure 3-5). This indicates bilinear flow (flow from the fracture and formation) with no or minor well bore storage effect.

In UO20, the log-log diagnostic plots show that the early time curve has a slope of 0.25 to 0.5, indicating bilinear flow (flow from the fracture and formation). The bilinear flow of the aquifer system can also be seen in the fourth root of time curves.

The position of the fracture was also determined by semi-log versus time graphs. The results showed fracture zones. It is concluded that aquifer tests may not be the most effective way to determine the position of a fracture, due to the fact that the pump rate and depth can have a significant influence on data accuracy.

See Table 3-2 for a summary of the fracture positions obtained for the three boreholes.

Table 3-2 Summary of the fracture positions (depth in mbgl and mamsl) determined by aquifer tests in UO7, UO14 and UO20.

Fracture positions	Zone 1	Zone 2
Borehole nr	Depth	Depth
UO7	21.08 - 21.45	22.8
UO20	20.9 - 21.2	23.67 - 23.71
UO14	21.95 - 22.31	29.06 - 29.64

Fracture positions	Zone 1	Zone 2
Borehole nr	Mamsl	Mamsl
UO7	1390.2 - 1389.8	1388.42
UO20	1390.19 - 1389.9	1387.42 - 1387.38
UO14	1389.65 - 1389.29	1382.54 - 1381.96

3.4 BOREHOLE VIDEO CAMERA OBSERVATIONS

The next method to determine the exact position of the fracture was borehole video camera observations. The borehole video camera is very effective for such determinations. The borehole video camera consist of a depth determination meter. Fracture positions were measured for all three boreholes.

Visible fractures could be observed in Figure 3-10 to Figure 3-12 and their positions can be obtained in Table 3-3. The images show the depth (L) of the fracture at different rotations (ROT). This method provides visible indications of apparent fracture apertures

and may not indicate transmissive fractures. See DVD for borehole video camera observations.

Table 3-3 Fracture positions measured by borehole camera observations.

Borehole Nr	Fracture positions	
	Small fracture	Large fracture
U07	21.5	22.8
U020	21.3	21.85
U014	22.4	22.7

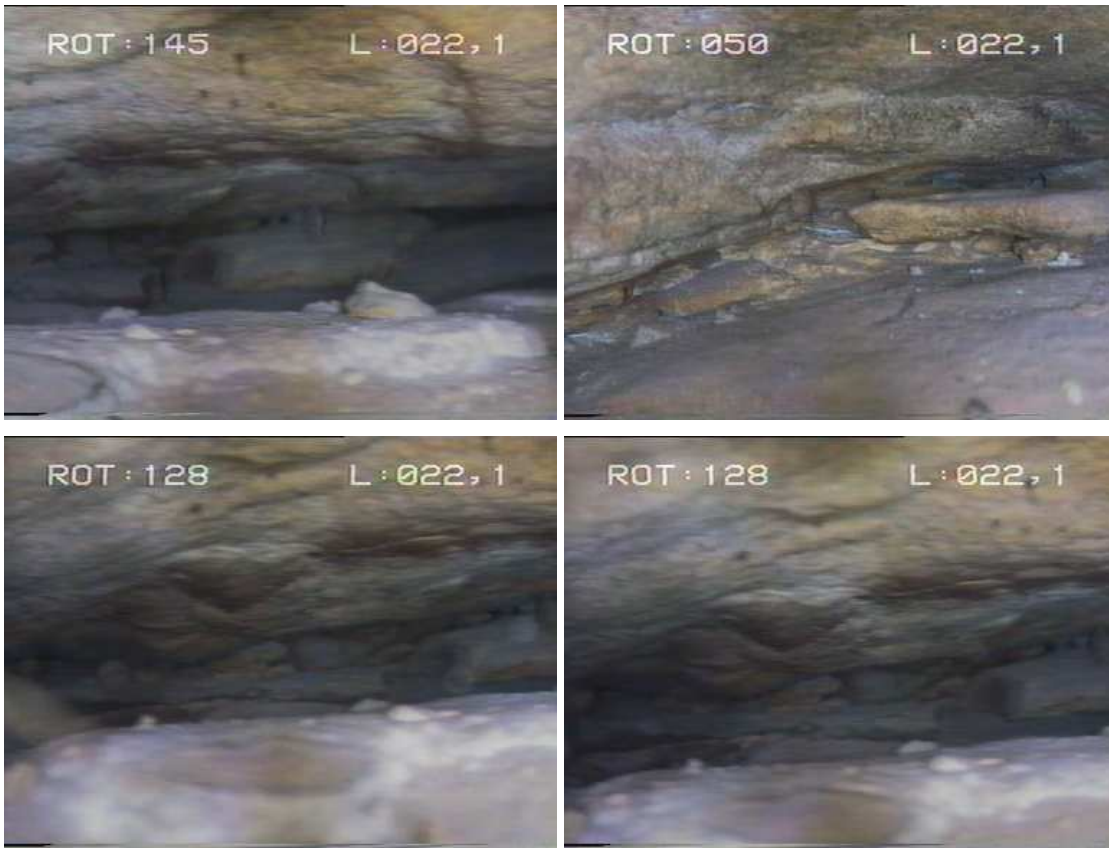


Figure 3-10 Borehole video camera observations in U07. (Fracture zone).



Figure 3-11 Borehole video camera observations in UO20. (Fracture zone).



Figure 3-12 Borehole video camera observations in UO14. (Fracture zone).

3.4.1 Discussion

When comparing the camera logging and the aquifer test results, the following preliminary conclusions can be drawn about the fracture positions. For example, the fracture position located by camera at 22.7 m in UO14 would seem a more reasonable depth for the larger fracture than at 29 m as was indicated by the aquifer test data. A large fracture at 29 m in UO14 would imply a steep dip in the horizontal plane over a 9.65 m distance between UO14 and UO20 where the fracture is found at 21.8 m.

The borehole camera is thus a very effective tool to determine the visible position of the fractures. The camera observations showed that two fractures intersect the three boreholes at different depths. Thus, borehole video camera observations may be more effective in determining the major fractures in the aquifer.

3.5 GEOPHYSICAL BOREHOLE LOGGING

Geophysical borehole logging was performed on UO20 and UO14. Three probes were used to determine the fracture position in UO20, namely the caliper probe, the full wave sonic probes and the Neutron-Neutron probe (N-N). The results of UO20 can be seen in Table 3-4. The full wave sonic probe specification makes it ideal for the measurement of lithology identification, formation porosity, fracture and permeability indication in hard rock, and mechanical properties.

The fracture position in UO20 was detected at a depth of approximately 21.3 m, by making use of three different probes (See Table 3-4 and Figure 3-13). The results from UO14 (not shown) were not as clear as for UO20.

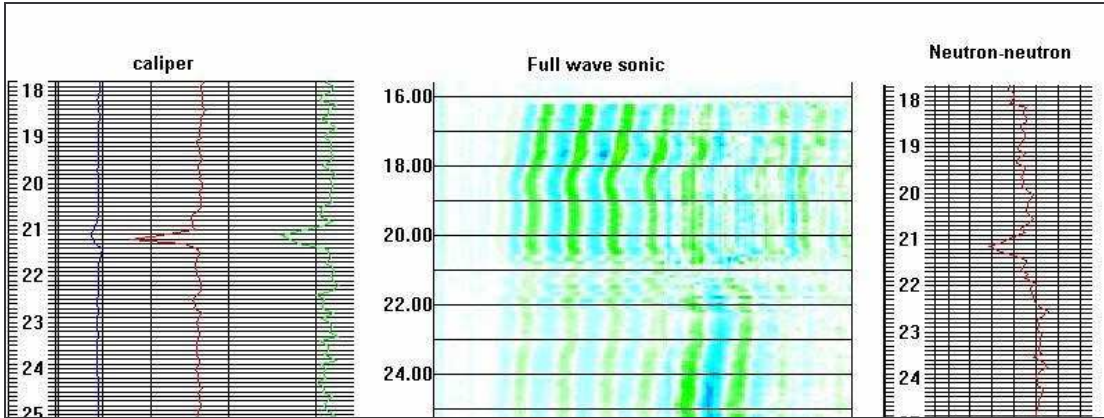


Figure 3-13 Results from geophysical logging in UO20 by the caliper probe, the FWS and the Neutron-Neutron probe.

Table 3-4 Results from geophysical logging in UO20 (mbgl).

Geophysical logging			
Fracture positions			
Borehole no.	Caliper probe	FWS probe	Neutron-neutron probe
UO20	21.3	21.3	21.3

3.6 MULTIPLE-PARAMETER LOGGING (PH, EC, REDOX POTENTIAL AND TEMPERATURE)

Multi-parameter logging was done on one of the boreholes at the campus test site to determine the pH, EC, redox potential, dissolved oxygen and temperature of the aquifer. See Figure 3-14 for the results of the logging. From the results it can be seen that the EC is on average between 80 and 100 mS/m. Temperature varies between 19.5 and 20° C, and the redox potential between 90 and 130. It can also be seen that the dissolved oxygen (DO) is depleted with depth, with the highest DO at the static water level (8 mg/l), a DO of 1.70 mg/l in the location of the fracture and a DO of 0.5 mg/l at the bottom of the borehole (46 m). The pH varies between 7 and 7.7. For application of biobarrier formation in the field, micro-aerophilic or anaerobic bacteria must be used.

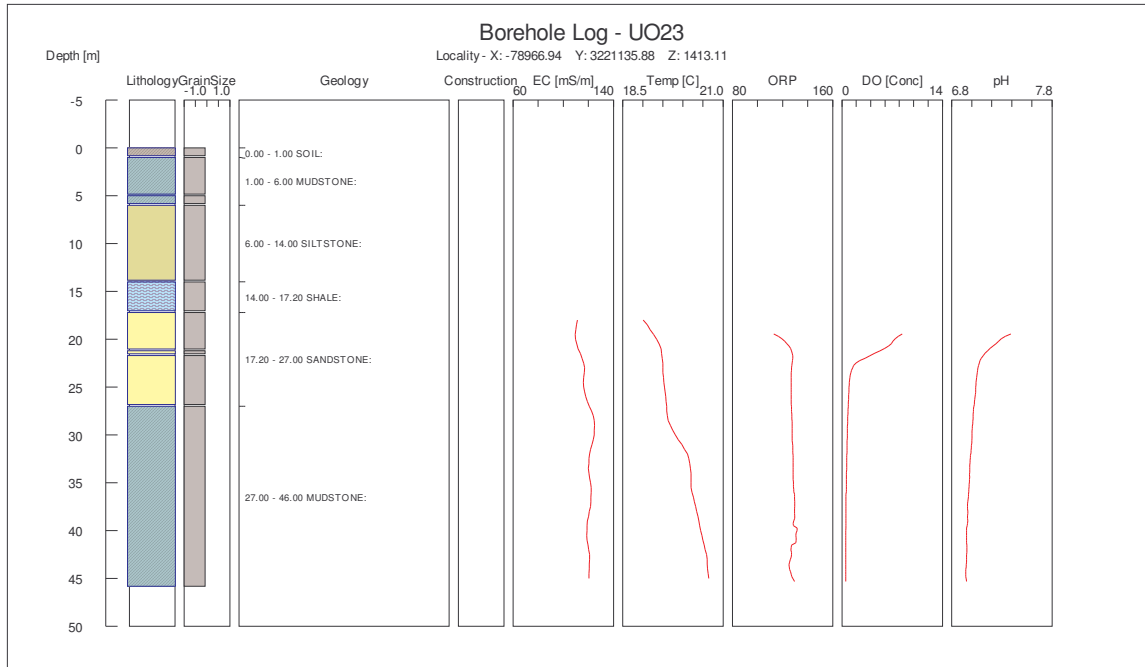


Figure 3-14 Multi-parameter logging in UO23.

3.7 FRACTURE POSITION DETERMINATION - EC LOGGING

The last method to determine the position of the fracture was conductivity logging. This test was conducted on the same principle as a point dilution tracer test (refer to section 3.9.2.3). By injecting a conservative tracer (NaCl) into the borehole over an interval (1-18 m), and by making use of an EC logger, the major and minor fractures in the borehole were obtained by determining the areas of greatest dilution. Fracture determination tests were conducted on UO7, UO20 and UO14.

For the purpose of this tracer test, different injection intervals were chosen. Large injection areas can be used to identify the exact position of the fracture. When the exact position of the fractures is known, the injection area can be decreased to cover only the fracture zone. The results of the two methods were compared to estimate which is the more accurate.

3.8 TRACER TESTS

3.8.1 Point dilution tests in UO20, UO7 and UO14

Two tests were conducted on UO20. For the first test, a large injection interval (18 m) was used to obtain an approximate indication of the fracture positions. The results were then compared and verified by means of a second test, with a smaller injection area (4 m).

The water volume in the injected section and the injection time were calculated as stated in Riemann 2002.

3.8.1.1 Large interval set-up and methodology

The set-up and methodology for the fracture determination test were as follows:

- An injection interval of 18 m was used, stretching from 15 to 33 m.
- The abstraction pipe (pump) was situated at 33 m and the injection pipe at 15m below the surface.
- The abstraction rate of the pump was measured to calculate the injection and circulation time of the tracer substance. An abstraction rate of 0.9 l/s was measured.
- The abstraction and injection pipe were then connected with the flowcell, and a closed system was created.
- The EC value (C_0) of the borehole was measured in the flowcell before the tracer was injected.
- 900 g NaCl was dissolved in 5 l of water (50 g NaCl injected per 1 m interval).
- Five litres of tracer solution was injected over a period of 7 minutes, as calculated in Riemann (2002). The system was then left to circulate for 7 minutes (circulation time is equal to injection time) to ensure the equal distribution of dissolved salt through the injection area.
- The EC increase was measured in the flowcell during the injection and circulation time.
- After the injection and circulation period (14 min), the pump was stopped.

- The EC over the injection area (18 m) was then measured at 10 cm intervals by making use of a down-hole EC logger.
- The EC in boreholes will be measured over several time intervals (t_0 - t_X) of the logging period to ensure sufficient data.
- After the logging period, the injection pipe can be disconnected from the flowcell.
- A discharge pipe can be connected to the flowcell and the pump-back phase can start.
- The EC of the water during the pump-back phase can then be measured.

3.8.1.2 Small interval set-up and methodology

The small and large interval tests operate on the same principle:

- An injection area of 4 m, located between 19.5 and 23.5 m, was used to include the fracture zone.
- 300g NaCl was dissolved in 2 l of water (75g NaCl injected per 1 m interval).
- 2 l of tracer solution was injected over a period of 2 minutes. The system was then left to circulate for 4 minutes (circulation time is double injection time) to ensure the equal distribution of salts through the injection area.
- The EC increase was measured in the flowcell during the injection and circulation time.
- After the injection and circulation period (4 min), the pump was stopped.
- The EC in the borehole was measured over ten intervals (t_0 - t_X) of the logging period to ensure sufficient data.
- After the logging period, the injection pipe was disconnected from the flowcell.
- A discharge pipe was connected to the flowcell and the pump-back phase started.
- The EC of the water during the pump-back phase was measured.

3.8.1.3 Interpretation of fracture determination for UO20

Figure 3-15 shows the data for four time periods (t_1 - t_4). From the results of the small and large interval tests (cumulative change over time), it can be seen that the large interval (Figure 3-16) shows more data points, but not necessarily more detail than the small interval (Figure 3-17). A prominent fracture can be seen at 21.3 m in both the small and large interval tests.

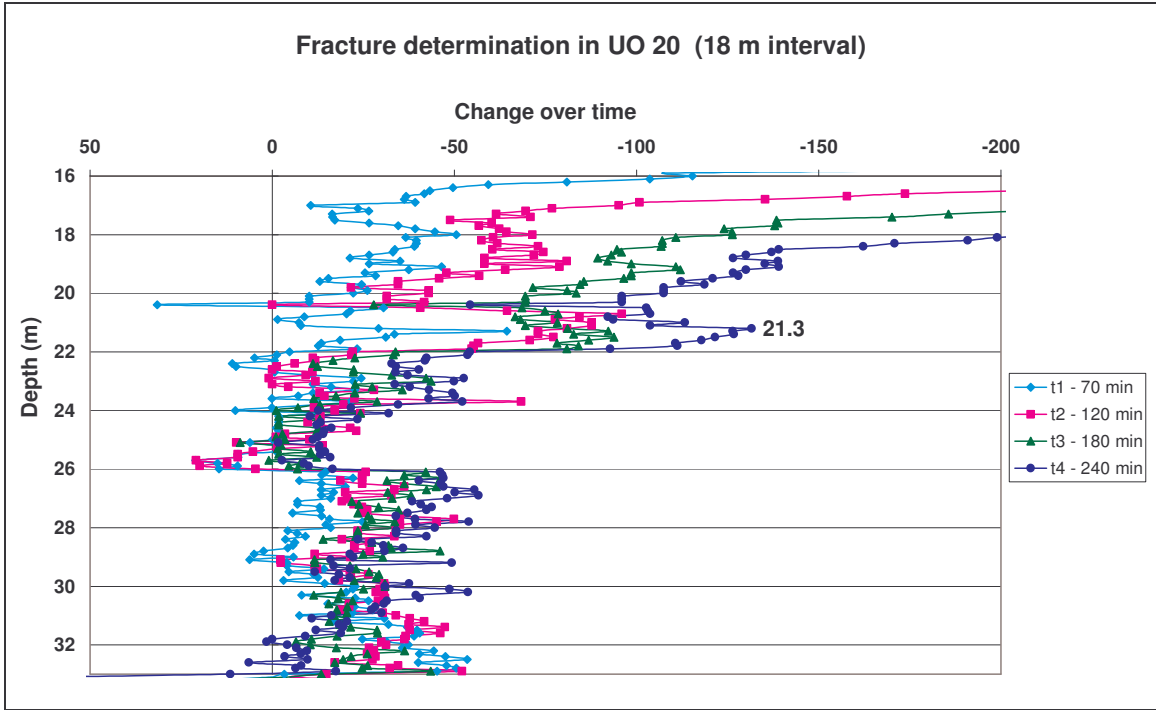


Figure 3-15 Fracture determination graph for UO20 - 18 m interval (t1-t4).

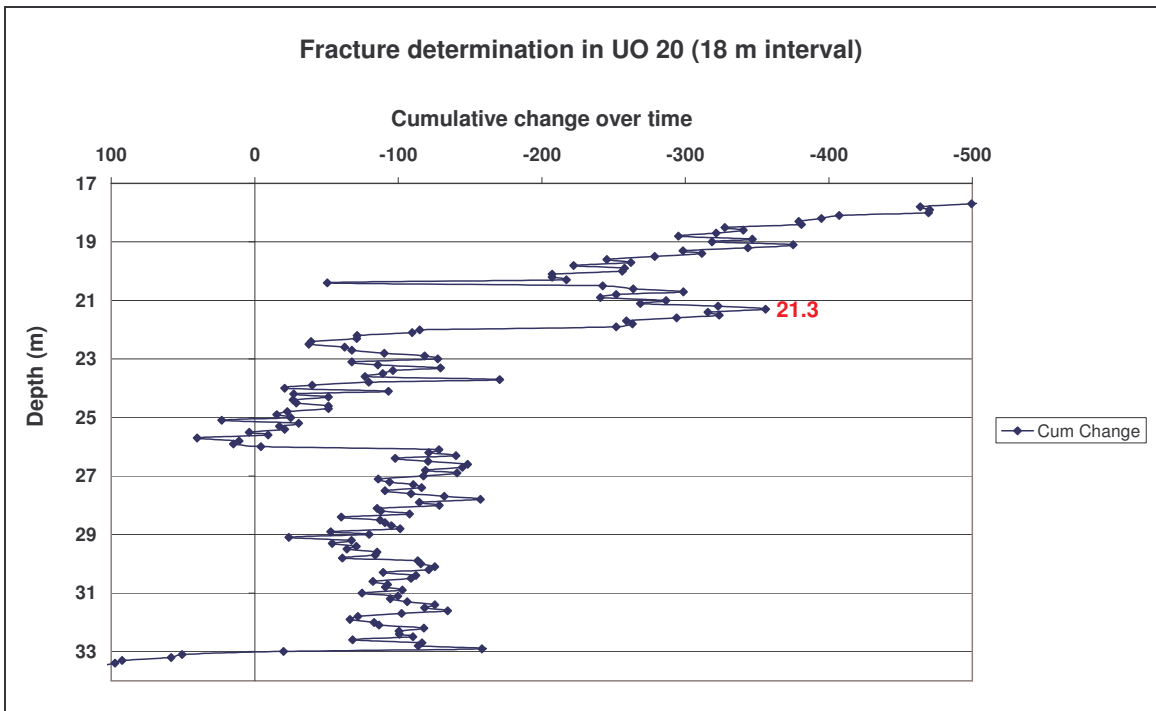


Figure 3-16 Cumulative change over time graph. Fracture determination for UO20 - 18 m interval.

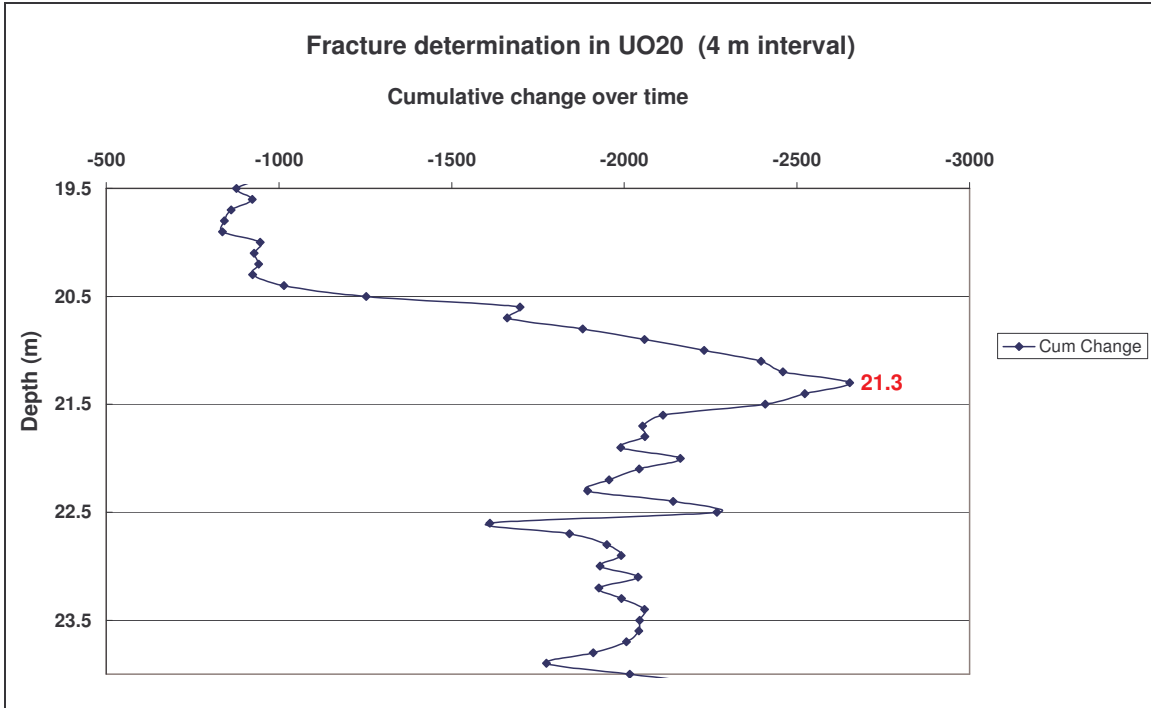


Figure 3-17 Cumulative change over time graph. Fracture determination for UO20 - 4 m interval.

Fracture determination tests were also conducted on UO7 and UO14.

See Figure 3-18 for the results of fracture determination tests on UO7. For UO7 a 14-metre interval was used (between 18 and 32 m).

From the results, it can be seen that the hydraulically dominant fracture is located at 22.8 m.

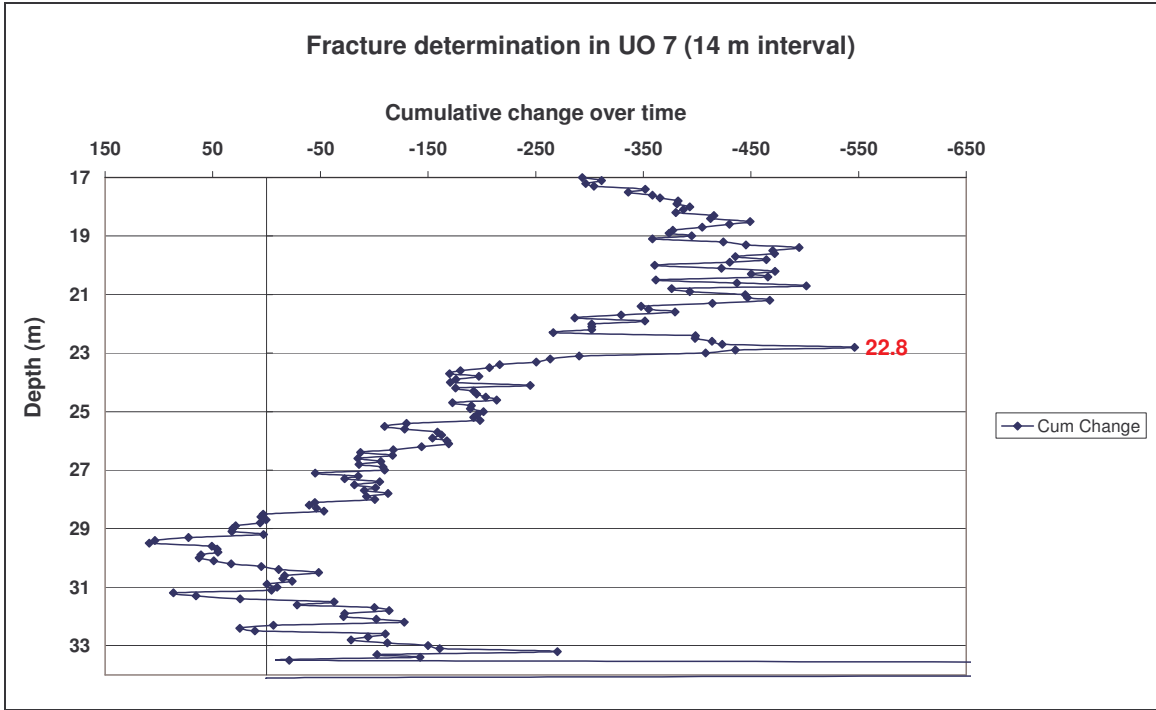


Figure 3-18 Cumulative change over time graph. Fracture determination for UO7 - 14 m interval.

A 14-metre interval (between 18 and 32 m) was used for UO14.

See Figure 3-19 for the results of the fracture determination test on UO14. From the results, it can be seen that the dominant fracture is located at 22.7 m.

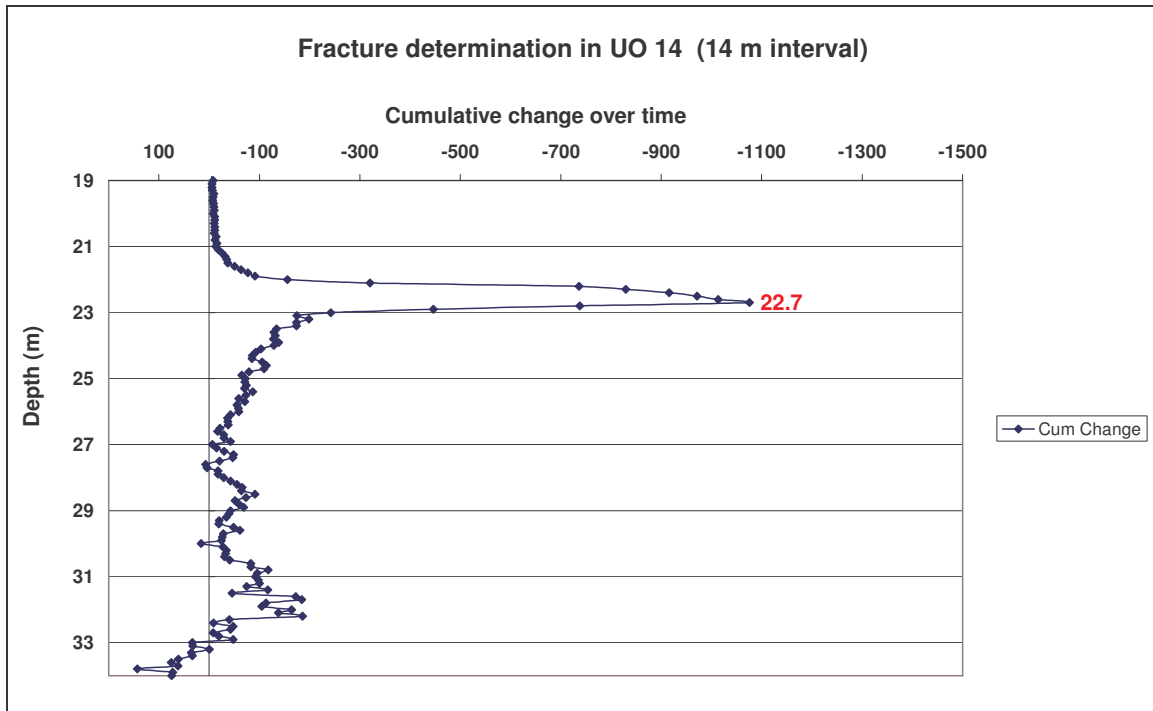


Figure 3-19 Cumulative change over time graph. Fracture determination for UO14 - 14 m interval.

The results show, as already seen from the aquifer test and observation borehole data of UO7, that the fracture positions in UO14 and UO7 are approximately on the same level, namely 22.7 and 22.8 m, respectively. The fracture at 21.3 m in UO20 is not directly connected with the fractures in UO7 and UO14.

3.8.1.4 Discussion

The EC logging method was found to be most effective in determining major fractures. Large interval point dilution tests were conducted in all three boreholes to determine the fracture positions over a range of between 14 and 18m. The large fractures could immediately be identified from the result.

Small interval point dilution tests were conducted to compare the results for accuracy. The results were the same. The large interval shows more data points but the detail is the same for both boeholes.

3.8.2 Conclusion and discussion for the three methods to determine the fracture position

From the four methods to determine the position of the fractures, the aquifer test method was the least effective. Only large zones could be identified. It was found that the abstraction rate plays a very important role in determining the fracture position. If the pump rate is too high, fractures will be dewatered rapidly and not observed.

The geophysical logging data show that some of the probes will detect the fracture positions very accurately.

The EC logging method was found most effective, This method shows the position of the fracture and identifies the major fracture in the borehole, whereas the borehole camera can only show the position of the fracture. Due to the fact that the size of the fracture is not necessarily an indication of its yield, the borehole camera cannot be classified as the best method to determine the major fractures in an aquifer.

See Table 3-5 for the results of the three methods to determine the fracture positions.

Table 3-5 Summary of the three methods to determine the fracture positions.

Pump tests		
Fracture positions	Fracture zones	
Borehole no.	Depth	Depth
UO7	21.08 - 21.45	22.8
UO20	20.9 - 21.2	23.67 - 23.71
UO14	21.95 - 22.31	29.06 - 29.64

Borehole camera observation		
Fracture positions	Fracture position	
Borehole no.	Small fracture	Large fracture
UO7	21.5	22.8
UO20	21.3	21.85
UO14	22.4	22.7

EC logging		
Fracture positions	Fracture position	
Borehole no.	small interval	Large interval
UO7	22.8	22.8
UO20	21.3	21.3
UO14	22.7	22.7

Geophysical logging			
Fracture positions			
Borehole no.	Caliper probe	FWS probe	Neutron-neutron probe
UO20	21.3	21.3	21.3

3.9 TRACER TESTS

Measurements of the transport properties of geological materials are usually taken on the field scale by monitoring the migration of existing pollution, or by conducting a tracer experiment. The most common method for conducting a tracer experiment involves establishing an advective flow field, into which a tracer is introduced (Novakowski *et al.*, 1998). The subsequent migration of the tracer is monitored in wells located down-gradient from the tracer source, and the transport properties are estimated by interpreting the tracer arrival with an analytical or numerical model.

3.9.1 Types of tracer tests

Depending on the purpose of the investigation and the site-specific situation, the type of tracer test can vary.

3.9.2 Types of tracers

Tracers are identifiable substances. The behaviour of a tracer can be studied by examination their flow behaviour (Riemann, 2002). Artificial tracers are used in the field of geohydrology in order to trace fluid movement and dispersion.

An ideal groundwater tracer has the following characteristics (Van Wyk, 1998):

- It is conservative and will follow the movement of the water without loss from the flow due to physical or chemical processes like adsorption on sediments or equipment.
- It is non-toxic, and can be applied with no administrative or legislative requirements.
- It is detectable with high sensitivity and can be measured accurately in the field.
- It will not contaminate the area of investigation or affect the results of further tests.
- The tracer substance and analysis are cost effective.

Depending on the purpose of the investigation and the local situation, the type of tracer test can vary. During this research, inorganic salt tracers such as the anions Cl^- (NaCl) and Br^- (NaBr) were used to trace groundwater movement in laboratory and field scale tests. An organic dye was also used during field tests (fluorescent dyes - uranine).

3.9.2.1 Point dilution test - Single-well tracer test

Single-well tracer tests should be conducted if only one borehole is available, or for a first approximation of specific transport parameters. Single-well tracer tests can be conducted at different depths of the borehole to estimate the vertical distribution of matrix and fracture porosity. The results should be verified with a radial convergent test.

3.9.2.2 Radial convergent test

A radial convergent tracer test is performed when two boreholes close to each other are available. For most of the transport parameters, this kind of test, usually in combination with a point dilution test, yields reliable results. For a radial convergent tracer test, two pump rigs are required, one for the injection and one for the abstraction borehole.

3.9.2.3 Point dilution tests - Injection borehole

The equipment for the injection borehole must fulfill several tasks:

- Mixing and circulating the water in the tested section sufficiently.
- Injecting the tracer at the depth of the tested section.
- Allowing for continuous measurements of tracer in the tested section.

For the purpose of the tracer test, an injection interval is chosen. This interval can vary depending on the purpose of the tracer test. Large injection areas can be used to identify the exact position of the fracture. When the position of the fractures is known, the injection area can decrease to target the flow zone of interest. See Figure 3-20 for the set-up of a tracer test.

3.9.3 Set-up in injection borehole

The circulation area is the area between the abstraction pipe (submersible pump) and the injection pipe. The system works as follows (see Figure 3-20 and Figure 3-21 for set-up):

- Water is abstracted by submersible pump.
- Abstracted water flows through the flowcell at the surface.
- The injection pipe is connected to the flowcell and flows back into the borehole.
- Tracer is injected into the flowcell.
- EC in the flowcell is measured by a portable EC meter on a regular basis.
- EC in the borehole (in the tested section) is measured by the EC logger.

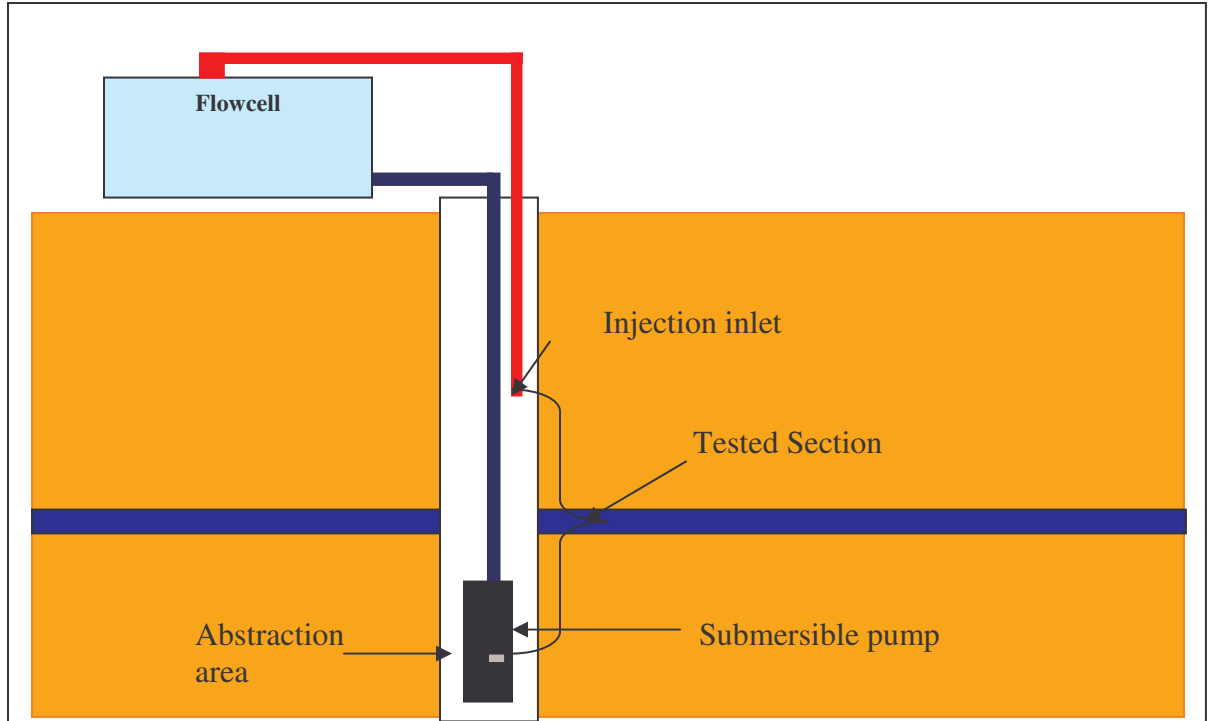


Figure 3-20 Set-up of tracer test in the injection borehole.



Figure 3-21 Set-up around the borehole and the flowcell.

3.9.3.1 Point dilution test results

A point dilution test was conducted on UO7A Darcy velocity (flux) of 3.1 m/d was measured. A seepage velocity of 34.9 m/d was calculated. The conservative tracer will therefore be transported in the fracture at a rate of 34.9 m/d.

3.10 RADIAL CONVERGENT TRACER TESTS

Three boreholes, namely UO7, UO14 and UO20, were selected for the radial convergent tests. The fracture is located in a sandstone formation. It is the most significant fracture on the campus site.

Tracer experiments were conducted using a radial flow field established by circulating water in one borehole and withdrawing it from another, while the third, located between the first two, was used to investigate the movement and dispersion of tracers through the horizontal fracture (see Figure 3-22).

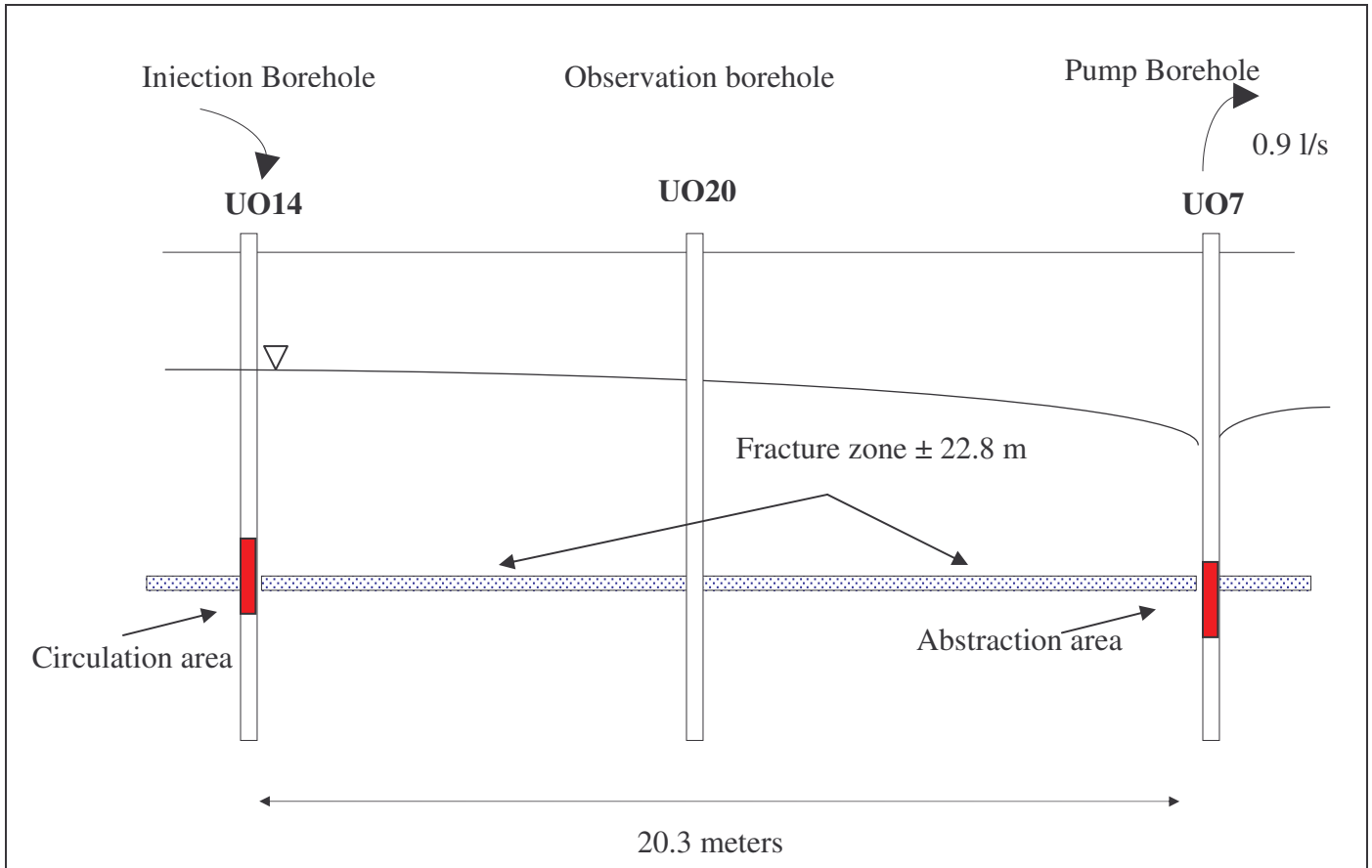


Figure 3-22 Set-up of a radial convergent test on the campus test site.

To explore the utility of the injection-withdrawal method as a general investigative tool, and with the intent to resolve the transport processes in a discrete fracture, two tracer experiments were conducted using the radial convergent tracer test method. One experiment was conducted from west to east, from UO14 to UO7, and the other in the opposite direction, from UO7-UO14. UO20 was used as an observation borehole to detect the tracer movement between the injection and abstraction boreholes.

Three conservative tracer substances (NaCl, NaBr, and fluorescein) were used to determine the movement and dispersion through the horizontal fracture. The dye used was uranine, a sodium-derivative of fluorescein.

The methodology for the radial convergent tracer test between UO14 and UO7 was as follows:

- An injection interval of 2.5m was used, between 21 and 23.5 m.
- The abstraction pipe (pump) was situated at 23.5 m and the injection pipe at 21 m below the surface.
- The abstraction rate of the pump was measured to calculate the injection and circulation time of the tracer substance. An abstraction rate of 0.9 l/s was measured.
- The abstraction and injection pipe were then connected to the flowcell, and a closed system was created.
- The EC value (C_0) in the flowcell was taken before the tracer was injected.
- 1000g NaCl, 350g NaBr and 20g uranine were dissolved in 5 l of water.

To provide for the optimal interpretation of the breakthrough curve, Novakowski (1992) suggested that the tracer be injected as a slug and that the withdrawn water should not be re-circulated into the injection borehole. In addition, because groundwater is pumped or injected through both the injection and withdrawal wells, residence times in the instrumentation and test intervals are sufficiently short that mixing conditions in the well bores need be accounted for.

- 5 l of tracer solution was injected over a period of 1.8min. The system was then left to circulate for 1.8 minutes (circulation period is double to injection period) to ensure the equal distribution of salts through the injection area.
- The EC increase was measured in the flowcell during the injection and circulation time.
- After the injection and circulation period (3.6 min), the pump was stopped.
- After 10 minutes, EC measurements with an EC data logger on UO20 began.
- The fluorometer was switched on after 10 minutes and measurements on the abstraction borehole taken every 10 seconds.
- Samples were taken every 10 minutes at the abstraction borehole to measure the NaBr and NaCl concentration to determine the breakthrough curves of the tracer substances. The concentrations were measured by making use of a Bromide and EC meter.

See Figure 3-23 for photograph of the fluorometer and Figure 3-24 for the set-up of the radial convergent tracer test.

The methodology for the radial convergent tracer test between UO7 and UO14 worked on the same principle as the test between UO14 and UO7, except for the following differences:

- An injection area of 3 m was used, reaching between 20.5 and 23.5 m.
- The abstraction pipe (pump) was situated at 23.5m and the injection pipe at 20.5 m below the surface.
- 1000g NaCl, 350g NaBr and 20g uranine were dissolved in 5 l of water.
- 5 l of tracer solution was injected over a period of 2 minutes. The system was then left to circulate for four minutes.
- After the injection and circulation period (4 minutes), the pump was stopped.

The software program TRACER (Riemann, 2002) was used to analyse the test results. The dispersion in the fracture and natural flow (velocity-m/d) were calculated.

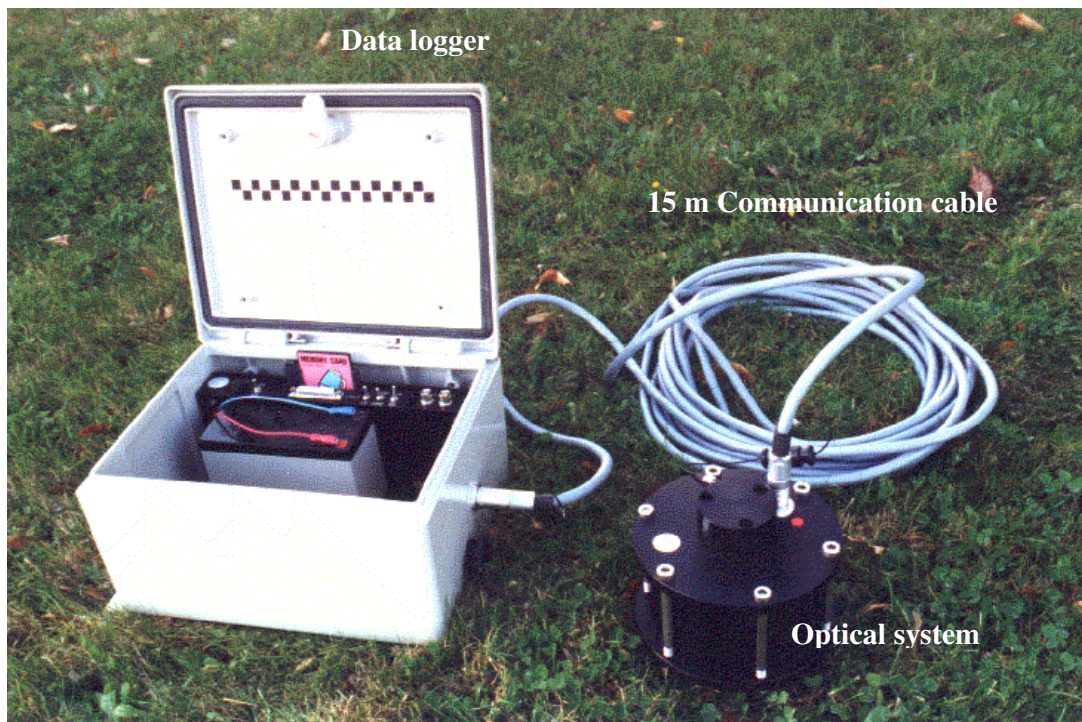


Figure 3-23 The GGUN-FLO2 filter fluorometer.

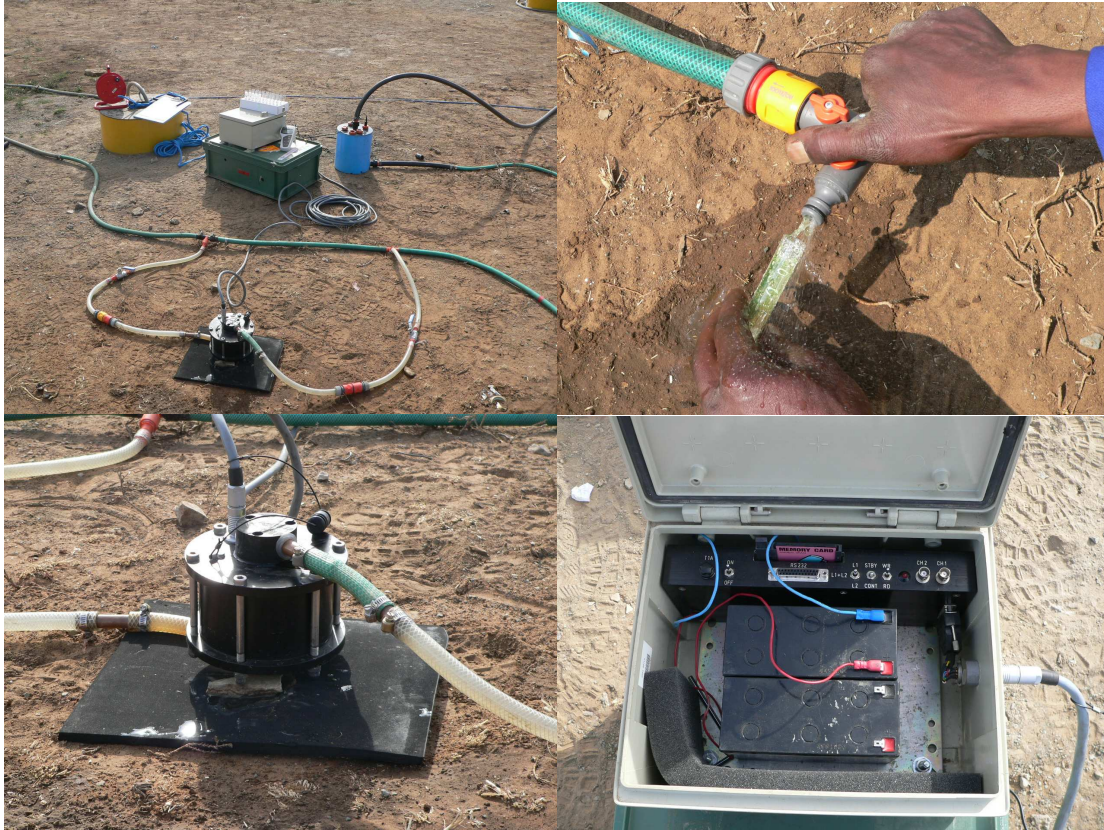


Figure 3-24 Set-up of a radial convergent test in the field.

3.10.1 Results

The interpretation of the tracer experiments in the abstraction as well as the observation borehole yields unique results. Although all three boreholes are connected with the Mode I fracture, it can be seen from the graphs that the tracer solutions use different flow paths to move from one point to another. See Figure 3-26, Figure 3-27 and Figure 3-28 for breakthrough curve graphs and results of the three tracer solutions.

The tracer test from UO14-UO7 (blue line graph) was conducted in the direction of groundwater flow and the test from UO7-UO14 (pink line graph) was conducted in the opposite direction.

3.10.2 Radial convergent test – UO14-UO7

From Test UO14-UO7 (blue line graphs), it can be seen that the tracer front of the NaCl, NaBr and uranine passes through the system after 200 minutes. After 200 minutes, the tracer concentrations start to increase over time. The sequence of breakthrough for the three tracers was as follows: NaBr reaches peak concentrations first, after 440 minutes. The second was uranine, after 458 minutes, and the third NaCl, after 490 minutes.

The results of these experiments show significant tailing in the shape of the breakthrough curves, which can be attributed to the arcuate shape of the flow field and large values of dispersivity. These kinds of results were interpreted by Raven *et al.* (1988), Hadermann and Heer (1996), Kunstmann and Kinzelbach (1998), and Becker and Shapiro (2000), with the assumption that a component of the tailing observed in the experimental data could be attributed to solute transfer from the flowing fluid into adjacent immobile zones or into the unfractured matrix. Raven *et al.* (1988) assume that the exchange is an advective process, whereby fluid entrapped in dead-end pore spaces adjacent to the fracture is “slightly” mobile as a result of the intrusion of vortices and eddies emanating from the main body of fluid in the fracture.

The software program TRACER (Riemann, 2002) was used to analyse the tracer test data to determine the shape of the flow field, dispersion, thickness and natural flow (velocity-m/d) in the fracture. See Figure 3-29 and Table 3-6 The results for the dispersivity and the velocity of the tracers can be seen in Table 3-6 From the results, it can be seen that uranine has the highest velocity (44 m/d) and the lowest dispersivity. NaCl is transported at the slowest rate (30 m/d), and the highest dispersion (3.1 m) was calculated for NaCl.

In Figure 3-31 (blue line graphs), a large preferred flow path is detected in UO20, between 21.3 and 22.3 m below surface, which causes tracer dispersion. It can also be seen that the recoverable tracer concentrations are much lower in the blue line graph.

The spatial maximum (mass midpoint) of the tracer plumes were calculated for each tracer. The spatial maximum represents the mean pore velocity of the medium, indicated with a circle. Since dispersivity lowers the peak concentration of the tracer plume in time the maximum concentration is detected at the position of the borehole at time = $t + x$ while the spatial maximum of the plume reaches the borehole at time = $t + 2x$. That illustrates that the tracer breakthrough curve peak does not represent the spatial maximum of the tracer plume, which is related to the pore velocity of the medium (van Wyk 1998). See Figure 3-25 for a schematic diagram of the spatial maxima of the tracer plumes.

From the result it can be seen that the mass midpoint of all three tracers were detected after the curve peak. See Table 3-7 for comparison between mass midpoint times and curve peak times.

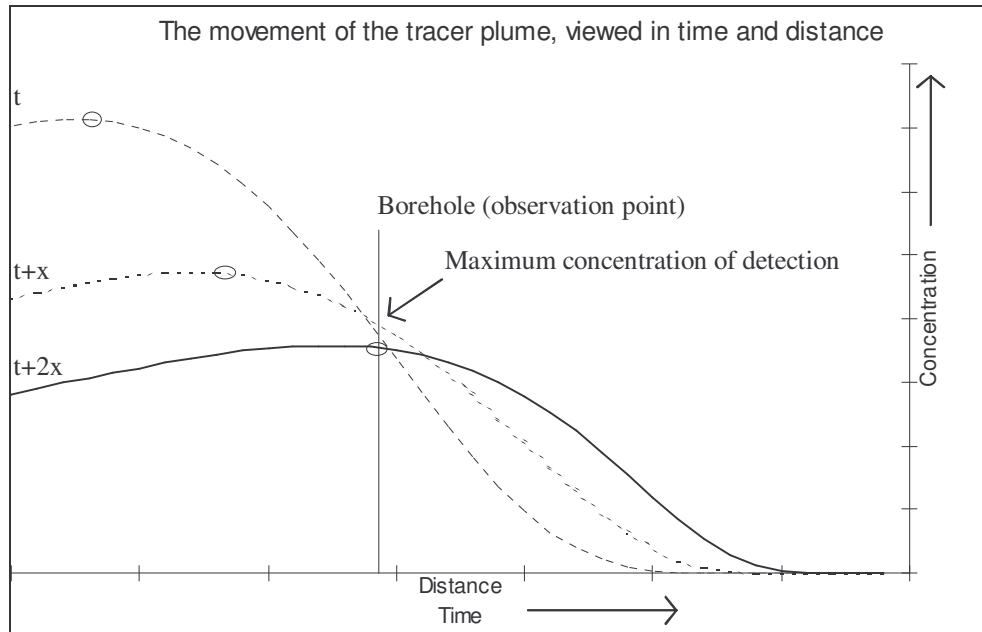


Figure 3-25 Spatial maxima of the tracer plume (after van Wyk. 1998).

3.10.3 Radial convergent test – UO7-UO14

From Test UO7-UO14 (pink line graphs), it can be seen that the tracer front of the NaBr and uranine passes through the system after 100 minutes. The tracer front for the NaCl passes through the system after 15 minutes. After respectively 100 and 15 minutes, the tracer concentrations start to increase very rapidly. The NaCl, NaBr and uranine reach peak concentrations after respectively 270, 310 and 249 minutes, and decrease over time.

The spatial maximum (mass midpoint) were calculated for each tracer. The spatial maxima of the tracer plumes were measured after the curve peak. See Table 3-7 for comparison between mass midpoint times and curve peak times.

From the result it can be seen that the mass midpoint of all three tracers were detected after the curve peak.

From these results, it can be assumed that the tracer used a different pathway. Compared to the blue line graph, dispersion is much lower and might be attributed to the presence of fewer dead-end pores between UO7 and UO14.

The TRACER program was used to analyse the data of all three tracers. See Figure 3-30 and Table 3-6. The results from the TRACER program show that the uranine has the highest velocity, at a transport rate of 86 m/d. NaBr was transported at the lowest velocity, causing the tracer to disperse.

In Figure 3-31 it can be seen that the active transport zone in UO20 is also much smaller (between 21.1 and 21.8 m) when the mass transport is from UO7-UO14. When the experiment is reversed, a larger active transport zone (between 21 and 22.5 m) was measured.

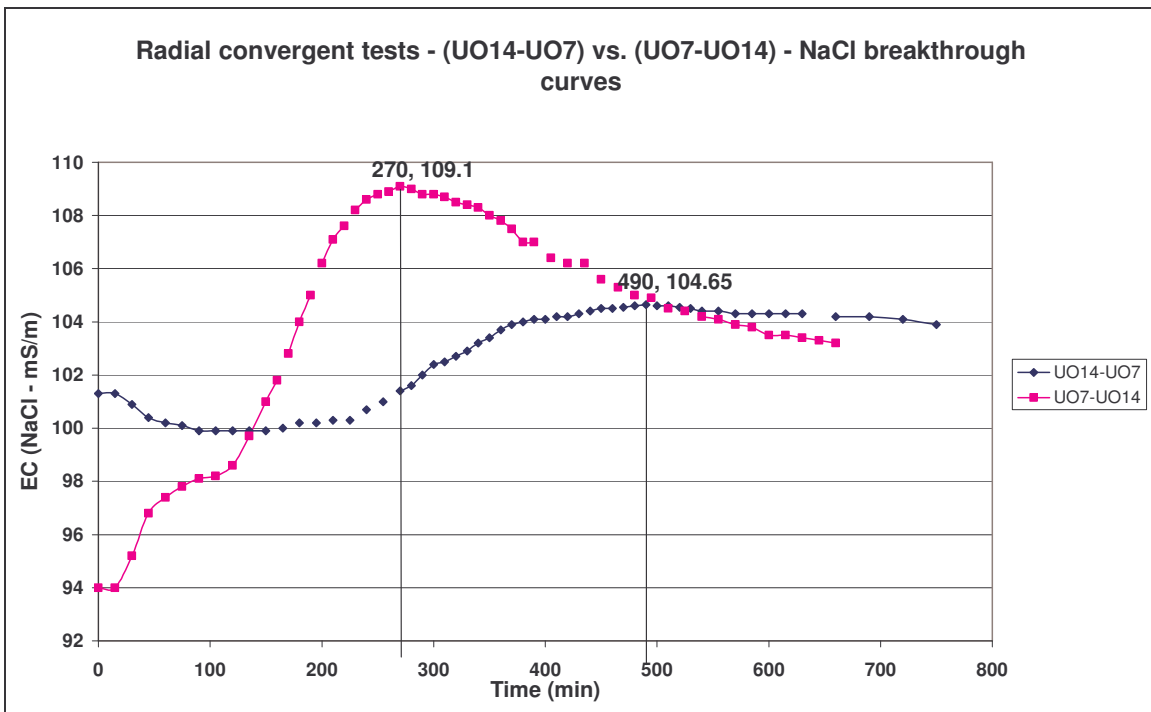


Figure 3-26 Radial convergent tests - NaCl breakthrough curves. UO14 - UO7 vs. UO7-UO14.

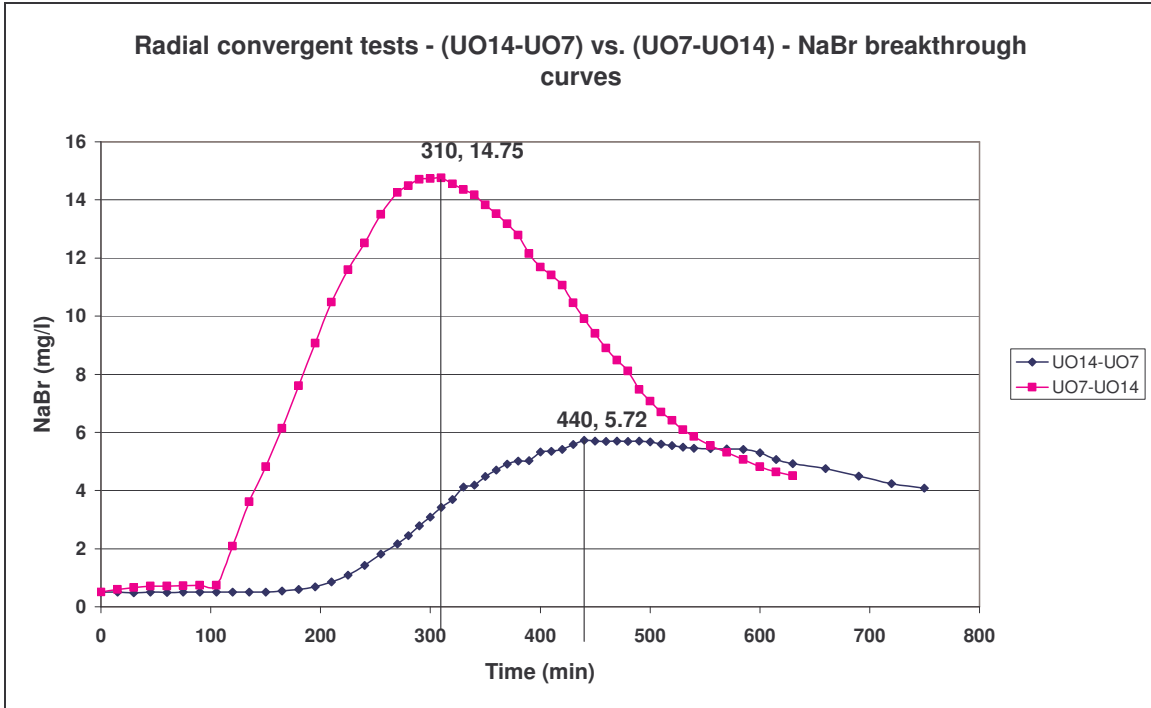


Figure 3-27 Radial convergent tests - NaBr breakthrough curves. UO14 - UO7 vs. UO7-UO14.

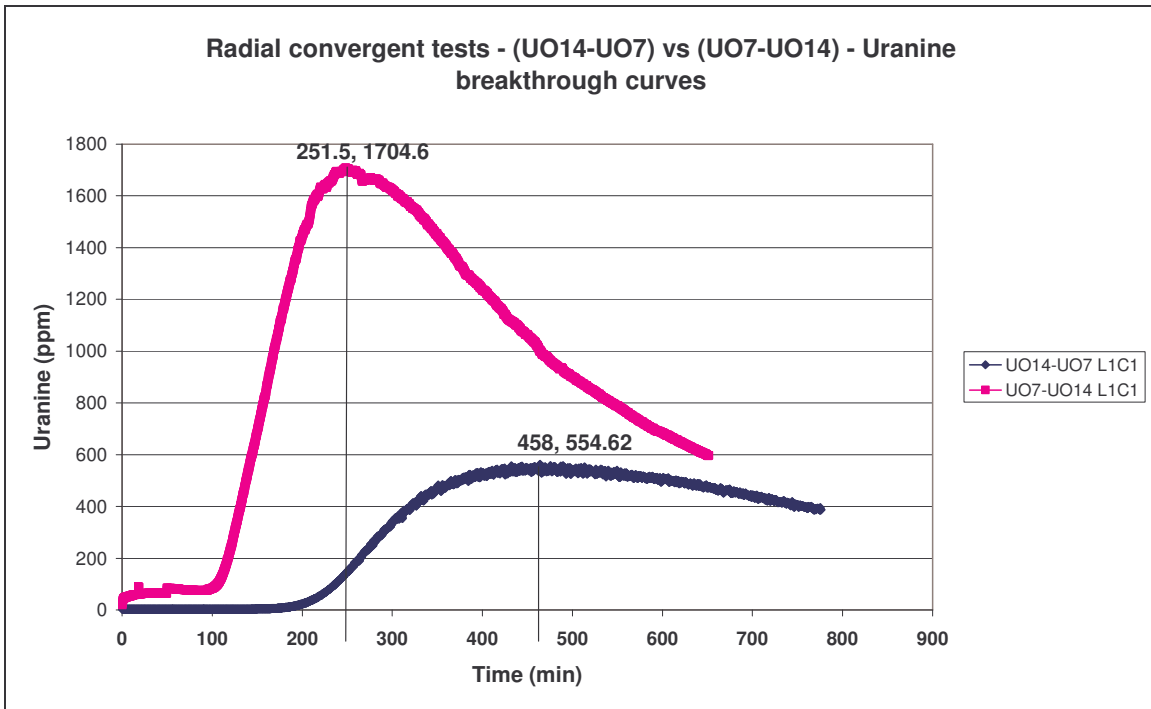


Figure 3-28 Radial convergent tests - Uranine breakthrough curves. UO14 - UO7 vs. UO7-UO14.

Table 3-6 Summary of the transport parameters for the three tracers.

UO14-UO7			
Tracer	Thickness (m)	Velocity v_f (m/d)	Dispersivity (m)
NaCl	0.14	46	1.9
NaBr	0.16	52	1.4
Uranine	0.15	49	1.7

UO7-UO14			
Tracer	Thickness (m)	Velocity v_f (m/d)	Dispersivity (m)
NaCl	0.15	79	1.7
NaBr	0.15	69	2
Uranine	0.15	81	1.6

Table 3-7 Comparison between breakthrough time and mass midpoint. (UO14-UO7) and (UO7-UO14).

UO14-UO7	Curve peak (min)	Mass midpoint (min)
NaCl	490	540
NaBr	440	510
Uranine	460	520

UO7-UO14	Curve peak (min)	Mass midpoint (min)
NaCl	270	350
NaBr	310	370
Uranine	250	312

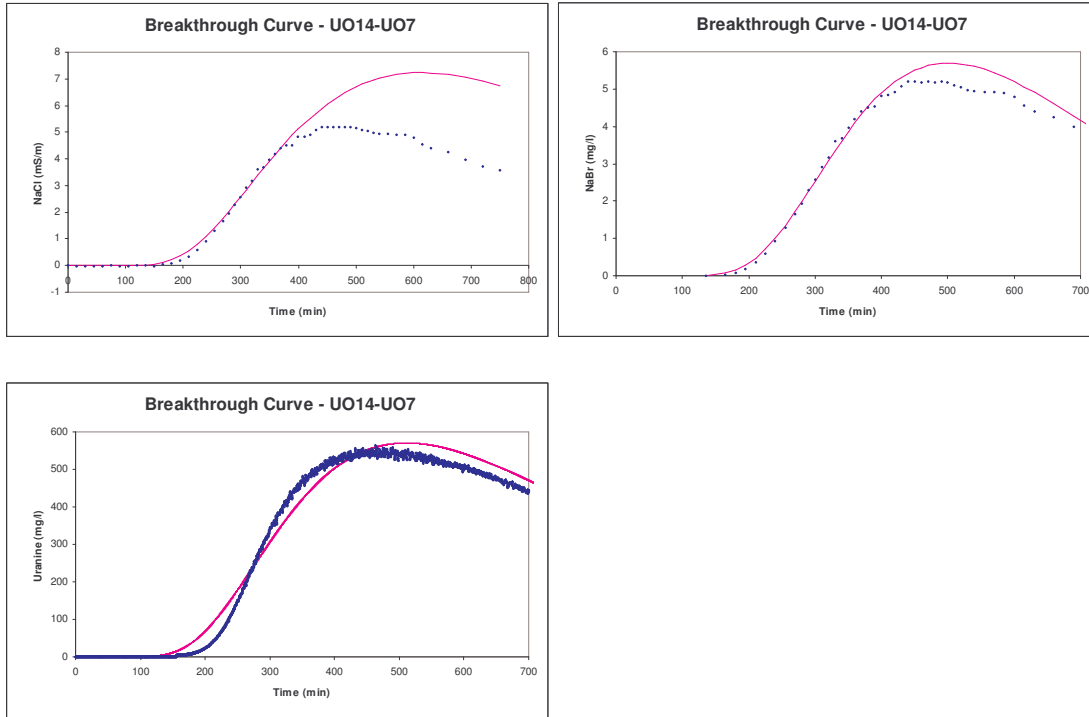


Figure 3-29 TRACER fits of the three tracers for the radial convergent test between UO14-UO7.

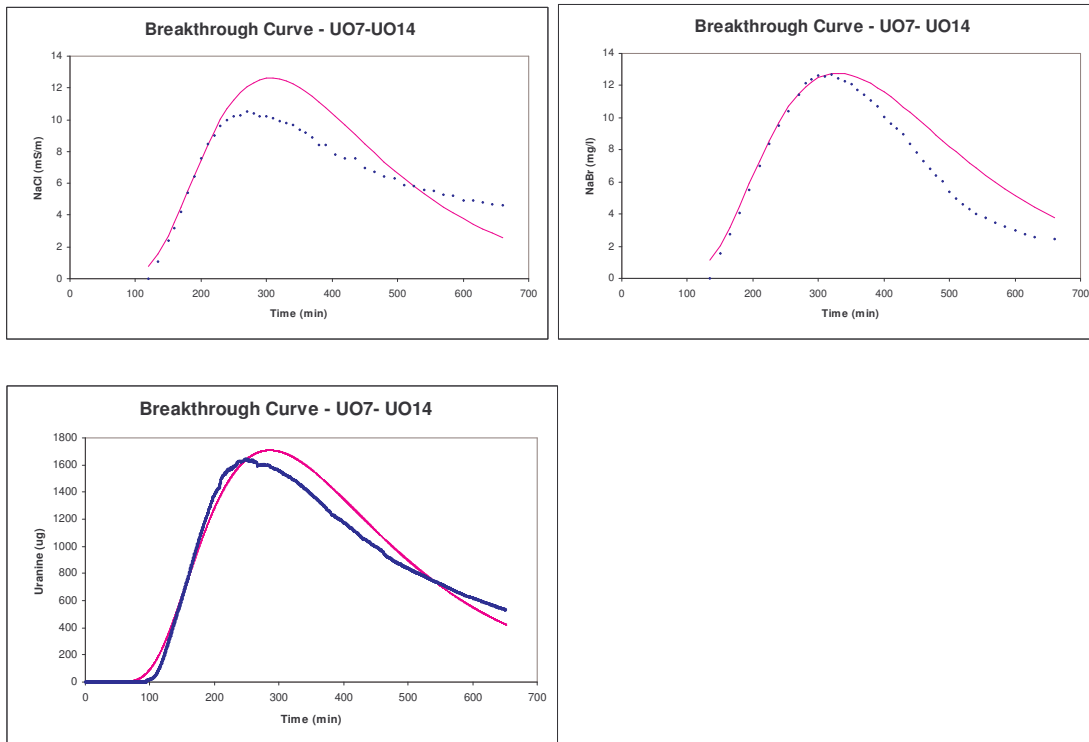


Figure 3-30 TRACER fits of the three tracers for the radial convergent test between UO14-UO7.

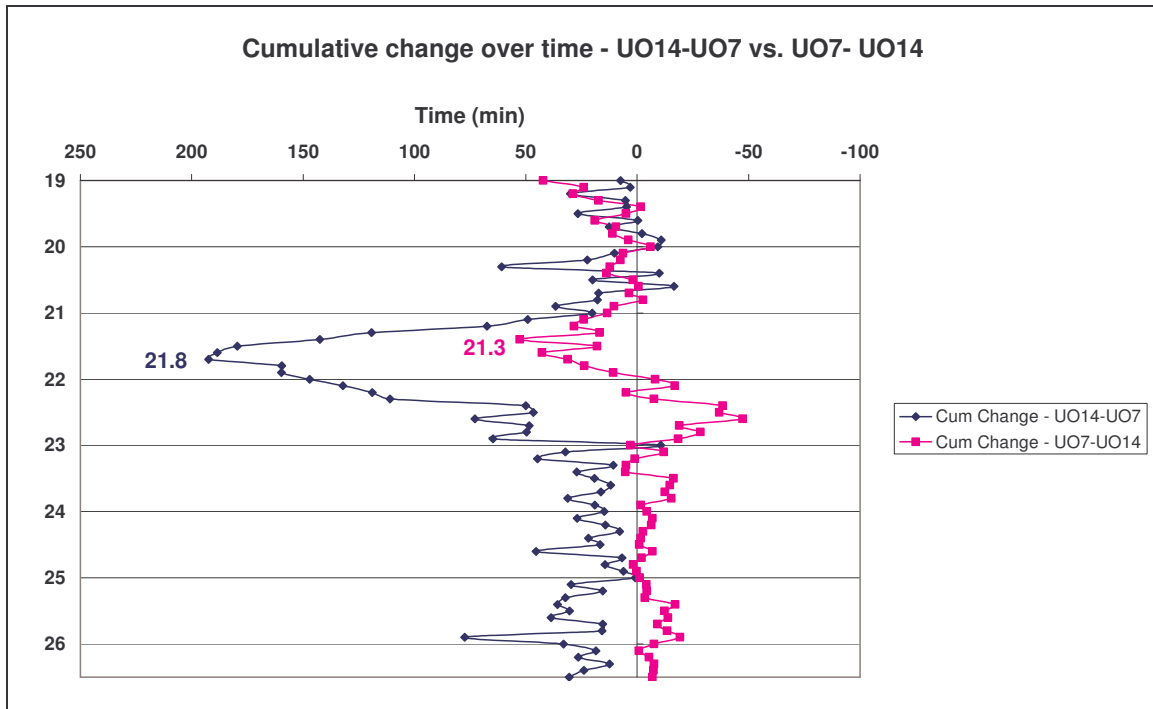


Figure 3-31 Cumulative change over time in UO20 during radial convergent tests (UO14-UO7 vs. UO7-UO14).

3.10.4 Discussion of results

The results from the radial convergent tracer tests in two directions showed that a tracer substance does not necessarily follow the same flow path when reversed. Although all three boreholes are connected with the Mode I fracture, it can be seen that the tracer solutions followed different flow paths to move from one point to another.

The assumption was that the tailing observed in the experimental data could be attributed to solute transfer from the fluid flowing into adjacent immobile zones or into the unfractured matrix. It is also known that dispersivity controls the shape of the breakthrough curve.

When comparing the results of the two tracer tests, it can be seen that much lower velocities were measured for the tracer test between UO14 and UO7 (in the direction of groundwater flow). A larger dispersivity value was also measured.

The results from EC logging in UO20 during the experiment between UO14 and UO7 showed a preferred pathway between 21.3 and 22.3 metres below surface. This causes

lower velocities and larger tracer dispersion. It can also be seen that the recoverable tracer concentrations are much lower.

3.11 CONCLUSIONS

The effectiveness of biobarrier technology relies on the successful injection and movement of bacteria through the aquifer, and in this case, movement in the fractures.

The exact positions of main fractures are thus important. Various tests were used to determine the position of the Mode I fracture in the three boreholes, namely (1) hydraulic tests (aquifer tests), (2) fracture determination tests - EC logging of boreholes, and (3) borehole camera recordings. The results from these tests are as follows:

Aquifer tests

The results from the aquifer test did not yield any significant indication of fracture positions. Only large fracture zones could be identified. The T values for all the boreholes were of the same order.

Fracture determination tests - EC logging

Fracture determination tests were conducted at small and large injection intervals. These were conducted to compare the results from the different injection areas. Not surprisingly, the results were exactly the same: the exact position of the fractures was obtained from all three boreholes. The fracture positions in UO7 and UO20 are on the same level, at respectively 22.8 and 22.7 m. The fracture in UO20 is a little higher at 21.3 m.

Radial convergent tracer tests

Tracer tests were conducted in both directions (from UO7-UO14 and from UO14 to UO7) to determine the transport of three conservative tracers through the fracture system. Unique interpretations were obtained with the use of multiple tracers, while accounting for the presence of natural flow in the fracture.

Although all three boreholes are connected with the Mode I fracture, it can be seen from the graphs that the tracer solutions followed different flow paths to move from one point to another.

UO14-UO7 (direction of groundwater flow)

The software program TRACER was used to analyse the tracer test data. From the results between UO14-UO7, it is seen that uranine has the highest transport velocity, moving at 44 m/d. The tracer with the lowest velocity was NaCl at 30 m/d. Due to its lower flow velocity, NaCl has the highest dispersion (3.1 m).

Very interesting results were obtained from EC logging in UO20. A large preferred pathway was detected between 21.3 and 22.3 metres below surface. This causes the tracers to disperse. It can also be seen that the recoverable tracer concentrations are much lower in this experiment than for the experiment between UO7-UO14. The results of these experiments show significant tailing in the shape of the breakthrough curves, which can be attributed to the shape of the flow field and large values of dispersivity.

UO7-UO14 (opposite direction of groundwater flow)

The TRACER program was used to analyse the tracer test data. From the results between UO7-UO14, the highest velocity was measured for uranine (86 m/d). In this case the NaBr was transported at the slowest velocity of 65 m/d. The highest dispersivity was measured for NaBr, at 2 m.

The results from this experiment differ completely from the tracer test between UO14-UO7. The assumption is that the tracer substance follows a preferred pathway from UO7 to UO14. Dispersion is much lower in this direction, and might be attributed to the presence of fewer dead-end pores between UO7 and UO14.

During this experiment, the preferred pathway in UO20 was much smaller.

Implications

From the field characterisation test the following was learned for the application of biobarriers in the field:

- Important hydraulic parameters were obtained from the aquifer tests and tracer tests, namely, transmissivities of the aquifer, velocities and dispersivities.
- By making use of fracture determination tests, the position of the fracture was obtained for all three boreholes. From this information, injection areas can be determined to ensure effective injection of bacteria and media into the fracture system and thus increase the effectiveness of biobarrier formation.
- By performing radial convergent tracer tests in both directions, the shortest injection time was obtained. Thus injection of bacteria will occur from UO7 to UO14.

To conclude: Although all three boreholes are connected with the Mode I fracture, the tracer solutions followed different flow paths to migrate from one point to another.

For the preparation and application of biobarrier technology in the field, the latter is very important. One cannot make assumptions about the transport characteristics of an aquifer. Very thorough site characterisation is necessary prior to the biobarrier field experiment to ensure that bacteria transport will be easy, fast and effective.

4 LABORATORY TESTING OF DIFFERENT BACTERIA FOR SUITABILITY OF BIOBARRIER PROPERTIES

The first and most important step towards efficient biobarrier application is the use of the correct bacterial species. During the course of this research, three bacterial species were tested and evaluated to determine the one with the most effective biobarrier properties. This chapter provides detailed information on the evaluation and testing of the bacteria *Raoultella planticola*, *Burkholderia vietnamensis* and *Serratia marcescens* for sustainable biobarrier formation in porous media (sand) under laboratory conditions. These tests include adhesion tests, conservative tracer and bacteria transport tests, and testing the effectiveness of the bacteria in reducing the hydraulic conductivity of porous fine and coarse sand.

The three bacteria species were chosen due to their ability to form EPS and glycocalyx and to successfully resuscitate after a starvation period.

4.1 BACTERIA TRANSPORT

Bacteria transport is of increasing interest to those involved in the remediation of contaminated subsurface environments, because adding and dispersing bacteria that can degrade or transform contaminants (bioaugmentation) is an attractive and viable remedial option (DeFlaun *et al.*, 2001).

Understanding bacterial transport in porous and fractured media is of great importance for the successful implementation of bioremediation strategies in subsurface environments (Dong *et al.*, 2002).

The aim of the bacterial transport test is to inject vegetative and starved bacteria into porous media to determine their transport characteristics. Vegetative bacteria are bacteria in their full grown size.

Bacteria transport through porous media is influenced by many parameters, including the unique properties of the bacterial cell, solution chemistry, porous media characteristics, and the physical properties of the environment (Gerlach *et al.*, 1998).

Cell properties that influence bacterial transport include surface proteins (extracellular), polysaccharides, pili, filaments, motility, chemotaxis, cell size, cell shape, surface charge, hydrophobicity, buoyant density, growth state and nutritional status (Gerlach *et al.*, 1998).

Starvation or reduction in cell size may also affect bacteria transport by reducing the effects of filtration. In the absence of filtration, a smaller bacterium may have a reduced level of interaction with the porous medium along a pore channel and therefore may be more effectively transported (Camper *et al.*, 1993).

Bacteria transport through porous media can be prevented by filtration; for example blocking bacterial movement by pores that are smaller than the bacteria. It is assumed that binding bacteria to particle surfaces also prevents movement, and that bacteria must be non-adhesive for extensive bacterial transport through porous media. Solute characteristics such as ionic strength, pH, temperature, presence of specific ions, and concentration of dissolved organic matter and presence of surfactants have also been shown to influence bacterial attachment to surfaces (Gerlach *et al.*, 1998).

Porous media properties such as mineralogy, organic matter and clay content, grain and pore size distribution, surface charge, and surface roughness can also influence bacterial attachment to surfaces (Gerlach *et al.*, 1998).

4.2 PREPARATION OF INOCULUM FOR BACTERIUM RAOULTELLA PLANTICOLA

R. planticola (DSM 4617) (Bagley *et al.*, 1981) was obtained from the Deutsche Sammlung von Microorganismen und Zellkulturen (DSMZ), as supplied by BHP Billiton.

R. planticola (DSM 4617) is also called *klebsiella planticola*, or *klebsiella trevisanii*.

R. planticola represents the general characteristics of the family Enterobacteria.

The bacterium was cultivated by the Department of Microbiology, Biotechnology and Food Biotechnology at the University of the Free State in South Africa.

A pre-inoculum of *R. planticola* was prepared with a loopful of culture from nutrient agar plates into 25 ml medium in a 250 ml Erlenmeyer flask and incubated at 30°C for 12h

before inoculation into the inoculum flask. The pre-inoculum of *R. planticola* was transferred to 200 ml inoculum medium in a 1000 ml Erlenmeyer flask and was incubated at 30°C for 8h. The inoculum medium contained (per litre): 10 g glucose, 1g citric acid, 0.25g MgSO₄·7H₂O, 0.01g CaCl₂·2H₂O, 10g K₂HPO₄; and 1 ml trace elements solution ; adjusted to pH 7.4.

The minimum temperature for growth of *R. planticola* is 11°C, with an optimum of 35°C and a maximum of 46°C. *R. planticola* is, therefore, a mesophile (organism living in the temperature range close to that of warm-blooded animals, and usually showing a growth temperature optimum between 25 and 40°C).

4.3 CULTIVATION OF RAOULTELLA PLANTICOLA

The medium used for cultivation was prepared by the Department of Microbiology, Biotechnology and Food Biotechnology. The medium, under nitrogen limitation, comprised (per litre): 10 g glucose, 1g citric acid, 0.25g MgSO₄·7H₂O, 0.01g CaCl₂·2H₂O, 10g K₂HPO₄; and 1 ml trace elements solution ; adjusted to pH 7.4.

Batch cultivations (closed-system bacterial culture of fixed volume) were performed by the Department of Microbiology, Biotechnology and Food Biotechnology. This was done in a 15 l Braun Biostat C bioreactor with 10l working volume. Chemostat cultures (continuous culture controlled by the concentration of limiting nutrient and dilution rate) were grown in a 2 l Multigen Model F-2000 bioreactor (New Brunswick Scientific Co., New Jersey) with an 800 ml working volume. Cells were grown at a control pH of 6.8 at 30°C, with varying agitation rates, maintaining the dissolved oxygen level (DO) above 30%.

4.4 ANALYSES

4.4.1 Optical density

Optical density (OD) was measured with a spectrophotometer at a wavelength of 690 nm. OD can be used to estimate cell concentrations. The OD values were read against a blank before inoculation. When dilutions were made, the blank tube reading was subtracted and the dilution factor taken into account when calculating the OD reading.

4.5 GROWTH CONDITIONS

According to the literature, *R. planticola* is a facultative aerobe (an organism that is able to grow in either the presence or absence of oxygen). This is because of the fact that it is a nitrifying bacterium (microbiological conversion of ammonia to nitrate).

During the tests at the Department of Microbiology, Biotechnology and Food Biotechnology, different kinds of electron acceptors and donors were used to determine whether the bacteria can survive anaerobically.

In anaerobic conditions, the results showed that the bacteria preferentially use glucose as the electron donor and NO_3^- as the electron acceptor.

4.6 ADHESION ABILITY OF BACTERIUM

Adhesion tests were performed on *R. planticola* (DSM 4617), to reveal the capacity of the cells to adhere to surfaces over a specific time period. The purpose of these tests was to give an indication of the retention properties of the cells.

Factors that may influence the attraction of the cell surface to the mineral surface include the electrostatic charge on each, and the chemical composition of the conducting fluid, as some balance of attractive and repulsive forces is achieved (Mills *et al.*, 1994).

Mills *et al.* (1994) demonstrated in the laboratory that increasing the ionic strength of the aqueous solution can also increase the extent of bacteria sorption to a variety of natural and artificial surfaces, as well as enhancing retention in sand columns during transport experiments.

4.6.1 Adhesion assay methodology

The ability for vegetative bacteria to adhere to fine sand was tested. Adhesion assay was performed as described in the protocol given by DeFlaun during a visit to the University of the Free State in July 2004 (DeFlaun *et al.*, 1998). Tests were performed as follows:

1. A 20 ml syringe was filled with 20 g of sand. The tip of the syringe was plugged with a small bit of glass wool. A piece of tubing was placed over the tip of the syringe and clamped off to prevent liquid from leaking.

2. Cells were prepared and suspended into artificial groundwater (AGW). Artificial groundwater is distilled water with different minerals added to represent groundwater. The composition of the artificial groundwater is as follows: (per litre of distilled water) 60mg $\text{MgSO}_4 \cdot 7\text{H}_2\text{O}$, 20mg KNO_3 , 36mg NaHCO_3 , 36mg CaCl_2 , 35mg $\text{Ca}(\text{NO}_3)_2$, 25mg $\text{CaSO}_4 \cdot 2\text{H}_2\text{O}$, 28mg NaH_2PO_4 , and 0.35 ml 1.0 N HCl, (pH 5.99) (DeFlaun *et al.*, 1998). For preparation of the artificial groundwater, the distilled water was autoclaved (sterilised) (refer to section 4.6.2.1 for description of autoclave/sterilisation process). The mineral solutions were prepared and aseptically (filter sterilised) introduced into the distilled water.
3. 3 ml of the culture was added to the syringe and covered with parafilm. The syringe was left to stand for 2 hours.
4. After 2 hours, the clamp was released and the effluent allowed to flow into a sterile tube.
5. Cell counting was done on the original culture added as well as the effluent to determine the percentage adhesion of the bacteria.

4.6.2 Results

The results showed that the vegetative bacteria have an adhesion of 85%.

From the results of the adhesion assay, it can be concluded that the vegetative bacteria have good adhesion properties, with the ability to adhere to the soil surface.

4.6.2.1 Autoclave/sterilisation process

Solutions (distilled water) and glassware must be sterilised in an autoclave at 121°C. Autoclave sterilisation time works as follows: For solutions: 15 minutes for the first litre and then 5 minutes for every additional litre. For sterilisation of glassware it will take 20 minutes.

4.7 TRACER TRANSPORT IN POROUS MEDIA

Conservative tracer transport tests and bacterial transport tests were performed in laboratory-scale test columns.

4.8 POROUS MEDIA COLUMN EXPERIMENT

4.8.1 Test column design

Test columns were designed to evaluate the movement of a conservative tracer and the bacteria *R. planticola* through fine and coarse sand.

Test columns were constructed from perspex. The column consists of three pieces: a base with four inlet pipes, the centre part consisting of a cylinder (27 cm long and a diameter of 7 cm) and the top part consisting of two outlet pipes. Connected to the bottom piece are four steel rods to support the column. The centre part of the column fits in-between the rods. The apparatus is assembled, secured together with four nuts and bolts. See Figure 4-1 for a photo of the test column.

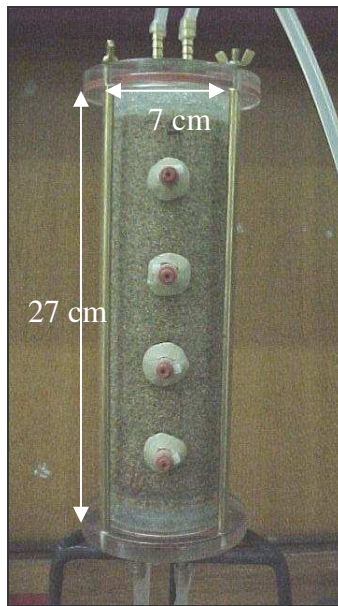


Figure 4-1 Schematic of the test column with dimensions.

Each column was fitted with four sample ports, spaced linearly along the column at distances of 5.6, 11.2, 16.8 and 22.4 cm from the column inlet. A sampling port consists of a syringe needle sunk into the column. Each needle is sealed with a septum to prevent fluids from draining. The purpose of the side sampling ports is to allow withdrawal of fluid samples to monitor the concentration and distribution of cells and tracer at each port and through the column. See Figure 4-2 for picture of sampling ports and methods.



Figure 4-2 Sampling ports.

4.8.2 Packing materials

Three types of packing materials were used for the test columns, namely glass beads, fine sand and coarse sand. The sand was supplied by BHP Billiton. The columns were packed as described in the following sections.

4.8.2.1 Packing of fine sand columns

Three differently sized packing materials were used for the fine sand column.

- Glass beads with a mesh size of approximately 2mm were placed at the bottom of the column (2 cm). Coarse sand with a mesh size between 1200 and 1500 μ m was placed on the glass beads (2 cm). The rest of the column was then packed with fine sand with a mesh size between 500 and 850 μ m. The last 2 cm of the column was packed with glass beads. The reason for the different layers is to ensure consistent and uniform infiltration and flow through the column. See Figure 4-3 for photo of packing material.

4.8.2.2 Packing of coarse sand columns

Two differently sized packing materials were used for the coarse sand column.

- Glass beads with a mesh size of approximately 2 mm were placed at the bottom of the column (2 cm). The rest of the column was filled with coarse sand (between 1200 and 1500 μ m), with the exception of the last 2 cm, which was filled with glass beads. See Figure 4-3 for photo of packing material.



Figure 4-3 Packing material - fine sand, coarse sand, and glass beads.

4.8.3 Determination of the hydraulic conductivity of the fine and coarse sand

The hydraulic conductivity of the fine and coarse sand was determined with a Darcy apparatus. See Figure 4-4 for the set-up of Darcy apparatus. The experiment was conducted as follows: Water was injected into the inlet side of the Darcy apparatus. A constant head was supplied at the inflow side by making use of a peristaltic pump connected to a water container. The flow at the outflow side was measured every 1 minute to determine the average flow rate (Q).

The hydraulic conductivity of the sands was calculated with the Darcy equation:

$$K = Q/A (dh/dl) \quad (\text{Equation 4.1})$$

Where:

Q = flow-rate,

A = cross-sectional area of the column, and

(dh/dl) = piezometric gradient.

A hydraulic conductivity of $230 \text{ m}^3/\text{d}$ was calculated for the fine sand, and a hydraulic conductivity of $350 \text{ m}^3/\text{d}$ for the coarse sand.

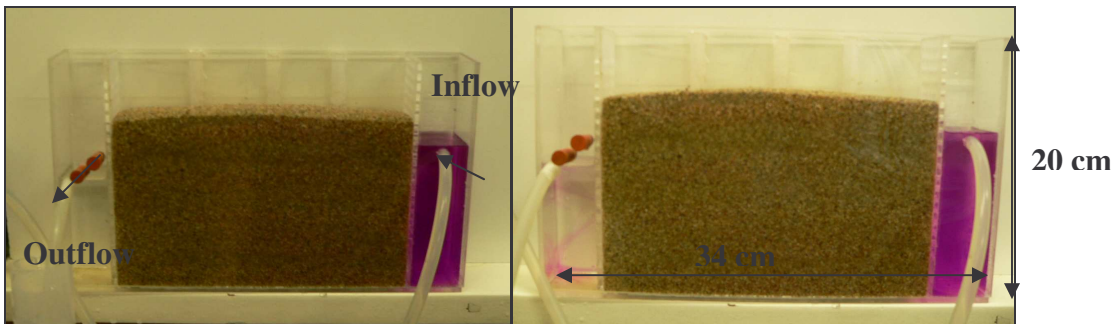
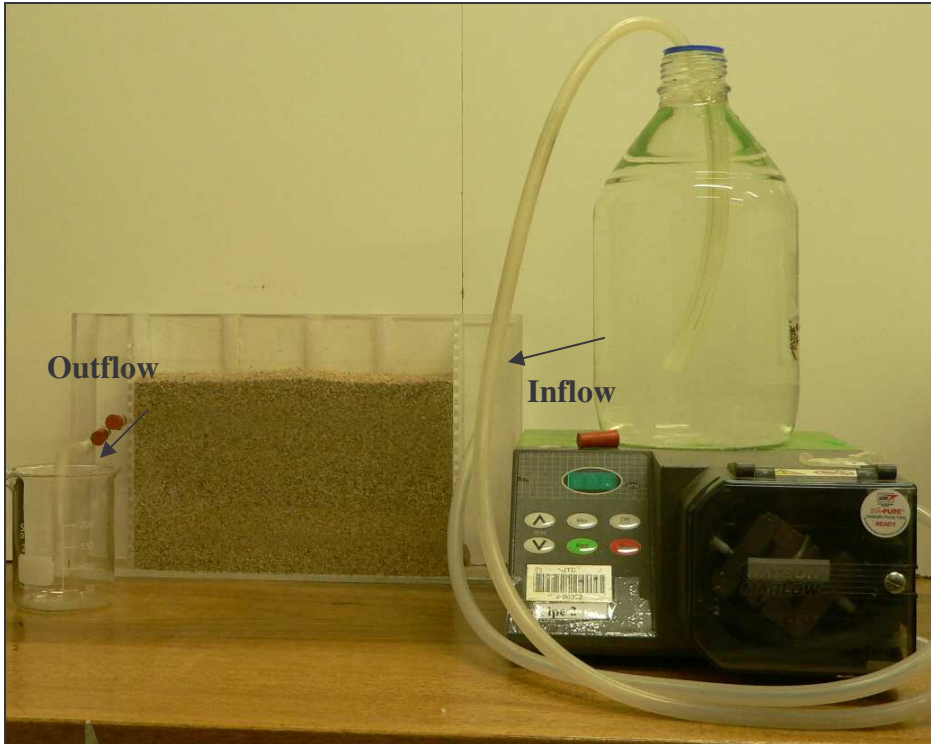


Figure 4-4 Set-up of the Darcy apparatus - calculation of the hydraulic conductivity of the fine and coarse sand.

4.8.4 Pore volume determination

The pore volume of the columns packed with fine and coarse sand was determined as follows: Columns were packed as described in sections 4.8.2.1 and 4.8.2.2. Columns were sealed at the bottom. The top was left open. Water was poured into the columns until the sand was saturated. A pore volume of 350 ml and 370 ml was measured for the fine and coarse sand columns, respectively.

4.8.5 Porosity determination (Total porosity)

The porosity of the fine and coarse sand was calculated with the use of a graduated measuring cylinder and sand. The sand was poured into the cylinder to a certain volume. The same volume of water was then used to determine the saturation volume of the sand. The porosities of both sands are in the order of 30%, respectively 0.33 and 0.36.

4.8.6 Set-up and operation of the columns

Flow rates were determined using a graduated cylinder and stopwatch. Artificial groundwater (refer to section 4.6.1) was injected into the measuring cylinder at the top (level in the cylinder was kept constant). The water flows into the column through four inlets at the bottom and via two outlets at the top. The outflow volume was measured every 2 minutes. See Figure 4-5 for the set-up of the columns.

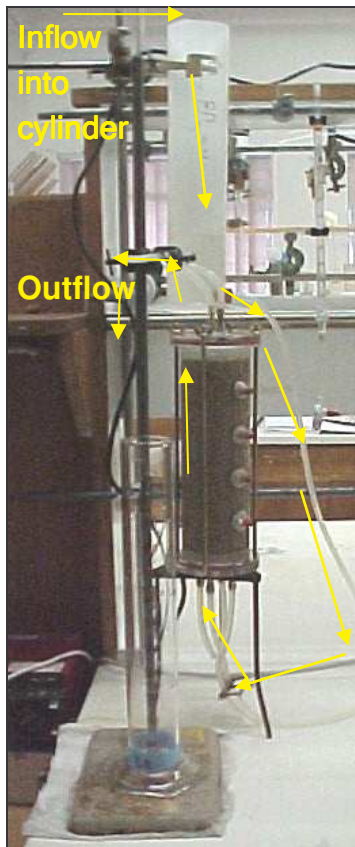


Figure 4-5 Set-up of the columns.

4.9 LABORATORY TRACER TESTS

Transport tests were performed to evaluate the movement and dispersion of a conservative tracer as well as bacterial transport in laboratory-scale test columns. With the use of a conservative tracer solution (NaCl), the movement and dispersion was measured through fine and coarse sand columns. The concentration versus time relation of the column outflow, known as the breakthrough curve, was determined.

The columns were prepared for tracer tests by flushing with two pore-volumes (PV) of sterilised artificial groundwater.

Artificial groundwater was used for the following reasons:

- To test if bacteria will grow in groundwater conditions.
- The use of groundwater is important for upscaling to aquifer conditions.
- The groundwater could be prepared and sterilised (autoclave) to eliminate any foreign bacteria growth.

4.9.1 Tracer test methodology

Artificial groundwater was used in the columns to saturate the sand by using a peristaltic pump.

When the columns were saturated, the NaCl tracer solution was pumped into the columns at a constant rate of 2 ml/min (120 ml/hour). The injection rate was the same for both columns; thus flow (Q) is constant.

One hundred millilitres of the NaCl tracer was injected into the columns. After the injection of the tracer solution, artificial groundwater was added to the system, thereby allowing the tracer to pass through the packing material. The electrical conductivity (EC) of the tracer solution was measured with an EC-meter at the outlet side of the column. Because of the injection of the tracer solution and advective and dispersive mass transport, a tracer breakthrough curve was observed from the EC measurements.

The concentration decrease was measured until it reached the initial background value, or until the concentration levelled out at a lower value. See Figure 4-6 for experimental set-up.

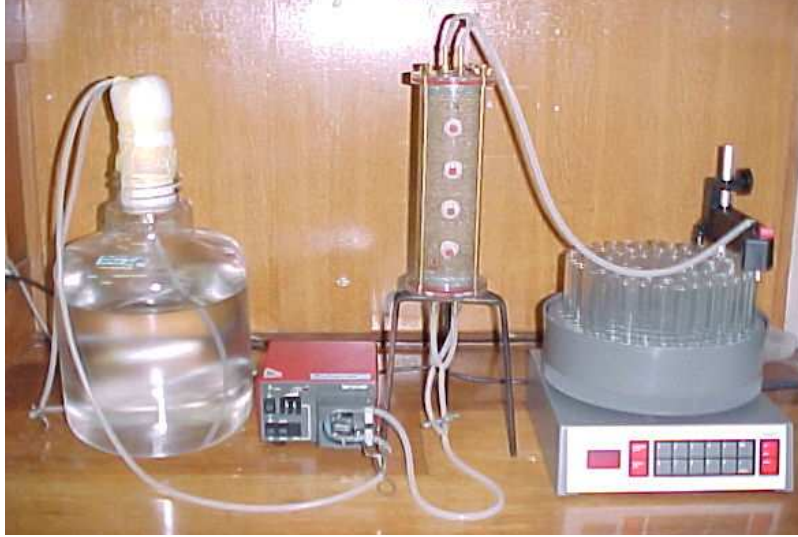


Figure 4-6 Tracer and bacteria test set-up.

4.9.2 Tracer test interpretation and results

During conservative tracer transport tests, the invading solute-containing water does not travel at the same velocity, and mixing occurs along the flow path. Due to mechanical dispersion and molecular diffusion, the breakthrough curve (conservative tracer) spreads out, causing the tracer to appear in the outflow of the column. This results in a dilution of the solute at the advancing edge of flow.

The results measured as concentration versus time data were converted to C/C_0 versus pore volume. The relative concentration (C/C_0) refers to the concentrations measured (C) divided by the original concentration injected (C_0).

For the coarse sand column (Figure 4-9), it can be seen that the leading edge of the tracer front passes through the system after 0.7 of a pore volume. After 1 pore volume, (370 ml) the tracer solution reaches a peak and decreases over time. The system reverts to pre-tracer levels after 2.5 pore volumes.

From Figure 4-8 (fine sand column), it can be seen that the leading edge of the tracer plume exited the system after 0.7 of a pore volume. After 1 pore volume (350 ml), the tracer plume reaches a peak and decreases over time. The tracer has been flushed after 1.8 pore volumes.

The data for the conservative tracer breakthrough through porous media, were analysed by a software program called PULSE. The equation for one-dimensional flow can be simulated by the tracer equation:

$$c(x,t) = \frac{M}{4\pi D \varepsilon \sqrt{D_L t}} \exp\left[-\frac{(x-vt)^2}{4D_L t}\right] \quad (\text{Equation 4.2})$$

with:

- M = injected mass of tracer (kg)
- D = aquifer thickness (or effective thickness of fracture zone)
- D_L = longitudinal dispersion coefficient (m^2/s); $D_L = \alpha_L v$
- v = groundwater velocity under natural gradient (m/s)
- ε = kinematic porosity
- x = distance (m) between the column inlet and outlet in x-direction (direction of groundwater flow)

The function of this program was to determine transport parameters from tracer tests in porous media.

See Figure 4-7 for the breakthrough curves fitted by the PULSE program. Velocities and dispersivities were calculated for both the fine and coarse sand.

From the results of the breakthrough curves, the following can be seen:

The fine sand had a velocity of 11.31 m/d and the coarse sand 10.8 m/d. Due to the lower velocity of the coarse sand, dispersivity is higher. Higher dispersivity in the medium causes increased mixing of the solute front as it advances.

The results were surprising. According to the theory, the velocity should be higher in the medium with the higher K-value (refer to section 4.8.3 for K-values of the fine and coarse sand). Darcy's equation was used to determine a solution.

From the equation of velocity calculations, the following can be assumed:

$$Q = KIA \quad (\text{Equation 4.3})$$

$$Q = K_{(coarse)} * A * I_{(coarse)} = K_{(fine)} * A * I_{(fine)} \quad \text{(Equation 4.4)}$$

$$Q = I_{(fine)} / I_{(coarse)} = K_{(Coarse)} / K_{(fine)} \quad \text{(Equation 4.5)}$$

Where:

- Q = Volume rate of flow
- K = hydraulic conductivity
- i = hydraulic head

A = Cross-sectional area normal to flow direction

The results showed that since the flow rate was kept constant, the gradient was 1.5 times higher in the fine sand than in the coarse sand, and thus the tracer flows faster in the fine sand.

See Table 4-1 for the velocities and dispersivities of the fine and coarse sand.

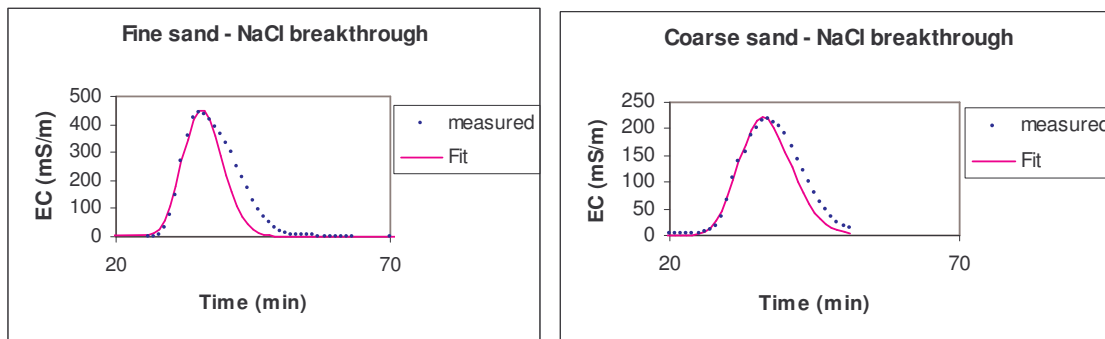


Figure 4-7 Conservative breakthrough curve fit with the PULSE software.

Table 4-1 Results from the fine and coarse sand - PULSE calculations for the velocity and dispersivity of the sand.

Column study	Velocity (m/d)	Dispersivity (m)
Coarse sand	10.8	0.0033
Fine sand	11.31	0.0014

4.9.3 Bacteria transport test

The movement of bacteria is of interest in groundwater for the following reasons (Kinoshita *et al.*, 1993):

- The subsurface migration of bacteria is an important determinant of subsurface ecology.
- Introduction of mobile bacteria or enzymes into contaminated aquifers is a potential *in-situ* clean-up strategy.
- Bacteria can contribute to aquifer clogging.
- Bacterial pollution of drinking water boreholes is a potential public health problem.

Bacteria transport tests were performed to test the movement of the bacteria species

R. planticola through test columns packed with respectively fine and coarse sand.

The bacterial transport test was performed on the same principle as the tracer test. Starved bacteria are produced when cells are suspended into a starvation solution, which results in changes in bacterial morphology and physiology, with significantly less exopolysaccharides that bacteria excrete to adhere to solid surfaces and trap nutrients. Vegetative bacteria are bacteria in their fully grown stage.

Optical density (OD) measurements were used to estimate the cell concentrations or mass in each fraction. Optical density can be measured with a spectrophotometer and readings are recorded in photometer units. Graphs were then plotted as C/C_0 versus pore volume, where C/C_0 is the total number of cells measured in optical density in a sample divided by the total number of cells (measured in OD) in the inoculum.

Two types of bacteria transport tests were performed on both the fine and coarse sand columns. The concentration and volumes are as follows:

- 10^8 vegetative bacteria cells/ml (grown in shake flasks) were suspended in 100 ml artificial groundwater.
- 10^8 starved bacteria cells/ml (batch culture) were suspended in 100 ml artificial groundwater.

See Figure 4-8 and Figure 4-9 for bacteria C/C_0 vs. pore volume graphs for the fine and coarse sand columns.

4.9.4 Bacteria transport data interpretation

4.9.4.1 Fine sand column

By making use of 100 ml vegetative bacteria, the following can be seen (see Figure 4-8 - vegetative bacteria (green line)):

- The vegetative bacteria start to exit the system after 0.69 pore volumes. After 1.17 pore volume, the bacteria concentration reaches a peak and decreases over time. The tracer is flushed after 1.9 pore volumes. Retardation relative to the conservative tracer is evident. It is possible that a percentage of the bacteria adhered to the bottom of the column and will remain there because of their vegetative state, and because only a 100 ml pulse of bacteria was injected into the column. If a continuous source is used, the bacteria will be forced through the column.

With the use of 100 ml starved bacteria, the following can be seen (see Figure 4-8 - starved bacteria (red line)):

- The leading edge of the bacteria front passes through the system after 0.72 pore volumes. After 1.06 pore volume, a peak is reached, which decreases over time. The system reverts to pre-tracer levels after 1.4 pore volumes.

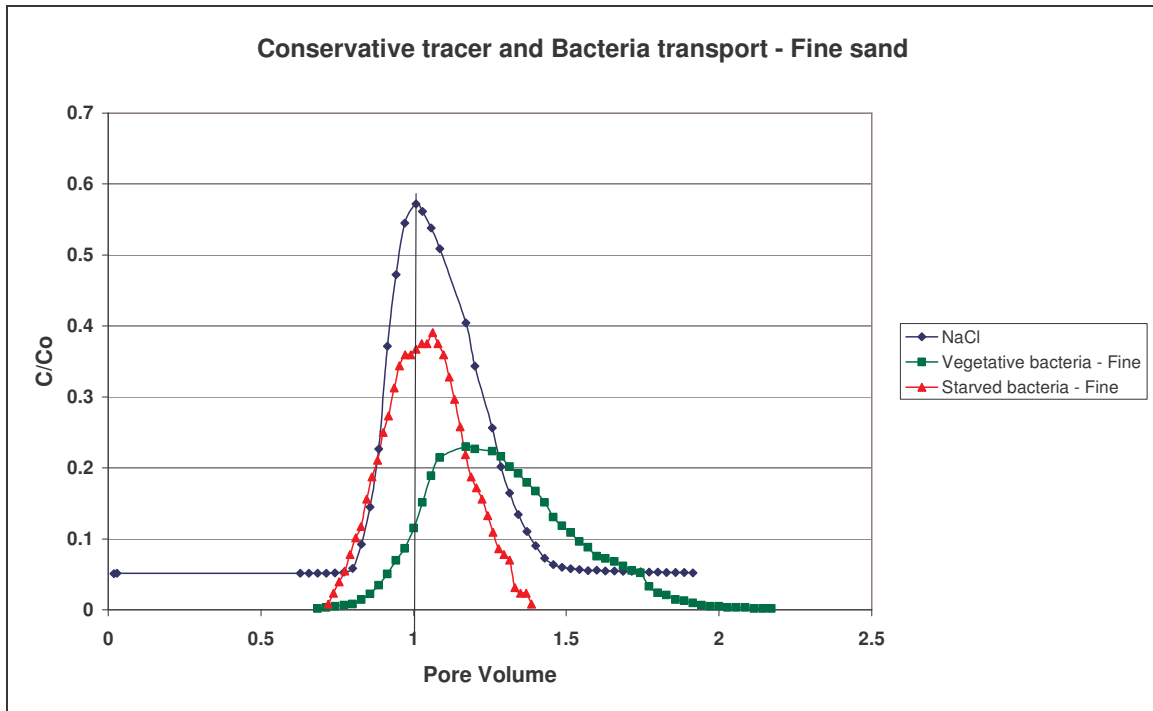


Figure 4-8 Tracer (EC) and bacteria test (OD) results - fine sand. C/C_0 vs. pore volume.

4.9.4.2 Coarse sand column

With the use of 100 ml vegetative bacteria, the following can be seen (see Figure 4-9 - vegetative bacteria):

- The leading edge of the bacteria front passes through the system after 0.645 pore volumes. After 1.05 pore volume, a peak is reached, which decreased over time. The system reverts to pre-tracer levels after 1.49 pore volumes.

With the use of 100 ml starved cells, the following can be seen (see Figure 4-9 - starved bacteria):

- The starved cells start to exit the system after 0.65 pore volumes. After 1.050 pore volumes, the bacteria solution reaches a peak and decreases over time. The tracer is flushed after 2 pore volumes. A retardation phase can be seen after 1 pore volumes is reached.

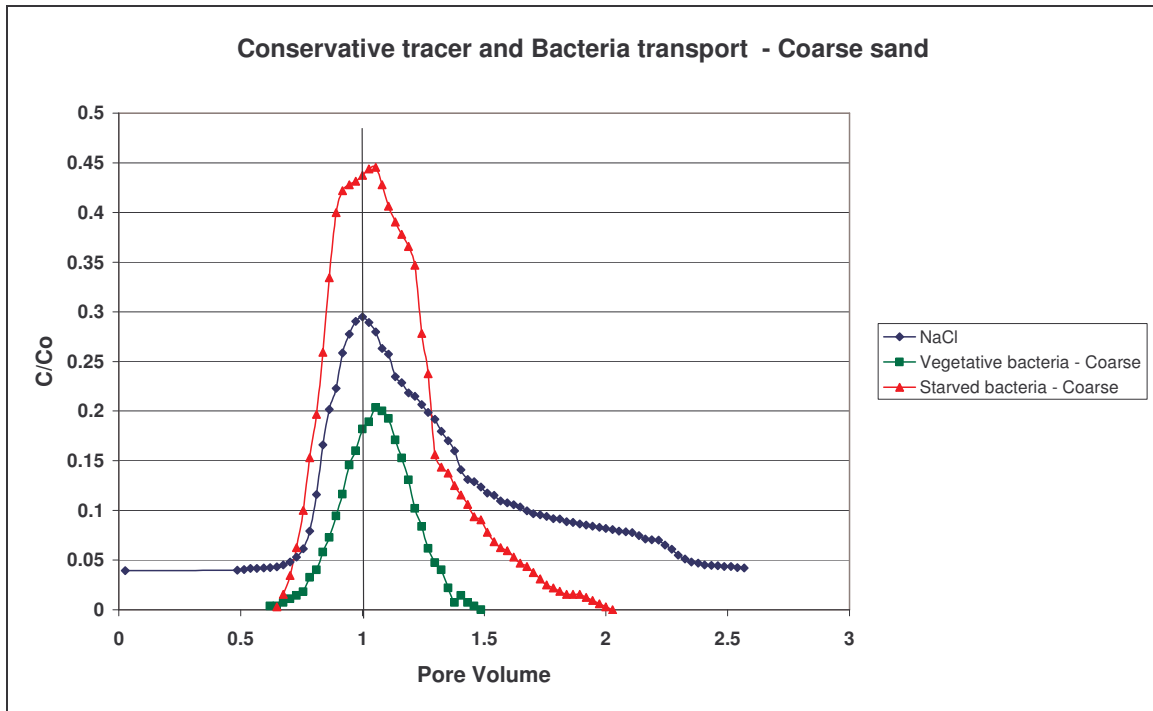


Figure 4-9 Tracer (EC) and bacteria test (OD) results - Coarse sand. C/C_0 vs. pore volume.

4.9.5 Bacteria transport results and discussion

The purpose of the breakthrough studies was to determine how bacteria size will affect the breakthrough of bacteria under the same flow rate conditions in fine and coarse sand. Although there were slight differences, all bacteria had similar average breakthrough curves, except for the breakthrough of the vegetative bacteria in the fine sand.

The data were also plotted using the PULSE software to determine velocity and dispersivity

The results of the conservative tracer and bacteria transport for the fine and coarse sand can be seen in Table 4-2. See also Figure 4-10 and Figure 4-11 for curve fitting with PULSE to determine the transport parameters.

In the fine sand column, the conservative tracer has the highest velocity and the lowest dispersion in the column. For the vegetative bacteria transport, it can be seen from the graph as well as from the PULSE calculations that the velocity of the vegetative bacteria

transport is much lower compared to the conservative tracer and transport of the starved bacteria. Due to the fact that bacteria cannot dissolve, diffusion cannot take place, and thus does not have an effect on the dispersion of the bacteria. Due to good adhesion properties as well as filtration of the bacteria in fine sand, some retardation can be seen during the transport of vegetative cells in fine sand.

From the transport through coarse sand, it can be seen that the velocities are generally lower than that of the fine sand. This can be attributed to a higher hydraulic gradient used which, causing the velocities to be slower.

In the coarse sand, the highest dispersivity was measured for the vegetative bacteria.

From the results of bacteria transport in fine and coarse sand, it can be concluded that bacteria size and particle size of the transport medium (sand) has an influence on the transport of bacteria. The transport of starved bacteria is effective in both fine and coarse sand, as well as vegetative bacteria transport in coarse sand. However, the transport of vegetative bacteria in fine sand is not very effective. Bacteria adhere to the sand near the inlet of the column and at low flow rates, disperse throughout the column.

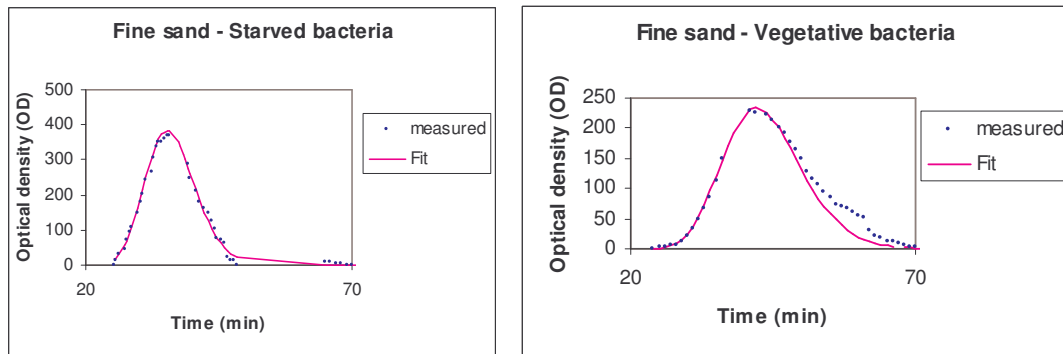


Figure 4-10 Curve fit with the use of PULSE to determine transport parameters for the fine sand.

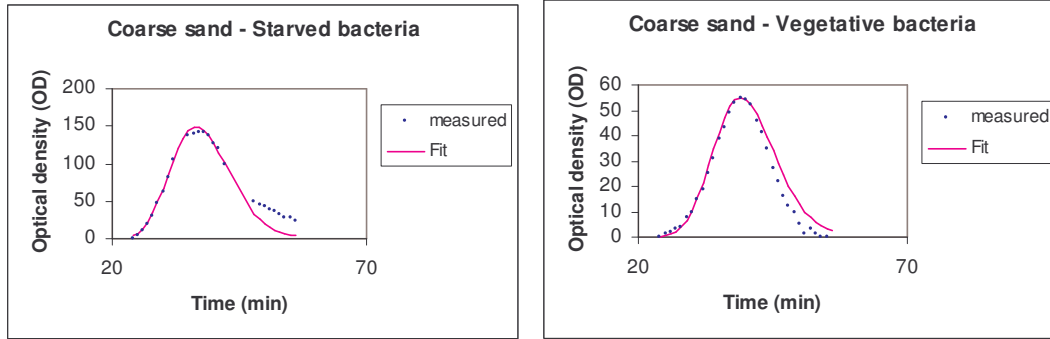


Figure 4-11 Curve fit with the use of PULSE to determine transport parameters for the coarse sand.

Table 4-2 Results of the bacteria transport in the fine and coarse sand - PULSE calculations for the velocity and dispersivity of the sand.

Fine sand		
Tracer	Velocity (m/d)	Dispersivity (m)
NaCl	11.31	0.0014
Vegetative bacteria	9.46	0.0036
Starved bacteria	11.32	0.0022

Coarse sand		
Tracer	Velocity (m/d)	Dispersivity (m)
NaCl	10.8	0.0033
Vegetative bacteria	10.22	0.0025
Starved bacteria	10.89	0.0024

4.10 IN-SITU REDUCTION OF SATURATED HYDRAULIC CONDUCTIVITY (BACTERIA CLOGGING)

4.10.1 Hydraulic conductivity (K) reduction test

Fine and coarse sand columns were used to determine the potential reduction in hydraulic conductivity that could be obtained in one-dimensional columns under controlled conditions. 10^8 cells/ml were suspended in artificial groundwater and injected into the columns.

Samples were taken at each port after every half pore volume. Optical densities were measured to monitor the bacteria distribution in the column. Bacteria injection stopped when an even distribution of bacteria was measured.

After injection, the columns were left to stand for two hours, giving the bacteria time to adhere, and then 1 pore volume of nutrient media was injected.

A constant head test was done every second day to determine the decrease in the hydraulic conductivity of the column. The reduction and % reduction in hydraulic conductivity for the fine and coarse sand is relative to the K-values measured in section 4.8.3.

4.10.2 Hydraulic conductivity (K) reduction test results

4.10.2.1 Fine sand column

After five days, a 54.3% reduction in hydraulic conductivity was measured after 1 pore volume of media flown through the column (Figure 4-9). Between the 10th and the 26th day of the experiment, the reduction in hydraulic conductivity varied between 80 and 100% after 1 pore volume.

On the 17th and the 26th day of the experiment, a 100% decrease in the hydraulic conductivity was measured. (A higher % reduction in the hydraulic conductivity means more effective clogging of the sand). On the 17th day, the column was clogged for over 25 hours (no flow for 25 hours).

Over the course of 30 days, an average reduction of 69% was measured in the hydraulic conductivity after 1 pore volume of media flowing through the column.

See Figure 4-12 for a detailed graph on the reduction of the hydraulic conductivity over time. The results from the fine sand column show that it is possible to decrease the hydraulic conductivity of the fine sand as well as clog the sand.

The increase in hydraulic conductivity with time is attributed to the fact that bacteria are flushing out of the column. The result is that a more adhesive bacteria will be needed to ensure that they are not flushed out of the column or aquifer, as the biobarrier will then not be effective.

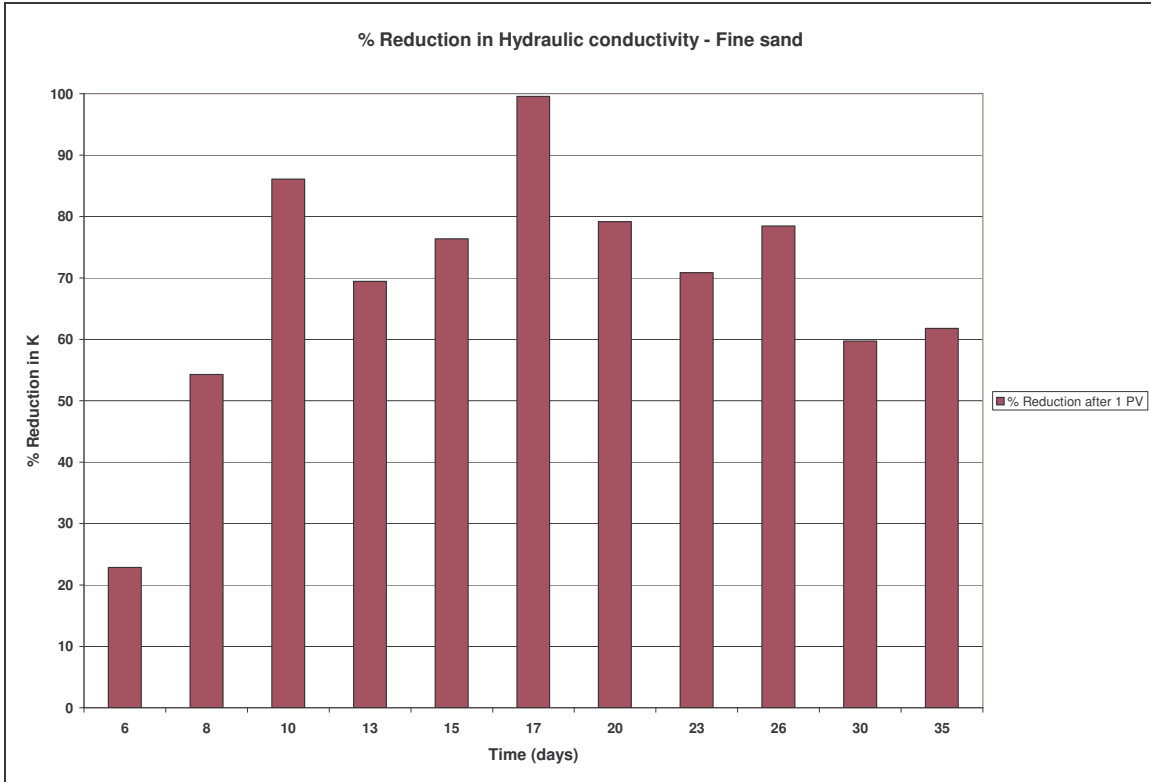


Figure 4-12 Percentage reduction in hydraulic conductivity for the fine sand column.

4.10.2.2 Coarse sand column

From Figure 4-13, it can be seen that the hydraulic conductivity reduced very slowly over time in the coarse sand column and that the reduction is not consistent.

In Figure 4-13, the following trends can be seen. During the first eight days, an average reduction of 30% was measured in the hydraulic conductivity after 1 pore volume of nutrient media has flown through the column. Between the 10th and the 17th day, the reduction in hydraulic conductivity varied. Over the last five sampling dates, the decrease in hydraulic conductivity was very similar. A reduction in the hydraulic conductivity of between 46 and 54% was measured after 1 pore volume. These sudden higher reduction rates be attributed to the fact that the bacteria were left for longer periods before nutrient media were added. Over the course of 35 days, a hydraulic conductivity decrease of 36% was measured. Results from the coarse sand column show that it is possible to decrease the K of coarse sand.

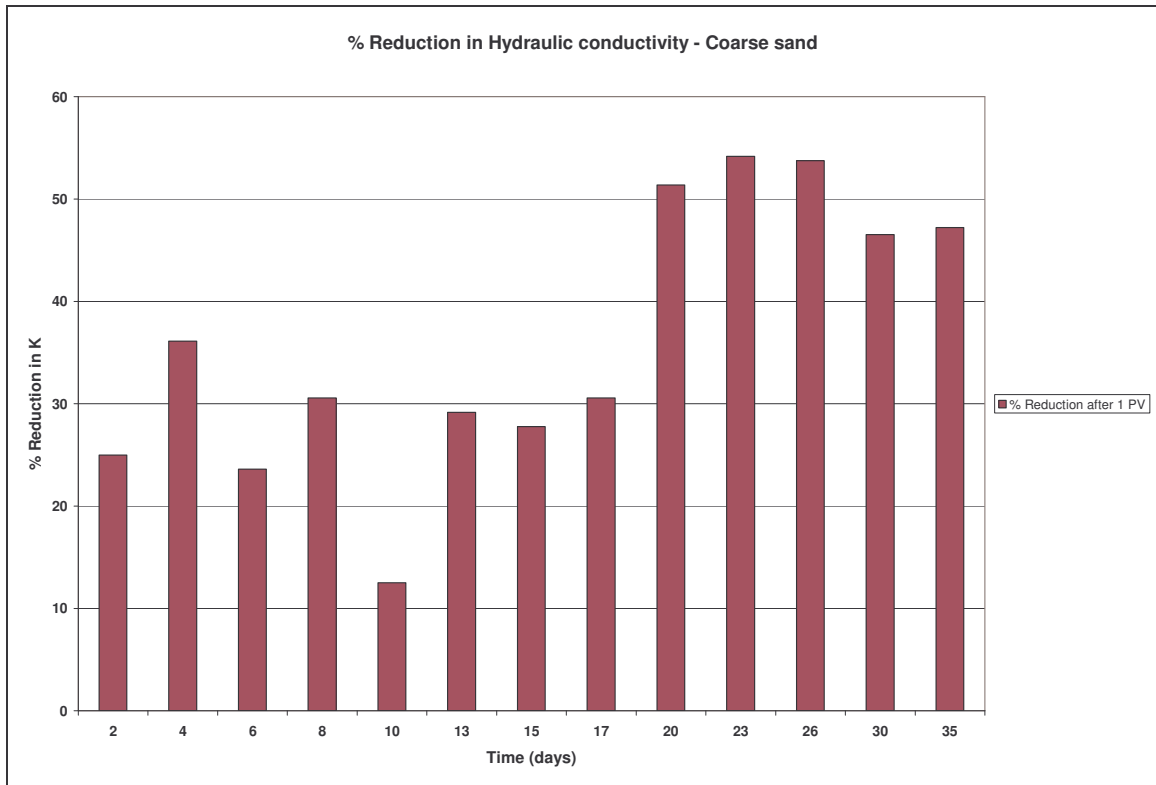


Figure 4-13 Percentage reduction in hydraulic conductivity for the coarse sand column.

4.11 CONCLUSIONS

Conservative tracer transport

The results of conservative tracer transport tests show that the tracer solute does not travel at the same velocity in the column and thus mixing occurs along the flow path. Due to mechanical dispersion and molecular diffusion, a breakthrough curve develops, causing the tracer to appear in the outflow of the column. The fine sand has a high velocity and less dispersion was observed. A lower flow velocity was measured in the coarse sand. Due to the lower velocity of the coarse sand, advection becomes the dominant contributor to the dispersion.

It was also determined that porosity has an influence on the velocity of a tracer. A higher velocity (lower porosity), was measured for the fine sand.

Bacteria transport

The bacteria transport test results show that the velocity of the vegetative bacteria are slightly lower, (especially for coarse sand) compared to the conservative tracer transport and the transport of the starved bacteria. Due to the good adhesion properties of the bacteria in fine sand, retardation can be seen during vegetative transport in fine sand.

From the results of the transport through coarse sand, it can be seen that the velocities are mainly lower than those of the fine sand. This can be attributed to retardation, due to adhesion of the bacteria. Larger dispersion was also measured for the vegetative bacteria.

From the results of bacteria transport, it is concluded that bacteria size and porous media size have an influence on the transport of bacteria. The transport of starved bacteria is effective in both fine and coarse sand, and vegetative bacteria transport is more effective in coarse sand. The transport of vegetative bacteria in fine sand is not effective and can be attributed to the size of the bacteria in relation to the pore size.

Hydraulic reduction test

The results from the hydraulic reduction tests in coarse sand show that, over the course of 30 days, an average reduction of 48% in the hydraulic conductivity was measured after two minutes.

In the fine sand column, an average reduction of 85% in the hydraulic conductivity was measured after two minutes, and an average reduction of 69% in the hydraulic conductivity after 1 pore volume of media had flowed through the column. A 100% reduction in the hydraulic conductivity was measured twice during the experiment.

It can thus be concluded that bacterium *R. planticola* has the ability to clog a fine sand column completely. In the case of the coarse sand, it is suggested that bacteria must be given more time between the hydraulic conductivity reduction tests (3-4 days) to enhance the growth and multiplication of the bacteria before the hydraulic reduction is tested.

Implications

For the purpose of this study, namely clogging coarse porous media and fractures, it is necessary to use a bacterium with high adhesion properties as well as very good biobarrier potential.

It was decided to use only vegetative bacteria for further study.

The results of the hydraulic reduction test on *R. planticola* show that the bacterium can clog fine sand 100% for a short period, but lacks the ability to clog coarse sand. During testing on *R. planticola* in coarse sand, it was evident that the bacteria cannot adhere sufficiently to the coarse grains, and cannot keep the barrier intact, which leads to large increases in the hydraulic conductivity after just one pore volume of flushing with nutrient media.

It was decided to cease all further research on the bacterium *R. planticola*, and search for bacteria with more effective biobarrier potential.

4.12 LABORATORY TESTING OF BACTERIUM BURKHOLDERIA VIETNAMENSIS

Due to problems associated with *Raoutella planticola*, as discussed in sections 4 to 4.11, it was decided to extend the study to include other bacterial species with biobarrier potential. The bacterial organism *R. planticola* was replaced with two new organisms, namely *B. vietnamensis* and *S. marcescens*.

4.12.1 Burkholderia vietnamensis

The *B. vietnamensis* strain G4 is the best trichloroethene (TCE) co-oxidising strain yet discovered (Fries *et al.*, 1997). TCE and its sister chloroethenes are the most widespread hazardous environmental contaminants in groundwater (<http://genome.jgi-psf.org>). Strain G4, when grown on toluene or phenol, produces an oxygenase that degrades TCE. The strain has been used at a number of polluted sites to aid groundwater clean-up (<http://genome.jgi-psf.org>). Strain G4 was isolated from an industrial waste treatment facility at Pensacola Naval Air station in Florida for its TCE oxidising ability (Nelson *et al.*, 1989).

4.12.2 Preparations and bacteria growth

Bacteria were grown at room temperature (22-25°C) and shaken at 120rpm. *B. vietnamensis* was grown in BSM media, consisting of four components, namely BSM A, BSM B, 1.2 M sodium lactate and 5% glucose.

- Component A (20X BSM A) contained (20X concentrated) potassium phosphate (diabasic). 17g $K_2HPO_4 \cdot 3H_2O$, 4g $NaH_2PO_4 \cdot H_2O$ and 8g NH_4Cl .
- Component B (20X BSM B) contained: (Nitrilotriacetic acid (NTA), trisodium salt $N(CH_2CO_2Na)_3 \cdot H_2O$ 2.46g). 4g $MgSO_4 \cdot 7H_2O$, 0.24g $FeSO_4 \cdot 7H_2O$, 0.06g $MnSO_4 \cdot H_2O$, 0.06g $ZnSO_4 \cdot 7H_2O$ and 0.02g $CoCl_2 \cdot 6H_2O$. In addition, 1.2 M sodium lactate stock and 5% glucose.

4.12.3 Inoculum preparation

The bacterium was cultivated by the Department of Microbiology, Biotechnology and Food Biotechnology at the University of the Free State.

Pre-inocula of *Burkholderia* were prepared with a loopful of culture from agar plates. The pre-inoculum flasks contained 50 ml medium (BSM media) in 250 ml Erlenmeyer flasks. Bacteria were incubated on shaker at 25°C for 20.5 h. To make the inoculum, 190 ml media were added to a 1 l Erlenmeyer flask. 10 ml pre-inoculum was added to each shake flask and incubated on a shaker for 6 hours at 25°C.

Bacteria were harvested by centrifugation at 10000 X g at 4°C for 10 minutes. The bacteria were suspended in AGW and dilutions were made of the culture.

Optical density measurements were used to estimate the cell numbers or mass in each fraction.

Bacteria were grown on a daily basis to ensure the viability of cells injected into the columns. A cell concentration of 2×10^6 cell/ml (OD = 0.3) was used for the injection of columns.

4.12.4 Adhesion tests

The adhesion tests on *Burkholderia* are outlined per methodology in section 4.6.1 (DeFlaun *et al.*, 1998). The results show that *B. vietnamensis* has the ability to adhere 95% (after 1 hour) to coarse sand.

4.12.5 Packing of columns

A fine and coarse sand column were packed. Columns were packed as described in section 4.8.2.1 and 4.8.2.2.

4.12.6 Bacterial transport test methodology

The columns were prepared for transport tests by flushing with two pore volumes (PV) of artificial groundwater. Artificial groundwater is sterilised, distilled water with different minerals added, so that it has the same composition as groundwater. One pore volume is respectively 350 and 370 ml for the fine and coarse sand (see section 4.8.4). Artificial groundwater (AGW) was also prepared for bacteria suspension.

For the bacteria transport test, 200 ml bacteria with a cell concentration of 2×10^6 cells/ml were suspended in artificial groundwater, and injected into the fine and coarse sand columns.

Ten millilitre fractions were collected from the outlet of the column every 5 minutes. The OD was measured for each sample to determine bacteria breakthrough.

4.12.7 Bacterial transport discussion

4.12.7.1 Fine sand column

After 18 hours, no bacteria breakthrough was measured. This can be attributed to the vegetative state and very good adhesion properties of the bacteria (95% adhesion after 1 hour).

4.12.7.2 Coarse sand column

The leading edge of the bacteria front passes through the system after 0.49 pore volume. After 1 pore volume, a peak was reached, which decreased over time. The system reverts to pre-bacteria levels after 1.6 pore volumes. It is important to note that the OD values (C) are much lower than the original injected concentration (C_0). It is possible that a high percentage of the bacteria adhered to the soil at the start of the column and will remain there because of their good adhesion properties (see Figure 4-14 for bacteria breakthrough results).

The bacteria transport data were analysed with the software program PULSE (porous media program).

From the results of Figure 4-14 and Table 4-3, the following interpretations can be made.

A very low velocity was calculated for the bacteria. This can be attributed to adhesion properties of the bacteria. Bacteria have the ability to adhere 95% after 1 hour. A breakthrough was obtained after 100 minutes. See section 4.12.4.

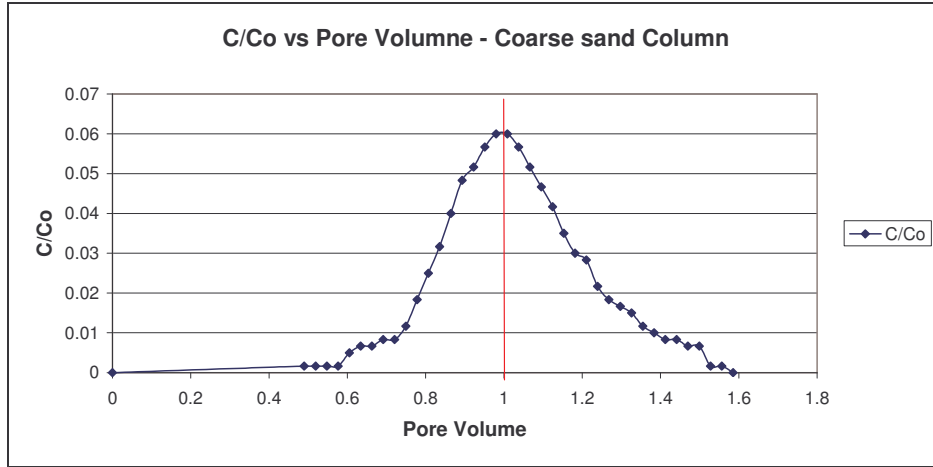


Figure 4-14 C/C_0 vs. pore volume - bacteria transport results.

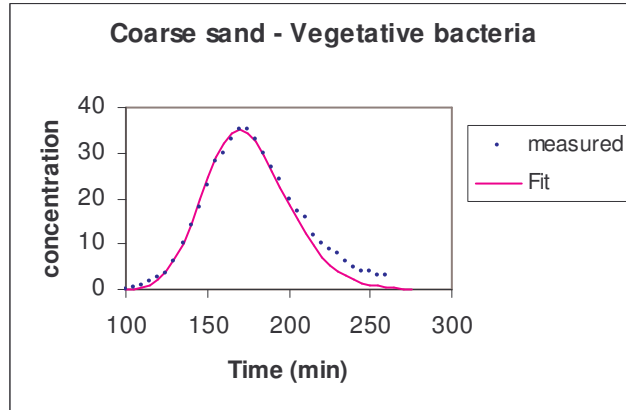


Figure 4-15 Bacteria breakthrough curve fitted with the PULSE software.

Table 4-3 Results of the bacterium (*B. vietnamensis*) transport in the coarse sand - calculations for the velocity and dispersivity of the sand.

Bacterium <i>Burkholderia vietnamensis</i>		
	Velocity (m/d)	Dispersivity (m)
Vegetative bacteria	2.35	0.003

4.12.8 Continuous injection of columns

4.12.8.1 Methodology

The columns (fine and coarse sand column) were repacked and saturated with artificial groundwater. Prior to the injection of bacteria and media, the flow rate through the packed columns was determined by means of a constant head test.

The test columns were then injected simultaneously with bacteria and media for ten days. A cell concentration of 2×10^6 cell/ml was injected into the columns to compensate for dilution in the column, because of simultaneous injection of bacteria and media. The reason for the simultaneous injection of bacteria and media is to ensure an even distribution of bacteria and media in the columns, as well as optimal growth situations in the column. The bacteria and media were injected at a rate of 0.5 ml/min each.

Vegetative bacteria were used daily to ensure the viability of bacteria. Approximately four pore volumes were pumped through the column each day.

4.12.8.2 Sampling of columns

Columns were sampled at the side ports on a daily basis. OD's were determined for the side port samples and the pH, electrical conductivity (EC) and OD's read for the outflow samples.

4.12.9 Results from the EC, pH and cell distribution

4.12.9.1 Fine sand column

The results from the EC showed that EC (C/C_0) varies between 0.45 and 0.55. The media concentration varied due to the consumption of nutrients by the bacteria.

For the first two days, the pH values were between 5.5 and 5.7. This lower pH level may result from the interaction of artificial groundwater and quartz mineral before any bacteria or media were injected. Quartz releases very low amounts of H^+ to the solution. After the sixth day, the pH stabilised at a value of 6.8. Details on the results of the EC and pH can be seen in Appendix A.

In the fine sand column, the optical density and outflow were measured daily at the four side ports. Port 1 is closest to the inflow side, while Port 4 is furthest away.

From Figure 4-16, it can be seen that the highest concentration of cells is measured at Port 1 (inflow side). These were attributed to the very high adhesion ability of the bacteria. Because of the fine texture of the sand, most of the bacteria adhered at the beginning of the flow path. The distribution of bacteria concentration decreases along the

flow path (towards the outflow side). The concentration of cells in the outflow was low, which is an indication that the cells were not flushed out of the column.

See Figure 4-16 for bacteria concentrations (cells/ml) in the column at each port, and Table 4-4 for information on the distribution of cells in the column. Optical density measurements of the outflow samples were taken twice per day (8:00 and 17:00). See Appendix A for information on the cell distribution concentration measured in optical density.

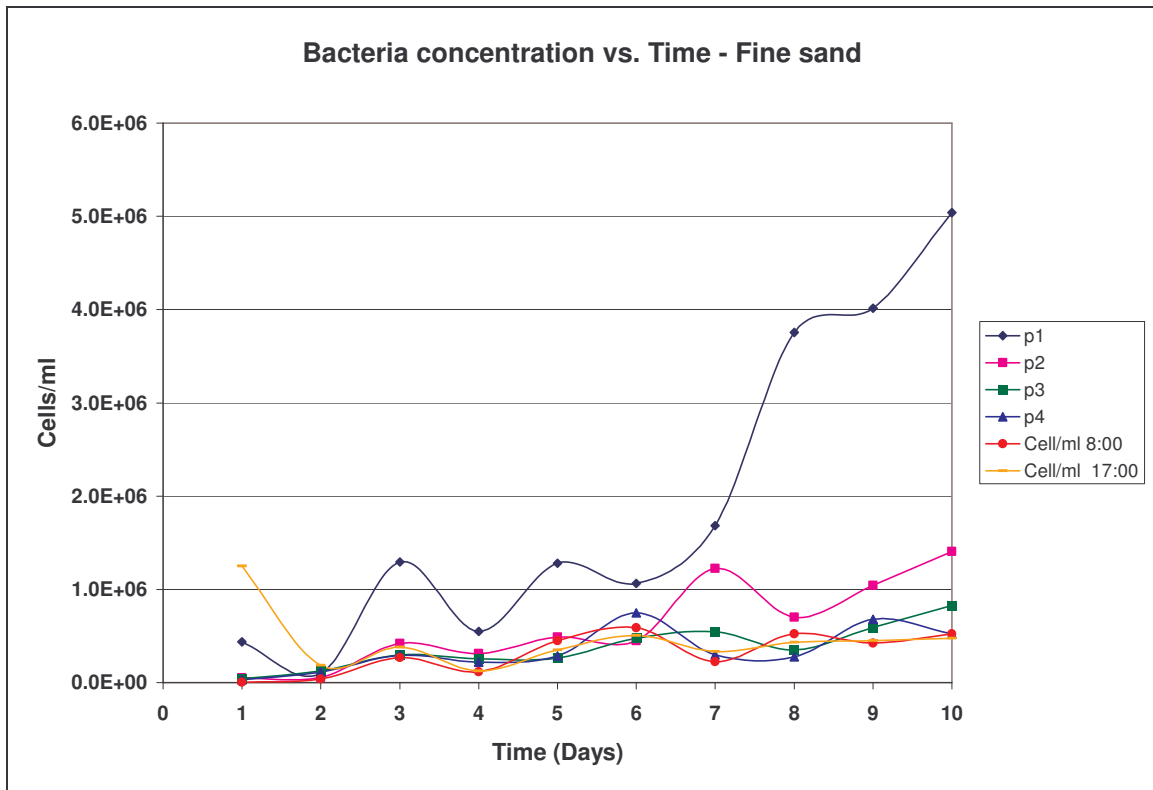


Figure 4-16 Cell concentration vs. time - fine sand column.

Table 4-4 Data - cell/ml, pH and EC data for the fine sand column.

Time	Cells/ml						EC (mS/m)	pH
	p1	p2	p3	p4	Outflow 8:00	Outflow 17:00		
							1053.00	
1	4.38E+05	5.00E+04	4.38E+04	3.13E+04	6.25E+03	1.25E+06	492	5.69
2	1.00E+05	5.63E+04	1.25E+05	1.13E+05	3.75E+04	1.88E+05	520	5.51
3	1.29E+06	4.19E+05	3.00E+05	2.94E+05	2.69E+05	3.81E+05	545	6.24
4	5.50E+05	3.13E+05	2.56E+05	2.19E+05	1.19E+05	1.25E+05	535	6.2
5	1.28E+06	4.88E+05	2.63E+05	2.88E+05	4.50E+05	3.50E+05	569	6.19
6	1.06E+06	4.50E+05	4.75E+05	7.50E+05	5.88E+05	5.06E+05	540	6.79
7	1.68E+06	1.23E+06	5.44E+05	3.00E+05	2.25E+05	3.31E+05	575	6.83
8	3.76E+06	7.00E+05	3.50E+05	2.75E+05	5.25E+05	4.31E+05	550	6.82
9	4.01E+06	1.04E+06	5.94E+05	6.81E+05	4.25E+05	4.50E+05	513	6.75
10	5.04E+06	1.41E+06	8.25E+05	5.25E+05	5.25E+05	4.75E+05	500	6.7

4.12.9.2 Coarse sand column

The EC varies between 500 and 640 mS/m. The lower EC concentrations over the first two days might be attributed to the presence of artificial groundwater in the column, which causes dilution. The pH varies between 5.6 and 6.9. Results of the EC and pH can be seen in Appendix A.

The optical density for each port, as well as for the outflow, was measured on a daily basis.

From Figure 4-17, it can be seen that the highest concentration of bacteria was measured in Port 1. If the two columns are compared, it can be seen that the concentration distribution of bacteria in the coarse sand column is much higher than in the fine sand column, except for Port 1. According to the cell/ml graphs, it can also be seen that the bacteria are active, because the concentrations (C) of the cells measured in all the ports over time were twice the original concentration (C₀) injected after 10 days. The concentration of cells measured in the outflow was lower. The high cell concentrations are attributed to the very high adhesion ability of the bacteria, and its ability to multiply and grow effectively. See Table 4-5 for information on the distribution of cells (OD) in the column and Figure 4-17 for cell concentrations (cells/ml) at each port vs. time. See Appendix A for cell distribution concentration measured (OD) for the coarse sand column.

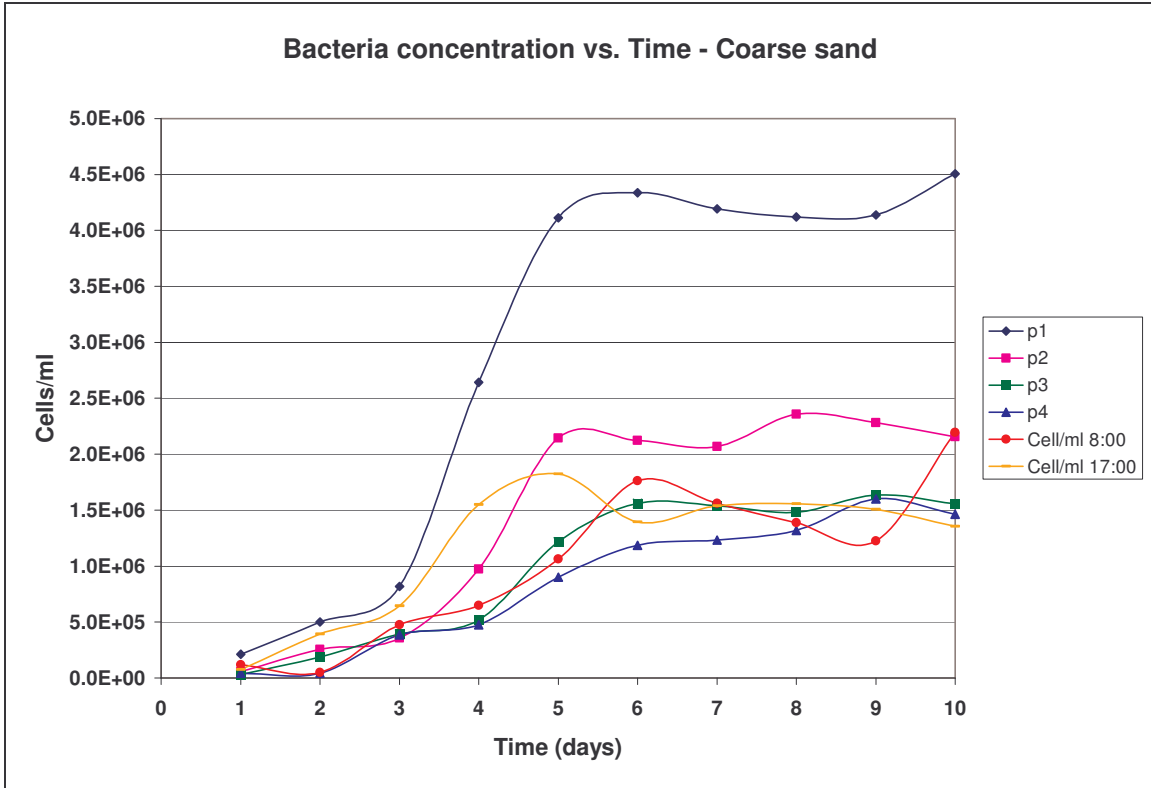


Figure 4-17 Cell concentration vs. time - coarse sand column.

Table 4-5 Data - coarse sand column.

Time	Cells/ml						EC (mS/m)	pH
	p1	p2	p3	p4	OD-out 8:00	OD-out 17:00		
							1053.0	
1	2.13E+05	5.63E+04	3.13E+04	4.38E+04	1.19E+05	7.50E+04	504	5.7
2	5.00E+05	2.56E+05	1.88E+05	4.38E+04	5.00E+04	3.94E+05	525	5.7
3	8.19E+05	3.56E+05	3.94E+05	3.88E+05	4.75E+05	6.44E+05	601	6.1
4	2.64E+06	9.75E+05	5.19E+05	4.75E+05	6.50E+05	1.55E+06	620	6.4
5	4.11E+06	2.14E+06	1.22E+06	9.00E+05	1.06E+06	1.83E+06	632	6.3
6	4.34E+06	2.13E+06	1.56E+06	1.19E+06	1.76E+06	1.39E+06	640	6.3
7	4.19E+06	2.07E+06	1.54E+06	1.23E+06	1.56E+06	1.54E+06	568	6.8
8	4.12E+06	2.36E+06	1.48E+06	1.32E+06	1.39E+06	1.56E+06	565	6.8
9	4.14E+06	2.28E+06	1.64E+06	1.60E+06	1.23E+06	1.51E+06	593	6.7
10	4.51E+06	2.16E+06	1.56E+06	1.46E+06	2.19E+06	1.36E+06	569	6.8

4.12.10 Hydraulic conductivity (K) reduction test

The hydraulic reduction test was performed to determine the potential reduction in the hydraulic conductivity of the sand columns, and whether the bacteria have the ability to successfully clog a fine and coarse sand column. Refer to Chapter 4, section 4.9.3 for hydraulic conductivity values for the fine and coarse sand.

After a ten-day period of continuous bacteria and media injection, the columns were stopped and the hydraulic conductivity (K) reduction measured by means of a constant head test. Artificial groundwater was used to perform the constant head test.

4.12.11 Results from the hydraulic conductivity reduction test - Fine sand column

When applying a constant head to the fine sand column, almost no flow was measured. For the first 2.5 hours, a very low flow was measured and an average of 92% reduction in the hydraulic conductivity was achieved. The hydraulic conductivity increase was very slow and the original flow (Q) was reached after 37 hours. The fact that the flow was not reduced 100% might be attributed to the poor distribution of cells throughout the column. The slow increase in the hydraulic conductivity over time might result from the very high concentration of cells in Port 1, which forms an obstruction at the inflow side. The increase in hydraulic conductivity might also be attributed to preferred pathways forming through the initial obstruction over time. See Figure 4-18 and Figure 4-19 for the graph of the % reduction in the flow and the hydraulic conductivity vs. time graphs.

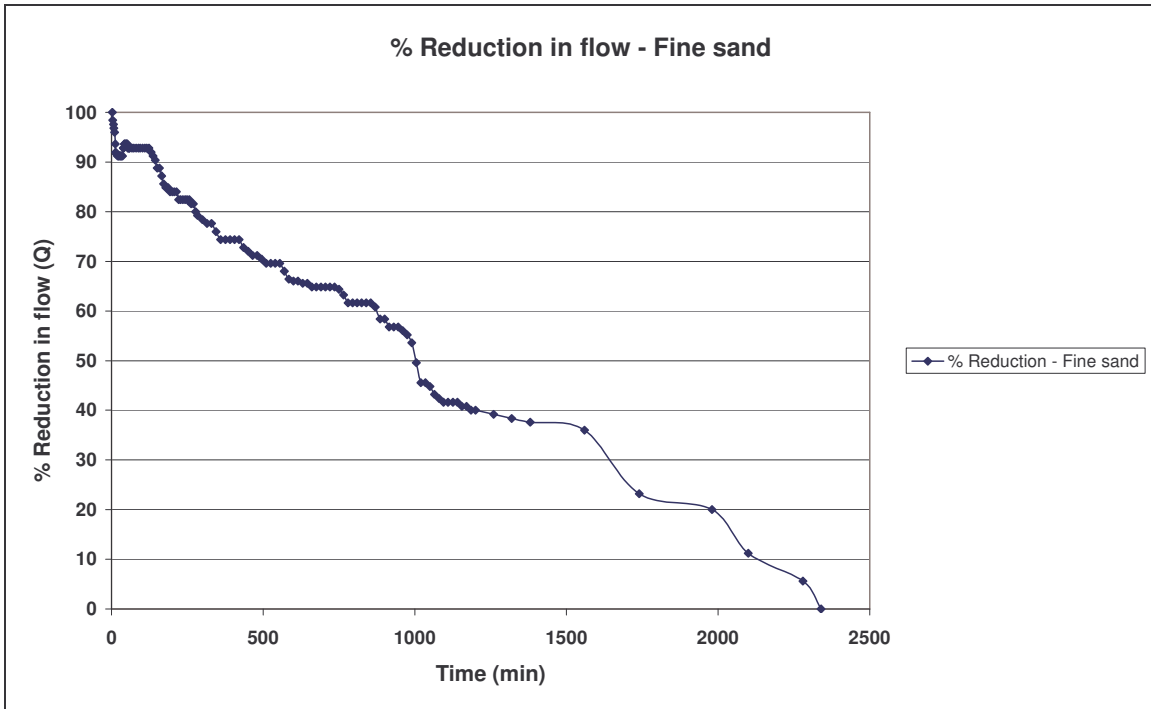


Figure 4-18 Results from the % reduction in flow for the fine sand column.

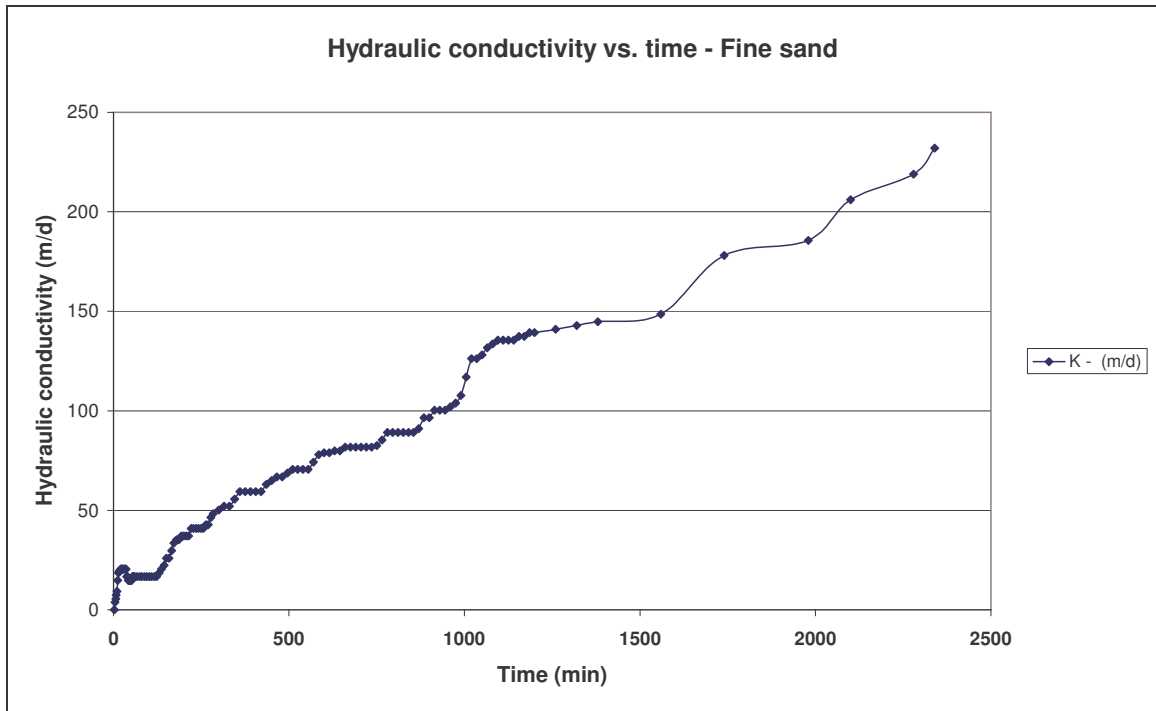


Figure 4-19 Results from the hydraulic conductivity vs. time for the fine sand column.

4.12.12 Results from the hydraulic conductivity reduction test—Coarse sand column

In the coarse sand column, a 100% reduction in the hydraulic conductivity was measured for the first four hours of the test.

After four hours, the hydraulic conductivity started to increase, and after fifteen hours, the hydraulic conductivity was back to its original value. The 100% reduction in the hydraulic conductivity can be attributed to the good distribution of cells in the column. The bacteria have more space to adhere and grow. It is problematic that the reduction is not sustainable. Injecting media instead of artificial groundwater for the hydraulic reduction test might be the answer to a sustainable reduction in K . See Figure 4-20 for the graph of % reduction.

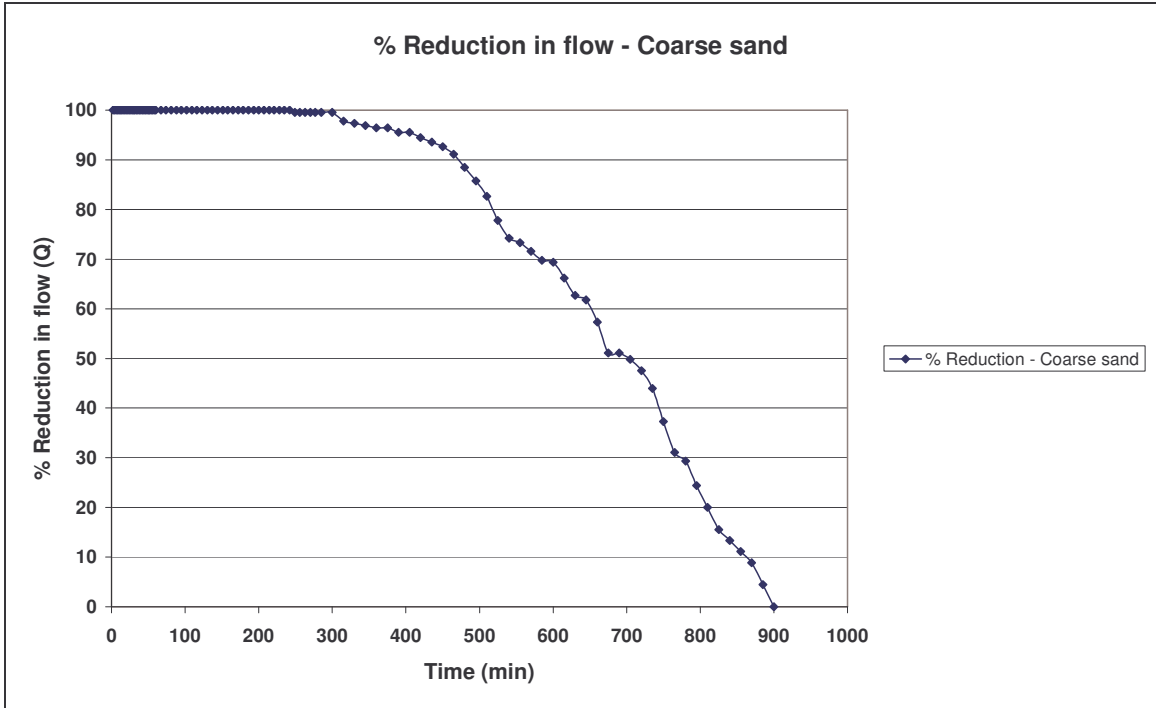


Figure 4-20 Results from the hydraulic conductivity reduction test for the coarse sand column.

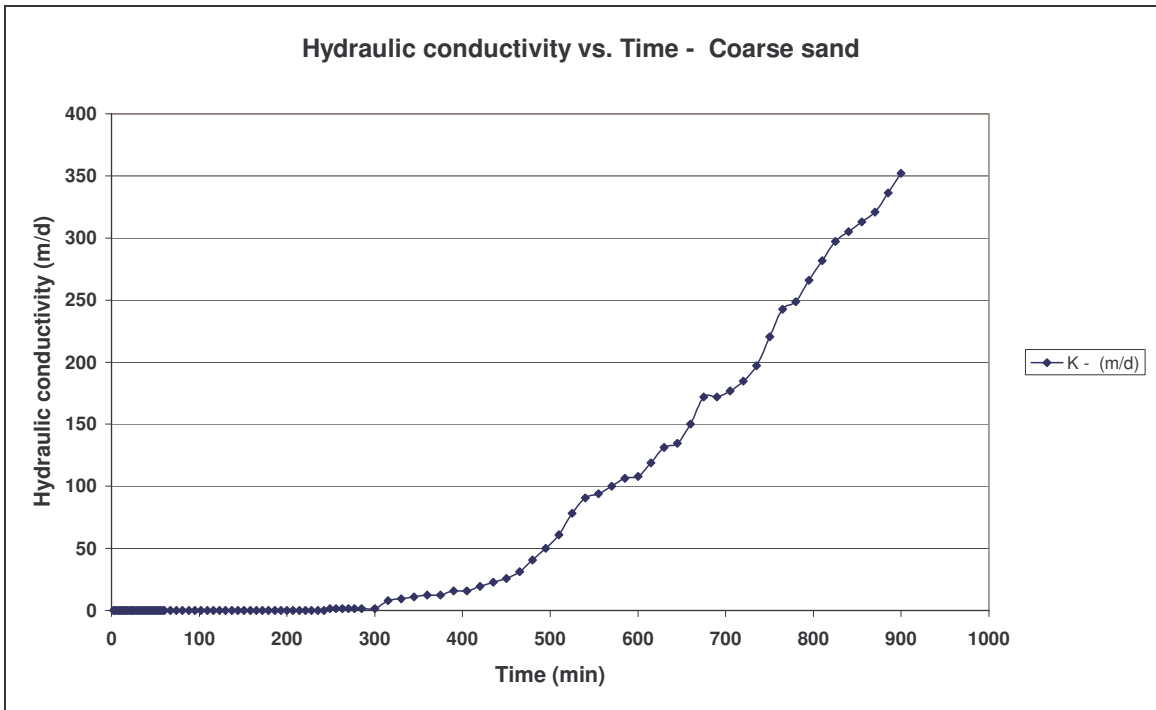


Figure 4-21 Results from the hydraulic conductivity vs. time for the coarse sand column.

The results from the hydraulic conductivity reduction test for the fine and coarse sand columns show that biobarrier technology is a feasible method for the manipulation of groundwater flow.

4.12.13 Conclusions

Bacteria transport

During the bacteria transport test in the fine sand column, no breakthrough of bacteria could be obtained. It is suspected that the bacteria adhered in the column. This is problematic, because the bacteria must have the ability to move through fine sand. Starving the bacteria for the purpose of transport in fine sand might be a possibility. Starvation of the bacteria will result in changes in the cell morphology and physiology (James *et al.*, 1995) of the bacteria. These changes often include a reduction in cell size, which may enhance the transport of these bacteria throughout the porous media.

During the bacteria transport test in the coarse sand, the breakthrough curve indicates that bacterial transport was viable. A high concentration of the bacteria adhered throughout the column. From this, it can be seen that *B. vietnamensis* has the ability to move and adhere in coarse sand.

Bacteria distribution

During continuous bacteria and media injection into the fine and coarse sand, the following was observed: In the fine sand column, the highest distribution of bacteria was measured in the port closest to injection. After ten days, the distribution of bacteria through the column was not even. In the coarse sand, the bacteria were evenly distributed throughout the column and the concentration (C) at each port had doubled from the initial concentration of bacteria injected (C_0).

Hydraulic reduction test

During the hydraulic reduction test in the fine sand column, the hydraulic conductivity increase was much slower than for the coarse sand, and the original flow was reached after 37 hours. In the fine sand, the bacteria have difficulty being transported through the sand. Most of the bacteria adhere at the start of the flow path and thus an even bacteria distribution is not possible. For the purpose of transport through very fine sands, starving

the bacteria might be an option. In principle, the concept of biobarrier formation by means of *B. vietnamensis* is shown in fine sand.

In the coarse sand column, a 100% reduction in hydraulic conductivity was attained over a period of four hours. The coarse sand has sufficient adhesion positions and the pores spaces are big enough to ensure transport of the bacteria as well as optimal growth in the pores spaces. *In situ* biobarrier formation is feasible in coarse sand. For application to high hydraulic conductivity surfaces, *B. vietnamensis* is a possible option.

Implications

B. vietnamensis appears to be a viable species to use. Unfortunately, if *B. vietnamensis* were to be manufactured or processed for a significant new use, the EPA must be notified at least 90 days prior to commencing the process. The EPA will then evaluate the intended new use and associated activities and, if necessary, prohibit or limit the activity before it occurs.

It was decided not to proceed with *B. vietnamensis*, and test *S. marcescens* to determine biobarrier potential.

4.13 LABORATORY-SCALE EXPERIMENTS ON BACTERIUM – SERRATIA MARCESCENS

4.13.1 Serratia marcescens

The genus *Serratia*, a member of the Entrobacteriaceae, is comprised of a group of bacteria related both phenotypically and by DNA sequence. Related terms are: *S. marcescens*, *S. plymuthica*, *S. liquefaciens*, *S. rubidaea*, *S. odoriferae* (*eMedicine.com*). The type species of the genus used in this research is *S. marcescens*. *S. marcescens* is a gram-negative bacillus-shaped bacteria.

Some strains of *S. marcescens* are capable of producing a pigment called prodigiosin, which ranges in colour from dark red to pale pink, depending on the age of the colonies (see Figure 4-22).



Figure 4-22 Plate with *S. marcescens*, showing the characteristic red pigment of the colonies.

Pigmented species and biotypes of *Serratia* also often exhibit pink or red colonies on nutrient agar. The use of low-phosphate agar without glucose, such as peptone-glycerol agar, can demonstrate pigmentation best. On nutrient agar, non-pigmented species or biotypes of *Serratia* yield opaque-whitish, mucoid, or transparent smooth colonies. The biotype used during this study is non-pigmented.

S. marcescens occurs naturally in soil and water, as well as in the intestines.

Pigmented bacteria are more often isolated from unpolluted water (from springs or wells) than from polluted water (river water downstream from cities).

Until as recently as 1964, researchers assumed that *S. marcescens* might play a role in the biological cycle of metals by mineralising organic iron and dissolving gold and copper.

S. marcescens is generally an opportunistic pathogen causing infections in immunocompromised patients.

A characteristic of *S. marcescens* is its ability to outgrow other bacteria and dominate the culture within days, which makes it ideal as a biobarrier species.

4.13.2 Source of bacteria

The bacteria used for the purpose of these experiments were collected by students from the Department of Microbiology, Biotechnology and Food Biotechnology, from Gravelotte Antimony Mine in South Africa.

Soil, water and sludge samples were collected aseptically at the mining and refining site located in the Limpopo Province of South Africa.

4.13.3 Preparations and growth of bacteria

S. marcescens was grown in BSM media, consisting of four components, namely BSM A, BSM B, 1.2 M sodium lactate and 5% glucose (refer to section 4.3. for the media components. The component B, 1 ml Trace Elements, 0.01g $\text{CuSO}_4 \cdot 5\text{H}_2\text{O}$, and 0.1g $\text{CaCl}_2 \cdot 2\text{H}_2\text{O}$ were added. Refer to section 4.3.2 for bacteria preparation.

4.13.4 Adhesion tests

The adhesion tests on *S. marcescens* were performed by the Department of Microbiology, Biotechnology and Food Biotechnology and are described in full detail in Van Heerden, (2005). The results showed that *S. marcescens* has an adherence capacity of 91% during the exponential growth phase and 90% during the stationary phase.

4.13.5 *In-situ* hydraulic conductivity reduction test

4.13.5.1 Methodology

In-situ biobarrier formation and reduction of saturated hydraulic conductivity were tested by means of different bacteria concentrations (10^2 , 10^4 , 10^6 , 10^8 cells/ml) in columns of coarse sand.

4.13.5.2 Packing of columns

Four columns were packed with coarse sand to determine the potential reduction that could be obtained under controlled conditions in laboratory columns (refer to Chapter 4, section 4.9.2.2 for packing a coarse sand column).

4.13.5.3 Continuous injection of columns with bacteria and media

Bacteria and media were injected simultaneously at a rate of 1 ml/min.

Simultaneous injection of bacteria and media occurred to ensure the even distribution of bacteria and media, and also to ensure optimal growth conditions in the column. See Figure 4-23 for set-up of the column experiments.

4.13.5.4 Sampling of columns

The outflow and the ports for each column were sampled on a daily basis. Optical density was measured for the outflow and side port samples. The following parameters were measured every day for the outflow samples: pH, EC (EC- mS/m), and optical density (OD- nm). The outflow was kept on ice to ensure no bacterial growth that could change the outflow parameters would occur.

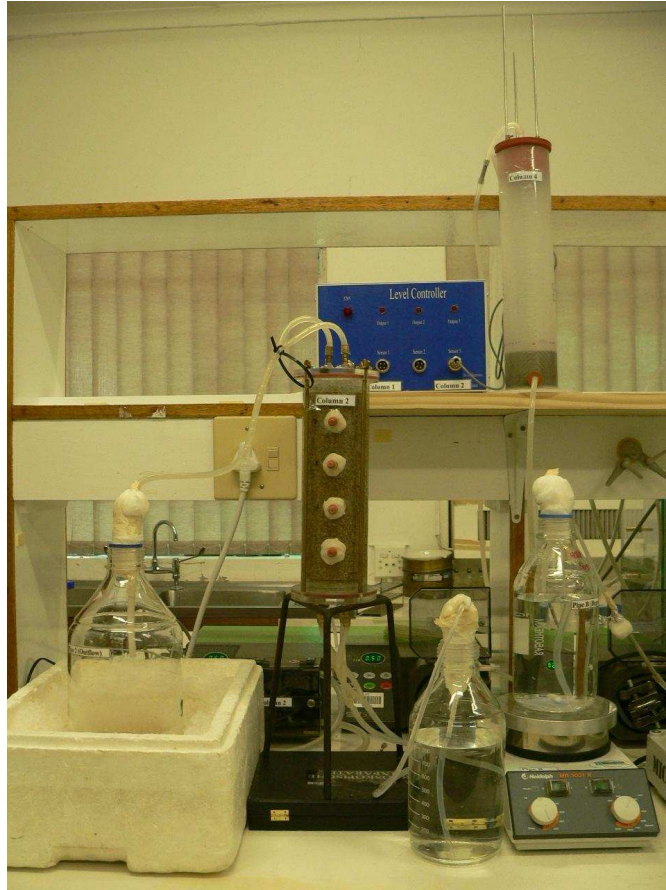


Figure 4-23 Set-up for the simultaneous injection of bacteria and media.

4.13.5.5 Results from the EC, pH and optical density

The results from the four columns were very similar.

For the course of the experiment the pH varied between 5.3 and 6, and can be attributed to simultaneous bacteria and media injection which causes mixing in the column.

The EC varies between 400 and 1000 mS/m. The lower EC concentrations over the first two days might be attributed to the presence of artificial groundwater in the column, which causes dilution. The results from the pH and EC can be seen in Appendix A.

From Figure 4-24, it can be seen that the optical density of the outflow samples for each column increased with time. The reason for this is bacteria growth and multiplication in the columns.

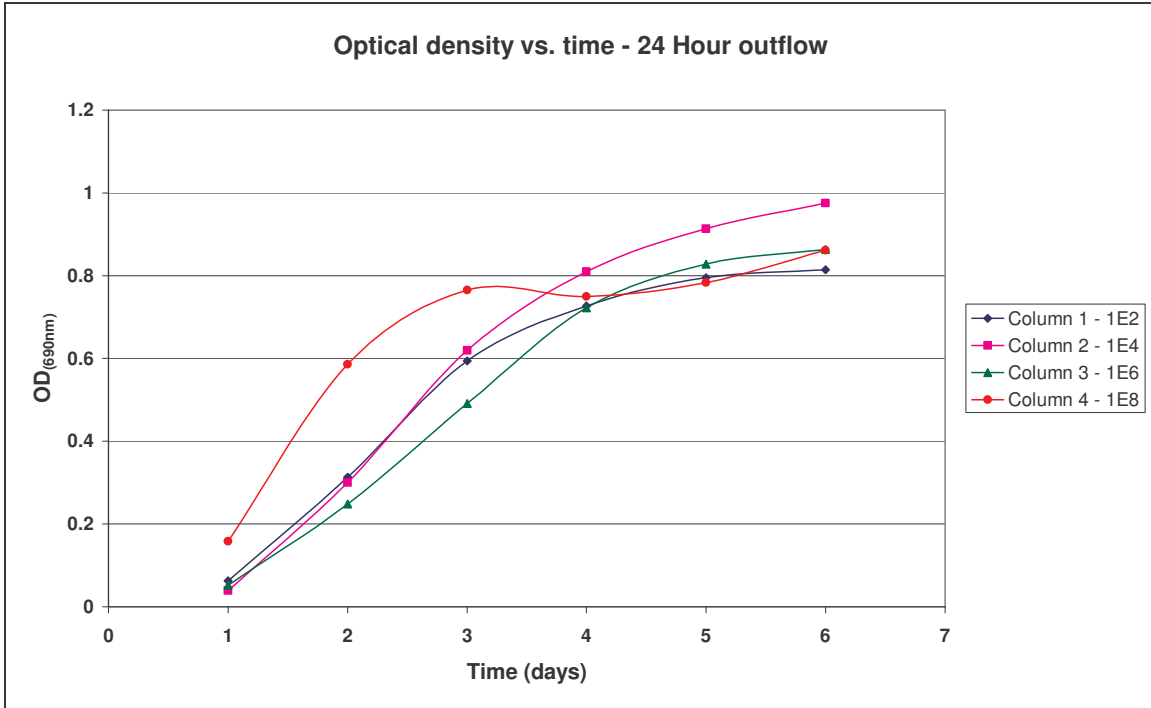


Figure 4-24 Optical density vs. time graph for the four coarse sand columns. 24-hour outflow.

4.13.6 Cell distribution in columns

The optical density for each port of the four columns were measured daily. See Figure 4-25 to Figure 4-28 for the distribution of cells (OD at each port) in the columns.

From Figure 4-25 to Figure 4-28, it can be seen that the concentration of the bacteria in each column is almost the same throughout the columns. A very good distribution was measured over a period of five days. The high cell concentrations in the column are attributed to the very high adhesion ability of bacteria.

From the graphs it can be seen that the highest bacteria concentration was measured on the fifth day of the experiment, except for Column 1, which had the highest concentration on the sixth day. A sudden drop in the OD on the sixth day was measured in all the columns, except Column 1. The assumption was that, due to bacteria concentration increases in the columns with time, oxygen will deplete with time. It is probable that the columns will start to react anaerobically after five days, causing the cell concentration to diminish.

Due to the decrease in the optical density, columns were stopped on the sixth day to determine the % reduction in the flow for the four columns. See Figure 4-28 for the bacteria distribution in the columns.

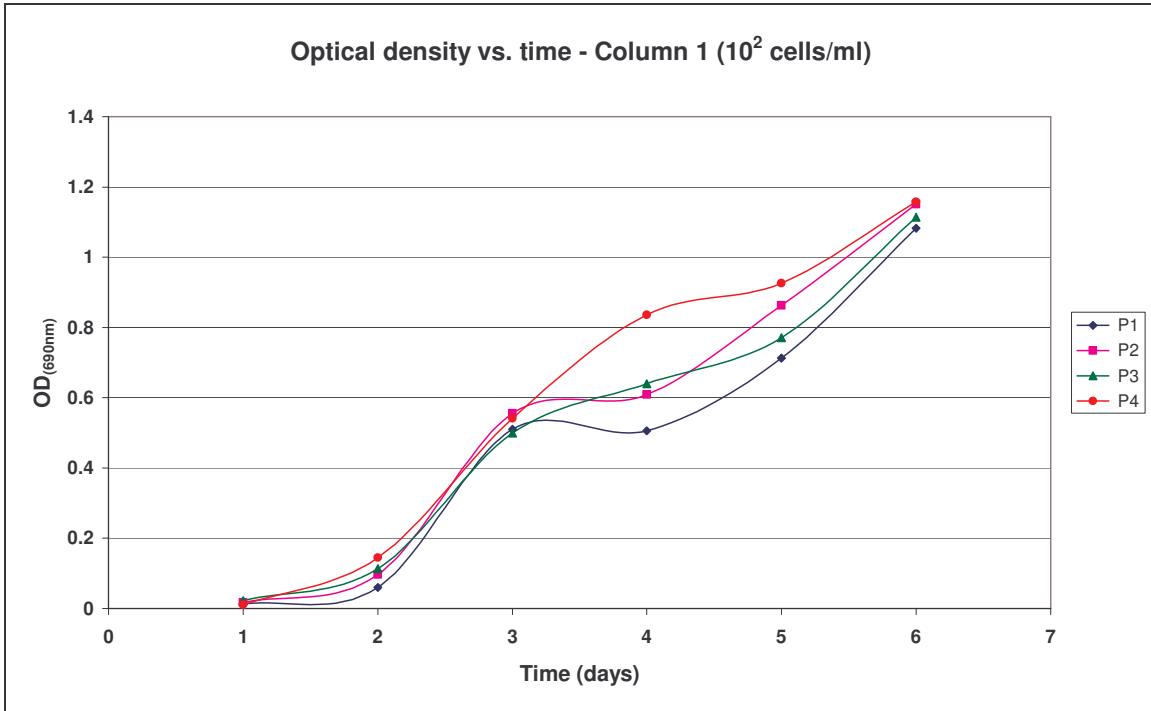


Figure 4-25 Cell concentration vs. time -Column 1.(10^2 cells/ml).

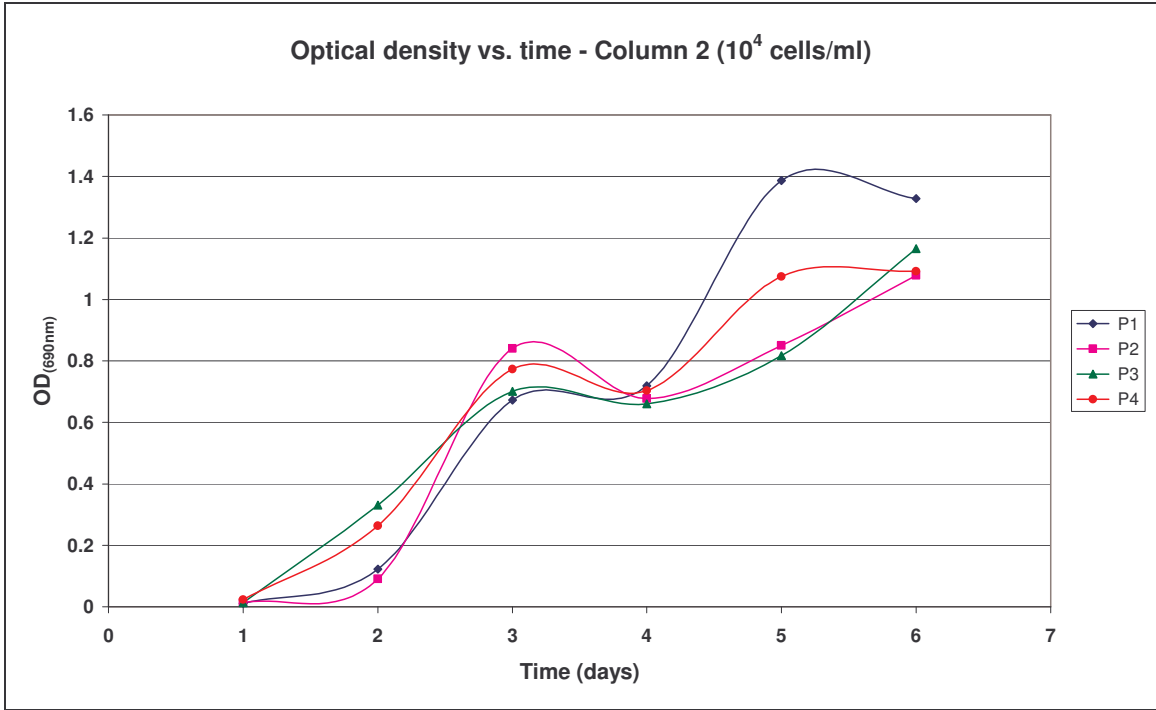


Figure 4-26 Cell concentration vs. time -Column 2. (10^4 cells/ml).

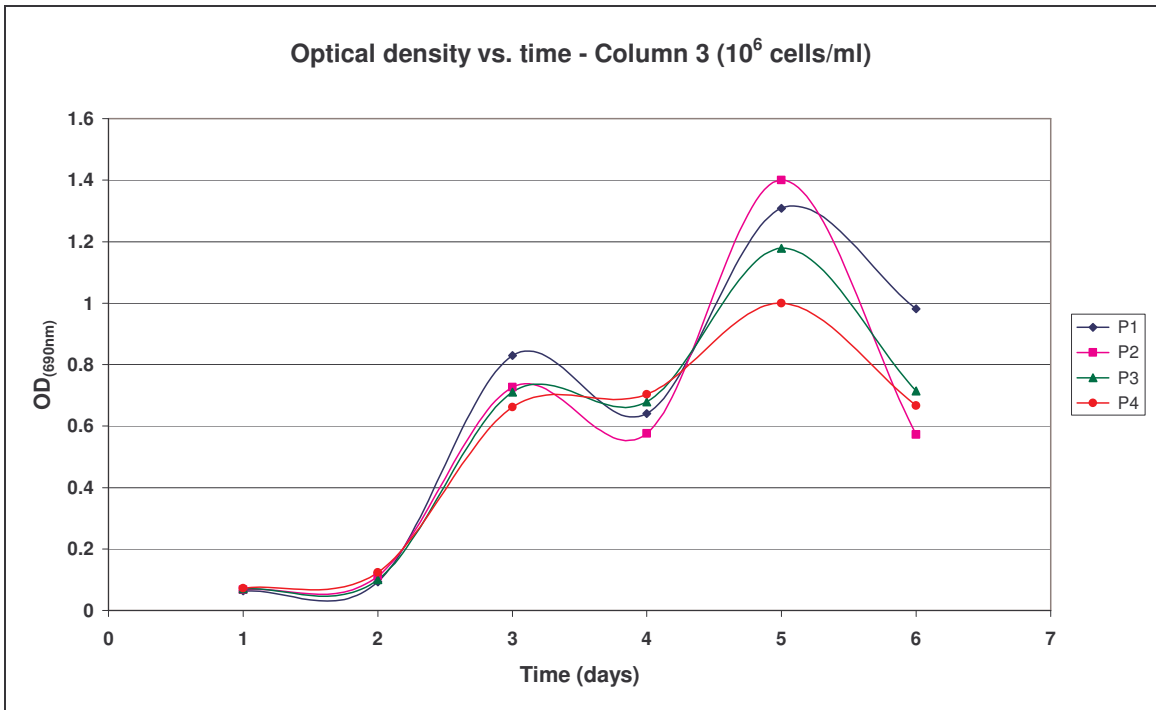


Figure 4-27 Cell concentration vs. time -Column 3. (10^6 cells/ml).

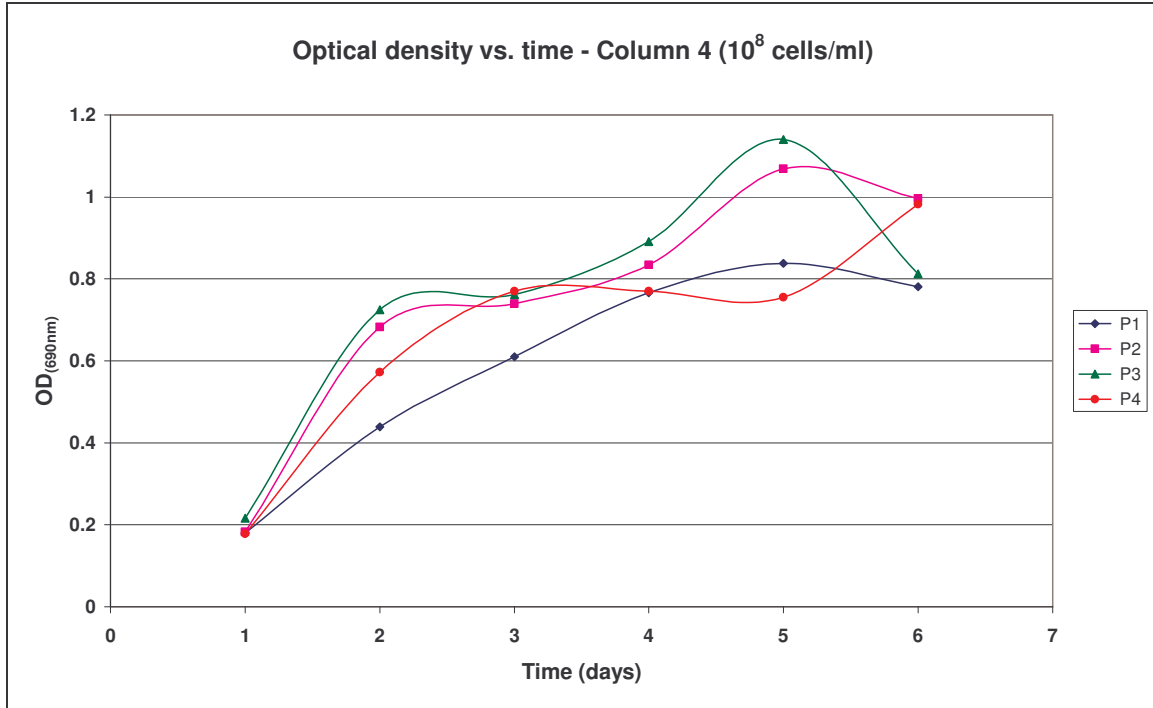


Figure 4-28 Cell concentration vs. time -Column 4. (10^8 cells/ml).

4.13.7 Discussion of results

The results of the parameter measurements for the outflow showed several important aspects. Due to the pH values of the media and groundwater, the pH of the outflow samples varied between 5.3 and 6. The electrical conductivity concentrations increase over time, due to continuous media injection.

Large optical density increases were measured in the ports of all four columns during the first five days. This can be attributed to good bacteria distribution throughout the column. A sudden drop in the OD was measured in Column 2 (10^4 cells/ml injected), 3 (10^6 cells/ml injected) and Column 4 (10^8 cells/ml injected) on the sixth day. This might be attributed to anaerobic conditions developing due to oxygen depletion in the columns.

A possible method to avoid total anaerobic conditions in the columns would be to aerate the bacteria on magnetic stirrers.

4.13.8 Hydraulic conductivity (K) reduction test

On the sixth day, the columns were stopped. The columns were left for three hours before the test started. The test was carried by means of a constant head test.

Groundwater from the campus test site was used to apply the constant head. See Figure 4-29 for the graphs of the reduction in flow for Column 1, 2 and 4.

For Column 1 (10^2 cells/ml), a 100% reduction in the flow was measured for a period of 14 hours. After 14 hours, the flow started to increase very rapidly. After an additional hour with an increased head, the flow was back to its original level.

For Column 2 (10^4 cells/ml), a 100% reduction in the hydraulic conductivity was measured for a period of 52.5 hours. After 52 hours, the head was increased. After ten minutes with an increased head, the columns started to flow, and after one hour the hydraulic conductivity was back to its original value.

For Column 3 (10^6 cells/ml), no results could be obtained, because the column started to flow immediately. The experiment was repeated and is discussed in detail in section 4.15.

Column 4 (10^8 cells/ml) was clogged for 52.5 hours. The head was increased, and the column started to flow after ten minutes.

The 100% reduction in the hydraulic conductivity can be attributed to the excellent distribution of cells in the column.

From the results of the hydraulic reduction test, it can be seen that columns must be inoculated with bacteria and media after 48 hours to ensure sustainable biobarrier formation. The effectiveness of biobarrier formation is also dependent on the head applied to the barrier.

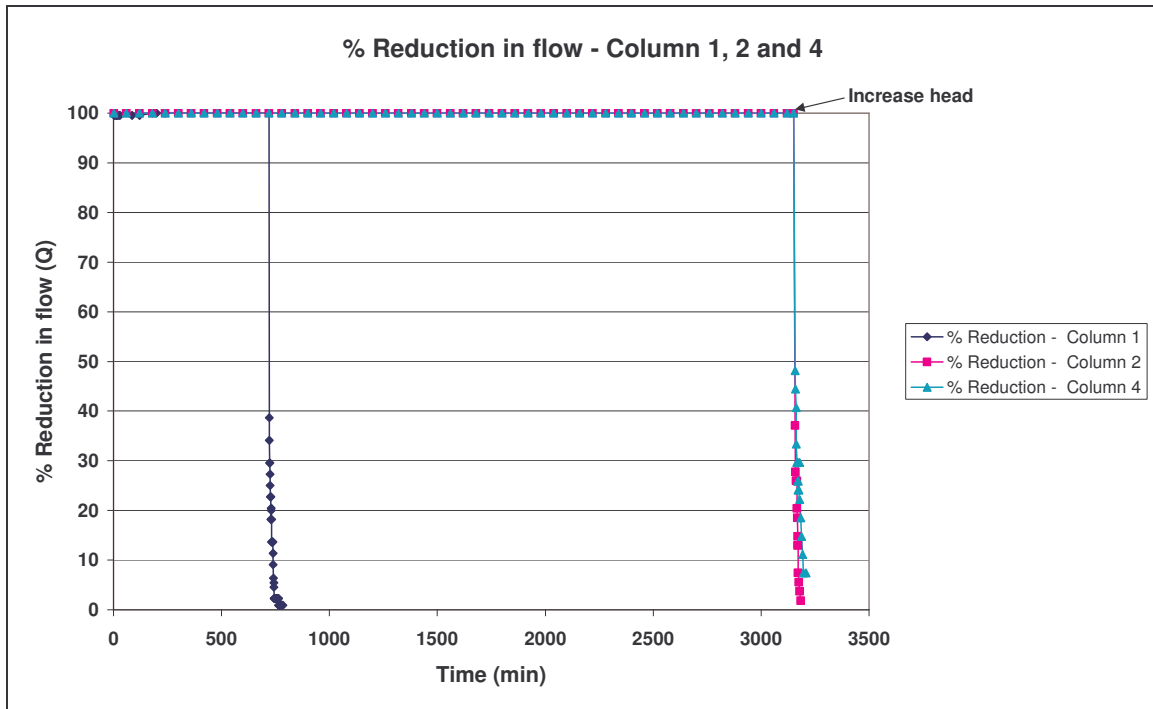


Figure 4-29 % Reduction in the flow for Column 1, 2 and Column 4.

4.13.9 Summary of the results and discussion

4.13.9.1 Hydraulic reduction test – coarse sand

- In Column 1, a 100% reduction in the hydraulic conductivity was maintained over a period of 14 hours (10^2 cells per ml).
- In Column 2, a 100% reduction in the hydraulic conductivity was maintained over a period of 52 hours (10^4 cells per ml).
- Unfortunately, Column 3 did not give any reduction in the hydraulic conductivity (10^6 cells per ml). The experiment was repeated and discussed in detail in section 4.15.
- In Column 4, a 100% reduction in the hydraulic conductivity was maintained over a period of 52 hours (10^8 cells per ml).

From the results of the hydraulic reduction test, it was found that barrier formation can be established with a minimum of 10^2 cells/ml. But the latter is not sufficiently effective to maintain the barrier. With cell concentrations between 10^4 and 10^8 , very effective barrier formation was established. Unfortunately, when the head was increased, the barrier

gave way very easily. This can also be the result of no media injection for more than two days.

For upscaling purposes and to make the biobarrier technology cost effective, the glucose concentration of the media was decreased from 10 g per litre to 3 g per litre. The KNO_3 was increased from 0.1 g to 10g per litre. The sodium lactate stock was eliminated. After this, optimal growth conditions could still be obtained (Van Heerden et al 2006).

Two columns, namely a column injected with 10^6 cells/ml and a column with 10^8 cells/ml, were repeated to determine the reduction in hydraulic conductivity.

4.14 REPETITION OF COLUMNS INJECTED WITH 10^6 AND 10^8 CELLS/ML

Column A was injected with 10^6 cells/ml and Column B with 10^8 cells/ml.

For both columns, the optical density of the four sampling ports were measured, as well as the dissolved oxygen in the outflow samples. See Figure 4-28.

The dissolved oxygen was measured for the outflow of Column A to determine how long it would take for the column to change from aerobic to anaerobic conditions. The results are displayed in Figure 4-30. It can be seen that the oxygen in the column was depleted .

The dissolved oxygen decreases very quickly, and from Day 2 onwards, the dissolved oxygen was lower than detection. The columns can therefore be classified as anaerobic.

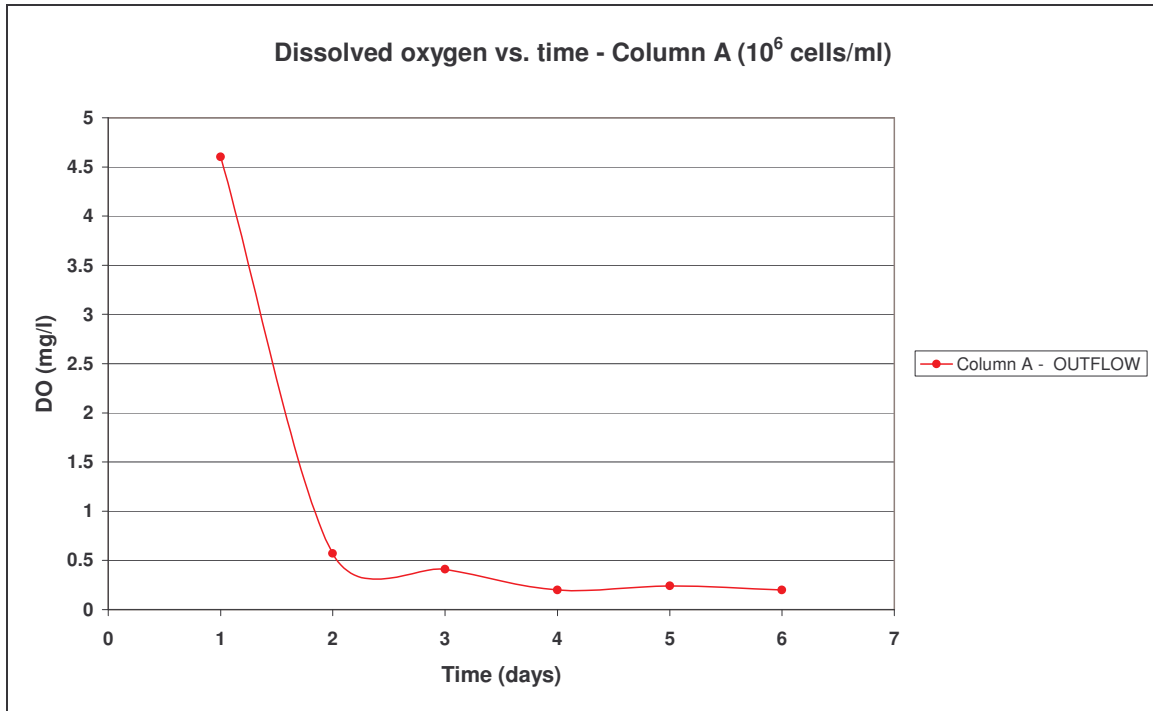


Figure 4-30 Dissolved oxygen vs. time graph for Column A (10^6 cells/ml).

4.14.1 Cell distribution in Column A and Column B

The optical density for each port was measured on a daily basis. See Figure 4-30 for information on the distribution of cells (OD) in Column A.

From Column A it can be seen that the concentration of the bacteria at each port over time is similar. A very good distribution was measured in Column A over a period of six days. The highest bacteria concentration was measured on the sixth day of the experiment.

For Column B, the bacteria concentrations vary on a daily basis. The OD of the outflow increased and the port OD decreased. The outflow samples were checked for viability by plating techniques on agar plates. Growth was obtained on the agar plates; thus the bacteria were still viable.

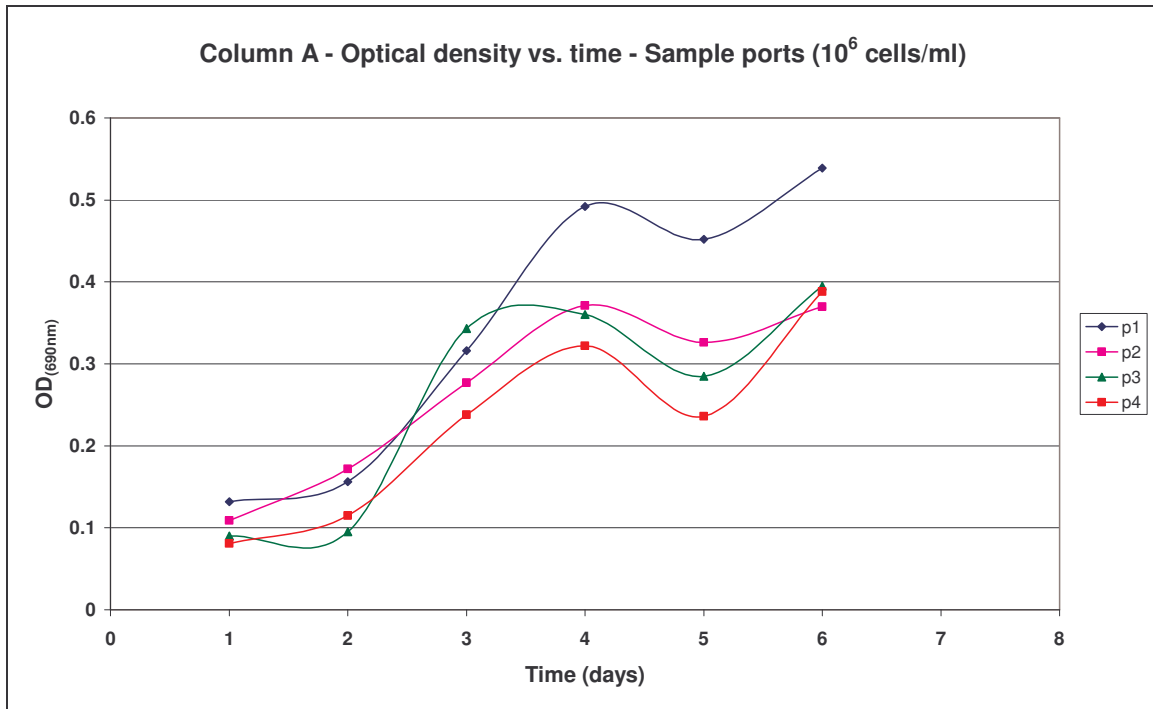


Figure 4-31 Cell concentration vs. time -Column A (10^6).

4.14.2 Hydraulic conductivity (K) reduction test – Column A and Column B

The columns were stopped on the sixth day and left for five hours before the hydraulic conductivity reduction test was performed by means of a constant head test.

Column A (10^6) and Column B (10^8) were clogged for a week. The original head of 0.05 was increased to 0.055 over a week's time to test the efficiency of the barrier. The barrier broke on the sixth day, when the head was increased to 0.065.

The 100% reduction in hydraulic conductivity can be attributed to the good distribution of cells in the column and optimisation of the media. It is important to note that the effectiveness of biobarrier formation is dependent on the head applied to the barrier.

4.14.3 Results and discussion

Dissolved oxygen measurements of the outflow showed that the columns can be classified as anaerobic after the second day. To prevent total anaerobic conditions in the coarse sand, injected bacteria and media must preferably be aerated to enhance optimal conditions for the bacteria to grow and multiply.

The results from Column A and B showed that it is possible to clog coarse porous sand 100% for a week. It appears that the barrier can withstand small head increases.

For the purpose of clogging coarse sand, *S. marcescens* is an excellent choice of bacterium

Adhesion and distribution of bacteria in coarse sand

Adhesion tests showed that bacteria *S. marcescens* has very good adhesion properties. The coarse sand have many adhesion positions and the pores are big enough to ensure transport of the bacteria as well as optimal growth between grains.

Hydraulic reduction tests

Results from the experiments showed that a biobarrier can be established in coarse sand with as little as 10^2 cells/ml, but is not effective over time. It was determined that an effective barrier can be established with cell concentrations of between 10^4 - 10^8 cells/ml. It was also determined that these barriers can withstand increases in the hydraulic gradient.

The conclusion made from the coarse sand column experiments is that the bacterium *Serratia marcescens* should be appropriate for biobarrier applications, especially in the case of fractures, where there are rough surface areas and large openings between surfaces.

Based on these results, it is clear that *in situ* biobarrier formation is feasible in coarse sand with high hydraulic conductivity.

5 TESTING AND APPLICATION OF BIOBARRIERS IN FRACTURED MEDIA

Laboratory testing methods were used in fractured media to obtain the required parameters for upscaling to the field. This includes testing the effectiveness of *S. marcescens* for reducing the hydraulic conductivity of a laboratory-scale horizontal parallel plate fracture with variable fracture apertures.

The effectiveness of these bacteria in clogging 11 m silicone tubing with a diameter of 3 mm was also evaluated. The significance of this experiment was to test the effect of different flow rates on bacteria adhesion and growth, as well as the effect of surface texture on the adhesion of bacteria.

The results from the pipe and horizontal parallel plate fracture were used for planning the field experiment.

5.1 TESTING BIOBARRIER FORMATION IN SMALL DIAMETER PIPES

5.1.1 Set-up of pipe experiments.

Two pipes, each with a length of 11 metres and an inner diameter of 3 mm were used. The 11 m pipe was rolled into a coil and placed in a water bath with a temperature of approximately 21°C. The reason for placing the pipes in a water bath was to represent a “fracture” in a saturated aquifer. The dimensions of the water bath were as follows: length = 0.5 m, width = 0.3 m and height = 0.5 m.

A bacteria concentration of 10^6 cells/ml was used.

5.1.1.1 Conservative tracer transport

The pore volume of both pipes was approximately 114 ml. Tracer tests were performed on both pipes to correlate the pore volume and determine the breakthrough curve of NaCl. The tracer was injected at a pump rate of 55 ml per hour. The results for the two pipes were almost identical. From Figure 5-1, it can be seen that the tracers reached a peak after 1 pore volume, and decreased over time. The tracer was flushed before two pore volumes have flowed through. The tracer data was also analysed by making use of

the software program TRACER (Riemann, 2002). The program was used to analyse the tracer test data, to determine the shape of the flow field, dispersion (m) and the flow (velocity-m/d) in the pipe. See Figure 5-2 for TRACER fit. During conservative tracer transport in fractures (in this case a pipe) under laminar flow conditions, the tracer will disperse both by molecular diffusion perpendicular to flow and by variation in the velocity profile across the fracture in the direction of flow. Fluid closer to the walls will flow more slowly than fluid in the aperture centre, so that mass advected with the fluid spreads longitudinally (Zimmerman *et al.*, 2002). This can create a concentration gradient in the transverse direction that, in turn, causes diffusion towards fracture walls.

The results from the TRACER program calculated a dispersivity of 0.07 m. The tracer velocity was measured at 124 m/d. Despite high velocities, there is insignificant dispersion and the NaCl is transported conservatively. The shape of the curve indicates almost “plug” flow conditions, and this is not expected typically in South African aquifers. See Figure 5-2 for breakthrough curve fitted with the TRACER software.

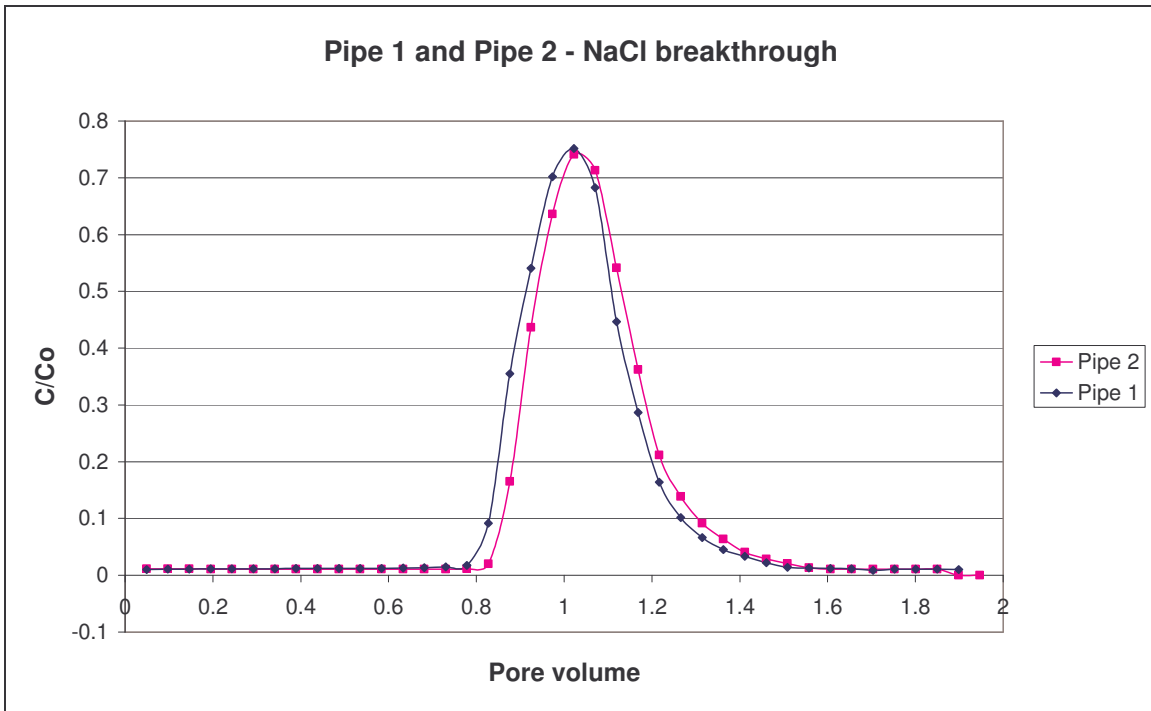


Figure 5-1 Pipe 1 and Pipe 2- Tracer breakthrough curve.

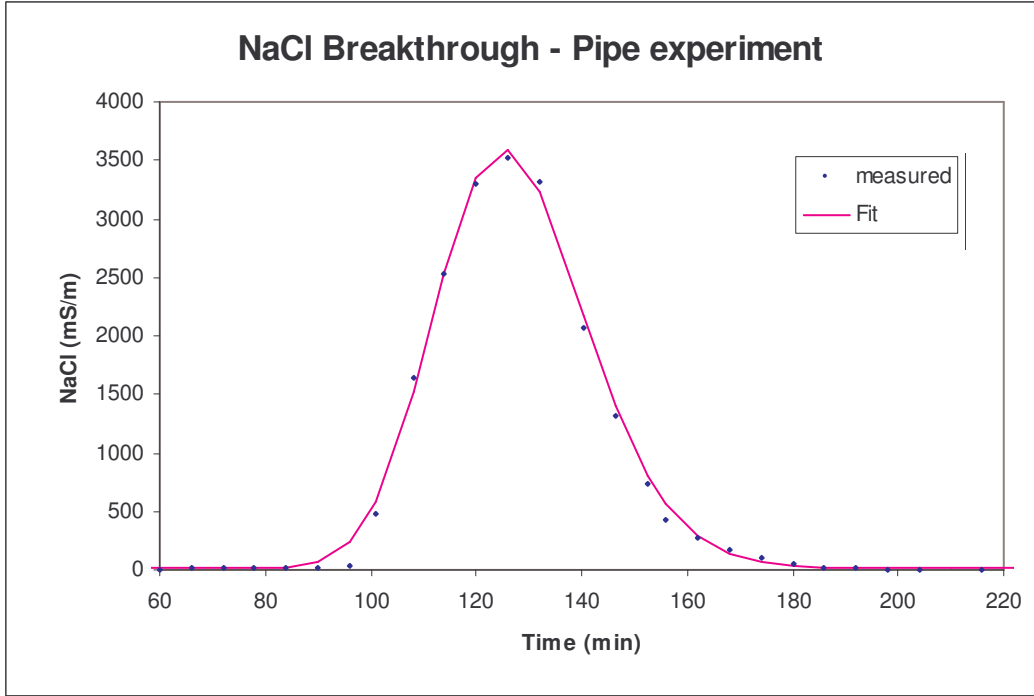


Figure 5-2 Pipe 1 and Pipe 2- Tracer breakthrough fitted by TRACER.

5.1.2 Continuous bacteria and media injection into pipes

For the transport and clogging experiment, a minimum of three pore volumes was pumped through Pipe 1 and a maximum of six pore volumes through Pipe 2. The reason for the different injection volumes per day was to test the effect of flow rate on bacteria adhesion in silicone pipes. Bacteria and media were pumped through the pipes simultaneously. The reason for the pipes to be under water was to simulate a “fracture” in a saturated aquifer, thus non aerobic conditions. Nitrogen gas was used to displace oxygen out of the water and ensure anaerobic conditions. Dissolved oxygen measurements were taken and were below 0.2 mg/l in the water above the pipes. The temperature of the water in the glass box was kept at approximately 22°C, to correlate with the aquifer temperature. The outflow samples were placed on ice to ensure that no growth occurs over the 24-hour outflow period.

See Figure 5-3 for the set-up of the pipe experiments.

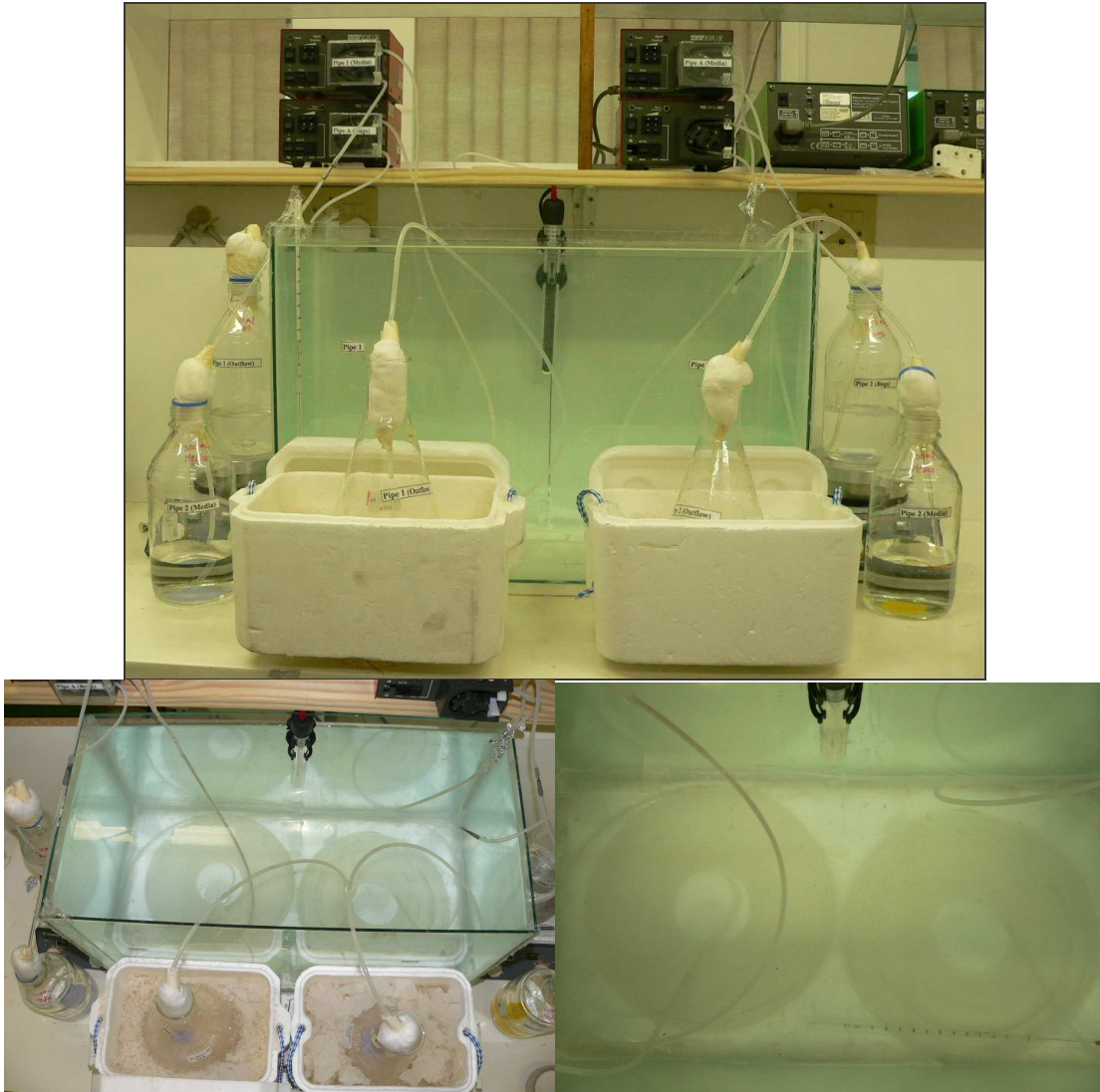
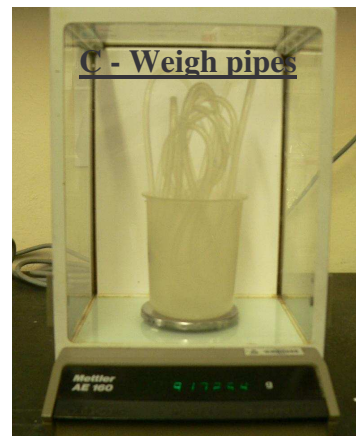
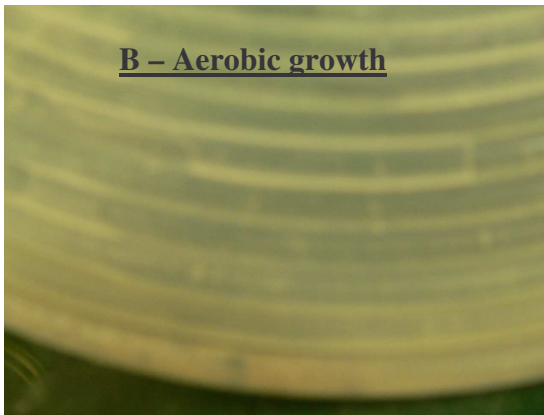
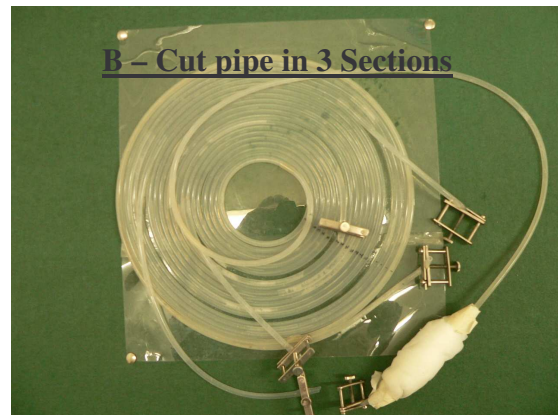
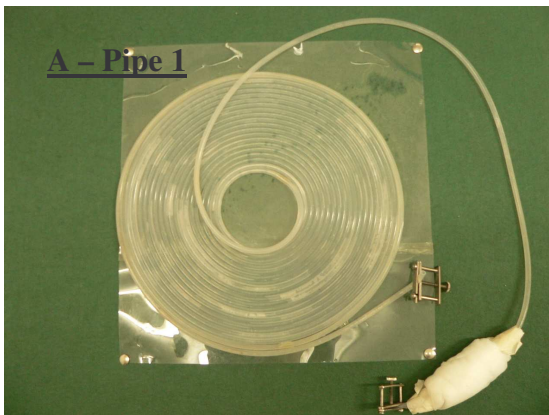


Figure 5-3 Set-up of pipe experiments.

After ten days, the experiment was stopped. The following methodology was used to determine the bacteria mass in the pipes (see Figure 5-4 (A - G)):

- (A) The pipes were taken from the glass box and put on a desk to dry.
- (B) The two pipes were both cut into three sections (respectively 4 m, 3.2 m and 3.8 m) and clamped off to ensure that no leakage occurs. The first section represents aerobic and semi-aerobic conditions, the second micro-aerophilic conditions, and the last anaerobic conditions and semi aerobic conditions near the outflow.
- (C) The mass of each pipe section was weighed.

- (D) The volume of each pipe section was then drained into an Erlenmeyer flask and the volume weighed (free-flow mass). The pipes were then rolled to loosen the bacteria adhering to the walls of the pipe and then flushed with methanol into an Erlenmeyer flask, and the volume weighed (adhered mass).
- (E and F) The volume drained from the pipes (free-flowing) and the adhering mass was filtered through 0.2 micron filters (filters were weighed before use).
- (G) Filters were then placed into the -80 °C fridge to stabilise before being placed into the -80 freeze dryer to dry.
- The filter papers were then weighed to determine the amount of dry mass for the free-flow and adhesion sections.



Testing and Application of Biobarriers in Fractured Media

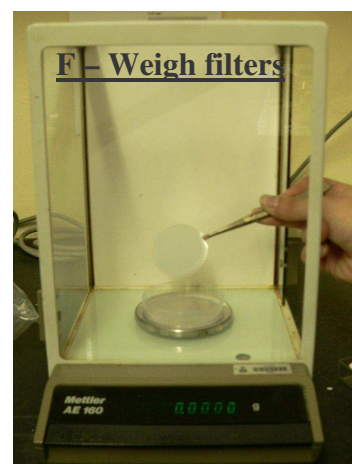
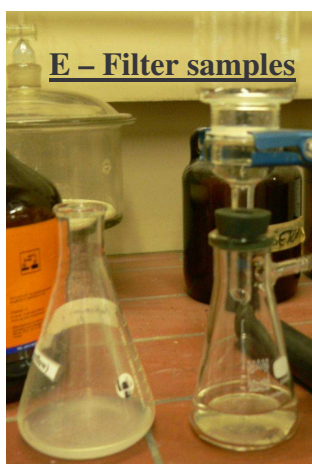


Figure 5-4 Steps to determine the free-flow and adhesive mass bacteria in Pipe 1 and Pipe 2.

5.1.3 Results and discussion

See Figure 5-5 to Figure 5-6 for the results of Pipe 1 and Pipe 2. Figure 5-5 compares the total adhered mass of bacteria in each section for Pipe 1 and 2 (mass adhered to the pipe per section). Figure 5-6 compares the free-flow mass (mass of bacteria in each section of Pipe 1 and Pipe 2).

In Figure 5-5, it can be seen that the adhesion in Pipe 1, section 1 is much higher than in Pipe 2, section 1. This is attributed to the lower flow rate in Pipe 1, which enables the bacteria to adhere to the pipe. The adhesion in section 2 for both Pipe 1 and Pipe 2 is almost the same. In section 2 of the pipes, the bacteria adhesion is lowest. Due to a lack of oxygen, the bacteria must adapt to anoxic conditions and switch to nitrate as an electron acceptor (micro-aerophilic and anaerobic conditions). The adhesion in section 3 is similar to section 2. The increase in adhesion near the end can be attributed to semi-aerobic conditions near the outflow side.

In Figure 5-6, it can be seen that the free-flow mass for Pipe 2, section 1 and 2 is higher than for Pipe 1. A reason for this might be the high flow rate in the pipe. It seems as if the bacteria have difficulty adhering to the pipe and remain in suspension. A very low percentage adhesion was obtained in Pipe 2.

The results of the pipe experiments showed very valuable information with regards to injection rates of bacteria and media. The results showed that with lower flow rates, higher adhesion will be obtained.

See Appendix B for pipe experiment data.

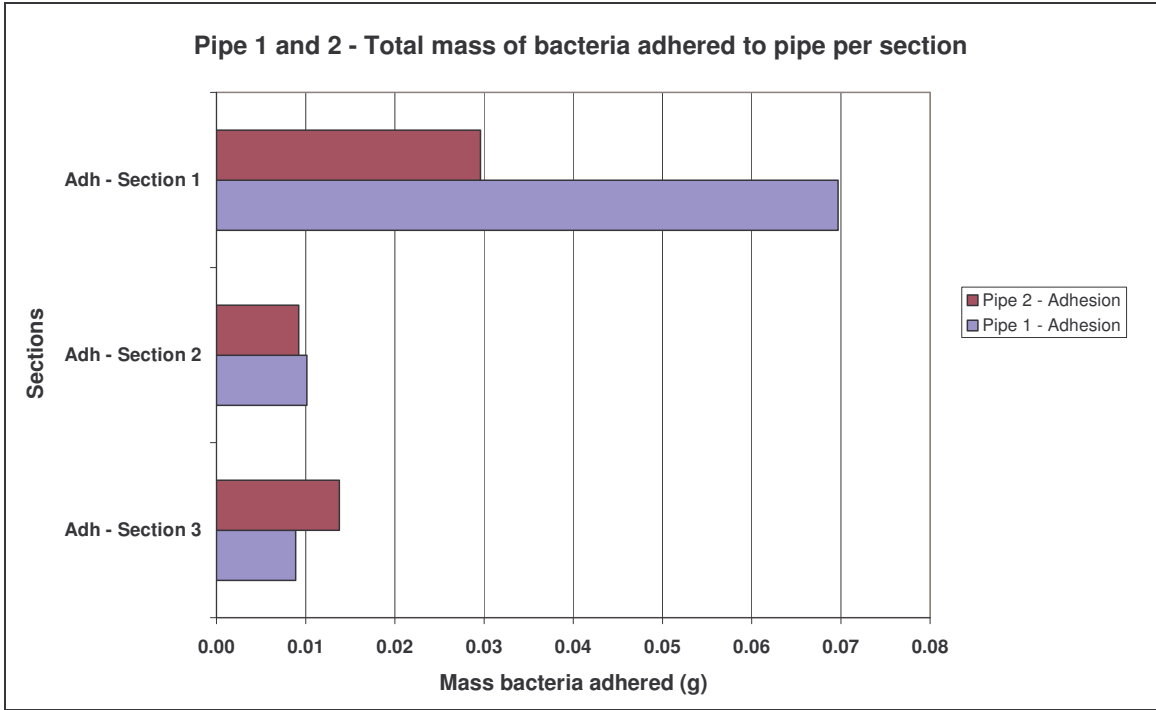


Figure 5-5 Results from the adhesion mass in Pipe 1 and Pipe 2.

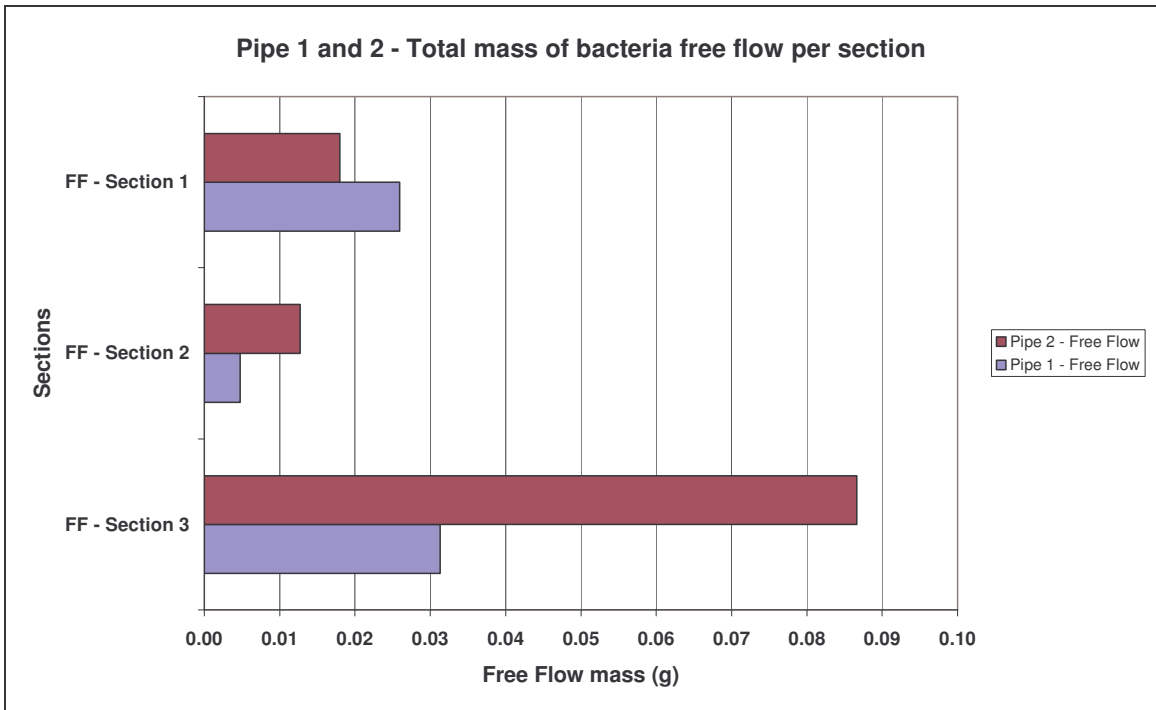


Figure 5-6 Results from the free-flow mass in Pipe 1 and Pipe 2.

5.1.4 Conclusions for the pipe experiments

From the pipe experiment, the following conclusions can be made:

During the ten-day period, it was observed that the bacteria have the ability to create a blockage in the pipes, but due to constant pumping (and therefore changes in hydraulic head) and the non-adhesive surface of the pipes, the blockage moves through the pipe. To prevent this from happening, a constant head system was installed, with the same results.

From the results of the pipe experiments, it can be seen that the bacteria have the ability to adhere especially in lower flow systems. Because of adhesion and growth in Pipe 1 (low flow rate), the free-flow volume decreased in the first two sections.

From this experiment, it can be seen that lower flow rates are advisable for upscaling experiments, and that the bacteria need adhesion surfaces to enhance growth and clogging. It can thus be concluded that the pipe experiment is not an ideal representation for bacteria clogging in a fracture system, since fracture flow characteristics are very different from pipe flow.

5.2 TESTING BIOBARRIER IN A SANDSTONE PARALLEL PLATE FRACTURE

The concept of the sandstone parallel plate fracture experiment was inspired by the research done by Hill and Sleep (2001). Laboratory-scale experiments were performed by Hill and Sleep (2001) to assess the effects of biofilm growth on flow and transport through a sandblasted glass parallel plate fracture.

In the experiment of Hill and Sleep (2001), the fracture for the experiment was constructed from two sandblasted glass plates, 6 mm thick, 21 cm wide and 28 cm long. The aperture of the fracture was 560 μ m (0.56 mm).

The effect of biofilm growth on flow and transport through porous media has been studied by many researchers. Hydraulic and tracer tests through rock fractures and artificial fractures have also been performed by many researchers in both laboratory experiments (Cliffe *et al.*, 1993; Dronfield and Silliman, 1993; Grisak and Pickens, 1981; Moreno *et al.*, 1985; Sonnenborg *et al.*, 1999) and field experiments (Becker and Shapiro, 2000; McKay *et al.*, 1993; Novakowski and Lapcevic, 1994).

5.2.1 Experiment 1 – 1.3 mm aperture

Laboratory experiments were performed to assess the effects of biofilm growth on transport through a controlled sandstone fracture and the effect on the hydraulic conductivity of the fracture.

The reason for using sandstone plates was because the site used for the field application of biobarrier formation is underlain by a series of mudstones and sandstones from the Adelaide Subgroup. The Mode I fracture at the campus test site at the University of the Free State is located in the sandstones.

This apparatus was built to represent the Mode 1 fracture at the campus test site. The purpose of this experiment was to assess the viability of biobarrier formation in fractures and expected constraints on the upscaling.

5.2.1.1 Materials and set-up of experiment

The apparatus was made of glass. The dimensions for the apparatus were as follows: 0.5 m high, 1 m long, and 0.4 m in width. See Figure 5-7 for set-up of the apparatus.

The apparatus was divided into three sections (see Figure 5-8):

The upper section was constructed above the sandstone fracture. This area was sealed from the other sections and filled with water to represent a saturated aquifer above the fracture.

The centre section (fracture section) consisted of two sandstone plates (0.8 m long, 0.4 m in diameter and 0.02 m thick). The aperture between the two sandstone plates was 0.0013 m (1.3 mm). The plates were separated using 12 plastic shims (0.02m long, 0.01 m in diameter and 0.013 m thick). The fracture section is connected to the in- and outlet areas. These are both 0.5 m high, 0.4 m in diameter and 0.1 m in length. The in- and outlet areas represent the injection and abstraction boreholes of the field experiment. Although the shims represent some deviation from a perfect parallel plate, their presence makes the experiment more representative of the field conditions.

The bottom section is located below the sandstone plates. This area was also filled with water to represent saturated conditions.

Light sensors were installed at the front of the apparatus in the area of the fracture. The purpose of the light sensors was to measure the optical resistance through the fracture aperture with time. A beam light was installed at the back of the apparatus in the location of the fracture. Light reflected through the fracture and the optical resistance was measured at the front, at the sensors, by making use of a volt meter. Fifteen sensors were installed over the fracture area, starting from the inlet side. See Figure 5-7 and Figure 5-9C for respectively the location and close-up photo of the light sensors.

Water level controllers were installed at the inlet side of the fracture. The purpose of the water level controllers was to regulate the gradient at the injection side (refer to section 5.2.2).

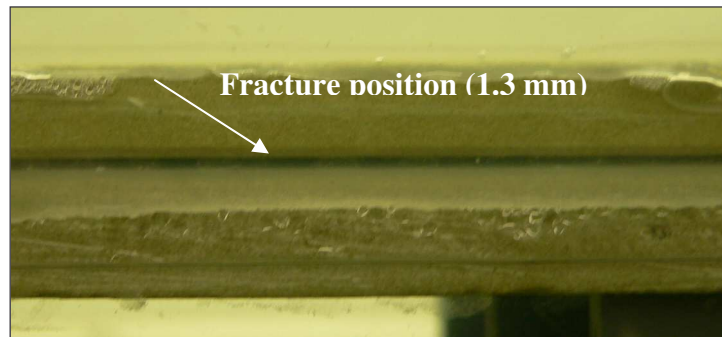
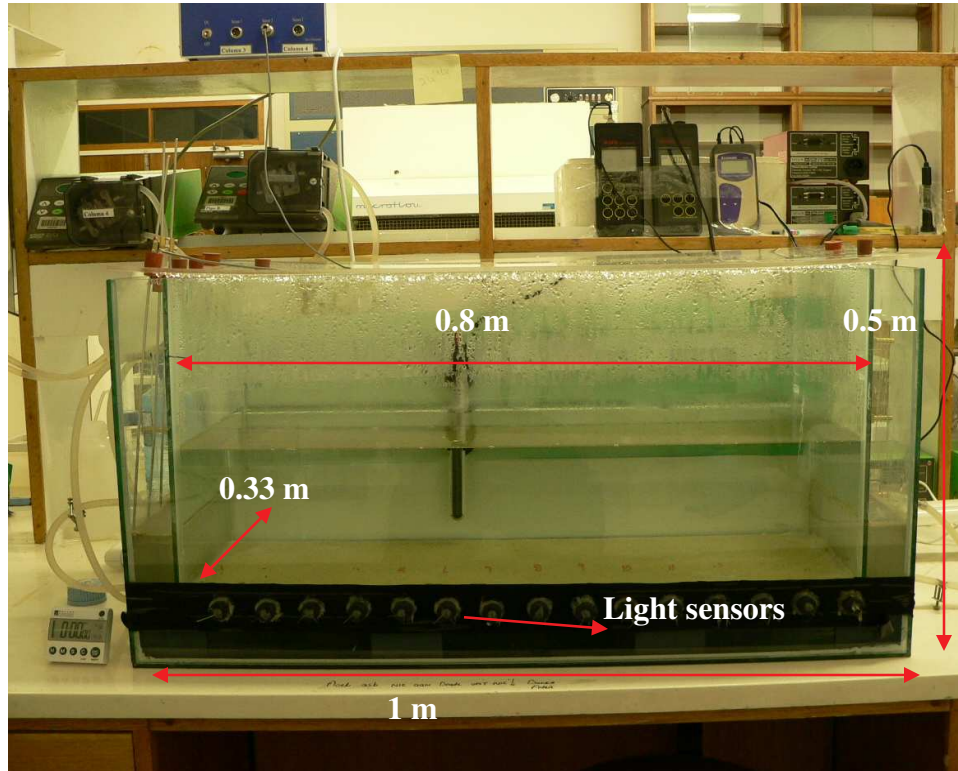


Figure 5-7 Set-up of the sandstone parallel plate experiment apparatus.

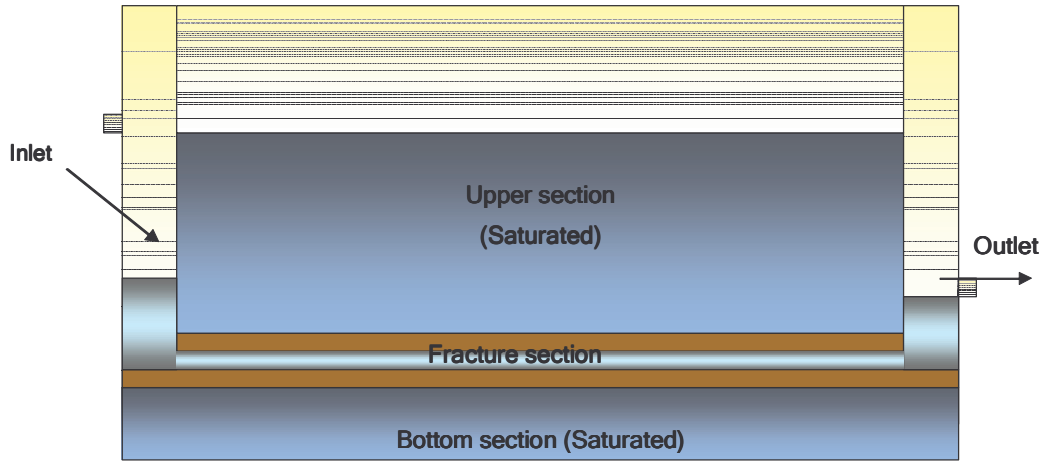


Figure 5-8 Horizontal parallel plate fracture apparatus showing the three sections.

5.2.2 Methodology

For the duration of the experiment, the fracture was operated under conditions of constant inlet and outlet head. Bacteria and media were injected simultaneously through the parallel plate fracture from supply bottles. The bacteria and media flowed through the fracture from the inlet side and exited via the outlet (outflow nozzles). The reduction in flow was determined by measuring the time for two pore volumes to flow through the fracture.

For the purpose of the experiment, a constant head was kept at the injection side of the parallel plate fracture. The gradient was maintained by means of a water level controller. The water level controller was operated as follows (see Figure 5-9): (A) Two peristaltic pumps were connected to an electric water level controller box (blue box). (B) The electric water level controller was connected to two floating sensors located at the injection side of the fracture. One sensor was at the water level and the other 1 mm above the water level. During the injection of bacteria and media, the sensors regulated the water level. When the water level dropped by 1 mm, the pumps switched on. When the water level gradient stabilised, the pumps stopped. This method successfully regulates the injection with little change in the gradient.

(C) Before the daily injection of bacteria and media, the optical resistance (ohm) was measured at each sensor to determine the growth of the bacteria in the location of each sensor.

5.2.3 Experimental approach

The following test was conducted on the sandstone parallel plate fracture:

- The theoretical hydraulic conductivity was determined using the parallel plate assumptions.
- A NaCl tracer and bacteria transport test were performed on the parallel plate fracture.
- The experiment was initiated by inoculating the fracture with bacteria and media on a daily basis to encourage growth. Two pore volumes (one pore volume of bacteria and one pore volume of media) were injected daily to test the reduction of the hydraulic conductivity of the fracture.
- Parameters (pH, EC, OD and DO) were measured at the fracture daily. The pH, EC, OD and DO and bacteria mass of the outflow were also measured.

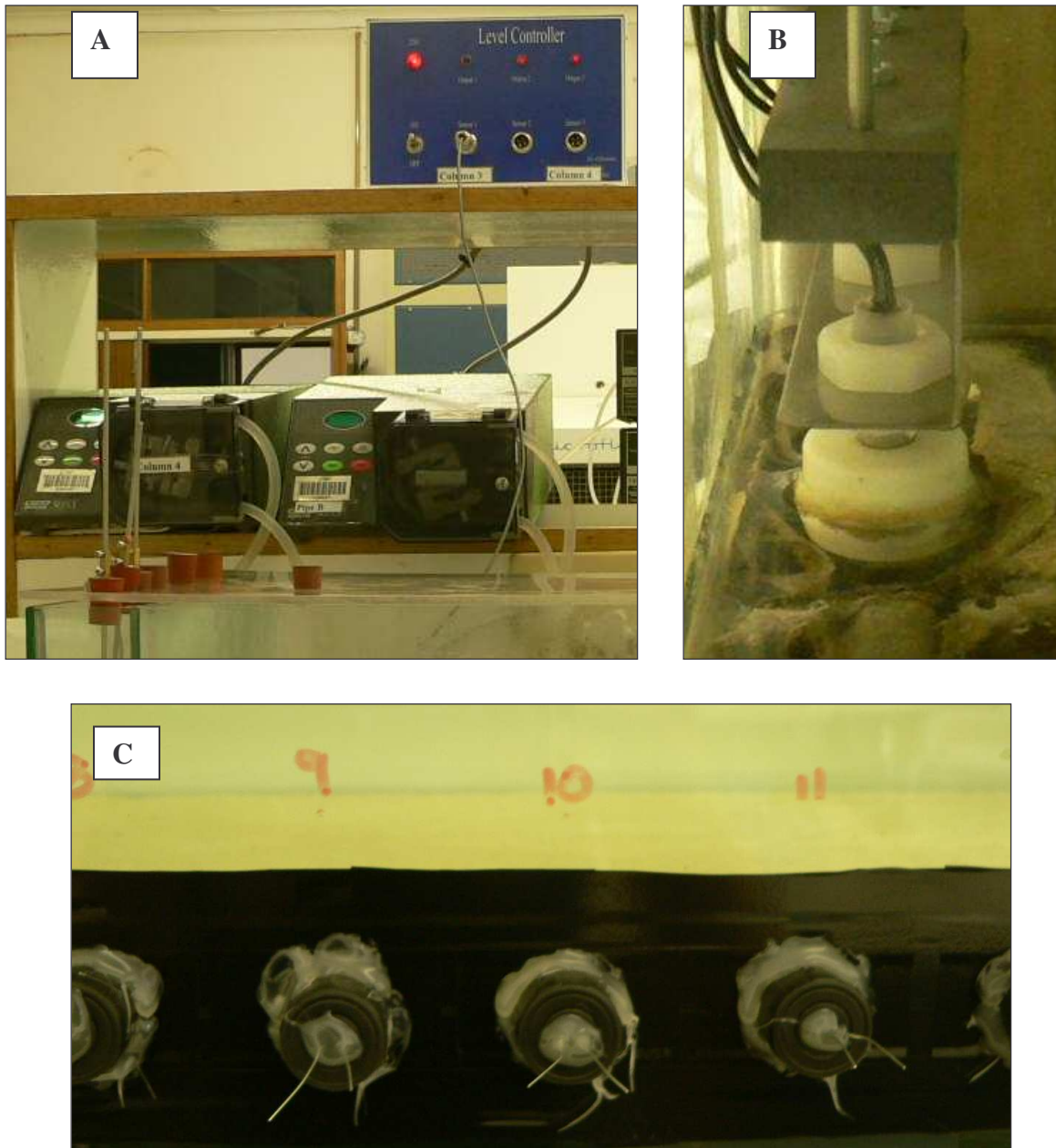


Figure 5-9 Set-up of the parallel plate fracture apparatus - Water level controllers and light sensors.

5.2.4 Procedure

Hydraulic and tracer tests were performed before the biofilm growth test to establish baseline conditions.

Researchers in the field of fracture flow used to consider a rock fracture as a pair of parallel plates separated by a constant distance, b , which represented the aperture of the fracture. Since fractures consist of rough walls, channeling and closings, they cannot be represented correctly by a unique fracture aperture. Therefore the term “equivalent aperture” was introduced to describe the effective aperture contributing to flow or transport in the fractured rock. There are three common definitions and estimations of the “equivalent aperture” with respect to different measurements. According to Tsang (1992), they are called mass balance aperture, frictional loss aperture and cubic law aperture (Riemann, 2002).

The hydraulic conductivity of the fracture was calculated using the parallel plate theory.

A hydraulic conductivity of approximately 17000 m/d was calculated for the fracture with an aperture of 1.3 mm.

5.2.5 Conservative and bacteria transport tests

A NaCl tracer was used to determine the conservative migration through the created fracture. A conservative tracer solution (NaCl) was prepared, with an electrical conductivity of 600 mS/m.

During conservative tracer transport in fractures under laminar flow conditions the following will happen: tracer will disperse both by molecular diffusion perpendicular to flow as well as variation in the velocity profile across the fracture in the direction of flow. The fluid closer to the walls will flow more slowly than fluid in the aperture centre. This will cause the tracer to advect with the fluid, and spread longitudinally. This can create a concentration gradient in the transverse direction that, in turn, causes diffusion towards fracture walls. From Figure 5-10 it can be seen that the fast flowing centre aperture fluid passes through the system after 0.0625 pore volume. Higher velocities and lower diffusion results in significant longitudinal dispersion and a nearly parabolic concentration profile across the aperture (Zimmerman *et al.*, 2002). Peak concentrations were measured after 1 pore volume and started to deplete over time.

A bacteria transport test was also performed to determine the transport of bacteria through the parallel plate fracture. Nine hundred millilitres of solution, with a bacteria concentration of 10^8 cells/ml (OD = 0.15) was used as a tracer. From Figure 5-10 it can

be seen that bacteria transport is much slower than the conservative tracer transport. The front of the bacteria exits the fracture after 0.5 of a pore volume. Peak bacteria concentrations were measured after 1.25 pore volumes. In the case of bacteria transport, adhesion to the fracture walls can occur. This results in significant longitudinal dispersion and a parabolic concentration profile across the aperture. From the results of the breakthrough curves it can be seen that the bacteria take much longer to be transported through the fracture than the conservative tracer.

The software program TRACER (Riemann, 2002) was used to analyse the NaCl and bacteria tracer data. A tracer velocity of 147 m/d was calculated for the conservative tracer and a velocity of 61 m/d for the bacteria in a fracture with an aperture of 1.3 mm.

The results from the TRACER analyses showed that the conservative tracer is transported twice as fast as the bacteria. The lower velocity of the bacteria might be attributed to bacteria adhesion to the fracture walls. See Figure 5-11 and Figure 5-12 for breakthrough fittings of the NaCl tracer and bacteria.

breakthrough curve. A summary of the transport parameters can be seen in Table 5-1.

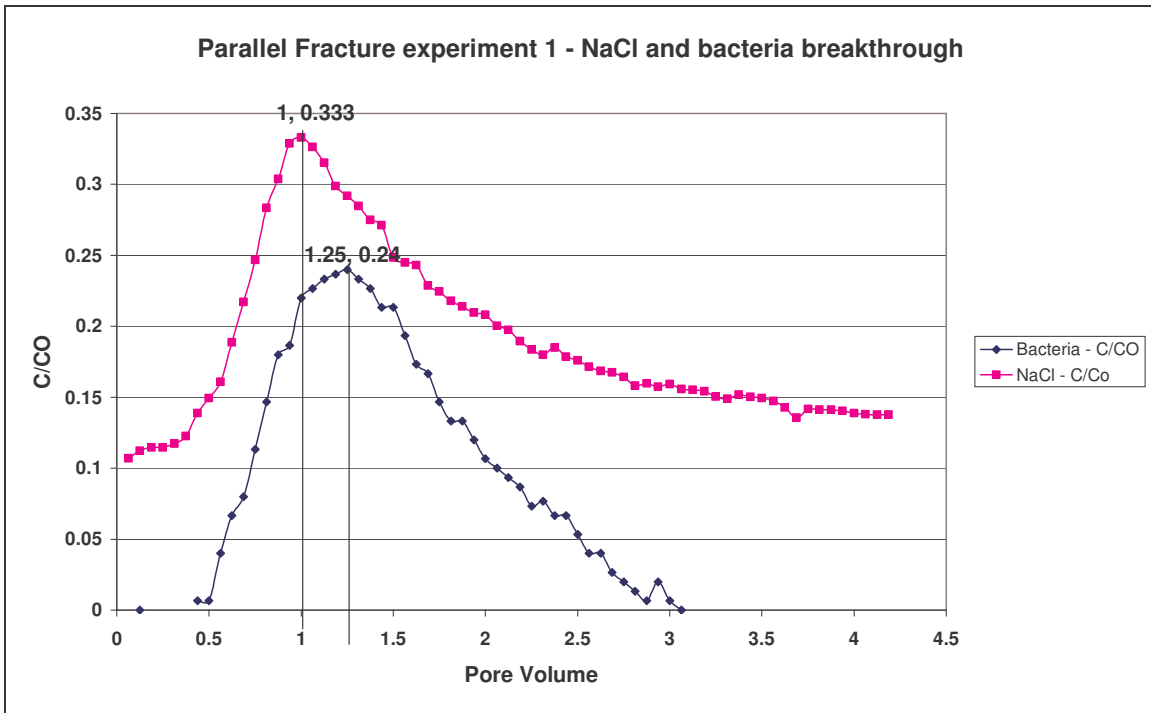


Figure 5-10 Sandstone parallel plate NaCl and bacteria breakthrough curve.

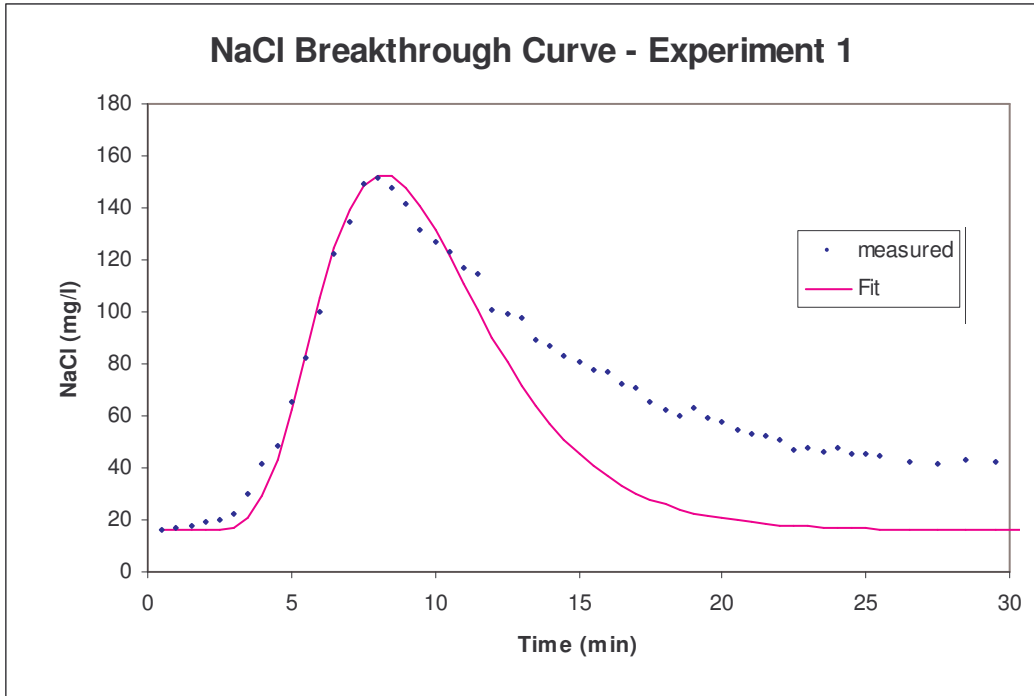


Figure 5-11 Results from the tracer fit for NaCl breakthrough curve in Experiment 1 of the horizontal parallel plate fracture.

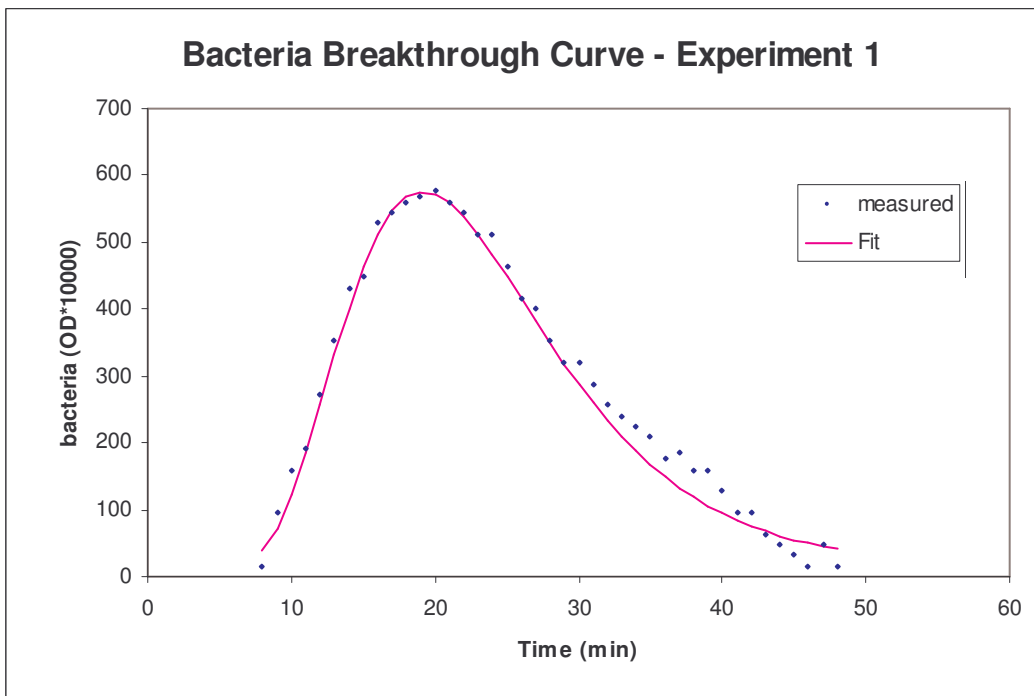


Figure 5-12 Results from the tracer fit for bacteria breakthrough curve in Experiment 1 of the horizontal parallel plate fracture.

Table 5-1 Summary of the transport parameters calculated by TRACER for Experiment 1.

Horizontal parallel plate fracture - Experiment 1		
Tracer	Velocity v_f (m/d)	Dispersivity (m)
NaCl	147	0.06
Bacteria	61	0.07

5.2.6 Results from the EC, pH, OD, mass outflow and DO measurements

Two pore volumes of bacteria and media were pumped through the fracture on a daily basis. The fracture was operated under constant hydraulic head (0.012) conditions for 30 days. The temperature in the fracture was between 21 and 23°C, which is representative of the aquifer. *In situ* effluent, dissolved oxygen concentrations, pH, EC, and optical density of the effluent were measured daily at the outlet side. The pH values in the fracture were very similar during the experiment, ranging between 6.2 and 7.2. A large increase was measured on the first day for the EC, but can be attributed to media injection. For the rest of the injection period the EC values were of the same order. See Appendix B for results for the pH and EC.

The optical density of the outflow was very high during the first seven days. After the seventh day, the OD started decreasing rapidly. The colour of the outflow changed from cream to grey. A distinct H₂S smell was also detected. During closer investigation, it was determined that, because of the SO₄ rich media, a sulphate reducing bacterium was activated. The bacterium was identified by the Department of Microbiology, Biotechnology and Food Biotechnology as *Desulfovibro*. Sulphate-reducing bacteria (SRB) are a diverse group of bacteria found in a variety of anaerobic environments, and all members possess the ability to use sulphate as a terminal electron acceptor.

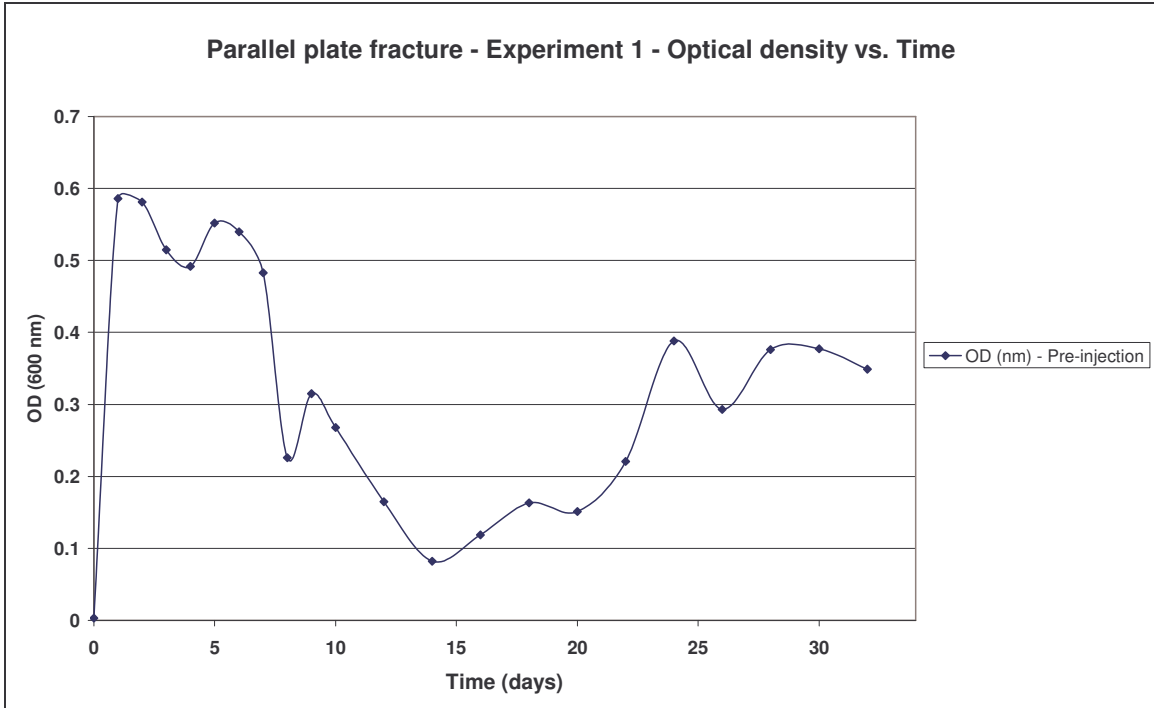


Figure 5-13 Parallel plate fracture experiment - OD vs. time graph.

Figure 5-14 shows the mass outflow vs. time. On the fourteenth day, very little mass was recovered. This can be compared to the good results for the reduction in flow on Day 16 (See Figure 5-17). Because very few bacteria flushed from the fracture, there were large numbers of bacteria to reduce the hydraulic conductivity of the fracture.

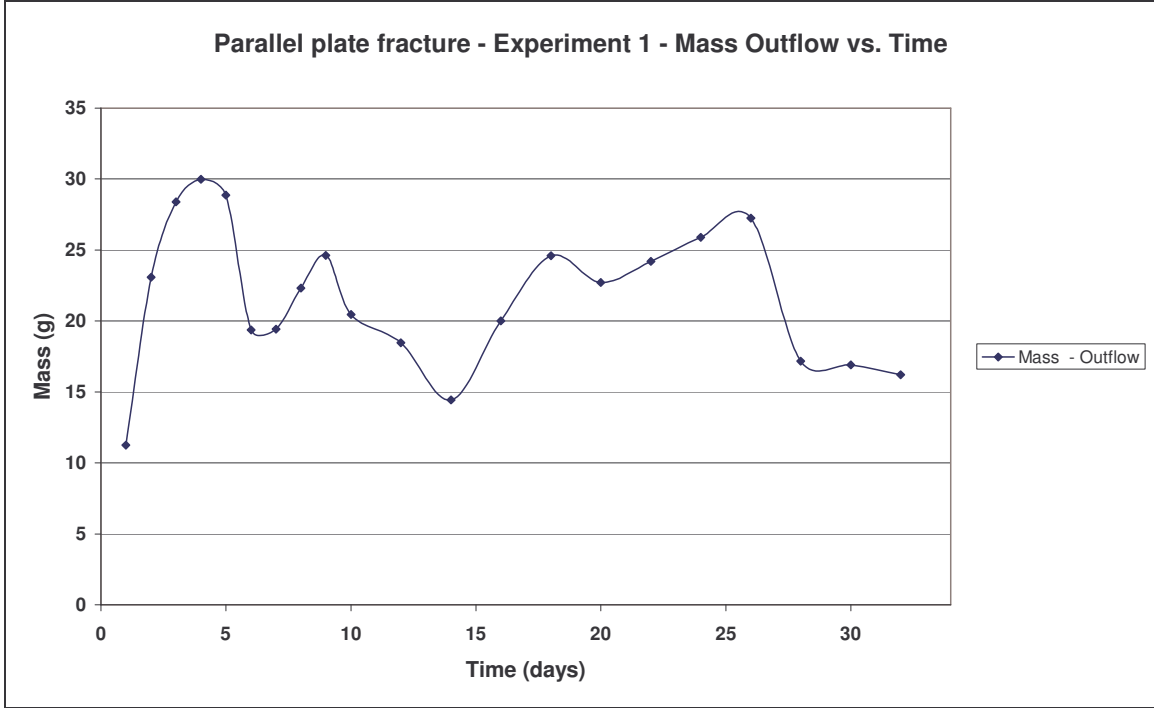


Figure 5-14 Parallel plate fracture experiment - Mass outflow vs. time graph.

The dissolved oxygen was generally lower than 0.2 mg/l. Thus, the system can be classified as an anaerobic system. See Figure 5-15 for the dissolved oxygen versus time graph. During Day 21, the bacteria and media injected, were placed on magnetic stirrers to aerate the injected solution. As can be seen in Figure 5-15, this caused the dissolved oxygen in the fracture to increase.

The EC versus time were measured at the outflow side on a daily basis, over the injection period of 2 pore volumes. From Figure 5-16, it can be seen that the EC is very stable (on average between 650 and 800 mS/m).

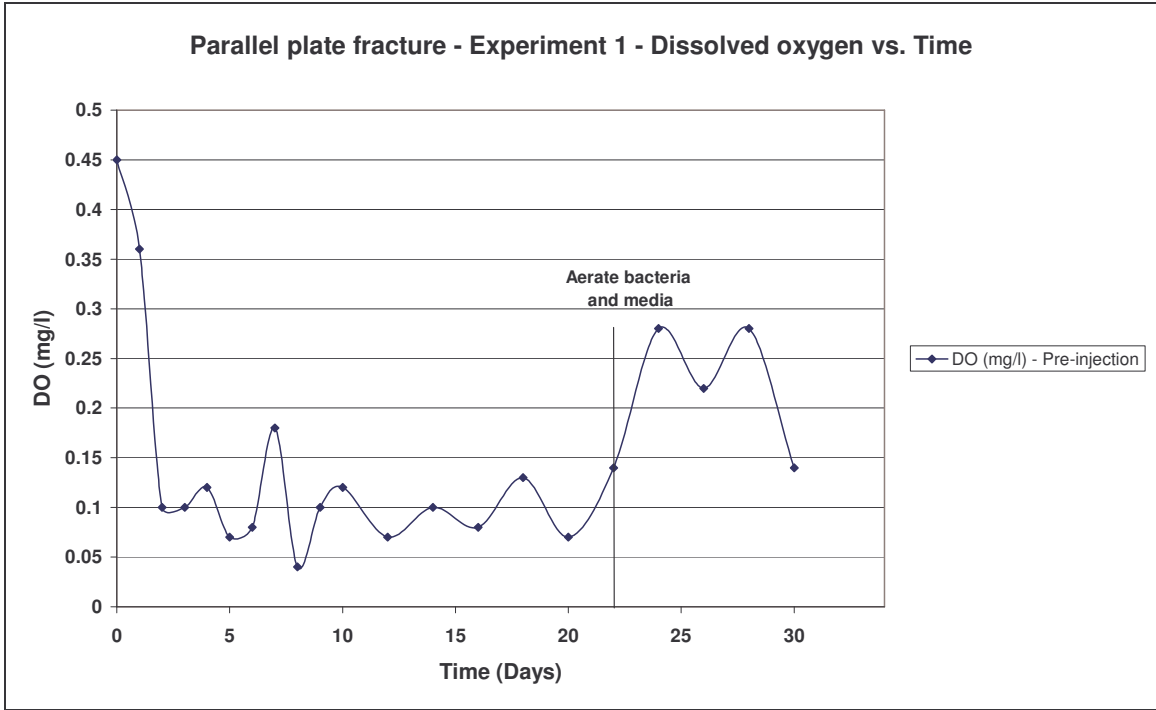


Figure 5-15 Parallel plate fracture experiment - DO vs. time graph.

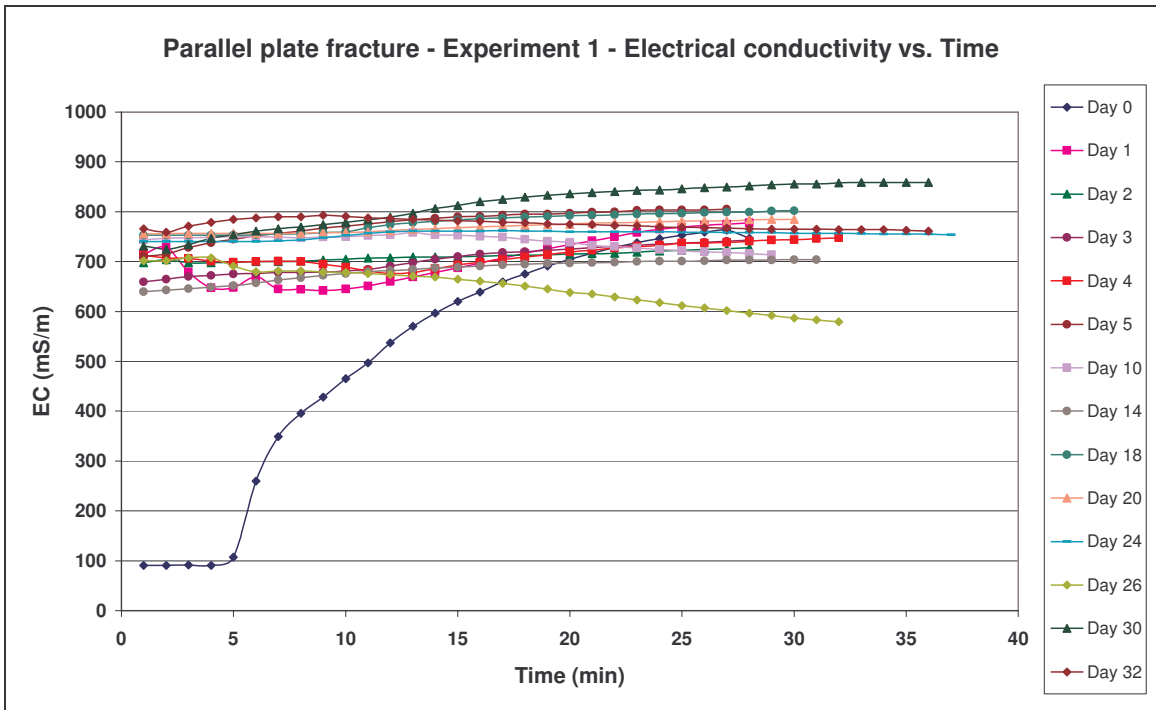


Figure 5-16 Parallel plate fracture experiment - EC variation during throughflow of 2 pore volumes.

5.2.7 Hydraulic conductivity (K) reduction test

A hydraulic conductivity reduction test was done on a daily basis during bacteria and media injection. From the results of the flow reduction, it can be seen that the bacteria have the ability to reduce the flow of the fracture. After four days, the flow was reduced by 16%, but unfortunately the experiment was disturbed by moving of the apparatus and the flow returned back to normal. After ten days, bacteria and media were injected every second day. A very gradual reduction in flow was measured over the first 16 days. The slow reduction in flow was attributed to the lower bacteria and media injection frequency.

The results demonstrate that the growth of biomass can reduce the hydraulic conductivity of a fracture with an aperture of 1.3 mm by approximately 35%. It is expected that this could be further reduced but the time period is considered too long for practical application.

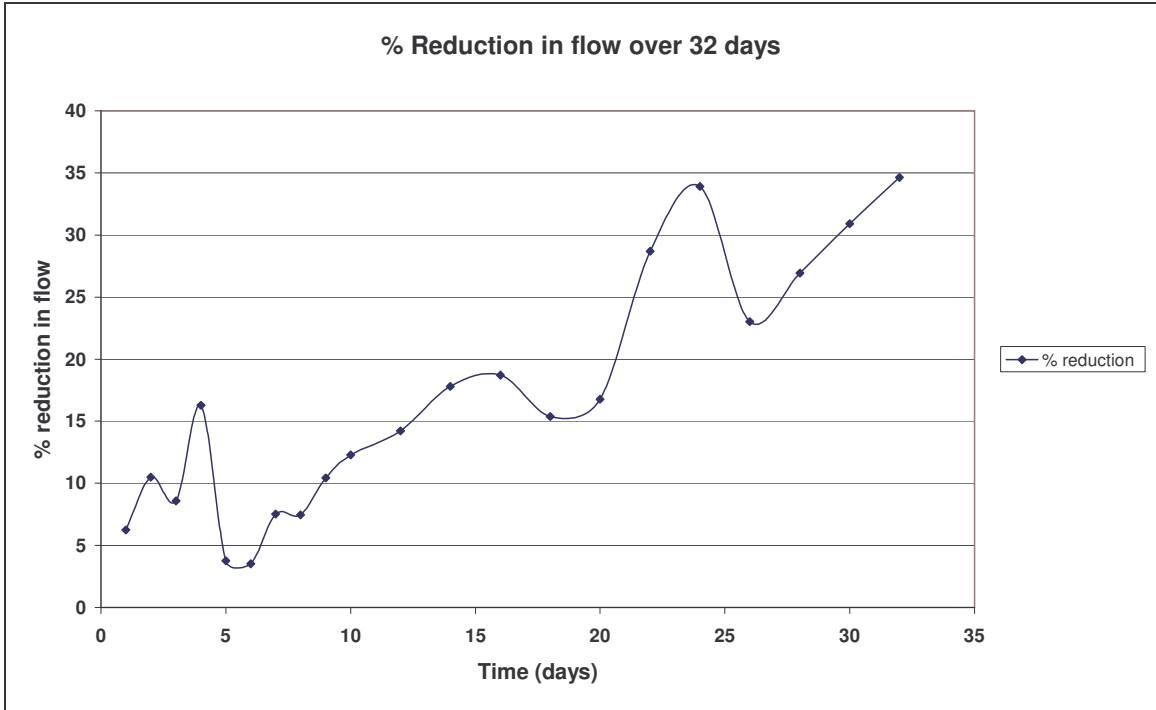


Figure 5-17 Parallel plate fracture experiment - Percentage flow reduction over two pore volumes.

5.2.8 Light sensors

The light sensors were read on a daily basis. The optical resistance for the light was measured. The highest value measured is 35 ohm which is an indication of no light measured at the sensor, and can be attributed to clogging of the fracture in the position

of the sensor. Lower values are an indication of no clogging in the position of the sensor. When the results from the flow reduction are compared with the light sensor data, it can be seen that reduction in flow is related to clogging in parts of the fracture. A very good example of this is during Day 14 and 16, very high values were measured (no light was measured) at sensor 1, 11, 14 and 15. This can be attributed to clogging of the fracture in these areas. Clogging is more prominent at the end of the fracture and can be attributed to blockages in the beginning and centre parts, moving to the end of the fracture.

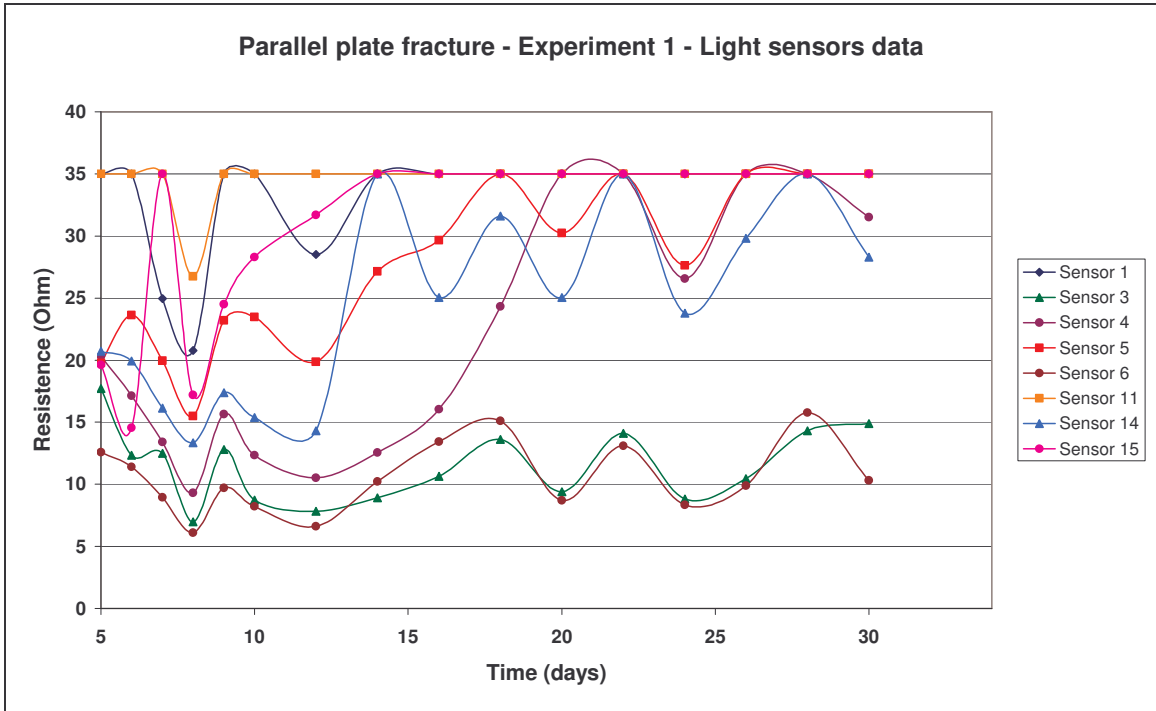


Figure 5-18 Parallel plate fracture experiment - Light sensor data.

5.2.9 Visible bacteria growth

During the experiment, the growth of biomass was visually inspected at the inlet and outlet sides. In Figure 5-19 bacteria growth can be seen on the sides of the glass and on the surface of the fluid at the inlet and outlet side.

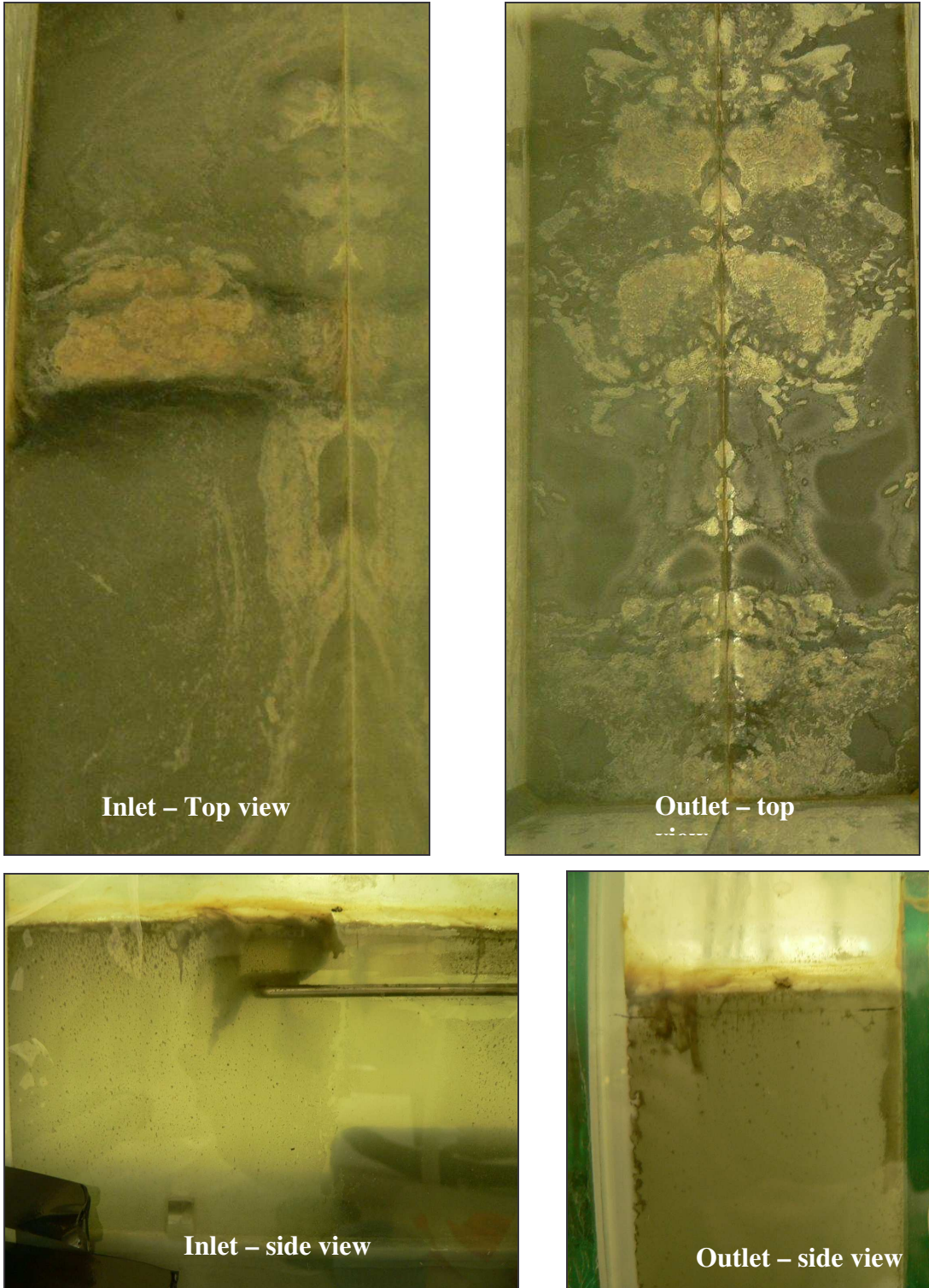


Figure 5-19 Bacteria growth at inlet and outlet sides.

5.2.10 Summary and conclusions of the parallel plate fracture – Experiment 1

Tracer and bacteria transport

Results from the TRACER software showed that due to the high velocity of the tracer, advection is dominant. Bacteria transport will be affected by longitudinal dispersion and bacteria adhesion.

Hydraulic reduction test

A 16% reduction in flow was measured after four days. Due to the movement of the apparatus after four days, the flow increased. After ten days, the media and bacteria injection was changed to every second day. After 16 days, a 16% reduction in the flow was measured. The highest reduction was measured after 24 days at 33%. The reasons for the low reduction values could be the following: (The following points can also be seen as recommendations for upscaling to a field test).

- Too little bacteria and media were injected prior to establishing biomass and thus biobarrier formation.
- The fracture aperture might be too large, causing the bacteria to flush out of the fracture instead of adhering and building a biobarrier.
- Because of the high sulphate concentrations in the media, a sulphate reducing bacterium, *Desulfovibro*, was activated. Due to anaerobic conditions, *S. marcescens* lost its ability to dominate due to a lack of nitrate which acts as the electron acceptor. *Desulfovibro* used the sulphate as an electron acceptor and started to dominate in the parallel plate fracture.
- The media must be optimised (nitrate concentrations must be increased) to ensure that *S. marcescens* is the dominant bacterium during biobarrier formation.

From the results of Experiment 1, it can be seen that it is possible to reduce the flow in a relatively large fracture by approximately 35%. This shows that it will take time to build biobarriers in fractures with larger apertures.

5.3 EXPERIMENT 2 – 0.8 MM APERTURE

The horizontal parallel plate fracture experiment was repeated to implement the recommendations made during Experiment 1. The fracture aperture was reduced to 0.8 mm, to assess the effects on transport, biofilm formation and reduction in the flow through the parallel plate fracture.

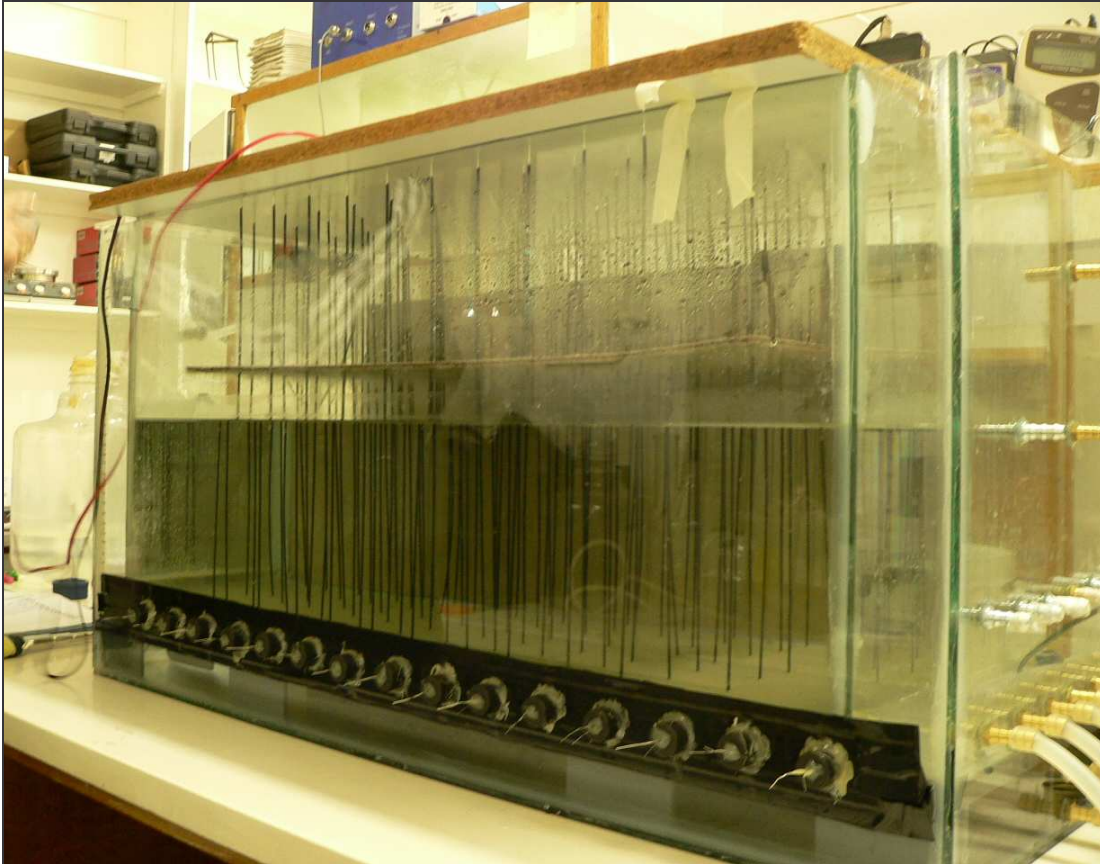


Figure 5-20 Parallel plate fracture experiment apparatus.

5.3.1 Experimental approach

The following test was conducted on the sandstone parallel plate fracture:

- The theoretical hydraulic conductivity was determined using parallel plate assumptions.
- A NaBr tracer breakthrough test and bacteria transport test were performed on the parallel plate fracture.

- A biofilm experiment was initiated by inoculating the fracture with bacteria and media on a daily basis to encourage growth. Two pore volumes (one pore volume bacteria and one pore volume media) were injected twice per day. The fracture was operated under a hydraulic head of 0.012. The hydraulic reduction in the fracture was measured on a daily basis.
- Several parameters (pH, EC, OD and DO) were measured daily at the outlet side.

5.3.2 Procedure

During Experiment 1, a sulphate reducing bacteria, namely *Desulfovibrio*, started to grow in the parallel plate. To prevent this, the two sandstone plates were autoclaved prior to the experiment, to sterilise the plates. Component B was also changed. The sulphate concentration in the media was decreased to prevent *Desulfovibrio* from growing and multiplying. The KNO₃ concentration was increased from 10 mg to 100 mg. Component B was prepared as follows: 20× BSM B. NTA 2.46g N(CH₂CO₂Na)₃·H₂O, 0.16g FeSO₄·7H₂O, 2g MgSO₄·7H₂O, 0.06g MnSO₄·7H₂O, 0.06g ZnSO₄·7H₂O, 0.02g CoCl₂·6H₂O and 1 ml trace elements. A glucose concentration of 1 g/l was used.

5.3.3 Conservative and bacteria transport tests

Hydraulic and tracer tests were performed prior to the biofilm growth test to establish baseline conditions. The hydraulic conductivity of the fracture was calculated with the cubic law equation.

A hydraulic conductivity of approximately 6000 m/d was calculated for the fracture.

A NaBr tracer (20 mg/l) was used to determine the breakthrough of a conservative tracer through the parallel plate. See Figure 5-21 for the tracer breakthrough curve. A 250 ml NaBr solution of the above-mentioned concentration was injected to determine the transport.

The leading edge of the NaBr tracer front passes through the system after 0.0046 of a pore volume. After one pore volume (1.2 l), a peak was reached, which decreased over time. The system reverts to pre-tracer levels after 2.7 pore volumes.

When comparing the total tracer recovery of experiment 1 and 2 (See Figure 5-11 and Figure 5-21), it can be seen that much higher tracer recovery was measured in

experiment 1. This can be attributed to very high concentration of NaCl (600 mS/m) used. For experiment 2, a much lower Br⁻ (20 mg/l) concentration was used.

A bacteria breakthrough test was also performed in the fracture to determine the transport of bacteria. When the breakthrough of the conservative tracer and the bacteria are compared, it can be seen that the bacteria transport is much slower than that of the conservative tracer. After 1.4 pore volumes, the bacteria solution reaches a peak and decreases over time. Lower transport rates of the bacteria can be attributed to bacteria adhesion and large dispersion in the direction of flow. See Figure 5-21 for NaBr and the bacteria breakthrough curve.

The dispersivity and velocity for NaBr and the bacteria were calculated with the TRACER software (Riemann, 2002). A dispersivity of 0.06 m and a tracer velocity of 151 m/d were calculated for the conservative tracer transport through the fracture (aperture 0.8 mm) showing that advection dominates. The bacteria transport was much slower. A velocity of 68 m/d was calculated for the bacteria.

When the results of the tracer test of Experiment 1 and 2 are compared, it can be seen that the velocities are almost the same although different apertures were used. This can be attributed to different gradients used. See Figure 5-22 and Figure 5-23 for the fitting of the NaBr and bacteria breakthrough curves and Table 5-2 for a summary of the transport parameters of the NaBr and bacteria.

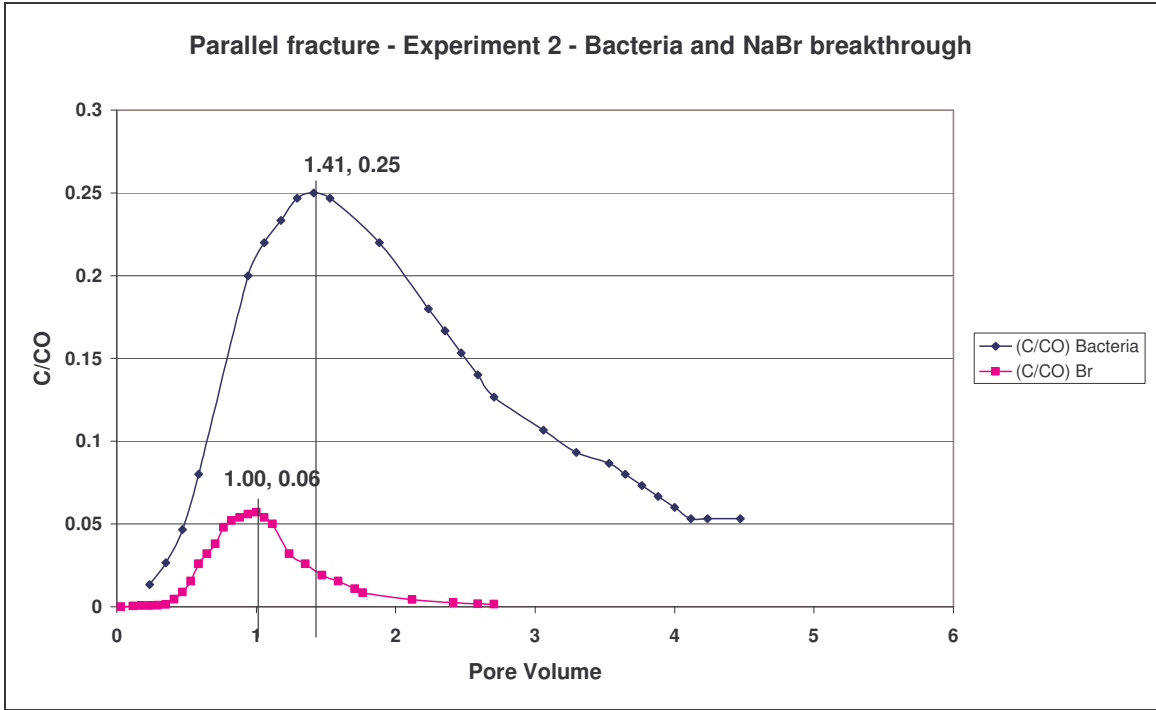


Figure 5-21 Parallel plate fracture - NaBr and bacteria breakthrough curve.

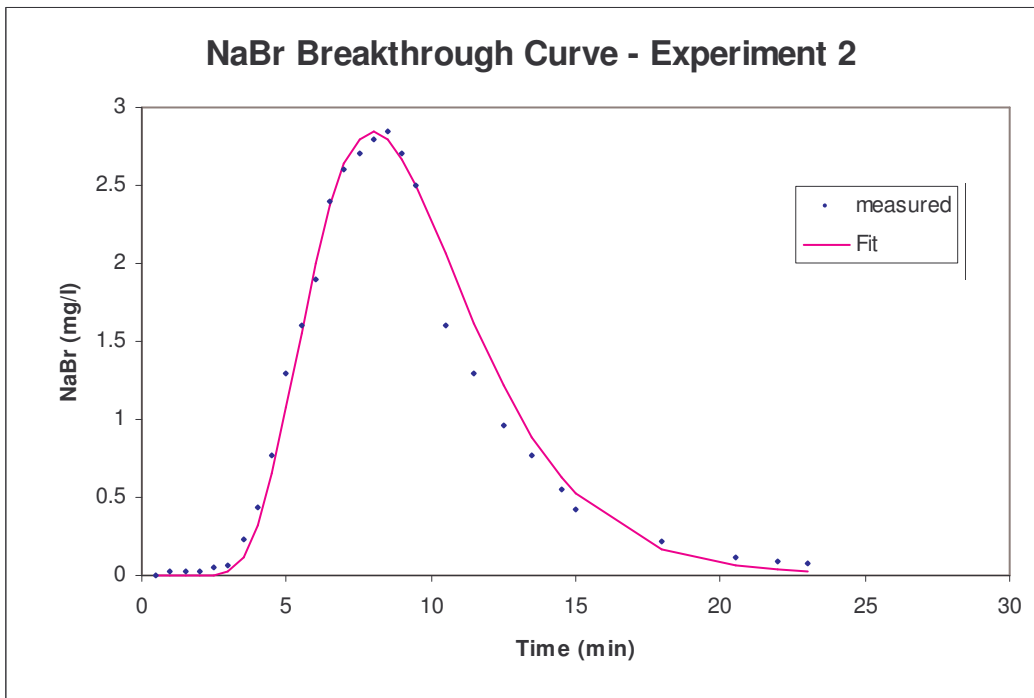


Figure 5-22 Results from the tracer fit for NaBr breakthrough curve in Experiment 2 of the horizontal parallel plate fracture.

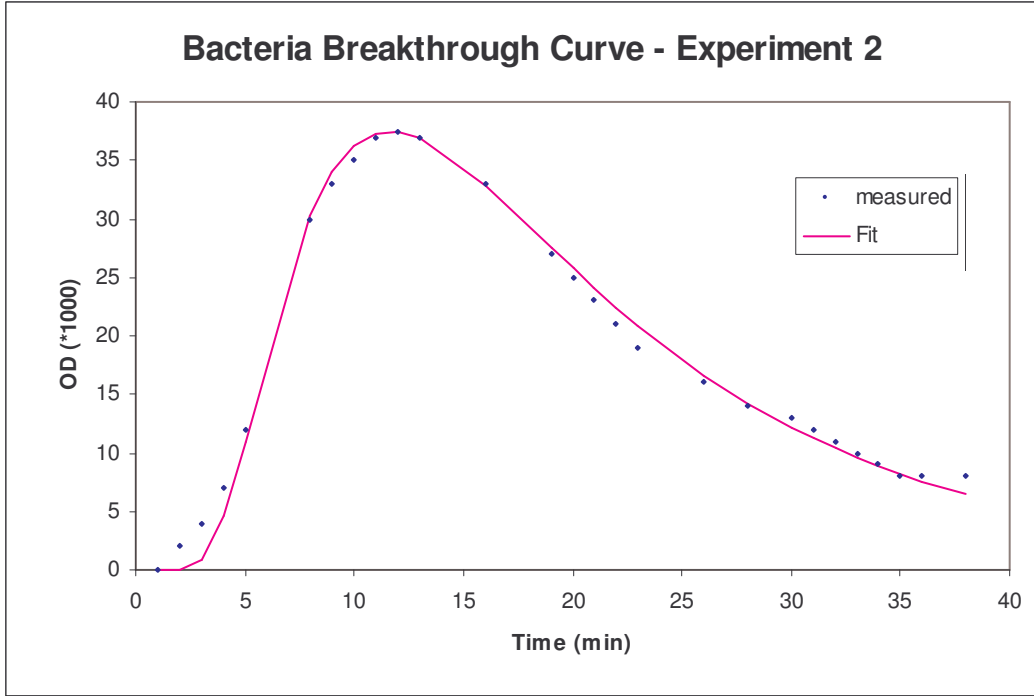


Figure 5-23 Results from the tracer fit for NaCl breakthrough curve in Experiment 2 of the horizontal parallel plate fracture.

Table 5-2 Summary of the transport parameters calculated by TRACER for Experiment 2.

Horizontal parallel plate fracture - Experiment 2		
Tracers	Velocity v_f (m/d)	Dispersivity (m)
NaBr	151	0.06
Bacteria	68	0.21

5.3.4 Results from the EC, pH, OD and DO measurements

The fracture was operated under a constant gradient of 0.012. Bacteria and media injection occurred twice per day for the first 20 days. Thereafter, bacteria and media injection occurred in the mornings and only media injection in the afternoons. The fracture was operated for 32 days under constant gradient conditions. The temperature in the fracture was between 21 and 23°C. Dissolved oxygen concentrations, pH, EC, and optical density of the effluent were measured daily at the outlet.

See Figure 5-24 to Figure 5-26 for results from the parameter measurements at the outlet on a daily basis. The pH values were very similar and varied between 6.5 and 7. See Appendix B for pH data.

The EC increases rapidly over the first few days. After five days, a sudden decrease in the EC values was measured. After seven days the EC stabilised and increased gradually. A very large increase in the EC was observed after Day 21 (See Figure 5-24). From the afternoon of Day 20 onwards, only 1 pore volume of media was injected. This effect can also be seen in the EC variation during the two pore volume injection (See Figure 5-25). The implications of only media injection is that the media is not diluted with bacteria during injection, thus higher concentrations of media are available for the bacteria in the fracture to consume.

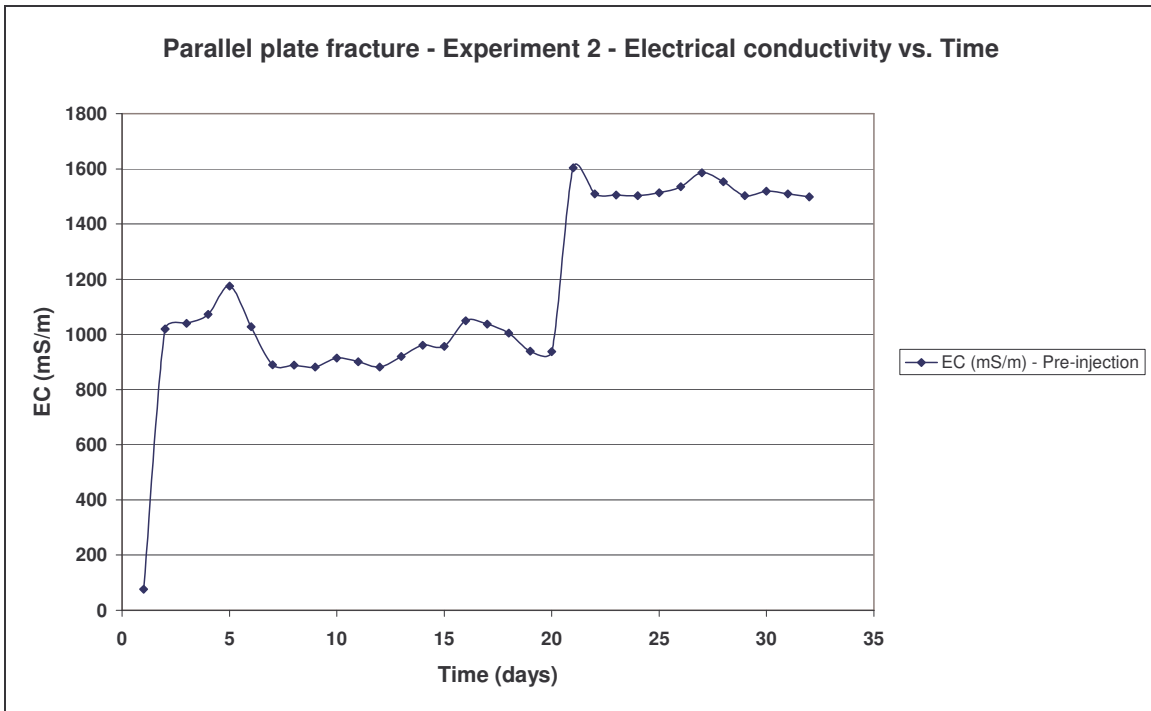


Figure 5-24 Parallel plate fracture experiment - EC vs. time graph.

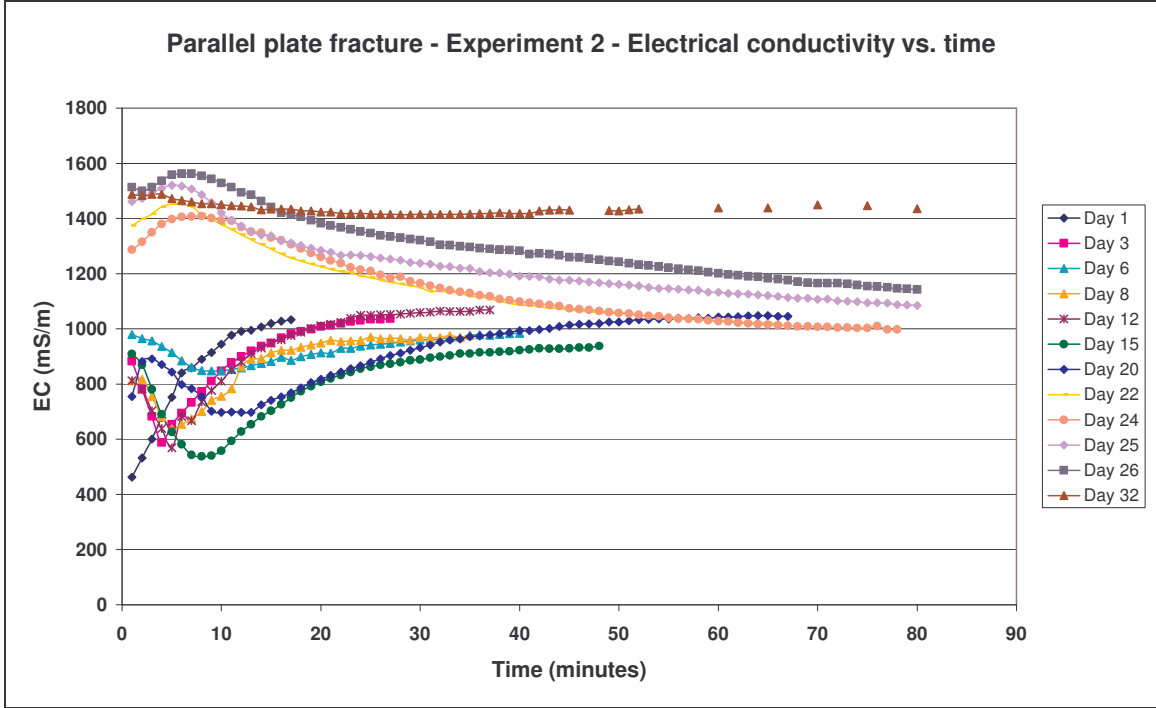


Figure 5-25 Parallel plate fracture experiment - EC vs. time graph.

The dissolved oxygen was measured every morning at the outlet side of the fracture, prior to bacteria and media injection. From Figure 5-26, it can be seen that the dissolved oxygen decreases very rapidly over time. After Day 10, the dissolved oxygen is on average lower than detection. The system can therefore be classified as an anaerobic system.

From Day 20, it was observed that the colour of the outflow started to change from cream to grey. It was decided to place the bacteria and media on magnetic stirrers during injection to aerate the bacteria and media before injection to discourage anaerobic conditions. This will also cause the bacteria to use both O₂ and nitrate as the electron acceptor. This prevents sulphate reducers from being activated and multiplying.

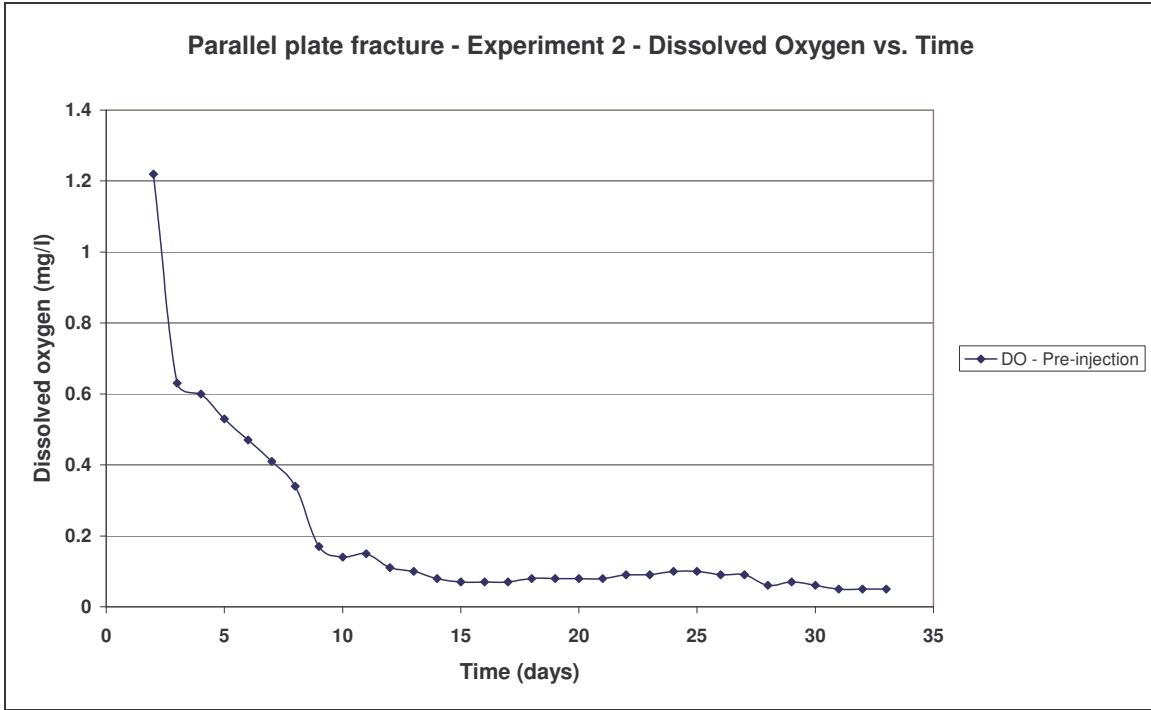


Figure 5-26 Parallel plate fracture experiment - DO vs. time graph for in-box and outflow samples.

5.3.5 Bacteria breakthrough – Real-Time PCR

The polymerase chain reaction (PCR) is a molecular biology technique for enzymatically replicating DNA without using a living organism, such as *E. coli* or yeast (Medicinenet.com). Like amplification with living organisms, the technique allows a small amount of the DNA molecule to be amplified exponentially. However, because it is an *in-vitro* technique, it can be performed without restrictions on the form of DNA and can be extensively modified to perform a wide array of genetic manipulations. DNA amplification is a laboratory process, in which a particular DNA segment from a mixture of DNA chains is rapidly replicated, producing a large, readily analysed sample of a DNA piece (Medicinenet.com).

Real-time PCR (RT-PCR) is a method that uses fluorescent dyes and probes to measure the amount of amplified product in real time (Medicinenet.com)

5.3.5.1 Bacteria breakthrough results

Samples of the outflow volumes were taken on a daily basis (every minute) during the injection of the bacteria and media, because the optical density is only accurate for the

first few days. The optical density readings measured by the spectrophotometer become inaccurate when the OD exceeds 0.9.

Real-time PCR analyses were conducted on some of the outflow samples by the Department of Microbiology, Biotechnology and Food Biotechnology (Van Heerden, 2006).

The results of some of the RT-PCR data are displayed in Figure 5-27 to Figure 5-28. From the graphs, it can be seen that the highest concentrations of bacteria occur during the first 10 to 15 minutes of the test. This might be attributed to bacteria at the end of the plate losing their adhesion properties because of anaerobic conditions. From the graphs, it can also be seen that the bacteria concentrations increase with time, which shows that the bacteria are capable of surviving and multiplying in micro-aerophilic-anaerobic conditions.

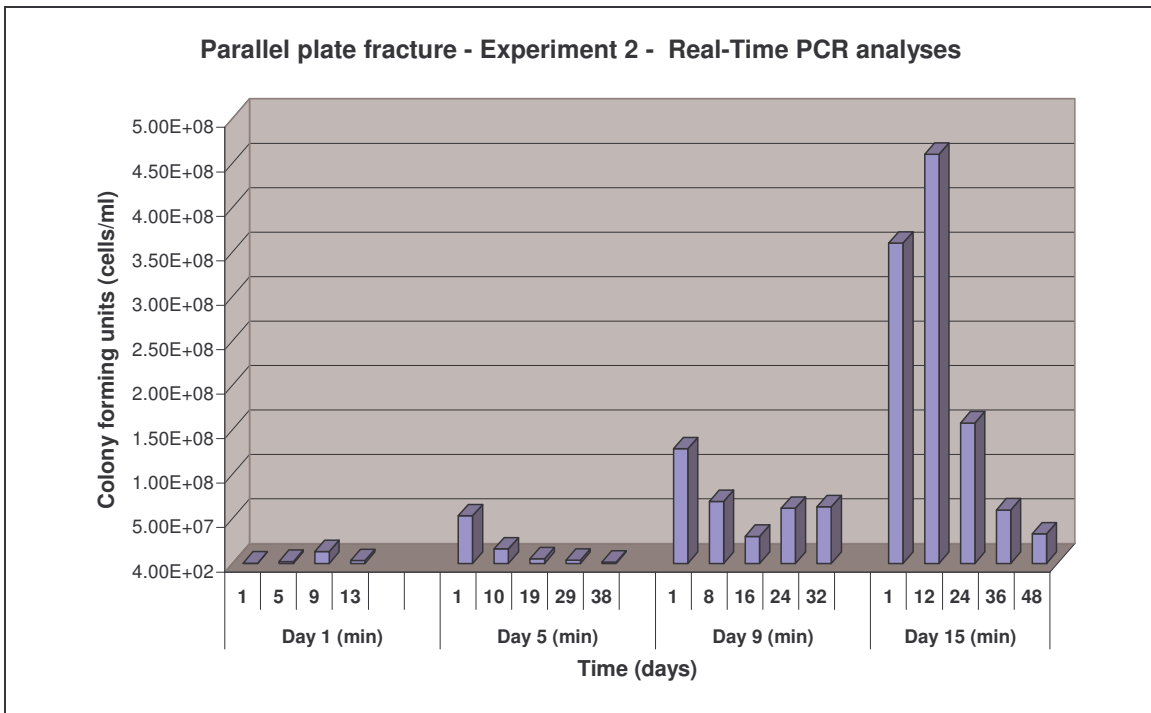


Figure 5-27 Parallel plate fracture experiment - R-T PCR vs. time graph for samples.

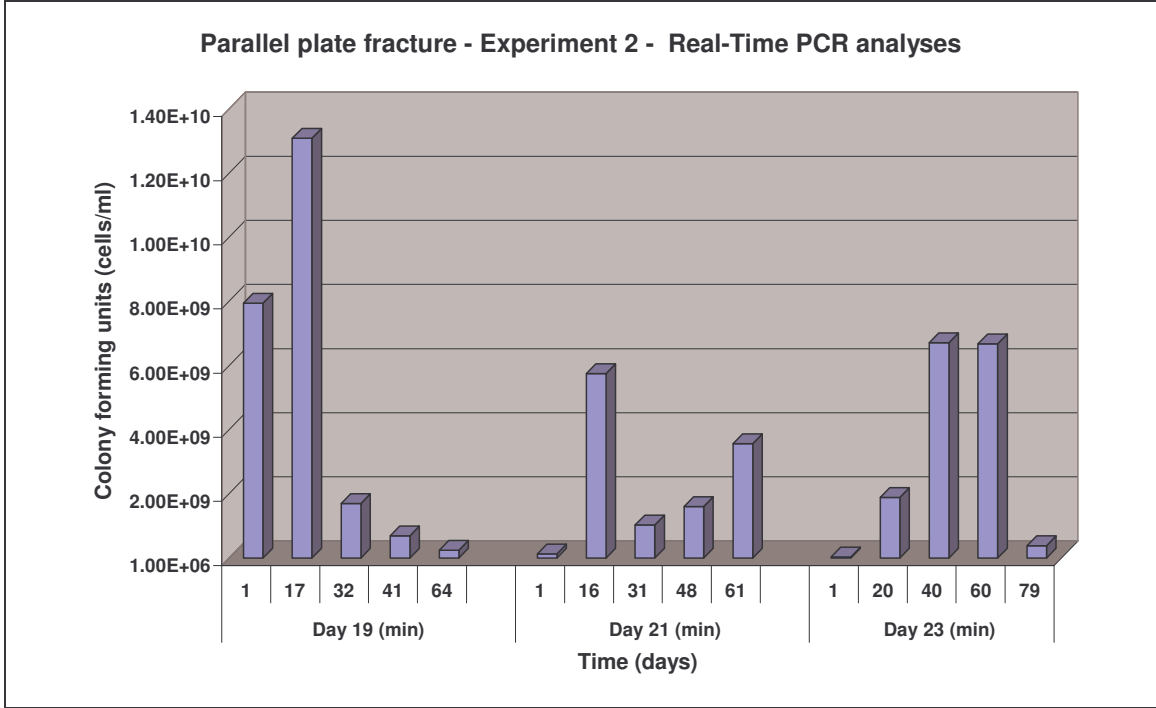


Figure 5-28 Parallel plate fracture experiment - R-T PCR vs. time graph for samples.

5.3.6 Calculation of the hydraulic conductivity

The hydraulic conductivity of the fracture was calculated using parallel plate theory. A hydraulic conductivity of approximately 6000 m/d was calculated for the fracture with an aperture of 0.8 mm. Prior to the hydraulic reduction experiment, the effect of increasing gradient was tested versus flow. From the results it can be seen that the increase in gradient causes the flow rate to increase.

Table 5-3 shows the effect of increasing gradient on the flow through the fracture.

Table 5-3 Initial flow under with changing hydraulic gradients.

	Gradient	Flow	
		(ml/min)	(l/s)
Gradient 1	0.012	138	0.0023
Gradient 2	0.022	260	0.0043
Gradient 3	0.032	380	0.00633

5.3.7 Hydraulic conductivity (K) reduction test

During the experiment, the reduction in flow due to biofilm growth was monitored on a daily basis. From the results (see Figure 5-29 and Table 5-5) a reduction of 53% was measured after only 6 days.

During Day 7, the flow increased rapidly. The reason for this phenomenon was investigated. Samples of the media used during Day 8 as well as freshly prepared media were submitted to the groundwater laboratory at the Institute for Groundwater Studies for analysis. See Table 5-4.

From the laboratory results, it appears as if the Cl and NO₃(N) mass were accidentally exchanged by the laboratory technician from the Department of Microbiology, Biotechnology and Food Biotechnology.

Table 5-4 Chemical analyses of the composition of the media.

Sample name	EC (mg/l)	pH (mg/l)	Cl (mg/l)	NO ₃ (N) (mg/l)	SO ₄ (mg/l)
Media (Day 8)	1891	6.95	2702	12.7	95
Original media	1850	6.9	12	2800	94

Since NO₃(N) concentrations were very low, the bacteria had no electron acceptor (nitrogen source). During Day 7, the dissolved oxygen at the fracture was already 0.4 mg/l, which placed the bacteria under enormous stress because of insufficient nitrate to act as an electron acceptor. This caused the bacteria to flush from the fracture, and an increase in flow was measured.

For the next four days (Day 8 - Day 10), the reduction in flow remained constant at an average of 40%.

Although the high chloride concentrations and low nitrate concentrations caused the bacteria to lose adhesion and flush from the fracture, this event can be interpreted as a positive development. A few days after this event, the flow started to reduce again. It can be concluded that it is possible to resuscitate bacterium *S. marcescens* when exposed to extremely high Cl and very low nitrate concentrations. Unfortunately, it will take a few days to overcome this problem, as the system cannot reactivate immediately.

The following is an overview of the flow reduction:

- From Day 12 onwards, the flow started to reduce rapidly.
- After 21 days, bacteria and media injections occurred only in the mornings, with only media injections in the afternoons.
- After 25 days, a reduction of 80% was measured in the flow.
- From Day 29 onwards, only media were injected in the mornings, because of difficulty in injection. Because of the very slow injection rate, the media became turbid during the injection period, which is an indication of possible growth and thus consumption of media before actual injection.
- During Day 29, a flow reduction of 95% was obtained.
- During Day 30, a 100% flow reduction was measured; where after the flow started to increase, but remained between 98 and 100%.

The injection of media was terminated on Day 31. At that stage of the experiment, a 98% reduction in the flow was measured.

Figure 5-29 was compiled to show the reduction in flow results by means of an average value for each day's flow. In Figure 5-29, the data were also extrapolated (eliminating the days affected by using wrong media) to show the actual time in days for the bacteria to clog the fracture. When extrapolated, it will take the bacteria approximately 23 days to clog the fracture to 98%.

From the results of the hydraulic reduction test, it can be seen that it is possible to reduce the hydraulic conductivity of a laboratory-scale parallel plate fracture by more than 98%.

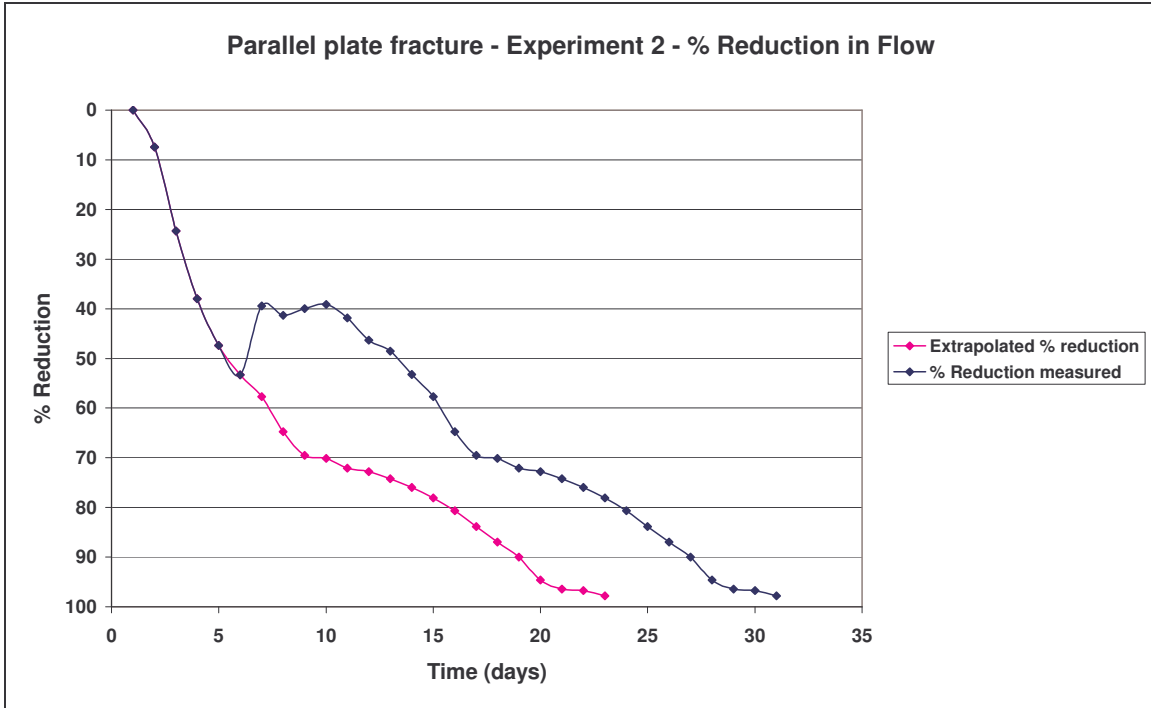


Figure 5-29 Parallel plate fracture experiment - % Reduction in flow vs. time graph.

5.3.8 Effect of increasing gradient on biobarrier stability

On Day 31, the experiment was terminated. After the hydraulic reduction test, the first challenge was to determine the effect of increasing gradients on the effectiveness (stability) of the biobarrier.

Groundwater was used to flush the fracture to determine how long the barrier would hold when not fed. See Table 5-3 and Table 5-5 for information on the original flow (ml/min) at each gradient, as well as the % increase in flow with time. See Figure 5-30 for the % increase in flow graph.

During the first 44 days after the experiment was stopped, almost no increase in the flow rate was measured. From Figure 5-30, it can be seen that, with a gradient of 0.012, the fracture was clogged to 98% for a minimum period of 44 days.

On Day 45, the hydraulic head was increased to 0.022. Groundwater was used again to flush the fracture. The gradient of 0.022 was applied for a 48 hours period. With gradient increase from 0.012 to 0.022, the flow increased between 2% and 2.3% of the original.

On the 47th day of the experiment, the gradient was again increased, this time to 0.032. After the increase, the flow increased to 7.9% of the original. For the next four days, the flow increased gradually with time, to 13.7%.

During the flushing experiment, three different gradients were applied to the clogged fracture. From the results, it can be concluded that the barrier in the fracture had the ability to withstand gradient increases of up to 0.032 without any significant signs of failure.

Table 5-5 % of the original flow with different gradients

Day	Gradient	Average daily flow rate (ml/min)	% Of original flow
Day 31	0.012	1	0.72
Day 33	0.012	1.8	1.30
Day 35	0.012	2.45	1.78
Day 37	0.012	4.2	3.04
Day 39	0.012	5.2	3.77
Day 41	0.012	2.62	1.90
Day 43	0.012	1.99	1.44
Day 45	0.022	1.3	0.50
Day 46	0.022	10.3	3.96
Day 47	0.032	30	7.89
Day 49	0.032	37	9.74
Day 51	0.032	45	11.84
Day 52	0.032	52	13.68

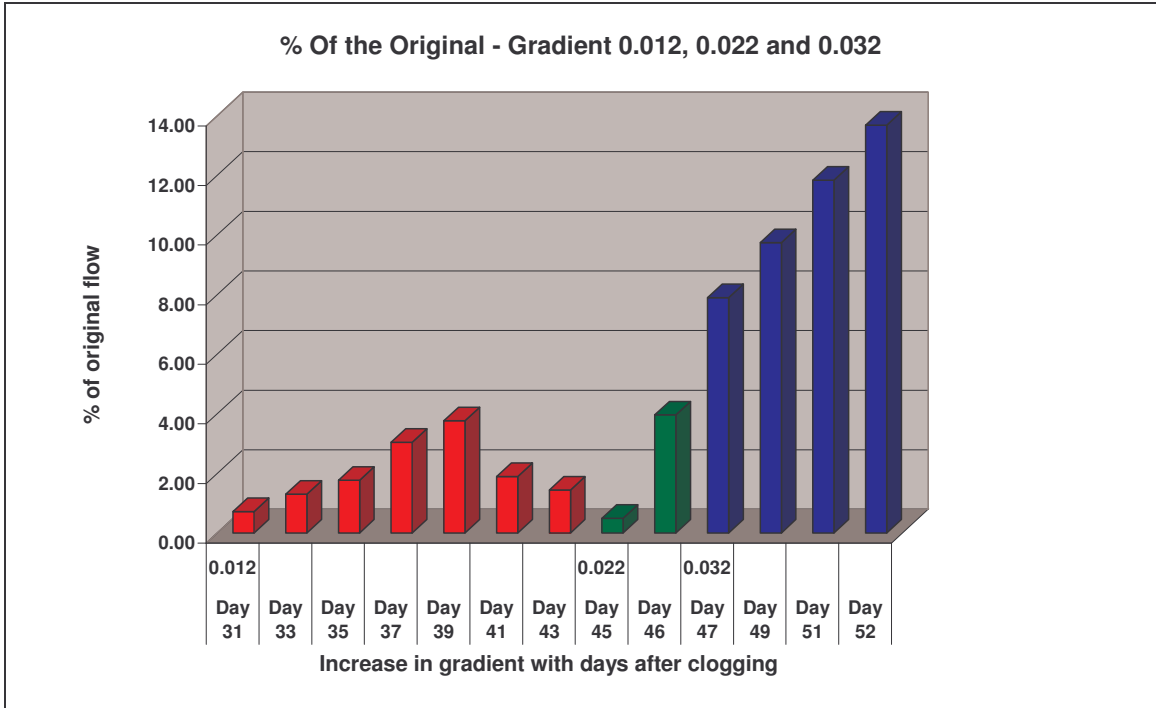


Figure 5-30 Parallel plate experiment -% Increase in flow with different gradients.

The EC was monitored daily during the flushing process (see Figure 5-31). From the EC data, it can be seen that the EC decreased rapidly and stabilised on day 35. The initial high EC values were caused by the media and, because of the gradient increase, *in situ* concentrations were replaced with groundwater, which has a much lower EC.

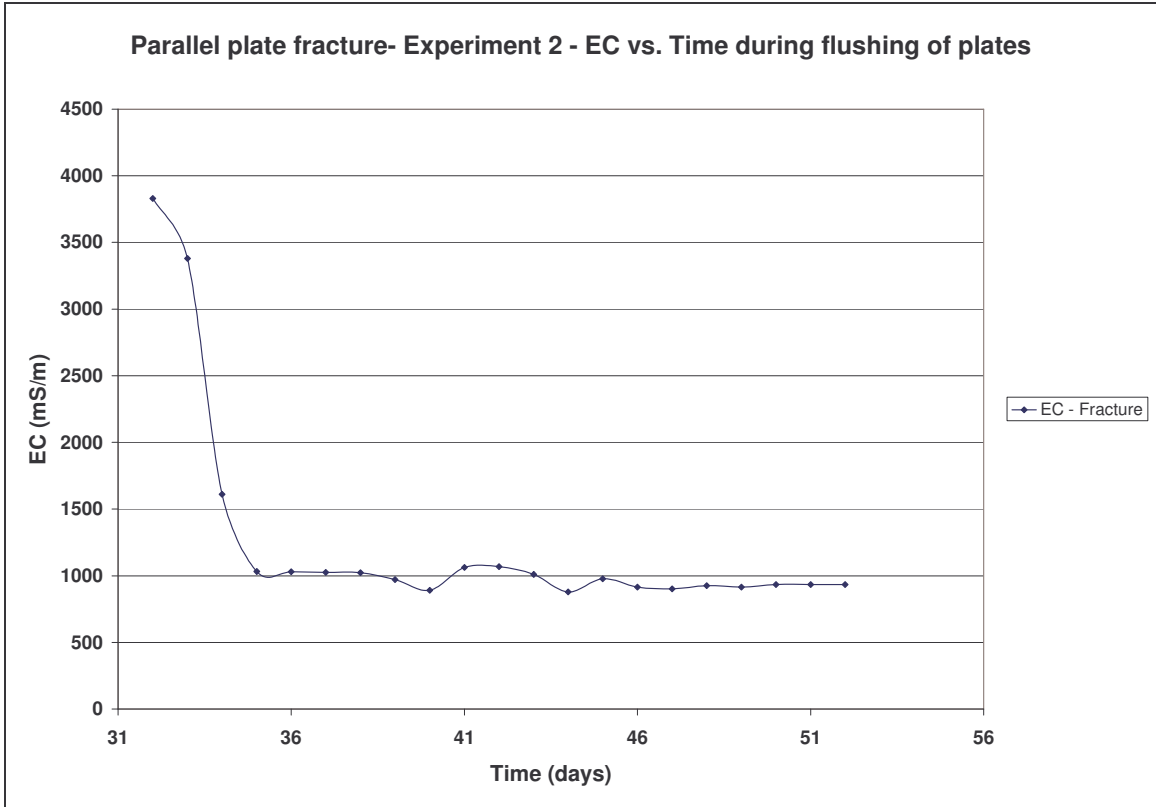


Figure 5-31 Parallel plate fracture experiment - Change in EC with time during flushing of the fracture.

5.3.9 Self potential techniques (SP)

Self potential measurements were carried out on the parallel plate.

Self potentials are measurements of the difference in natural ground potentials between two points on the ground or rock surface. They can be generated by a number of different sources, including groundwater flow, mineral deposits and chemical diffusion. Self potentials can vary from less than a millivolt to over one volt, and the sign of the potential is a diagnostic factor in the interpretation of self potential anomalies. Although there are many sources of self potentials, the common factor is groundwater. The potentials are generated by the flow of water, by water acting as an electrolyte and as a solvent of different minerals and compounds.

With an increasing demand for investigation methods with both high accuracy and high resolution across a variety of spatial scales, the new discipline “hydrogeophysics” evolved, which aims to combine knowledge from various disciplines such as

hydrogeology, soil physics, biogeochemistry, and geophysics, to improve subsurface hydrogeological characterisation and monitoring (Vereecken *et al.*, 2004).

Although self potential surveys are mainly used for mineral exploration, they can also be used in determining the movement of water or the delineation of potential fracture zones (Krishnamurthy *et al.*, 2003).

5.3.9.1 Methodology

Self potential techniques were employed on the parallel plate fracture. The idea behind the self potential experiment was to try to identify or determine possible flow patterns forming during the experiment due to bacteria growth in the fracture.

The instrument to measure the self potential was built by a Ph.D. student (Michael du Preez) at the Institute for Groundwater Studies at the University of the Free State. The self potential apparatus was constructed on the upper section of the experiment.. See Figure 5-32 for the set-up of the self potential experiment. (A) A wooden board was used to construct a grid consisting of 80 steel pins (pins were 55 cm long). This steel pins were isolated with a plastic tube. On top of the wooden board, 1 cm pins were visible to take the self-potential readings. The pins were evenly spaced in the wooden board. (B) The pins rested on the parallel plate fracture. A voltmeter was used to take the measurements (Ohm). Readings were taken on a daily basis for the 79 pins relative to the base point pin to analyse the iso-potential lines for identifying the changes in the flow path in the fracture zones due to bacteria growth.

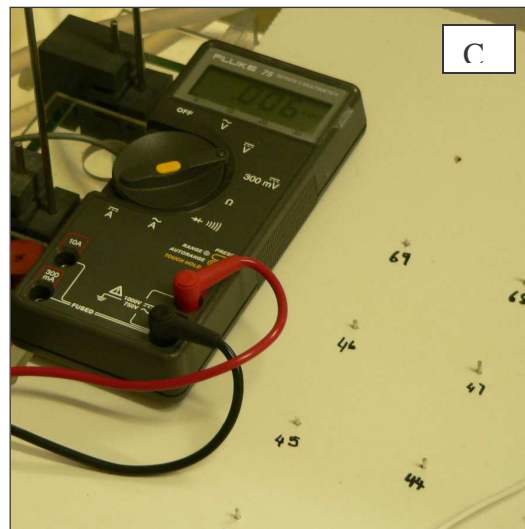
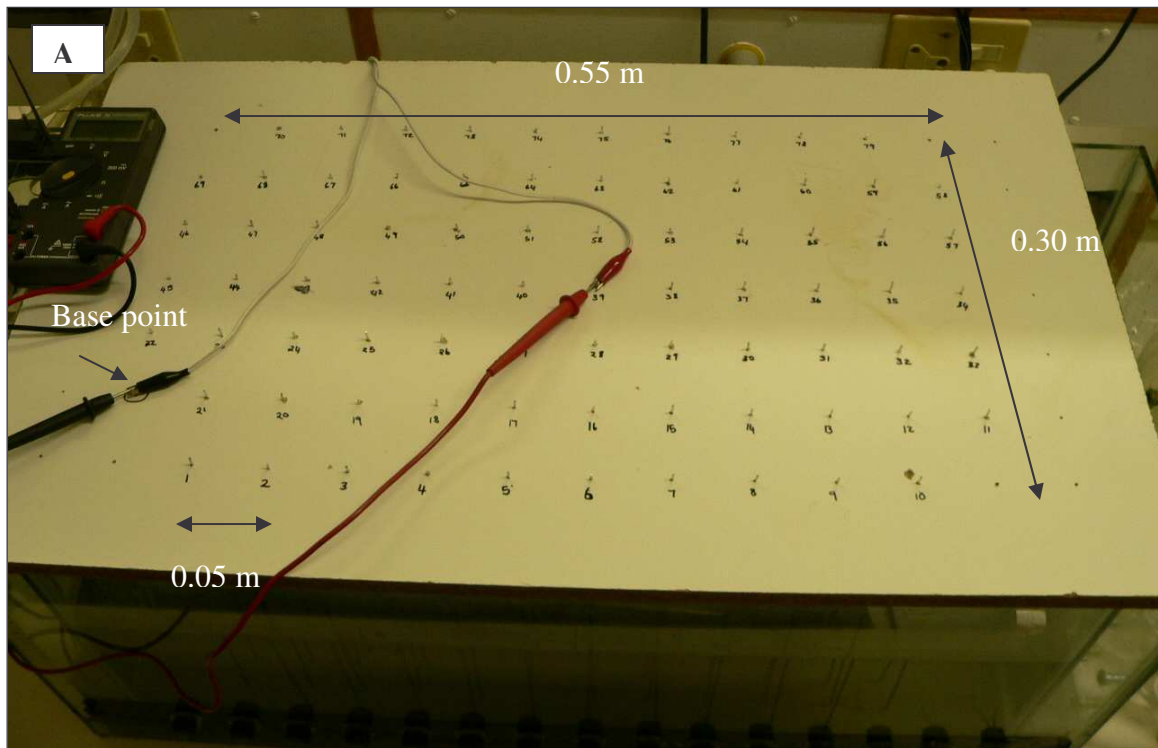


Figure 5-32 Self potential measurements. (A) grid with 80 pins. (B) Pins spaced on top of the fracture, (C) voltmeter used for taking self potential readings.

5.3.9.2 Results from the comparison between the % reduction in flow and the self potential

The processing of data and preparation of flow pattern figures was done by du Preez (unpublished data). Flow patterns (Figure 5-34 to Figure 5-36) show the influence of bacteria growth on the flow of the water in the fracture.

Very interesting results were obtained from the self potential readings. The flow patterns can be interpreted as follow: Dark blue colours are an indication of high flow, the lighter blue colours are associated with low flow and white is an indication of no flow. The light blue and white areas can be associated with high bacteria growth. Ten graphs were prepared to illustrate the flow patterns over a range of 30 days. The self potential results were also correlated with the reduction in flow measured over the time period and can be seen in Figure 5-33.

Looking at the results from the flow pattern data it can be seen that on Day 5, three distinct white areas can be identified. The shims keeping the aperture open are located in these areas. It can be assumed that bacteria growth started immediately in these areas, causing the flow to decrease rapidly. A 55% reduction was measured in the flow over the first five days. (Refer to Figure 5-29 for % reduction in flow after five days). On Days 8 and 10, an increase in the flow is visible and can be attributed to the mistake in media preparation. From Day 12 to 18 a gradual decrease in the flow can be seen in both the flow patterns as well as the flow reduction graph (see Figure 5-34 to Figure 5-36). From Day 20 onwards, the flow patterns show a decrease in the flow over the area. This can be seen from the light blue distributed over the whole area. An assumption can be made that during the course of the experiment, bacteria adheres on both sides of the plates, this accumulation increased with time, causing the fracture aperture to decrease. After 20 days, it seems as if the bacteria started to accumulate in the fracture. During this time the flow reduction was between 72 % and 96 %.

5.3.9.3 Discussion

The flow patterns obtained from the self potential measurements were correlated with the reduction in flow rate over time. Very good correlation was obtained. The flow pattern data mimicked the flow reduction data. During the first part of the experiment the first bacteria growth started in the vicinity of the shims. This caused the flow to reduce

rapidly. From Day 20 onwards, it seemed as if bacteria growth was dominant over the whole area, decreasing the fracture aperture and decreasing the flow.

From the results it can be concluded that self potential methods are a very good method to determine flow patterns in a parallel plate fracture.

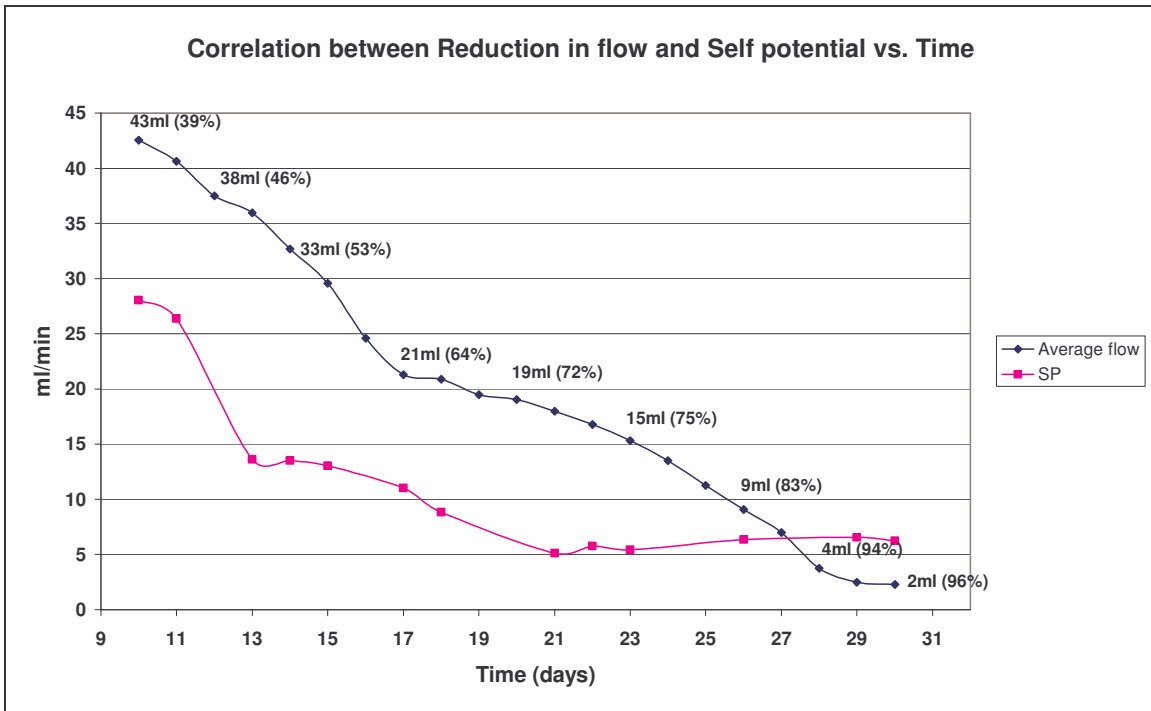


Figure 5-33 Comparison between the reduction in flow and the daily average self potential readings over time.

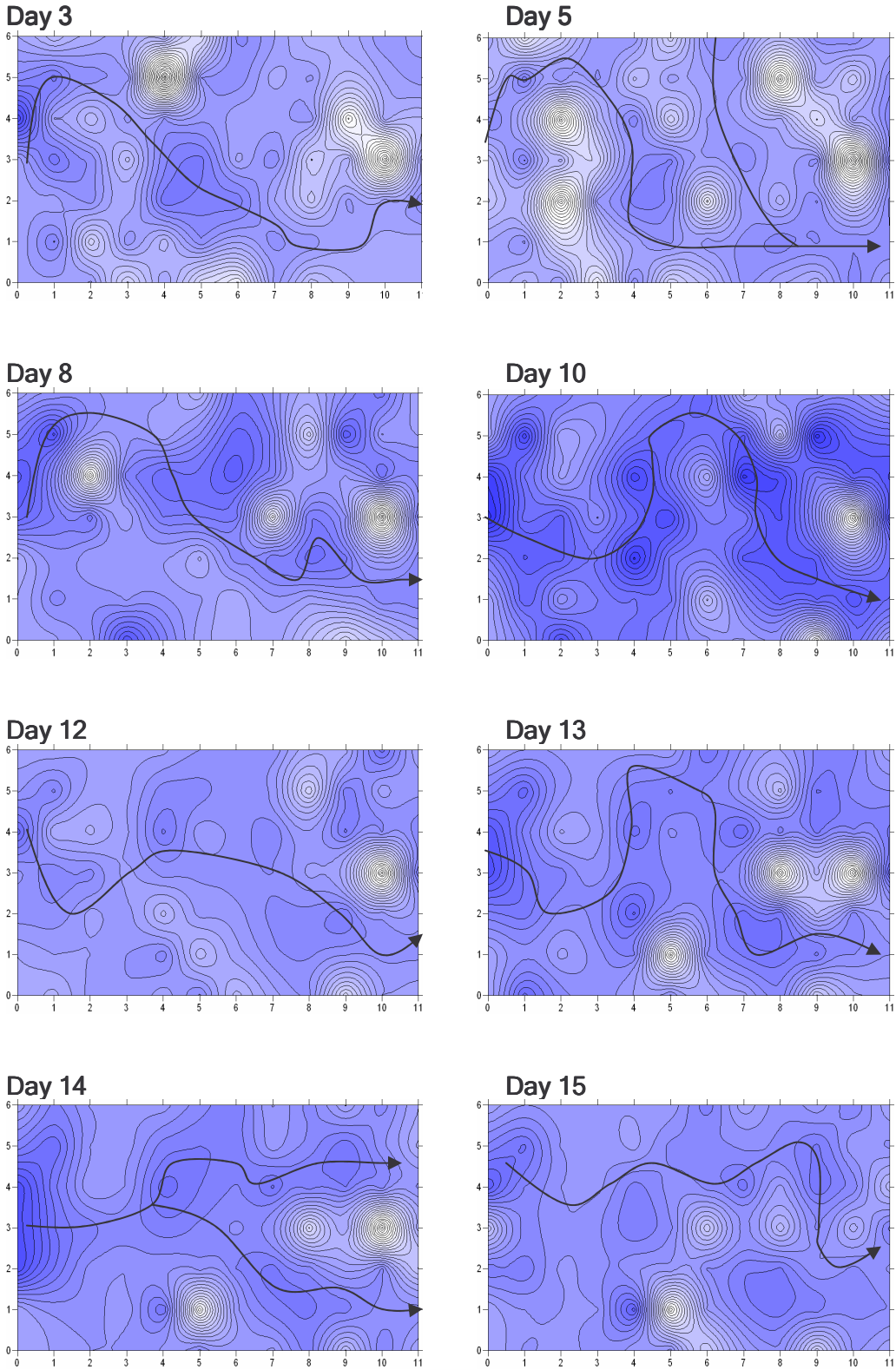


Figure 5-34 Self potential measurements - Flow pattern data (Day 3 to Day 15).

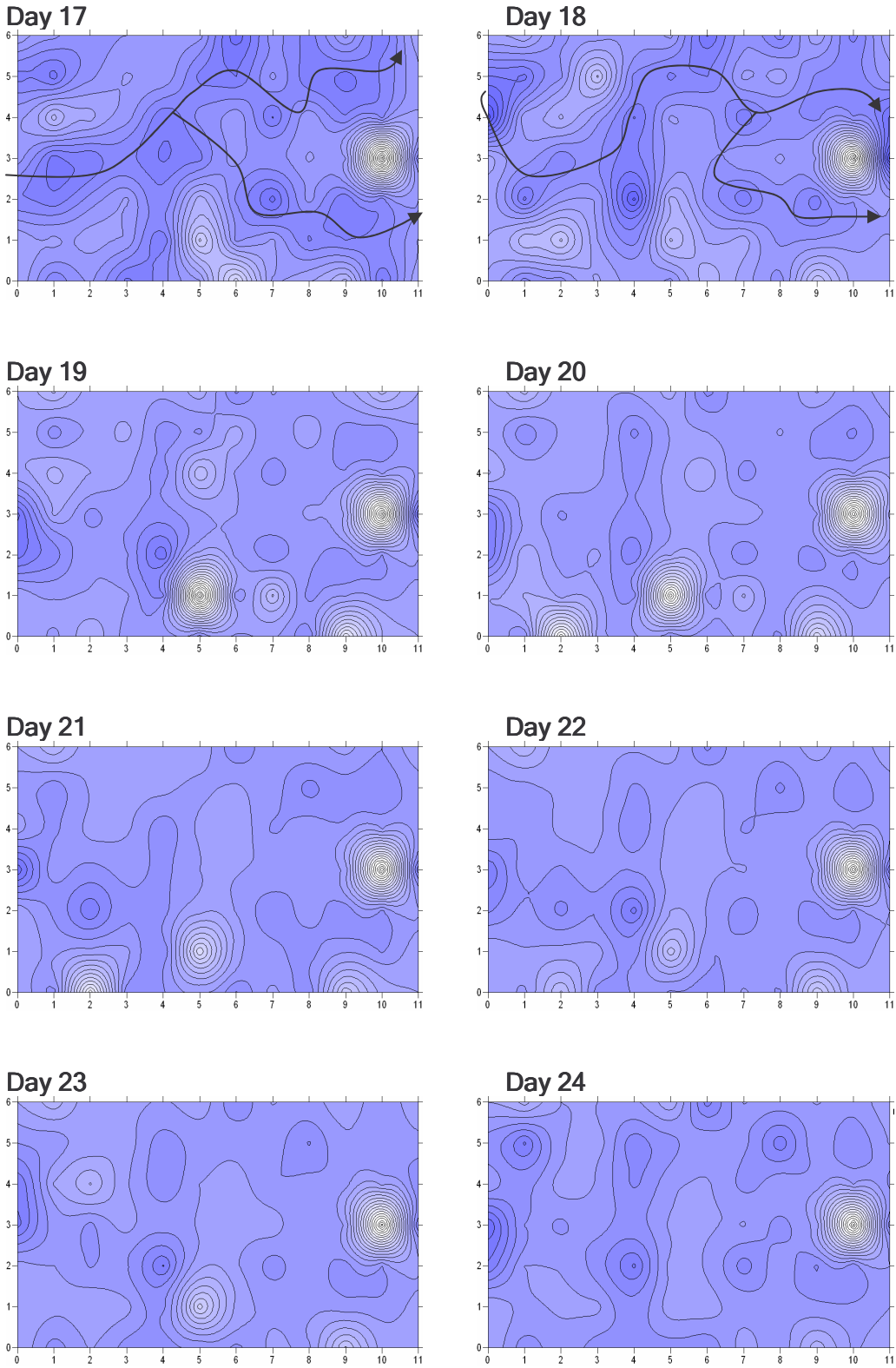


Figure 5-35 Self potential measurements - Flow pattern data (Day 17 to Day 24).

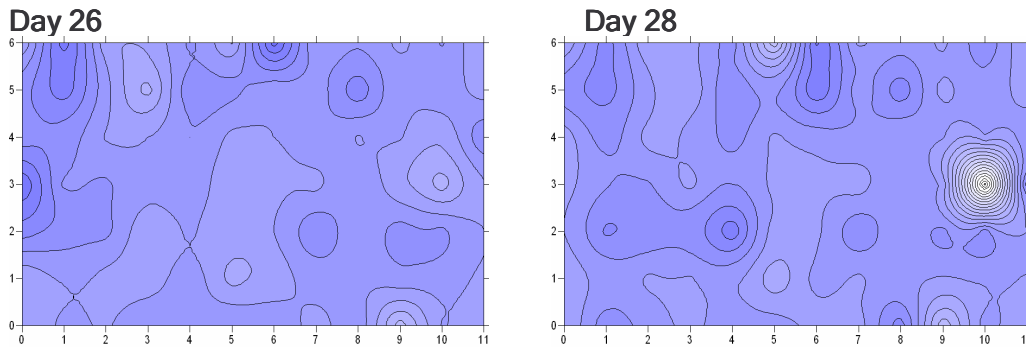


Figure 5-36 Self potential measurements - Flow pattern data (Day 26 to Day 28).

5.3.9.4 Effect of increasing gradient on the flow patterns

After the hydraulic reduction test, the effect of increasing gradients on the effectiveness of the biobarrier were tested (refer to section 5.3.8). Self potential measurements were taken during this time to determine the effect of increasing gradient on the flow patterns. The results of the flow patterns can be seen in Appendix D and the correlation between the self potential and the flow rate can be seen in Figure 5-37. A very good correlation between the self potential and flows was obtained. The results of the flow pattern gave very similar results. From the flow pattern data a white area at the outflow side can be observed in almost all the data. This might be attributed to the decreased flow. After nine days, the flow was 3.8% of the original flow. After 46 days, the flow decreases to just 0.5% of the original flow. On day 46, the gradient was increased and again on Day 48. On consideration of the postulated flow pattern, it can be seen that the white (no flow) areas have increased. This is speculated to be a result of the compaction of bacteria in the fracture.

To conclude, self potential appears to be a good method to obtain flow patterns in a parallel plate fracture on laboratory-scale.

5.3.9.5 Implication

From the self potential results obtained on laboratory-scale, it seems to be a very effective method to obtain flow patterns in fractures.

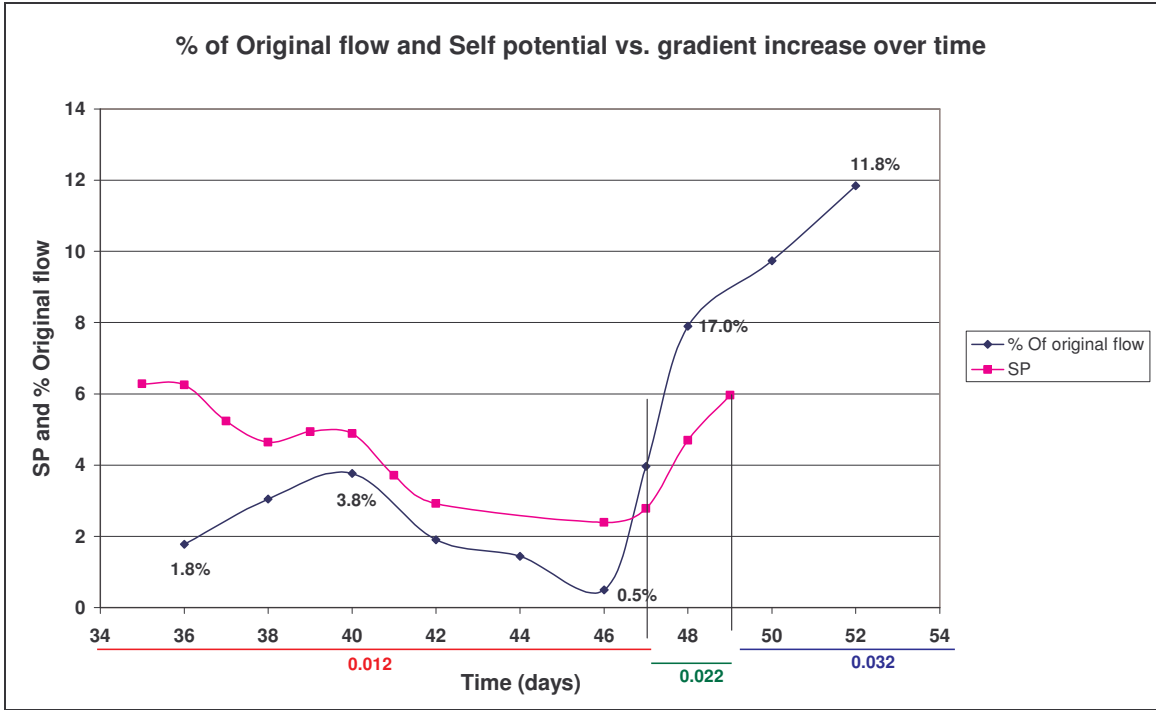


Figure 5-37 Comparison between the % of the original flow and the self potential readings over time.

5.3.10 Flushing with NaCl

The second challenge was to restore the fracture to its original hydraulic conductivity. Restoring the fracture system is a very important aspect of the experiment, especially for upscaling to field conditions. When barriers are no longer needed, the aquifer system must be cleaned. This includes eliminating the bacteria as well as removing bacteria mass to ensure the aquifer hydraulics return to the original state.

On the 52nd day of the experiment, the gradient was adjusted to the original value of 0.012. Due to the decrease in the gradient, the flow reduced to approximately 7.8% of the original.

A NaCl solution (35g/l) was prepared. The NaCl was used to flush the fracture, with very interesting results. Over a period of six hours, the flow decreased from 7.8% to 0.1%. The outflow nozzles were checked for possible blockages and none were found.

From this, it can be deduced that the barrier is not negatively influenced by a substance with a very high ionic strength (equivalent to seawater). The high NaCl concentrations was expected to be detrimental to the bacteria, but from the results it can be seen that it

will not affect the adhesion of the bacteria. See Figure 5-38 for the reduction in flow graph.

After six hours of flushing with NaCl, the experiment was terminated.

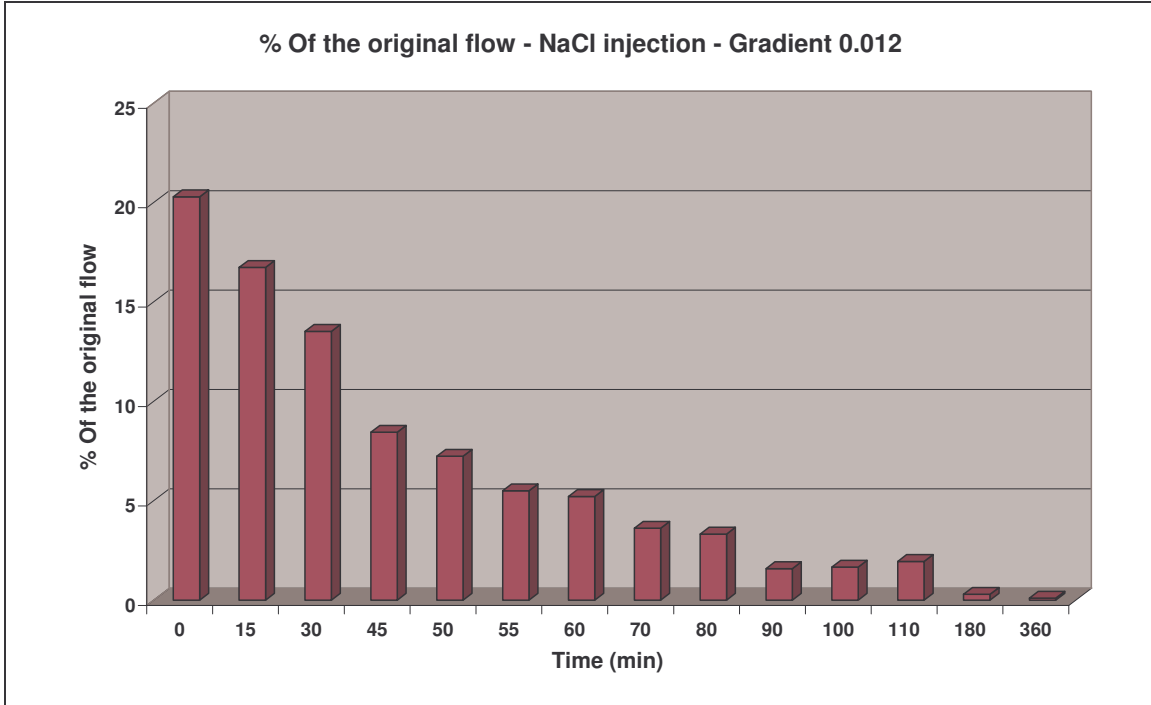


Figure 5-38 Parallel plate experiment -Reduction in flow during NaCl injection.

5.3.11 Flushing with sodium hypochlorite

Currently, many techniques exist to rehabilitate biological clogging. These techniques are described in detail by Smith (2003) and Smith (2005). One such technology is applying sodium hypochlorite.

A 15% hypochlorite solution was prepared and injected. The flow almost immediately began to increase. The bacteria growth at the injection side of the fracture began to disintegrate and flush through the fracture (see Figure 5-39). At the outflow side of the fracture, bacteria were visibly flushed from the fracture (see Figure 5-40). After two hours, the flow returned to its original value.

The implications of this technique are as follows:

- Biobarrier formation can be removed and the aquifers remediated very cost effectively with sodium hypochlorite. When biobarrier is no longer needed, a sodium hypochlorite solution can be injected into the aquifer system. This will chemically rehabilitate the system, and thus killing, dislodging, and dispersing the *in situ* bacteria.
- As part of the rehabilitation process, the boreholes must be pumped to remove dead bacteria mass from the boreholes and aquifer system.

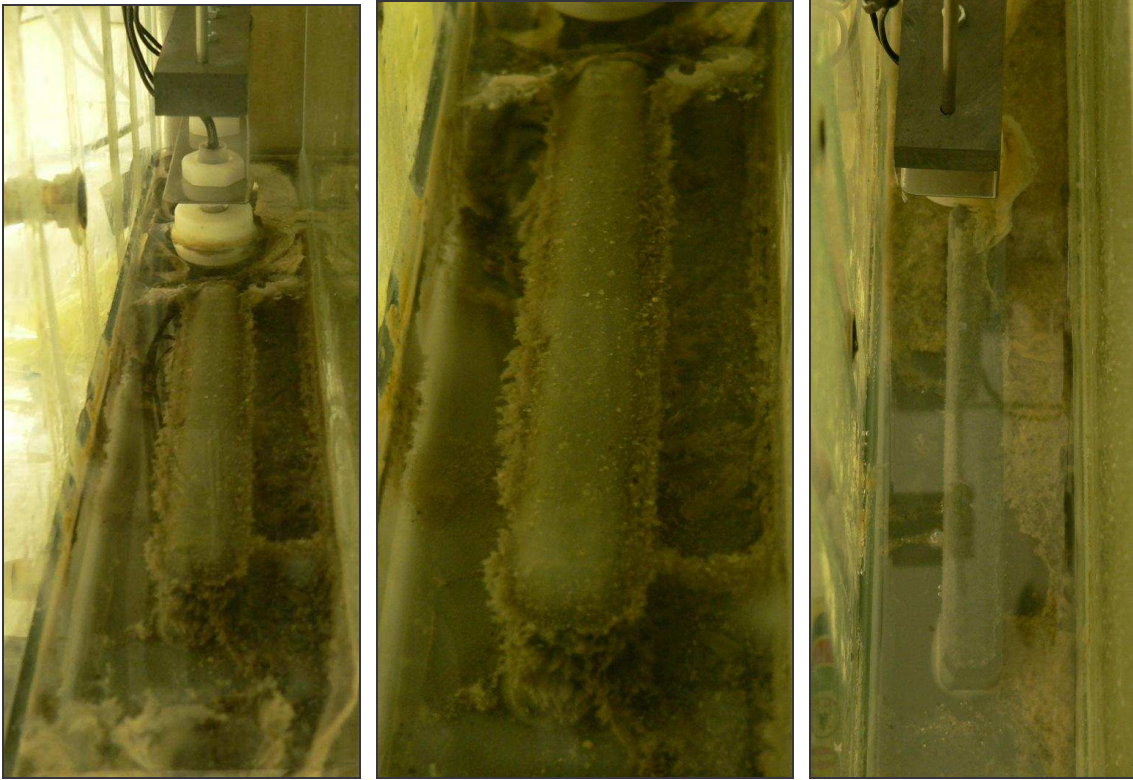


Figure 5-39 Bacteria mass at the inflow side of the fracture begins to disintegrate.

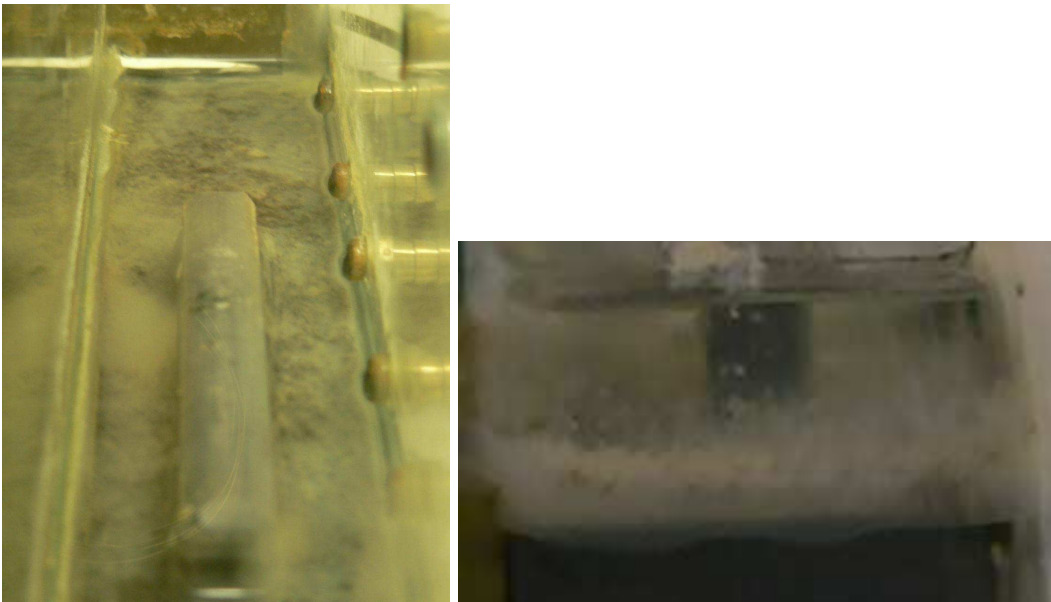


Figure 5-40 Bacteria mass flushing from the fracture - Outflow side of the fracture.

5.4 DISCUSSION

Pipe experiments

From the pipe experiment, the following conclusions can be made:

Pipes were operated for ten days. During this period, it was observed that the bacteria have the ability to create a blockage in the pipes, but due to constant pumping and the non-adhesive surface of the pipes, the blockage moves through the pipe. To prevent this, a constant head system was installed, but with the same results.

From the results of the pipe experiments, it can be seen that the bacteria have the ability to adhere, in lower flow systems. Because of adhesion and growth in Pipe 1 (low flow rate), the free-flow volume decreased in the first two sections.

From the pipe experiments, it can be seen that lower flow rates are advisable, and that the bacteria need adhesion surfaces to enhance growth and clogging. It can be concluded that the pipe experiment is not an ideal representation for biobarrier functioning in the field.

Parallel plate fracture - Experiment 1 (1.3 mm aperture)

Transport tests

From the NaCl and bacteria transport, the following was observed: The NaCl moved conservatively through the fracture. A dispersivity of 0.16 m and a tracer velocity of 111 m/d were calculated for the fracture with an aperture of 1.3 mm.

Bacteria transport was slower than for the conservative tracer but also successful through the fracture. The slower velocity can be attributed to adhesion of the bacteria to the rough surface of the parallel plate fracture.

Hydraulic reduction test

The highest reduction of 35% was measured after 24 days. The following may have contributed to the low reduction rate in the fracture:

- Fracture aperture might have been too large.
- Moving of experiment apparatus on the fifth day, causing the flow to return to the original flow. Low reduction can also be attributed to too few bacteria and low media quantities being injected prior to establishing biomass and biobarrier formation.
- Activation of *Desulfovibro* (sulphate reducing bacteria), due to high sulphate and low nitrate concentrations.

The following recommendations were made prior to application of biobarriers in the field.

Composition of media must be changed, lowering the sulphate concentrations and increasing the nitrate concentrations to ensure *Desulfovibro* is not activated.

Bacteria and media injection can be reduced after biobarrier formation is established.

From the results of the parallel plate fracture - Experiment 1, it can be seen that it is possible to reduce the flow in a relatively large fracture by approximately 35%. The results show that it will take time to built biobarriers in fractures with larger apertures.

Parallel plate fracture - Experiment 2 (0.8 mm aperture)

Transport test

From the NaBr and bacteria transport, the following were observed: The NaBr moved conservatively through the fracture. The dispersivity of the NaBr was calculated with the TRACER software. A dispersivity of 0.06 m and a tracer velocity of 151 m/d were calculated for the fracture with an aperture of 0.8 mm.

Electron acceptors (Dissolved oxygen and nitrate)

The results showed that after Day 10, the dissolved oxygen was depleted and the system could be classified as anaerobic.

On Day 20, it seemed as if the sulphate reducer was again activated due to the anaerobic conditions in the system. The bacteria and media were placed on magnetic stirrers to aerate the bacteria and media before injection and to discourage anaerobic

conditions. This encouraged the bacteria to use both O₂ and nitrate as the electron acceptor.

Real-time PCR

The results of the Real-time PCR showed that the highest concentrations of bacteria occur during the first 10 to 15 minutes of each day's outflow. This can be attributed to bacteria at the end of the plate losing their adhesion ability because of total anaerobic conditions. The mobile bacteria are then flushed from the column when injecting the next pulse of bacteria or media

Hydraulic reduction test

From the results of the hydraulic reduction test, the following were observed. A rapid reduction to 53% of the original flow rate was measured after just six days.

During Day 7, the flow increased rapidly. The reason for this phenomenon was that the Cl and NO₃(N) mass were exchanged by accident during the preparation of the media. Due to low NO₃(N) concentrations the bacteria had no electron acceptor and with the dissolved oxygen at 0.4 mg/l, the starved bacteria were flushed from the fracture, and an increase in flow was measured.

A few days after this event, the flow started to reduce. It can be concluded that it is possible to resuscitate bacterium *S. marcescens* (after stressing the bacteria).

From Day 12 onwards, the flow started to reduce rapidly. After 25 days, an 80% reduction was measured in the flow. After 29 days, a flow reduction of 95% was obtained. During Day 30, a 100 % flow reduction was measured; after the flow started to increase, but remained between 98 and 100%.

From the results of the hydraulic reduction test, it can be seen that it is possible to reduce the hydraulic conductivity of a parallel plate fracture by more than 98%. From the results of the parallel plate, it can be concluded that a parallel plate fracture with a fracture aperture of at most 0.8 mm can be clogged 100%.

Effect of increasing gradients on the biobarrier stability

Because media injection stopped on Day 31, the first challenge was to determine the effect of increasing gradients on the stability of the biobarrier.

Between day 32 and 45 (14 days) after media injection stopped), surprisingly almost no increase in the flow rate was measured. This is very reassuring, because it implies that the barrier can be maintained without media injection. The results showed that, with a gradient of 0.012, the fracture was clogged 98% for a minimum period of 14 days.

On Day 47, the hydraulic head was increased to 0.022. With a gradient increase from 0.012 to 0.022, the flow increased between 2% and 2.3% of the original over a period of 48 hours.

On the 49th day of the experiment, the gradient was increased again, this time to 0.032. The flow increased to 7.9% of the original. For the next four days, the flow increased gradually with time to 13.7% of the original. The 13.7 % of the original flow suggests that the barrier has lost some of its effectiveness at the end of the experiment.

From the results, it can be concluded that barriers in the fracture have the ability to withstand gradient increases of up to 0.032 without significant failure.

Self potential techniques

The flow patterns obtained from the self potential measurements were compared with the reduction in flow rate (% reduction) over time. The flow pattern data mimicked the flow reduction data. During the first part of the experiment the first bacteria growth started in the vicinity of the shims. This caused the flow to reduce rapidly. From Day 20 onwards, it seemed as if bacteria growth was dominant over the whole area, decreasing the fracture aperture and decreasing the flow.

From the results it can be concluded that self potential methods are a very good method to determine flow patterns in a parallel plate fracture.

Flushing with NaCl

The second challenge was to clean the fracture. A 35g/l NaCl solution was used to flush the fracture. Interestingly, over a period of six hours, the flow decreased from 7.8% to 0.1%. From this, it can be observed that the barrier is not negatively influenced by a substance with a very high ionic strength (equivalent to seawater).

Flushing with sodium hypochlorite

A 15% sodium hypochlorite solution was prepared and injected. The flow almost immediately began to increase. The bacteria growth at the injection side of the fracture began to disintegrate and flush through the fracture. At the outflow side of the fracture, bacteria were visibly flushed from the fracture (see Figure 5-40). After two hours, the flow returned to its original value. It can be concluded that biobarrier formation can be removed and the aquifers remediated very rapidly and cost effectively by applying sodium hypochlorite.

Overall conclusion

Biobarrier technology is definitely a viable method for reducing flow in horizontal fractures. A 100% clogging of a 0.8 mm fractured was obtained, and the effects of no media injection and increasing hydraulic gradients were minimal after initial formation of the biobarrier. For the removal of biobarriers, the injection of sodium hypochlorite is effective.

6 FIELD APPLICATION OF BIOBARRIER TECHNOLOGY

The process of pore or fracture clogging due to the accumulation of bacterial cell bodies forming extra-cellular polymers in an aquifer can be defined as biobarrier formation.

This thesis has two aims, namely to determine the viability of transport of bacteria through dual porosity fractured rock aquifers and to test the effectiveness of biobarrier formation for reducing the hydraulic conductivity of a dual porosity fractured rock aquifer.

No formal field test of biobarrier technology for reducing the hydraulic conductivity of a dual porosity fractured rock aquifer had been performed on South African aquifers prior to this research, thus it was somewhat challenging to conduct these experiments.

The area used for the tests was the campus test site at the University of the Free State.

Chapter 5 focussed on the different methods to determine the fracture position and hydraulic properties in three boreholes, namely UO7, UO14 and UO20. After the fracture positions were determined, radial convergent tracer tests were performed to obtain the mass transport properties. The first tracer test was between UO14 and UO7 and the second between UO7 and UO14. UO20 was used as an observation borehole. The results from these tests were used in preparation for the field application of biobarrier technology.

For the application of biobarrier technology in the field, bacterium *S. marcescens* was used.

6.1 SET-UP OF FIELD EXPERIMENT

6.1.1 Methodology

The set-up of the field experiment was the same as for a radial convergent tracer test. Tracer experiments were conducted using a radial flow field established by circulating water in one borehole (UO7) and withdrawing water from another (UO14). See Figure 6-1 for the set-up of each borehole.

UO7 was used as the injection borehole and UO14 as the abstraction borehole. A small air pump was connected to UO20 to aerate UO20 in an attempt to keep the system aerobic and thus stimulate bacterial activity.



Figure 6-1 Set-up of the three boreholes: UO7 (injection borehole), UO20 (observation borehole) and UO14 (abstraction borehole).

From the results of the fracture determination test in UO7, an injection area of 1 metre length, stretching from 22 to 23 metres, was used.

The abstraction pump was situated at a depth of 23 metres below surface and the injection pipe at 22 metres below surface. The abstraction and injection pipes were then connected to a 70 litre flowcell, and a closed system was created. Circulation in the 1 m tested section took place at a rate of 0.9 l/s.

The bacteria and media were injected into the flowcell at a rate of 1 l/min, by means of peristaltic pumps. The reason for the slow injection rate was to cause as little as possible disruption to the water levels in the boreholes, so that radial flow from the injection borehole would not occur.

In UO14, a pump was placed at 25 mbgl and the pump calibrated for an abstraction rate of 0.5 l/s. An abstraction rate of 0.5 l/s was used to encourage the transport of bacteria and media. If the abstraction rate is too low, bacteria and media might drift in the direction of groundwater flow, which is the opposite direction to the pump-induced flow.

Prior to injection of the bacteria, a pre-injection experiment was done to determine the effect of injecting 300 l/day of water on the water levels of the aquifer system. The results showed that injection has minimal effect (approximately 2 cm rise in UO7 and 1 cm rise

in UO20 and UO14) on the water levels. Thus the proposed volume for injection is possible, and no major effects are expected on the water levels of the aquifer system.

During the first day of bacteria and media injection, the abstracted water from UO14 was re-injected into UO7 at a depth of 21 metres as soon as the breakthrough curve was measured. This was done to calculate the biomass and media, ensure aerobic conditions and minimise the loss of nutrients. See Figure 6-2 for the set-up of the test site.

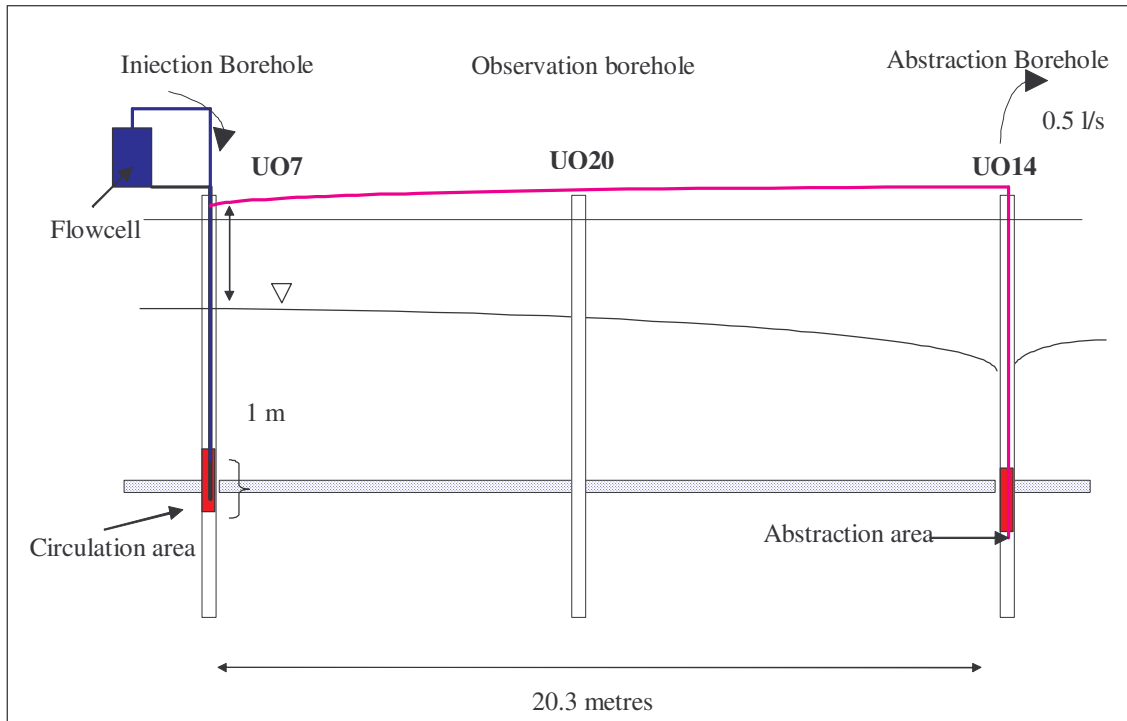


Figure 6-2 Set-up of the biobarrier test at the campus test site.

6.2 PREPARATION OF BACTERIA AND MEDIA USED FOR THE FIELD EXPERIMENT

The bacteria and media were prepared by the Department of Microbiology, Biotechnology and Food Biotechnology.

6.2.1 Media preparation

The media preparation for the upscaling experiment was the same as described in Chapter 4, section 4.3 and section 4.14.3. The concentrations were upscaled to a final

concentrated volume of 2.5 litres. The 2.5 l volumes of concentrated media solution were transferred to 25 l containers.

On site, each 25 l container was filled with groundwater pumped from one of the boreholes upstream of the biobarrier boreholes to give a 10 times dilution of the media solution. Three hundred litres of diluted media were injected each day for the first 11 days. See Table 6-1 for injection volumes.

6.2.2 Bacteria preparation

The bacteria were prepared according to the procedure described in Chapter 4, section 4.14.3.

For the inoculum, 380 ml BSM media, instead of 190 ml, were added to a 1 l Erlenmeyer flask. 20 ml, instead of 10 ml, of the pre-inoculum was added to each shake flask and incubated on a shaker at 25°C for 4½ hours.

The bacteria were harvested by combining all the inoculum flasks, which added up to 8 litres. The optical density (OD) was measured at 600 nm and the cell concentrations calculated from a standard curve. Four litres of the medium were added to the inoculum to give a final volume of twelve litres, with a cell concentration of approximately 10^9 cells/ml. One litre of this cell concentration was transferred to each drum (12 drums, 1 l per drum).

6.3 TESTING THE EFFECTIVENESS OF A BIOBARRIER IN FRACTURED ROCK AQUIFERS

6.3.1 Methodology for daily injection

On the first day, before injection started, the pumps were started in UO7 and UO14 to create a radial flow field.

The growth media was added using 25 litre drums. One hundred litres of media were injected before beginning the injection of 312 litres bacteria and media. The reason for this was to ensure media availability for the bacteria when arriving at the subsurface. The peristaltic pumps pumped the media from the injection container into the flow cell at a rate of 1 litre per minute. For the bacteria and media injection, 1 litre of bacteria was

added to a 25-litre container of growth media. With this, the bacteria concentration was diluted 25 times before injection, which brought the cell concentration to 4×10^8 cells/ml. (During laboratory column experiments, it was found that biobarrier formation can be established with a cell concentration of 10^4 to 10^6 cells/ml) therefore two orders of magnitude higher concentration was applied, based on the expected dilution in the aquifer.

The bacteria and media were thoroughly mixed and poured into the injection container. For the duration of the bacteria and media injection, each of the 12 drums was prepared immediately before injection. (See Figure 6-3 for the set-up of the injection borehole). See Table 6-1 for a summary of the bacteria and media injection volumes with time.

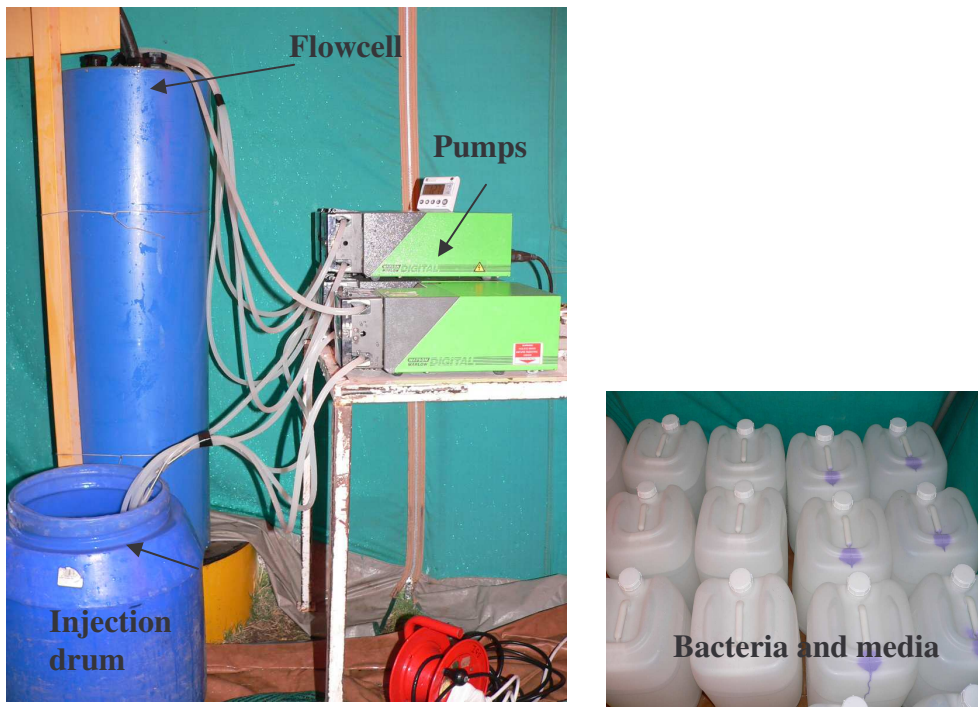


Figure 6-3 Set-up at the injection point.

Table 6-1 Volumes of bacteria and media injected over time. Bacteria concentrations were measured in cells/ml).

Field day	Volume media injected (l)	Volume bacteria injected (l) Cell concentration = (10^8 cells/ml)	Eventual (10^8 cells/ml)
Day 1	400	12 l	1.2×10^9
Day 2	300	12 l	1.2×10^9
Day 3	300	12 l	1.2×10^9
Day 4	300	12 l	1.2×10^9
Day 5	200		
Day 6	300	12 l	1.2×10^9
Day 7	300		
Day 8	300	12 l	1.2×10^9
Day 9	300	12 l	1.2×10^9
Day 10	300	12 l	1.2×10^9
Day 11	300		
Day 14	200		
Day 15	300		
Day 17	200		
Day 31	150		
Day 35	150	6 l	6×10^8
Day 36	100	4 l	4×10^8

6.3.2 Sampling

As seen from Table 6-1, the injection volumes differ over time. For each day, samples were taken at 15-minute intervals by means of a tap at the outflow of the abstraction borehole. The reason for this was to determine the breakthrough curve of bacteria and media each day. The electrical conductivity (EC) was measured by means of a hand-held instrument. The bacteria samples were sent to the Department of Microbiology and Biotechnology for real-time PCR analyses. Water level measurements were also taken every half hour to determine the effect of injection on the water levels.

6.4 DATA ANALYSES

6.4.1 Media breakthrough

Breakthrough curves were plotted for the EC over time. The EC over time was measured in the abstraction borehole to determine the distribution of the media concentration from UO7 to UO14. In Figure 6-4 (Day 1) and Figure 6-5, the relative concentrations were plotted versus time. The large drop in the EC concentration over the first 60 minutes for Day 1 can be attributed to removal of pre-existing salinity in boreholes due to previous

tracer tests. Further, a gradual increase in the EC can be seen with time and can be attributed to the large volume of media injected.

In Figure 6-5 it can be seen that the over the first few days, there is a relative increase of between 0.005 and 0.008 in concentration. From Figure 6-5 and Table 6-1 (injection times), it can be seen that the concentration decreased as the media injection decreased. The shape of the curve is also dependent on the volume injected.

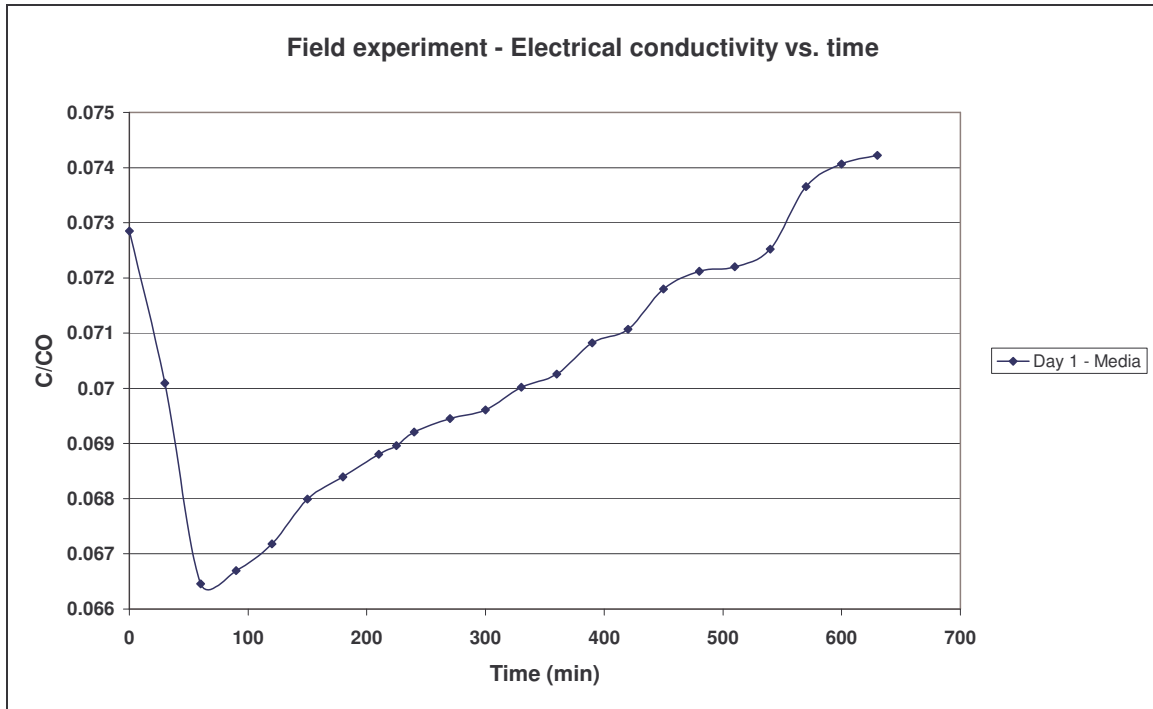


Figure 6-4 Media (C/C_0) breakthrough curves vs. time - Day 1.

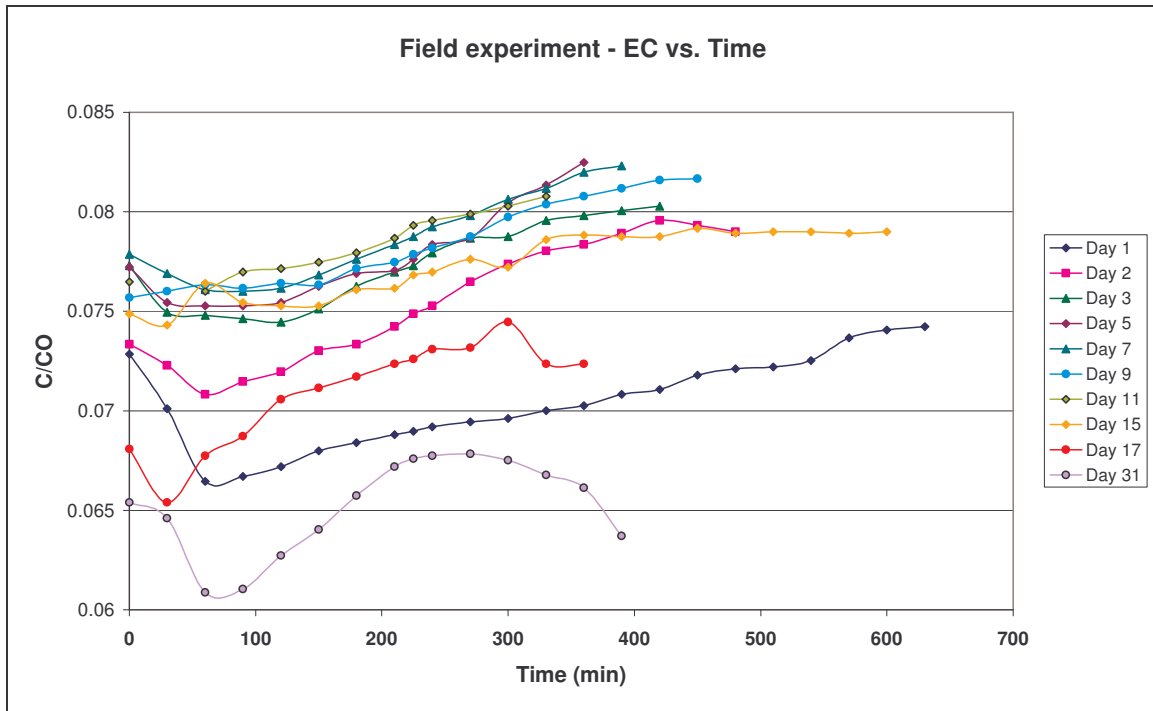


Figure 6-5 Media (C/C_0) breakthrough curves vs. time.

6.4.2 Bacteria breakthrough – Real-Time PCR

Refer to Chapter 5, section 5.3.5 for more information on real-time PCR and PCR methods. The PCR and real-time PCR analyses were performed by the Department of Microbiology, Biotechnology and Food Biotechnology.

During the first ten days, bacteria injection occurred on all the days, with the exception of Day 5 and Day 7. During each day, 12 litres of bacteria with a concentration of 10^9 cells/ml were mixed with 300 litres of media and injected into the aquifer. Samples were taken for PCR and RT-PCR analyses. The purpose of the analyses was to identify *S. marcescens* as well as to determine the concentration of *S. marcescens* in the aquifer system. From the results, it is easier to understand events in the subsurface. The samples were not analysed immediately, which made it very difficult to determine the progress of the bacterial biomass formation in the system. From the RT-PCR results, the following can be seen:

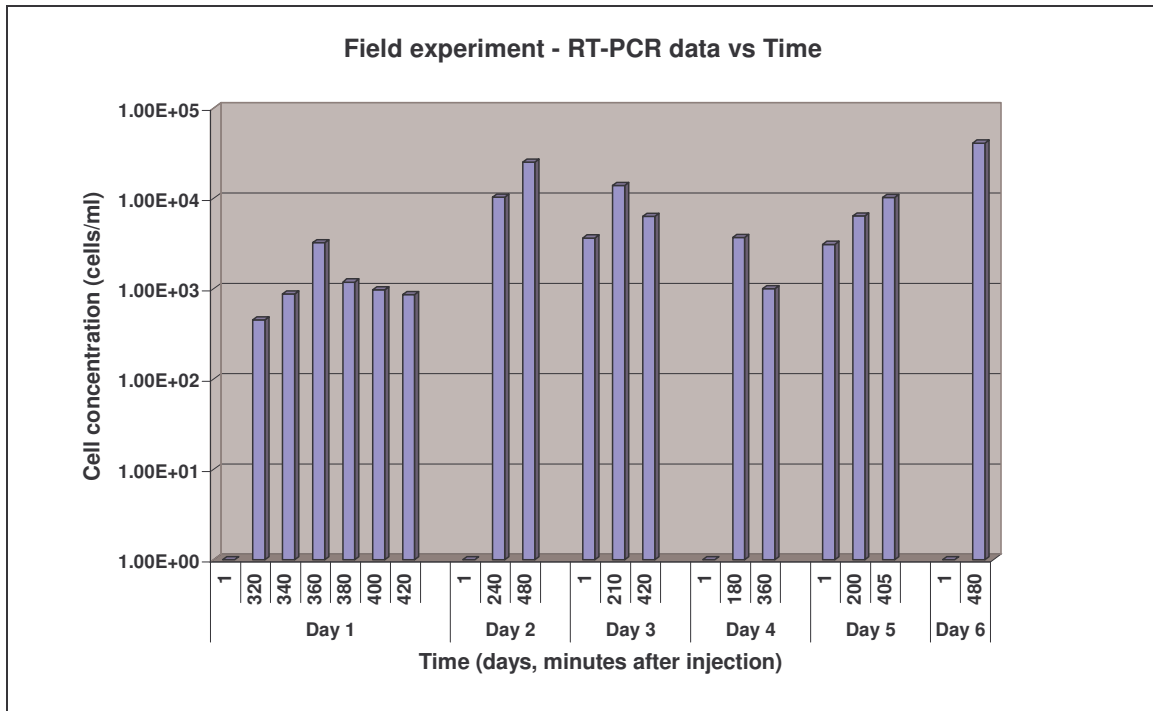


Figure 6-6 Bacteria breakthrough curves determined by real-time PCR - Samples taken from UO14.

See Figure 6-7 for the bacteria breakthrough curve of Day 2 (optical density). The results show that a maximum of over 10^3 cells/ml was measured during the first day. When comparing this to the breakthrough curve results of the uranine, and the NaCl and NaBr tracer breakthrough curves described in Chapter 3, the following were found: The sequence for breakthrough was as follows: the uranine was first, taking approximately 250 minutes to reach peak breakthrough at the abstraction borehole, NaCl was second, with a peak breakthrough time of 270 minutes, and then NaBr, taking 310 minutes to reach a peak. See Chapter 3, section 3.10.3 and Figure 3-26 to Figure 3-28 for the results and graphs of the uranine, NaCl and NaBr breakthrough curves.

Since there have been no formal field tests of bacteria transport on South African dual porosity fractured rock aquifers to date, it is encouraging to find that bacteria migration was measurable.

From Figure 6-8, the following can be seen: A very flat curve was measured, due to the large injection volume and adhesion of the bacteria to fracture surfaces.

The dispersion and velocity for bacteria transport was calculated with the TRACER software (Riemann, 2002). A very slow velocity of 21 m/d was measured for the bacteria. Due to the slow velocity of the bacteria, a very large dispersivity of 10.52 m was measured. In Table 6-2 the bacteria transport parameters were compared with the radial convergent tracer transport parameters. From the result it can be seen that bacteria transport is much slower, thus even distribution of bacteria will take longer in an aquifer.

Figure 6-6 shows the cell concentrations for Day 1 to Day 6. During the first six days, the cell concentrations increased to 4×10^4 cells/ml. Unfortunately, no RT-PCR data are available after Day 6.

During the last part of the experiment, 16S and PCR analyses showed that, apart from *S. marcescens*, there is a significant amount of biostimulation with the media used. This means that other *in-situ* bacteria can contribute to the barrier forming process.

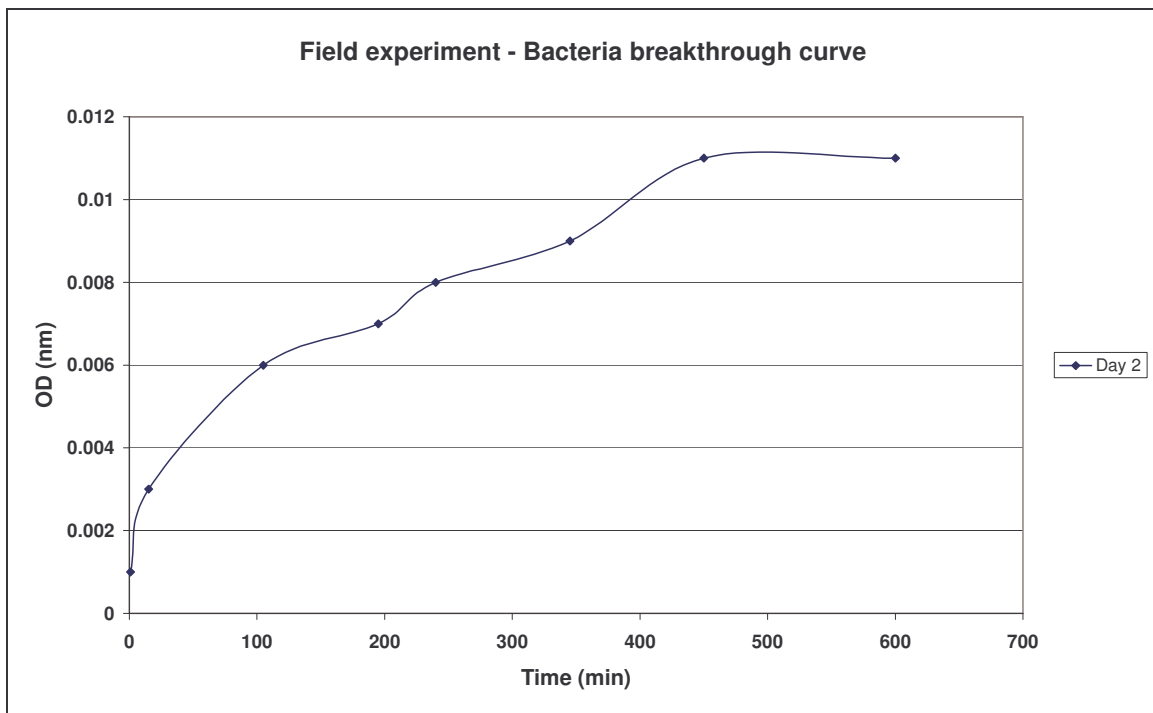


Figure 6-7 Bacteria breakthrough curve - Field experiment. - Day 2

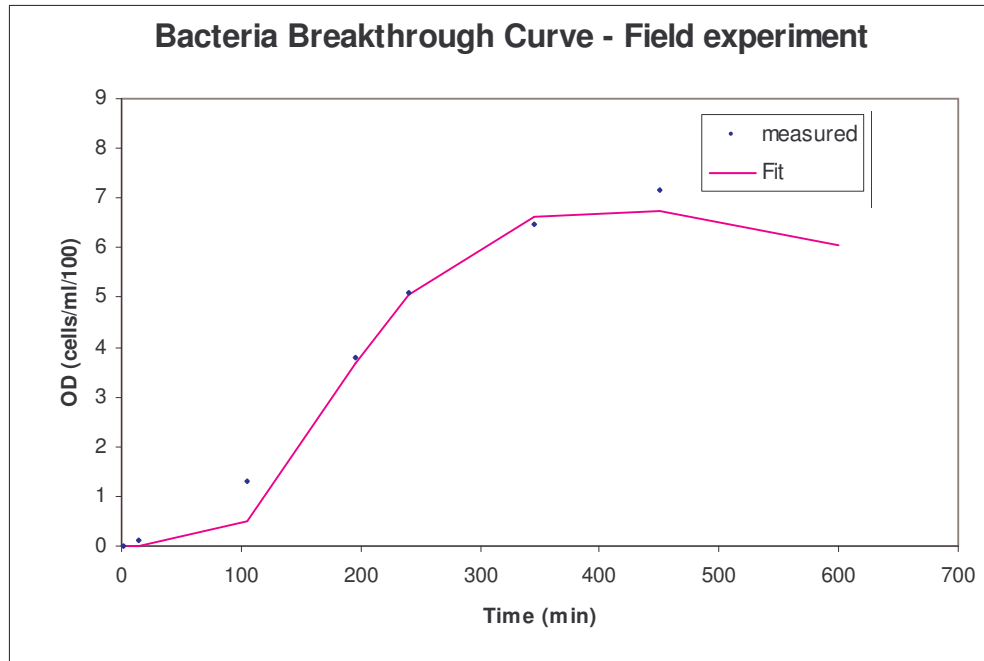


Figure 6-8 Results from the TRACER fit for the bacteria breakthrough curve - Field experiment.

Table 6-2 Summary of the transport parameters calculated by TRACER for the field experiment.

U07-U014			
Tracer	Thickness (m)	Velocity v_f (m/d)	Dispersivity (m)
NaCl	0.15	79	1.7
NaBr	0.15	69	2
Uranine	0.15	81	1.6
Bacteria	0.16	21	10.52

6.4.3 Water level measurements

Water level data can be used to determine possible bacteria growth due to water level increases measured during the injection period. The water level increases will occur due to obstructions forming in the fracture.

With regard to the water level data for UO7, UO20 and UO14, the following can be seen: During the first eleven days of the experiment, an average of 312 litres bacteria (12 l) and media (300 l) were injected per day, except on Day 5 (200 litres). Figure 6-9 shows the static water level data over the course of the experiment (and unrelated events that may have had an impact on water levels). See Table 6-1 for reference to injection days and volumes injected.

The rise in the water level of UO7 was much higher than in UO20 and UO14. This can mainly be attributed to injection in UO7. See Figure 6-9 and Figure 6-10 for graphs of the static water level versus time (water level measurements taken at the beginning of each day) and the water level versus injection times (water level measurements at the end of each day). During the 15 days, a sharp increase in the water level was measured in UO7. To a lesser extent, this can be attributed to the injection process, while the main cause is bacteria growth. UO7 and UO20 are relatively high yielding boreholes with high hydraulic conductivities and the effect of recharge due to injection is minimal. A water level increase of 1.069 m was measured in the injection borehole. A more gradual increase of the water levels in UO20 and UO14 was measured. The assumption was made that this increase can be attributed to bacteria growth. An increase of 0.595 and 0.600 was measured in UO20 and UO14, respectively. This can be attributed to the distance between the injection, observation and abstraction boreholes.

After Day 16, the injection was stopped. The sharp drop in the water level of UO7 was caused by the removal of the pump in UO7, as circulation no longer took place. A slow decrease in water levels can be seen between Day 18 and Day 28. Between Day 28 and Day 30, a sharp decrease in the water levels can be seen in all three boreholes. This is possibly a sign of barrier failure (see Figure 6-9). It was then decided to re-inject media to determine if the bacteria could be resuscitated *in situ*. The aim was to inject media during Day 31, and then bacteria and media during Day 35 and 36. A large drop in the water levels was observed between Day 31 and Day 34. This can be attributed to a combination of injection of media and cleaning of boreholes in the vicinity of the biobarrier boreholes. The bacteria and media injection during Day 34 and Day 35 caused a brief recovery in the barrier. After Day 37, water levels in all the boreholes decreased over time. Between Day 38 and 43, barrier failure was observed again. After Day 37, the biobarrier was no longer effective.

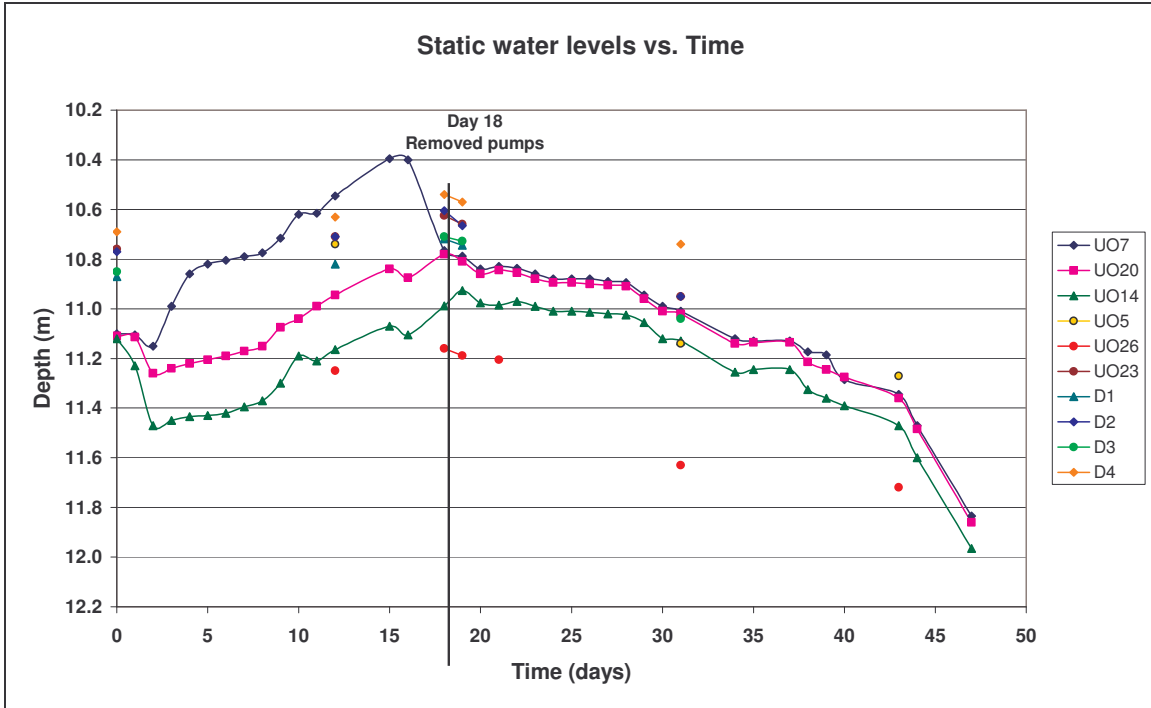


Figure 6-9 Variation in the static water levels vs. time (days).

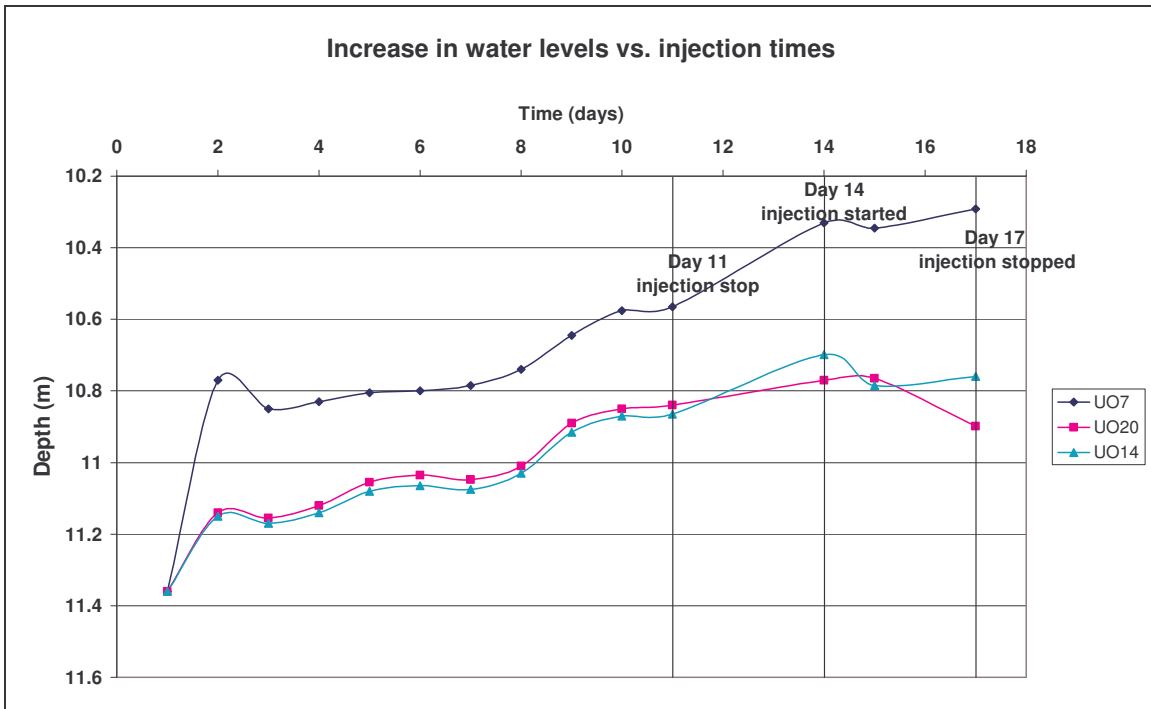


Figure 6-10 Increase in the water levels vs. injection times measured at the end of each injection day (days).

6.4.4 Testing the effect on aquifer properties

6.4.4.1 Methodology

Slug tests in South Africa are used with two objectives in mind: (i) to get a first estimate of the yield of a borehole (relationship obtained by Viviers *et al.*, (1995)) and (ii) to estimate the K-value (or T-value) of the aquifer in the vicinity of the borehole.

In a slug test, the static water level in a borehole is suddenly lowered or raised. This is usually done by lowering a closed cylinder into a borehole. The cylinder replaces its own volume within the borehole water, thus increasing pressure. As the equilibrium in the water level is changed, it will recover or stabilise to its initial level. If the rate of water level recovery or recession is measured, the transmissivity or hydraulic conductivity of the borehole can be determined (Kruseman and De Ridder, 1991).

For the purpose of the field-scale biobarrier test, slug tests were conducted to estimate the hydraulic conductivity (K) of the aquifer in the vicinity of the boreholes.

To ensure accurate slug-test recordings, a transducer was used to record the time vs. drawdown/recovery (recession) data. A pressure transducer can act as a discrete or continuous measuring device. The rate of recession was measured before and during the field experiment to determine the reduction in hydraulic conductivity of the fracture by using a pressure transducer (STS-DL/W version 232).

Pressure transducers commonly have a small capillary tube vented to the atmosphere that allows them to automatically compensate for barometric (atmospheric) pressure. Pressure transducers measure the pressure head (water column) above the transducer. The pressure transducer was connected to a data logger that contains micro-processors to convert pressure information to feet or metres of water column above the transducer, or depth to water from the top of the well casing.

The test was conducted as follows: The transducer was lowered to a depth of 15 metres in the borehole and the other end connected to a computer. Slug tests were conducted as described above. After the slug test was finished, the data was downloaded to a computer and subsequently used to calculate aquifer hydrogeologic properties. See Figure 6-11 for the set-up of the slug test.

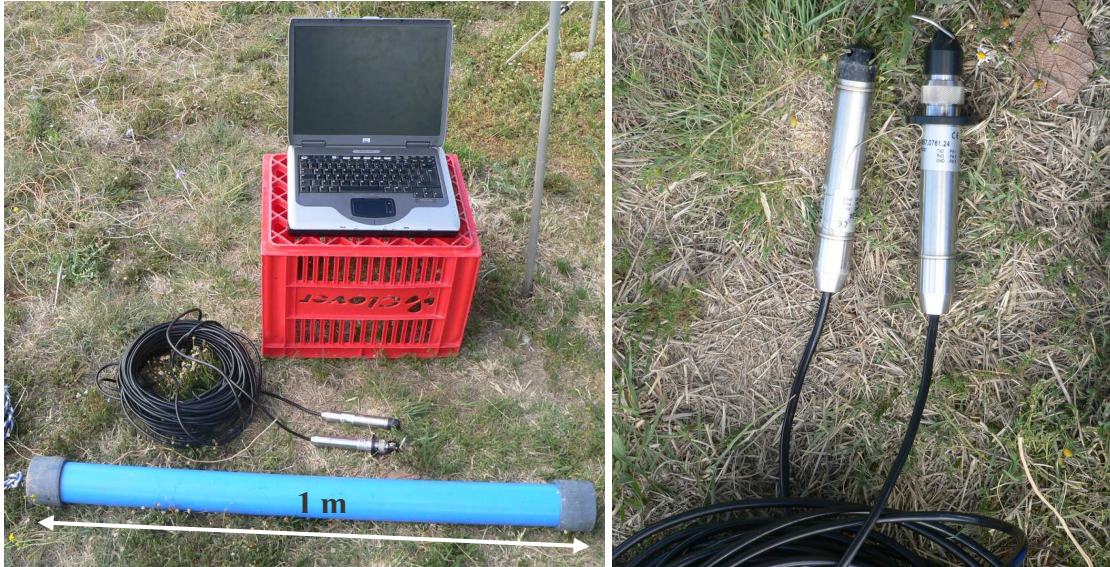


Figure 6-11 Set-up for a slug test by means of transducers.

Prior to the field experiment, slug tests were conducted on the three boreholes.

For the first 12 days of the field injection experiments, slug tests were not conducted because of constant injection. Slug tests were performed on Days 16, 20, 27, 30, 34, 38, 40, 42, 44, 48 and 51. Unfortunately, the slug tests done on Days 16 and 20 of the experiment, were done by measuring with a stopwatch and dipmeter because of electronic problems with the transducers. These slug tests are not as accurate as transducer data.

The results from the slug tests were analysed by means of the Bouwer and Rice method (1976) to estimate the K-values with time.

The Bouwer and Rice equation reads:

$$K = \frac{r_c^2 \ln(R_e / r_w)}{2d} \frac{1}{t} \ln \frac{h_0}{h_t} \quad (\text{Equation 6.1})$$

Where:

r_c =radius of the unscreened part of the borehole where the head is rising

r_w =horizontal distance from the borehole centre to the undisturbed aquifer

R_e =radial distance over which the difference in head h_0 is dissipated in the flow system of the aquifer

d =length of the borehole screen or open section of the borehole

h_0 =head in the borehole at time= t

h_t =head in the borehole at time t

According to Van Tonder and Vermeulen (2005), an incorrect hydraulic conductivity value will be obtained from the slug test if the thickness of the aquifer (total formation) is used as the flow thickness. For a flow thickness of 0.16 m (i.e. the thickness of the fracture zone), a hydraulic conductivity value of 541 m/d is estimated with the Bouwer and Rice (1976) slug-test method (Van Tonder and Vermeulen, 2005). This estimated K-value is more representative of the K-value of the fracture zone. The flow thickness value was used for the calculations.

6.4.4.2 Results from aquifer hydraulics

Consistent results were obtained for all three boreholes during the experiment.

See Figure 6-12, Figure 3-13 and Figure 6-15 for the variation in the hydraulic conductivity with time and for the % reduction in the hydraulic conductivity graph for all three boreholes.

Because UO7 served as the injection borehole, it is expected that the greatest reduction would be obtained there. The original hydraulic conductivity of the borehole (UO7) was 446 m/d. After 20 days, the hydraulic conductivity decreased to 70 m/d; thus an 84% reduction in the hydraulic conductivity was obtained. After Day 20, the hydraulic conductivity started to increase rapidly. This can be attributed to the fact that the bacteria were no longer supplied with media. Barrier failure was measured between Day 27 and Day 34, causing the hydraulic conductivity to increase from 70 to 207 m/d per day (see Figure 6-12). Media injection occurred again on Day 31 and bacteria and media injection on Day 33 and 34. From Figure 6-9, it seems as if the barrier was not rebuilt during injection and the hydraulic conductivity increased to 260 m/d. During Day 34 to Day 37, the barrier recovered slightly and caused the hydraulic conductivity to decrease. After 38 days, the barrier started to fail, and collapsed after 44 days. After 48 days, only 13% reduction in the original hydraulic conductivity was observed.

The fracture position is higher in UO20 than in UO7 and UO14, thus the expectation of barrier formation in UO20 was much smaller. It was unexpected to measure a 60%

reduction in the hydraulic conductivity after 16 days. The hydraulic conductivity decreased from 590 to 235 m/d. A sharp increase of 235 to 455 m/d in the hydraulic conductivity was measured between Day 16 and Day 30, and can be attributed to the absence of media injection. Between Day 30 and Day 34, the barrier recovered slightly, causing the hydraulic conductivity to decrease. After 34 days, a sharp increase in the hydraulic conductivity was measured and can be attributed to barrier failure.

In UO14, a 40% reduction was measured after 16 days. This is reassuring, as it means that bacteria transport can be successfully accomplished in dual porosity fractured rock aquifers. This shows that it is possible to establish the biobarrier over as distance. After 20 days, the barrier loses its effect very quickly, and must thus be more steadily supplied with media to maintain the barrier.

From the results of the slug test, it can be concluded that it is possible to reduce the hydraulic conductivity of fractures in the vicinity of the injected fracture. It is also possible to decrease the hydraulic conductivity of fractures over some distance from the injection point (at least 20 m). From the results of the field experiment, it can be said with confidence that biobarrier formation is a viable method to decrease the hydraulic conductivity of a dual porosity fractured rock aquifer.

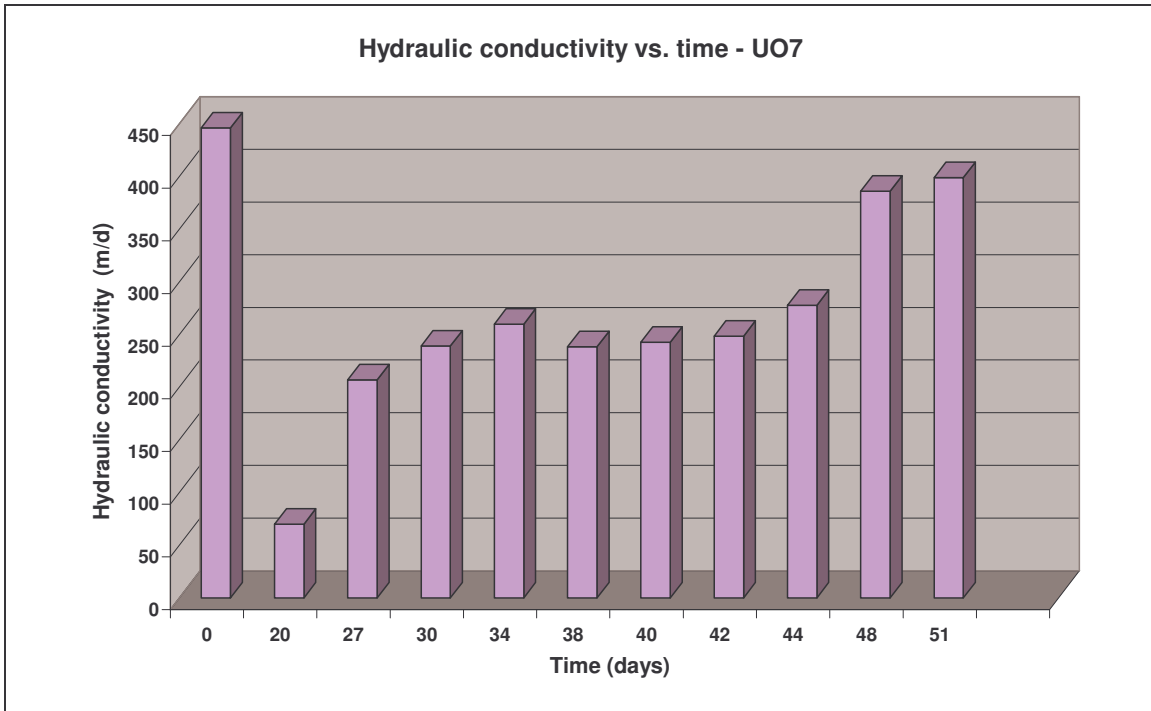


Figure 6-12 Variation in the hydraulic conductivity over time in UO7.

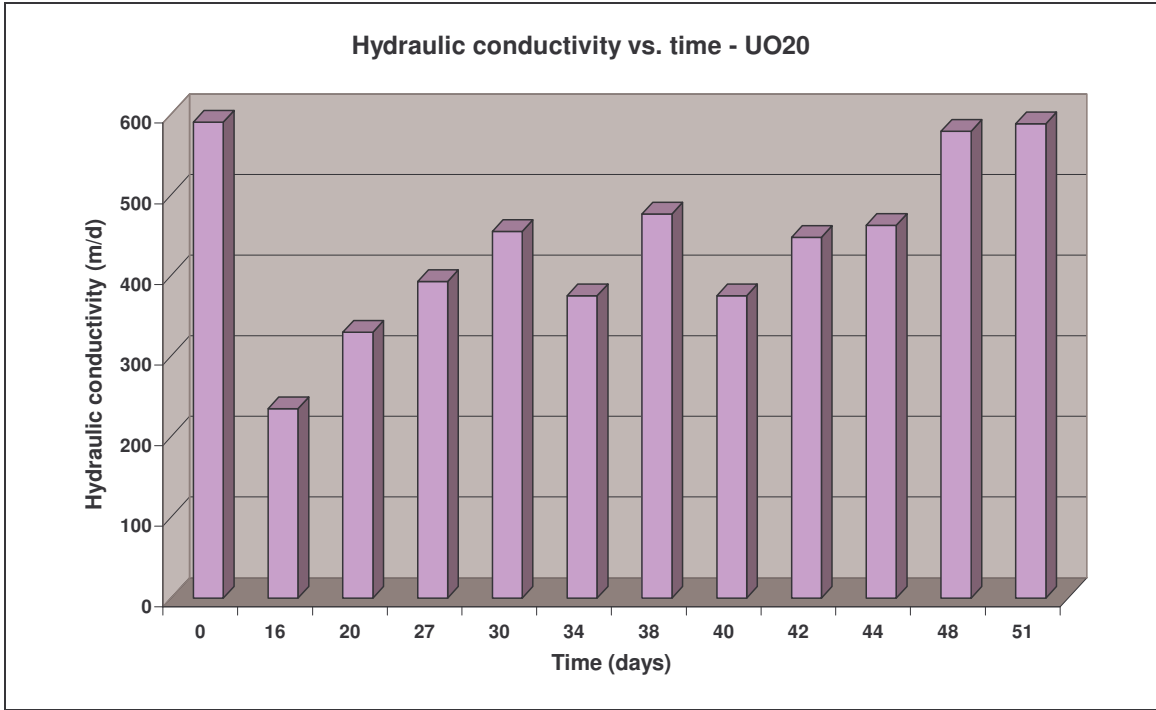


Figure 6-13 Variation in the hydraulic conductivity over time in UO20.

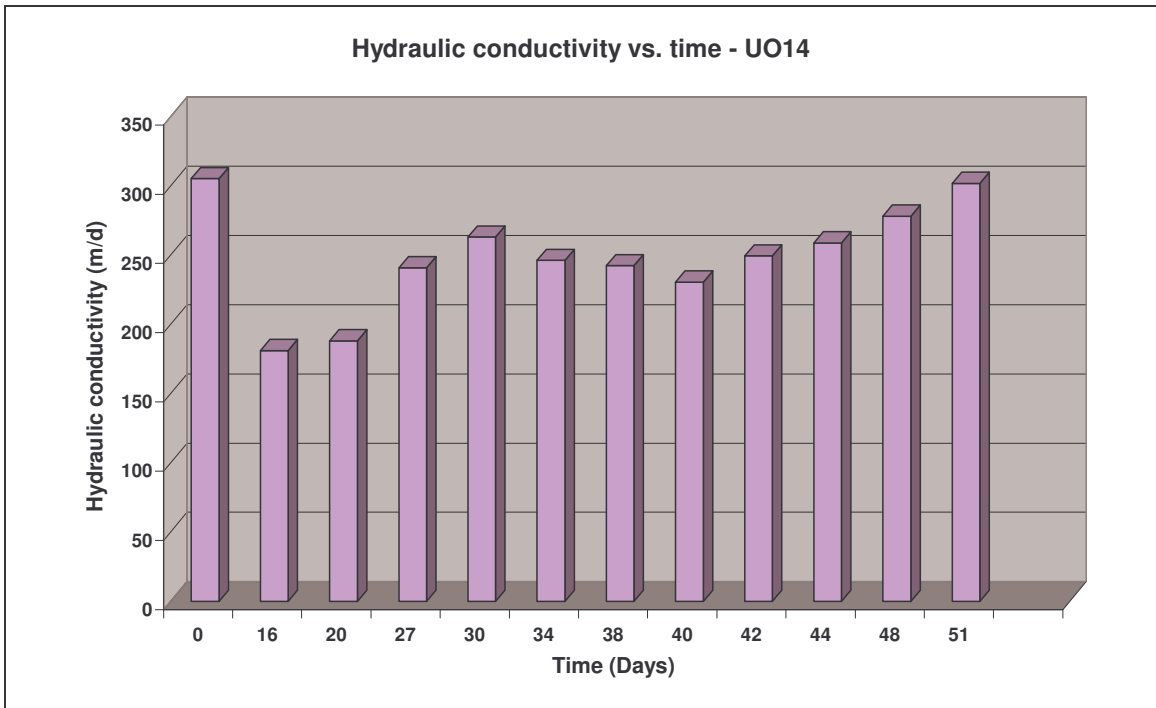


Figure 6-14 Variation in the hydraulic conductivity over time in UO14.

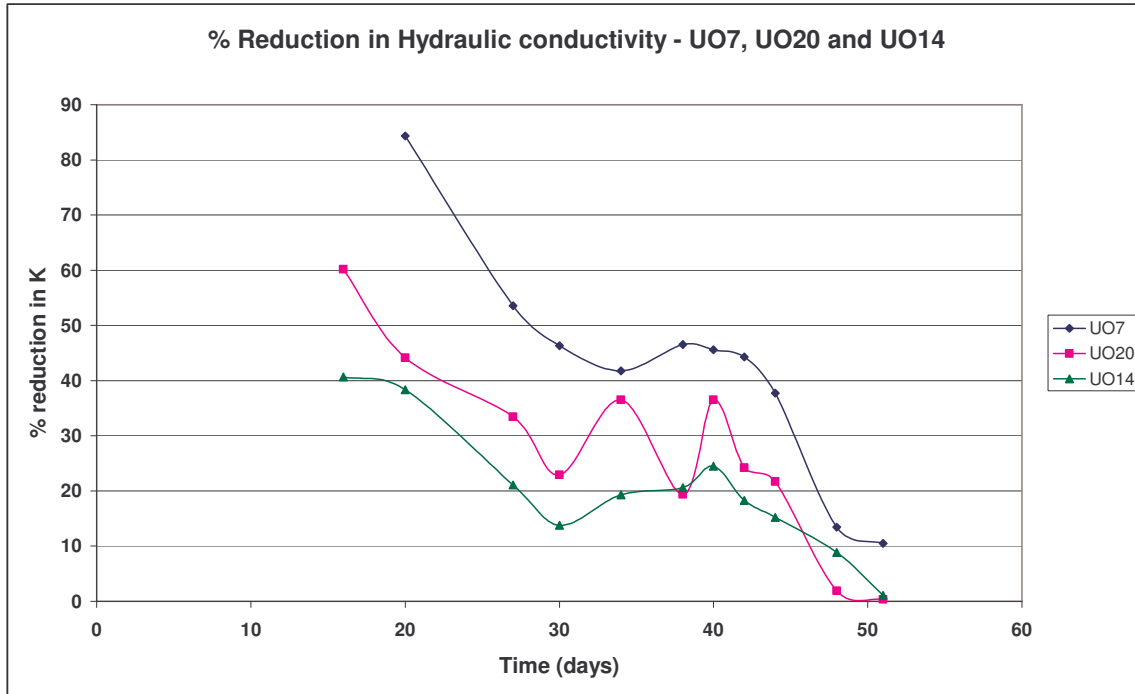


Figure 6-15 Reduction in hydraulic conductivity in UO7, UO20 and UO14 (%).

6.4.5 Flowmeter measurements

6.4.5.1 Methodology

The residual flow in the boreholes was measured by means of a Century System VI flowmeter logger.

During the field experiment, only UO20 and UO14 were logged. During borehole video camera observations in UO7, it was decided not to log UO7 because of bacteria growth on the sides of the borehole that could be damaged or disturbed if the flowmeter was lowered into the borehole.

See Figure 6-16 for the set-up of the flowmeter measurements.

The flowmeter consists of a 1.2 metre probe. A skirt was placed at the bottom of the probe to force flow upwards into the probe from the bottom. Logging was done from the top down. The area of investigation was between 20 and 25 metres below the surface.

The original flow was measured prior to the field experiment. After 20 days, the first flowmeter readings were taken. Flowmeter readings were taken on a weekly basis.

See Figure 6-17 and Figure 6-18 for the results of the flowmeter.



Figure 6-16 Set-up of the flowmeter (UO20 and UO14).

6.4.5.2 Flowmeter results

From the results, it can be seen that much higher flow values (litres per second) were recorded in UO14 than in UO20. The reason for this is that, because there are two fractures in UO14, there is vertical flow between these two fractures.

In UO20, the major fracture is located at a depth of 21.3 metres. From Figure 6-18, the fracture position can clearly be seen. Much lower yields were measured in UO20, because there is only one fracture in the borehole, and thus only horizontal flow is measured at the fracture position. Very small reductions in the flow were measured in both boreholes after biobarrier formation.

A way to obtain quality flowmeter data might be to pump at a very low rate in one of the boreholes. The reason for not doing these experiments accordingly was to decrease the possibility of disturbance to the barrier formation, but perhaps in future this could be done, as suggested.

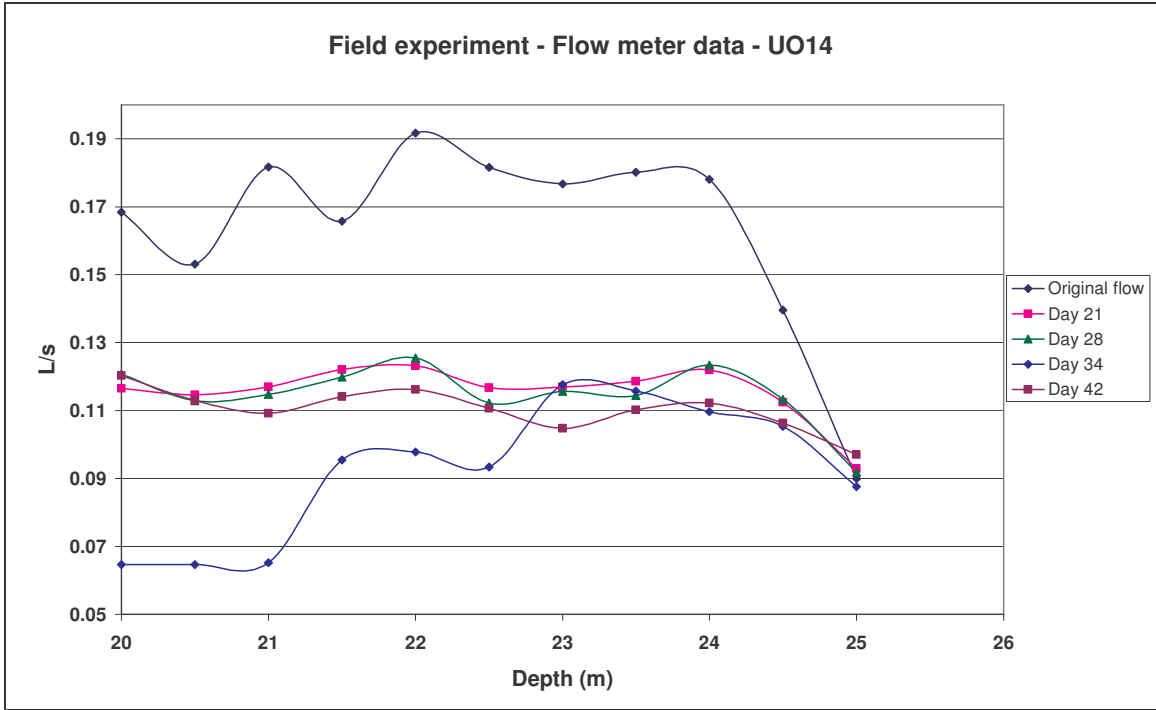


Figure 6-17 Flow rate vs. depth (UO14).

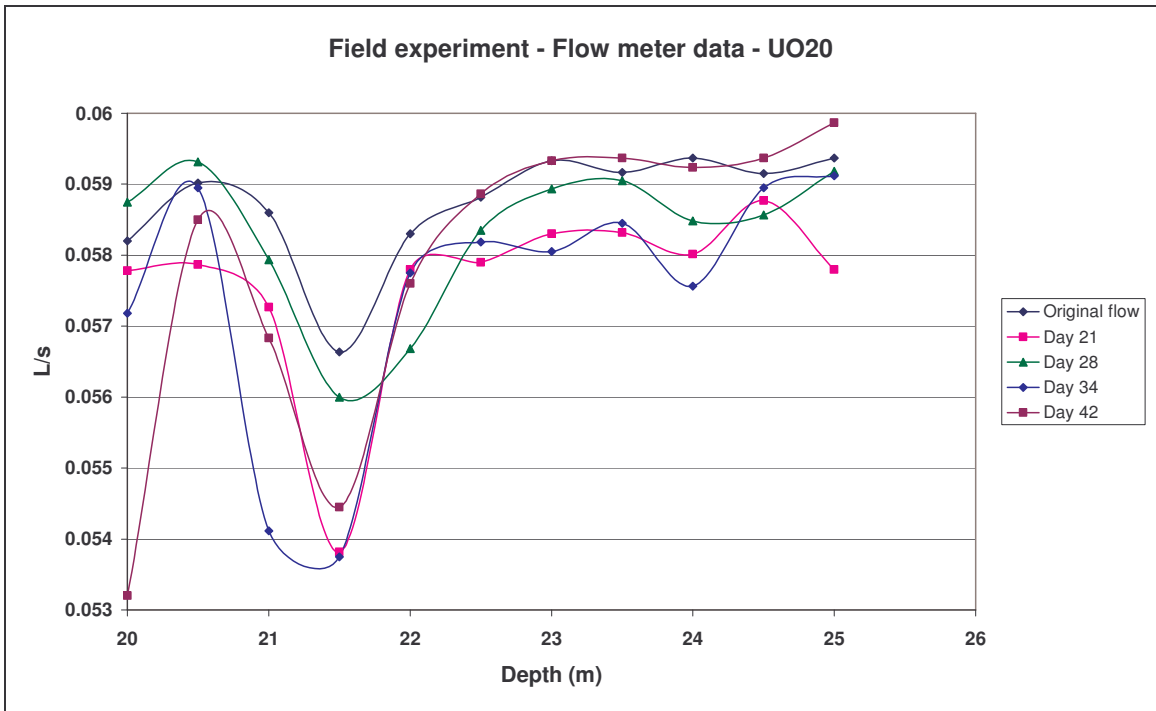


Figure 6-18 Flow rates vs. depth (UO20).

6.4.6 Borehole video camera

Borehole video camera investigations were conducted on a weekly basis, from Day 16 onwards. See Figure 6-19 for the set-up of the borehole video camera. See Figure 6-20 to Figure 6-23 for photographs of the bacteria growth in boreholes after 16 days of injection of bacteria and media. (See DVD for additional borehole video camera observations). This includes borehole video camera observations for all the boreholes prior to injection as well as observations during the application of biobarriers in the field. During the field experiment, only the fracture areas were targeted.

6.4.6.1 Borehole video camera observations

From the results of the borehole video camera, the following could be observed: In UO7, bacteria growth started almost at the static water level and continued to below the fracture. After 23 metres, bacteria growth started to decrease due to anaerobic conditions.

In UO20, the greatest bacteria growth was visible at the position of the fracture. The whole fracture area was covered with a whitish mat of bacteria.

In UO14, bacteria growth was visible in the small fractures as well as in the large fractures.

(See DVD for borehole video camera observations of the fracture zones).



Figure 6-19 Set-up of the borehole video camera (UO20 and UO14).



Figure 6-20 Borehole video camera observations (Day 16, UO7, 16- 21. m) (White material is biomass).



Figure 6-21 Borehole video camera observations (Day 16, UO7, 22.8. m). (White material is biomass).



Figure 6-22 Borehole video camera observations (Day 16, U20, 21.3 m).



Figure 6-23 Borehole video camera observations (Day 16, UO14, 22.7 m).

6.4.7 Rehabilitation of the aquifer

6.4.7.1 Flushing with sodium hypochlorite (NaOCl)

The aim of chemical borehole rehabilitation was to disinfect, dislodge, disperse and remove the *in situ* bacteria and to sterilise the borehole.

In the laboratory parallel plate fracture experiment good results were obtained by making use of a 15% hypochlorite solution to rehabilitate the parallel plate fracture. For the rehabilitation of biobarrier formation in the field situation, sodium hypochlorite was used.

The effectiveness of the rehabilitation was assessed by measuring the hydraulic conductivity of the boreholes before and after treatment, as well as by means of borehole video camera observations.

On the 45th day of the experiment, NaOCl was injected into the aquifer. 125 litres of 15% NaOCl solution were prepared and injected into UO7. The test was conducted in the same manner as the previous one, except that the abstraction water was disposed of rather than re-circulated.

After eight hours of pumping, 7 litres of NaOCl were injected into UO7, 11 litres into UO20 and 7 litres into UO14. The system was circulated by pumps for 48 hours to clean the boreholes. Slug tests were performed to determine if the yield had recovered to its original value. The hydraulic conductivity of all three boreholes recovered to their original values. See Figure 6-12 to Figure 6-15 for the results of Day 51.

6.5 CONCLUSIONS

During this study, the main aims of the thesis were to determine the transport properties of bacteria through fractured rock aquifers and to test the efficiency of bacteria in decreasing the hydraulic conductivity of a horizontal fracture in a fractured rock aquifer.

Prior to the field application of biobarrier technology, hydraulic tests (fracture position determination, hydraulic conductivity of fractures, flow velocities, dispersivity values, flow thickness, direction of groundwater flow, etc.), flowmeter observations and borehole video camera work were performed on all three boreholes to determine initial hydraulic

conductivity values, flow values, and to visibly observe events in the vicinity of the fracture position.

The site was set-up on the same principle as a radial convergent tracer test. For the first 11 days, bacteria and media were injected as described in Table 6-1.

Electrical conductivity measurements

Electrical conductivity was measured on a daily basis to ensure that the media injected was evenly distributed through the aquifer system. From the results, it can be seen that the media concentrations increased over the first 11 days, indicating that there are nutrients available for the bacteria. When the injection was stopped after 11 days, the EC of the aquifer decreased gradually, as the bacteria consumed the available nutrients in the groundwater.

Bacteria transport and bacteria identification

Bacteria transport was evaluated by means of RT-PCR techniques. Samples were taken on a daily basis to determine the breakthrough of bacteria. During the first day, a breakthrough was obtained. When comparing the bacteria breakthrough curve with the breakthrough curve of the conservative tracers used during the site characterisation test (NaCl, NaBr and uranine), it can be seen that bacteria retardation is greater than that of the other conservative tracers and may not be solely due to dispersion. There is visual evidence in the camera logs that some of the injected bacteria adhere to the aquifer surfaces. Also, the mass recovery of bacteria would not match the injected tracer amount for vegetative bacteria, as it should for a truly conservative tracer, because the bacteria are capable of reproducing in the aquifer.

This is very good news for biobarrier technology in South African fractured rock aquifers. Bacteria transport is easy and viable in fractures.

From the results of the PCR analyses, it was also evident that, in addition to *S. marcescens*, there is a significant amount of biostimulation with the media used.

Water level measurements

Static water level measurements as well as water level variation measurements were taken on a daily basis. This was to monitor the effect of recharge due to injection, as well as the effect of bacteria growth on the water levels.

During the first 16 days, sharp increases in the water levels were measured in UO7. This can be attributed to bacteria growth in the injection borehole. The water levels in UO20 and UO14 increased gradually and can be attributed to recharge from injection and, to a lesser extent, bacteria growth. Between Day 18 and 28, the water levels dropped gradually. Between Day 31 and 34, barrier failure was observed. Barrier formation was restored after a short injection period. Complete barrier failure was observed after 43 days.

Aquifer hydraulics

Slug tests were performed and measured by means of transducers. The Bouwer and Rice method was used to calculate the hydraulic conductivity of the fractures with time. The results were as follows:

The best reduction was obtained in the injection borehole. An 84% reduction in the hydraulic conductivity was measured after 20 days (hydraulic conductivity decreased from 446 to 70 m/d). After Day 20, the hydraulic conductivity started to increase rapidly. Barrier failure was observed between Day 27 and Day 34. This caused the hydraulic conductivity to increase from 70 to 207 m/d. During Day 34 to Day 37, the barrier recovered slightly and caused the hydraulic conductivity to decrease. After 38 days, the barrier started to fail, and collapsed after 44 days. After 48 days, only 13% of the barrier was still in position.

The 60% reduction in the hydraulic conductivity of UO20 after 16 days was unexpected. The hydraulic conductivity decreased from 590 to 235 m/d. A sharp increase in the hydraulic conductivity (from 235 to 455 m/d) was measured between Day 16 and Day 30, and can be attributed to the absence of media injection. Between Day 30 and Day 34, the barrier recovered slightly. After 34 days, a sharp increase in the hydraulic conductivity was measured and can be attributed to barrier failure.

From the results of UO14, it could be seen that it is possible to form a biobarrier over a distance. A 40% reduction was measured after 16 days. After 20 days, the barrier loses its effectiveness very quickly, and must be supplied more readily with media to maintain the barrier. This is very reassuring, as it means that bacteria transport can be successfully accomplished in a dual porosity fractured rock aquifer.

It is possible to reduce the hydraulic conductivity of the fractures in the vicinity of the injection borehole to an extent of 80% or more. It is possible to decrease the hydraulic conductivity of fractures at a distance from the injection borehole. From the results of the field experiment, it can be said with confidence that biobarrier formation is a viable method for decreasing the hydraulic conductivity of a dual porosity fractured rock aquifer.

Borehole video camera observations

From the results of the borehole video camera, the following could be observed: In UO7, bacteria growth started almost at the static water level and continued to below the fracture. After 23 metres, bacteria growth started to decrease due to anaerobic conditions.

In UO20, the greatest bacteria growth was visible at the position of the fracture. The whole fracture area was covered with a whitish mat of bacteria.

In UO14, bacteria growth was visible in the small fractures as well as in the large fractures.

Rehabilitation of the aquifer

For the rehabilitation of biobarrier formation in the field situation, sodium hypochlorite was used.

The effectiveness of the rehabilitation was assessed by measuring the hydraulic conductivity of the boreholes before and after treatment.

A 15% sodium hypochlorite solution was prepared and injected into UO7. The test was performed in the same manner as the bacteria injection experiment.

The effectiveness of the rehabilitation was determined by slug tests. All the hydraulic conductivities recovered to their original values. The use of sodium hypochlorite for the rehabilitation of boreholes is thus a viable method.

6.6 RECOMMENDATIONS

Prior to the field application of biobarrier technology, extensive site characterisation must be performed to determine the hydraulic properties of the site, including fracture positions, hydraulic conductivity, flow velocities, dispersivity values, flow thickness, flow direction, etc.

According to fracture determination data and borehole video camera observations, an injection area must be determined. When the site includes fractures at different depths, this must be taken into account when choosing the injection interval.

During the test, water level measurements must be taken for all the boreholes close the site (100-metre radius).

When building biobarriers, groundwater flow must always be kept in mind. Biobarriers will drift according to the direction of groundwater flow, thus it is recommended that the barrier be constructed a few metres upstream of the target area. This will decrease the flow (hydraulic conductivity) of the area upstream of the area. Bacteria will drift to the target area, and thus a more effective barrier can be built.

The theory and practice of radial convergent tracer tests are a viable method to construct biobarriers. Injecting bacteria and media into an injection borehole and pumping at another allows the bacteria to move, disperse and adhere in the fracture. Very good results were obtained with this method. Pumping must be constant and at low rate during the test. This will ensure the containment of biomass and aerobic conditions, and minimise the loss of nutrients.

7 APPLICATION OF BIOBARRIER TECHNOLOGY TO SOUTH AFRICAN AQUIFERS

7.1 INTRODUCTION

Groundwater is a source of drinking water for many people around the world, especially in rural areas. In South Africa, approximately two thirds of the rural population depends on groundwater (located in fractured rock aquifer systems) for their domestic needs (Pietersen, 2004). In such aquifers, groundwater is contained in fractures (hard rocks), fissures and dissolution cavities (dolomite and limestone) and to a lesser extent in pores in weathered rock (Vegter, 1995). As a result, the storativity and transmissivity compare poorly with primary aquifers, where water storage can represent up to 30% of the gross volume. Groundwater quality varies throughout South Africa, with rainfall and residence time being important factors in quality.

Pollution of groundwater with toxic and carcinogenic compounds is a serious concern for public health and environmental quality. Pollution is commonly manifested as a contaminant plume migrating in the direction of groundwater flow from a point source.

7.2 TYPES OF GROUNDWATER CONTAMINANTS

Pollution refers to levels of hazardous substances in the environment over and above what is ordinarily found in the absence of local activities. Groundwater pollution therefore refers to the occurrence of substances (inorganic species, organic compounds or bacterial agents) in concentrations above those found naturally in an aquifer. The substances themselves, both chemical and bacterial, are referred to as contaminants.

A wide variety of materials can be identified as contaminants in groundwater. Contaminants may include organic chemicals, hydrocarbons, inorganic cations, inorganic anions, pathogens and radionuclides.

7.3 GROUNDWATER REMEDIATION TECHNOLOGIES

Remediation goals vary from site to site. Remedial actions are usually selected on the basis of their effectiveness, practicability, durability and likely cost (www.environment-agency.gov.uk). Refer to Table 7-1 for a summary of remediation technologies widely used.

The following remediation technologies are used for groundwater remediation:

- Physical barriers (physical containment of the contaminant with sheet piling, grout injection, decant piling etc.)
- Groundwater pump and treat (extracting contaminated groundwater for treatment at the surface).
- Enhanced *in situ* bioremediation (injection of nutrients and other geochemical agents to stimulate biological activity to degrade some contaminants *in situ*).
- Air sparging (an *in situ* treatment technology that involves the injection of air directly into the saturated subsurface via either vertical or horizontal wells to exchange volatile contaminants from the dissolved phase to the vapor phase by way of air stripping (ITRC, 2005)).
- Water flooding (mobilisation and removal of a contaminant through increases in the hydraulic head).
- Chemical flushing to mobilise contaminants (surfactant and alcohol flooding to mobilise and remove residuals).

A few of the above remediation technologies will be discussed and compared to biobarrier technologies or suggested as complimentary techniques to biobarriers.

7.4 ADVANTAGES OF BIOBARRIER TECHNOLOGY OVER SOME REMEDIATION TECHNOLOGIES

The biobarrier concept typically involves the construction of a wall of porous carbon-based material (Strietelmeier *et al.*, 2001) placed in a line perpendicular to the direction of groundwater flow that extends at least to the width and depth of a contaminant plume. Biobarrier technology is believed to be very cost effective to implement, maintain and remove (Komlos, *et al.*, 1998).

For the successful implementation of biobarriers at a contaminated site, the groundwater system must be reasonably well characterised in terms of direction of flow, width and depth of plume, concentrations along the plume, flow velocity and hydraulic conductivity (Strietelmeier *et al.*, 2001).

In the next section, biobarrier technology is compared to currently used remediation technologies to show the advantages of biobarrier technology.

7.4.1 Physical barriers and biobarriers

Containment of the contaminant plume is important in preventing further migration and localising the plume for *in-situ* or *ex-situ* remediation.

Current containment methods (physical barriers) include sheet pilings and grout curtains. These barriers require extensive physical manipulation of the site (e.g. excavation and back-filling) and are expensive to construct (James *et al.*, 2000).

Biobarrier technology, however, involves the use of bacterial biomass produced *in situ* to contain or manipulate groundwater flow. Biobarriers can be maintained through a series of vertical or horizontal injection boreholes that feed the bacteria to maintain the biobarrier. Contaminants trapped in the biobarrier can be contained by maintaining the biobarrier. Once the objectives are reached, the subsurface can be returned to a more normal habitat by lowering the nutrient concentration to the subsurface community and allowing the organisms and biobarrier to die back and return to a bacterial community more consistent with the area and groundwater (www.srs.gov).

When comparing biobarriers with physical barriers, the following can be seen:

- Biobarriers are more cost effective and cause less surface disruption than physical barrier technologies. Biobarrier construction is achieved without excavation and therefore will be economically attractive at many sites. Examples include funnel and gate technology, where strings of biobarriers are used to funnel a contaminant into a specific area. Biobarriers are also easy to remove. When the barrier is no longer needed, the nutrient supply can be terminated, and the bacteria forming the barrier will die off. Cleaning the aquifer system is also very easy.
- There is no obvious depth or aquifer type limitation for biobarrier technology. Physical barrier technologies such as slurry walls and grout curtains are not usually cost effective at depths of more than 15 m (Cunningham and Hiebert, 2000) or in hard rock environments.

Refer to Table 7-2 for a summary of the comparison between biobarrier technology and current used remediation technologies.

7.4.1.1 Funnel and gate

Biobarriers can be used in funnel and gate systems to isolate contaminant plumes in groundwater, and funnel the plumes through *in situ* reactors. The biobarrier will act as the funnel, thus containing the contaminant plume. The *in situ* treatment area will act as the gate. The groundwater plume will be directed through the *in situ* reactors in the gates, where physical, chemical or bacterial processes remove contaminants.

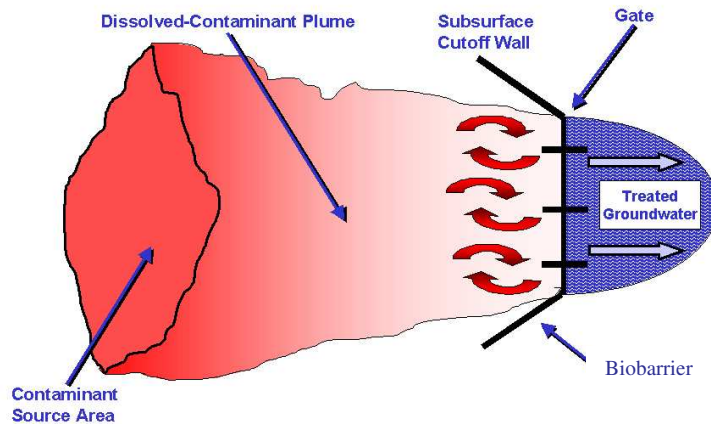


Figure 7-1 Example of a funnel and gate system.

7.4.2 Pump-and-treat systems and biobarriers

Conventional pump-and-treat systems are based on the concept of extracting contaminated groundwater for treatment at the surface. *Ex situ* remediation normally commences on abstracted water.

Pump-and-treat systems are designed for two possible objectives, namely, restoration or containment, or a combination of both (ITRC, 2005).

- Restoration is a process that actively removes and treats the contaminant.
- Containment prevents the contaminant from spreading and protects down-gradient receptors.

The efficacy of a pump-and-treat for remediation of groundwater contaminants depends primarily on hydrogeological and contaminant properties.

The ideal environment for pump-and-treat is a homogeneous aquifer with a relatively high hydraulic conductivity. Fractured rock and karst aquifers are more difficult to remediate, since regions within the fractured rock may store contaminants that the bulk of the groundwater does not reach (ITRC, 2005).

Removal of the contaminated water is often not viable because of the sheer volume of contaminated water to be pumped and treated. Furthermore, contaminants continue to leach out from the sediments and pollute more groundwater after the contaminated water is extracted. Clean-up time varies widely, ranging from years to decades or more.

The advantage of biobarrier technology over pump-and-treat is that biobarriers can be used as a containment technology and in conjunction with remediation technologies to degrade the contaminants *in situ*. Biobarriers can be placed in the subsurface to contain the contaminant, or decrease the hydraulic conductivity of the aquifer, causing the contaminant to slow down. With biobarrier technology, remediation could be effective in dual porosity fractured rock aquifers. Refer to Table 7-2.

Table 7-1 Summary of remediation technologies currently used.

Remediation technologies		
	Advantage	Disadvantage
Physical barriers		
Physical containment of the contaminant with sheet piling, grout injection, decant piling etc.	Containment of contaminant.	Physical manipulation of the site.
		Not cost effective at depths > 15 m.
		Expensive to construct.
Pump and treat		
Extracting contaminated groundwater for treatment at the surface.	Remediation of homogeneous aquifer with high K-values.	Fractured rock and karst aquifers are difficult to remediate.
	Containment of contaminant.	Large volume of contaminated water to be pumped and treated.
		Contaminants leach from sediments and pollute groundwater.
		Clean-up time varies from years to decades.
	Not cost effective.	
Air sparging		
Injection of air directly into the saturated subsurface via either vertical or horizontal wells.	Volatile contaminants from the dissolved phase to the vapor phase by way of air stripping	
	In situ treatment technology.	
Water flooding		
Mobilisation and removal of a contaminant through increases in the hydraulic head.	Mobilise and remove contaminants.	Not cost effective.
Chemical flushing		
Surfactant and alcohol flooding.	Mobilise and remove contaminants.	Not cost effective.
Biostimulation		
BioStimulation is the modification of contaminated materials and sites to enhance the growth of indigenous microbes already present. It can include the use of fertilizers and other nutrients in an attempt to stimulate the microbes.	Less costly than other remedial options.	
	Application involves equipment that is widely available and easy to install.	Effectiveness dependent on appropriate indigenous microbial population and organic material present.
	Technique does not produce waste products that must be disposed.	Testing the ability of indigenous microbes is costly.
	Time required for subsurface remediation may be shorter than other approaches (e.g., pump-and-treat).	Sites cannot always be cleaned and closed rapidly within budget amounts and target dates.
Bioaugmentation		
Addition of naturally occurring microbes to contaminated materials and sites. The correct microbes are added in sufficient quantities.	Applied with minimal cost, disruption and time.	Injection wells and/or infiltration galleries may become plugged by microbial growth or mineral precipitation.
	Sites can be cleaned and closed rapidly within budget amounts and time.	Difficult to implement in low-permeability aquifers.
	When correctly applied it is more effective, faster, and less costly than biostimulation.	May require continuous monitoring and maintenance.
	Time required for subsurface remediation may be shorter than other approaches.	Remediation may only occur in more permeable layer or channels within the aquifer.

Table 7-2 Summary of the comparison between biobarrier technology and currently used remediation technologies.

Remediation technologies vs. Biobarrier technologies					
Physical barriers	Advantage	Disadvantage	Biobarrier technology	Advantage	Disadvantage
Physical containment of the contaminant with sheet piling, grout injection, decant piling etc.	Containment of contaminant.	Physical manipulation of the site (e.g. excavation and back-filling).	Bacterial biomass produced <i>in situ</i> to contain or manipulate groundwater flow	Cause less surface disruption. Achieved without excavation.	Not effective in Karst aquifers.
		Not cost effective at depths > 15 m.		No depth limitation.	
		Expensive to construct.		Cost effective to construct.	
				Easy to remove barrier.	
				Funnel and gate.	
Pump and treat			Biobarrier technology		
Extracting contaminated groundwater for treatment at the surface.	Remediation of homogeneous aquifer with high K-values.	Fractured rock and karst aquifers are difficult to remediate.	Bacterial biomass produced <i>in situ</i> to contain or manipulate groundwater flow and degrade contaminant.	Containment of contaminant.	Not effective in Karst aquifers.
	Containment of contaminant.	Large volume of contaminated water to be pumped and treated.		Bacteria degrade contaminant <i>in situ</i> .	
		Contaminants continue to leach out from the sediments and pollute more groundwater.		Decrease the K-value of aquifer, (cause contaminant to slow down).	
		Clean-up time varies widely, ranging from years to decades.		Easy to remove barrier.	
		Not cost effective because of cost of rehabilitation at the surface.		Cost effective to construct.	

7.4.2.1 Comparison between pumping as hydraulic control and biobarrier as hydraulic control

Pumping methods can be used as hydraulic control, but not cost effectively. Pumping is effective in homogeneous aquifers but not in fractured rock aquifers. Pumping methods can contain a contaminant plume, but the pumped water must still be rehabilitated *ex situ*. Pumping is not cost effective in the long run because of the cost of rehabilitation at the surface.

Biobarrier technology works very effectively for hydraulic control. During testing of biobarrier technology on dual porosity fractured rock aquifers, it was found that bacteria *S. marcescens* can reduce the hydraulic conductivity of an aquifer successfully.

Biobarrier technology can be used to reduce the hydraulic conductivity of a fracture and is effective in containing and reducing certain types of pollution (Wongsa *et al.*, 2004, Montpas et al 1997, Bidlan and Manonmani, 2002). These barriers can be established and removed cost effectively.

7.5 BIOREMEDIATION TECHNOLOGIES

Biobarrier technology can also be combined with bioremediation technologies to simultaneously degrade a contaminant and hinder its migration (Komlos *et al.*, 1998). Bioremediation can be defined as any process that uses microorganisms, fungi or their enzymes to return the environment altered by contaminants to its original condition.

A biobarrier can be used as a stand-alone system when biodegradable materials are the only contaminants, or it can be used in combination with bioremediation technologies, to remediate contaminants (Strietelmeier *et al.*, 2001).

In-situ groundwater bioremediation is a technology that encourages growth and reproduction of indigenous microorganisms to enhance biodegradation of organic constituents in the saturated zone. *In-situ* groundwater bioremediation can effectively degrade organic constituents which are dissolved in groundwater and adsorbed onto the aquifer matrix.

The key parameters that determine the effectiveness of *In situ* groundwater bioremediation are: the hydraulic conductivity of the aquifer, which controls the distribution of electron acceptors and nutrients in the subsurface; biodegradability of the petroleum constituents, which determines both the rate and degree to which constituents will be degraded by microorganisms; and location of organic pollution in the subsurface.

Bioremediation may be employed to attack specific soil contaminants, such as degradation of chlorinated hydrocarbons by bacteria. Bioremediation technologies can be divided into three main types namely:

- bioaugmentation
- biostimulation and
- natural attenuation

All three types of bioremediation can be used at the site of pollution (*in situ*) or on pollution removed from the original site (*ex situ*).

Bioaugmentation can be defined as the addition of pre-grown bacterial cultures to enhance bacterial populations at a site to improve contaminant clean up and reduce clean up time and cost. Bioaugmentation is the addition of native or non-native bacterial cultures or “inocula” to the matrix to enhance or replace the native bacterial population. Indigenous or native microbes are those that occur naturally at a site. They are usually present in very small quantities. They may not be able to prevent the spread of the contaminant. In some cases, native microbes do not have the ability to degrade a particular contaminant. In general, biobarrier technology will be a form of bioaugmentation.

During the process of biostimulation, nutrients and oxygen, are added to contaminated water or soil to encourage the growth and activity of bacteria already existing in the soil or water. The disappearance of contaminants is monitored to ensure that remediation occurs. For example, hydrocarbon spills (specifically, gas spills) or certain chlorinated solvents may contaminate groundwater, and introducing the appropriate electron acceptor or electron donor amendment, as appropriate, may significantly reduce contaminant concentrations after a lag time allowing for acclimation. This is typically much less expensive than excavation followed by disposal elsewhere, incineration or

other *ex situ* treatment strategies, and reduces or eliminates the need for pump-and-treat, a common practice at sites where hydrocarbons have contaminated groundwater.

Intrinsic bioremediation (natural attenuation) occurs naturally in contaminated soil or water. This natural bioremediation is the work of microorganisms and is seen in petroleum pollution sites, such as old gas stations with leaky underground oil tanks.

Unfortunately not all contaminants, however, are easily treated by bioremediation using microorganisms. For example, heavy metals such as cadmium and lead are not readily absorbed or captured by organisms.

7.5.1 Bioremediation technologies for remediation of polluted sites

Like human beings, bacteria require a constant supply of organic nutrients to survive. Since most contaminants are compounds of hydrogen and carbon atoms, known collectively as hydrocarbons or organic compounds, many bacteria can digest the contaminants that pose a hazard to an ecosystem, its wildlife, and the health of the surrounding human population.

Until recently, practical applications of *in situ* bioremediation focused mainly on aerobic bacteria (Alexander, 1999), which absorb energy from the oxidation of organic compounds to carbon dioxide, with oxygen serving as the electron acceptor. However, this approach is limiting because oxygen is a requirement for aerobes and is scarce in the subsurface and many other contaminated environments. The amount of oxygen dissolved in groundwater is low and the rate of oxygen supply through diffusion from overlying unsaturated soils is slow.

The use of anaerobes or facultative anaerobe bacteria is a much better option for *in-situ* bioremediation at contaminated sites. Anaerobes grow in the absence of oxygen and oxidise organic compounds to carbon dioxide, using nitrate, sulphate or Fe^{3+} oxides instead of oxygen as electron acceptors.

Some anaerobes can degrade PCE and TCE by using these compounds as electron acceptors for the anaerobic oxidation of organic compounds or hydrogen gas (Lee *et al.*, 1998). Under ideal conditions, the reduction process removes the chlorine atoms from the contaminants, yielding ethylene as the final product; the chlorine is released as

chloride, PCE and TCE contaminants may thus be remediate by adding organic compounds to the subsurface (Lee *et al.*, 1998).

Nitrate pollution as a result of fertiliser use or the introduction of waste into the subsurface can be treated in an analogous manner. Denitrifying bacteria in the subsurface can oxidise added organics or hydrogen, reducing nitrate to harmless nitrogen gas.

Toxic metals and metalloids are often soluble, and thus mobile, in aerobic groundwater; however, under anoxic conditions, bacteria can reduce these to insoluble forms that precipitate from the groundwater. The metals and metalloids are thus immobilised, which limits their spread and threat to water resources. This typically occurs in the presence of sulphide ions, since many metal sulphides are insoluble, some microorganisms could also reduce sulphate to sulphide in the presence of oxygen and nitrate.

Biobarrier and bioremediation technology can also be combined with air sparging remediation technologies. Air sparging is an *in-situ* treatment technology that involves the injection of air directly into the saturated subsurface via either vertical or horizontal boreholes to exchange volatile contaminants from the dissolved phase to the vapor phase by way of air stripping (ITRC, 2005). The stripped compounds are then biodegraded in the vadose zone. The dissolved oxygen introduced by sparging may also stimulate biodegradation of contaminants in the dissolved phase.

7.5.2 *Serratia marcescens* applied for biobarrier formation as well as bioremediation

During this research bacteria *S. marcescens* was used to test the effectiveness of reducing the hydraulic conductivity of a dual porosity fractured aquifer.

From the results of the field test, it could be seen that *S.marcescens* has the ability to establish a biobarrier over a distance from the injection borehole. Field experiments with this bacterium showed that it is possible to clog fractures in the vicinity of the injected fracture to an extent of 80% or more and to decrease the hydraulic conductivity of fractures at a distance from the injection borehole. The results showed that *S. marcescens* is capable of forming a biobarrier and decreasing the hydraulic conductivity of a dual porosity fractured rock aquifer.

Other studies have shown that *S. marcescens* can also be used for bioremediation purposes.

Research conducted by Wongsa, *et al.*, 2004, showed that *S. marcescens* possessing the ability to degrade a wide spectrum of hydrocarbons. *S. marcescens* were able to degrade kerosene by more than 50%, diesel oil more than 60%, gasoline to an extent of 44%, and lubricating oil about 50%.

S. marcescens was also identified by Montpas *et al.*, (1997), as the most effective TNT-degrader. They established that bacterium *S. marcescens* is able to degrade TNT rapidly and that the rate of this transformation is dependent on the presence of a surfactant (Tween 80 (polysorbate 80)). This study suggests that a versatile microorganism such as *S. marcescens* could play a role in a biological depollution system.

Research conducted by Bidlan and Manonmani, (2002) also showed that *S. marcescens* is capable of aerobic degradation of DDT, and the uptake of nickle II by *S. marcescens* was investigated by Kennan *et al.*, (2002).

It can thus be concluded that bacterium *S. marcescens* is a versatile microorganism and can play a role in biobarrier formation as well as in a biological depollution system.

7.6 IMPLEMENTATION OF BIOBARRIERS IN SOUTH AFRICAN AQUIFERS

South African aquifers are of four broad types and flow mechanisms, namely the intergranular, the dual porosity aquifers aquifers, the fracture flow aquifers, and the karst aquifers. See Table 7-3 for an overview and summary of the main aquifer types and suitability for biobarrier technology. (Refer to Chapter 2, sections 2.1 and 2.2 for description of the aquifer types).

Table 7-3 Summary of the main aquifer types and flow mechanisms in South Africa.

Aquifer Type	Porosity type	Properties of Importance	Implications for biobarrier	Overview of implementation of biobarrier
Intergranular Silts, sands and gravels	Primary	High matrix porosity	Flow occurs in matrix	Characterise flow system
		High organic and clay content	Target coarse sandstone and gravel	Injection withdrawal tests Starvation of bacteria Bacteria injection until equally distributed Nutrient supply Monitoring Rehabilitation
Intergranular and fractured Sandstone and shale	Dual	High fracture K	Water and pollution flow in fractures	Find most transmissive fractures
		Low matrix K	Target fractures	Characterise flow system Injection - small interval in fracture zone injection withdrawal tests Bacteria injection until equally distributed Nutrient supply Monitoring Rehabilitation
Fracture flow Granites	Fracture	Fracture flow is dominant	Water and pollution flow in fractures	Find most transmissive fractures
		Fractures serve as preferred pathways Matrix porosity is low	Target fractures	Characterise flow system Injection - small interval in fracture zone Injection withdrawal tests Bacteria injection until equally distributed Nutrient supply Monitoring Rehabilitation
Karst Limestone and dolomite	Karst	Fracture and karst flow	Flow in fractures is too high	Fracture areas are too big to target
		Dissolution of soluble rocks Low matrix porosity		Biobarrier will not be effective

7.6.1 Practical implementation of biobarrier techniques in South African aquifers

The first step in application is to choose a suitable bacterium for the situation. In case of an application of biobarrier technology for containment of a pollution plume, a combination between containment and bioremediation of the plume or just hydraulic conductivity reduction, the bacteria chosen for the technology is very important.

Bacteria isolated for the purposes of biobarrier formation, bioremediation formation or a combination of the two can be done as follows:

Bacterial inoculum must be prepared in the laboratory from soil or groundwater either from the site where they are to be used or from another site where the biodegradation of the chemicals of interest is known to be occurring or a known bacterium capable of containment or remediation can be used. Microbes from the soil or groundwater must be isolated and are added to media containing the chemicals to be degraded. Only microbes capable of metabolising the chemicals will grow on the media. This process will isolate the bacterial population of interest, which may contain several different strains of microbes.

The isolated microbes can then be propagated in a nutrient medium and concentrated to produce an inoculum. Using native soils has the advantage that the microbes are more likely to survive and propagate when re-injected at the site, and also there will be less regulatory resistance to their use.

Using microbes from a different site has the advantage that they can be chosen from bacteria that are known to biodegrade the chemicals of concern. However, there is a possibility that these microbes will not be able to adapt to their new environment and will not propagate. Typically the microbes will adapt if the new environment is similar to their native environment.

Secondly, there are many factors that will influence the ability of bacteria to be an effective biobarrier or a biodegrader. The effectiveness of the bacteria for biobarrier formation or biodegradation will depend on bacterial properties for example: cell size, bacteria transport and distribution, bacterial adhesion, aerobic or anaerobic conditions

etc. These bacteria properties have an influence on each other. These parameters will be discussed in section 7.6.3.

7.6.2 Site characterisation

Prior to application of biobarriers or bioremediation, detailed site characterisation must be done on the area. If no boreholes are available on the site, boreholes must be drilled starting away from the contaminant source and moving inwards. The reason for this is to determine the extent of the pollution that must be contained or remediated. After the drilling of the boreholes, the following tests should be done in the area: aquifer tests, slug tests, fracture determination, tracer tests, borehole camera observations, geophysical logging, measuring flow velocities in the boreholes by making use of a flowmeter, and multiple-parameter logging.

7.6.2.1 Aquifer tests

Aquifer tests (constant discharge test and recovery test) should be done on all the boreholes to determine the hydraulic parameters of the aquifer, which include transmissivity, hydraulic conductivity, and porosity values.

7.6.2.2 Slug tests

Slug tests must be done by making use of transducers to determine the recession time of the aquifer. Hydraulic conductivity values can be determined from slug test data.

7.6.2.3 Fracture determination

The position of the fractures in each borehole should be determined by making use of large and small interval electrical conductivity logging tests. Sodium chloride can be injected on the same principle as a point dilution test. Injection must first occur over a large interval in the borehole. After injection and circulation of a few minutes, the EC can be measured in the injection area. The fracture positions will be identified from the dilution of the sodium chloride in the fracture positions. Data can be correlated by decreasing the injection interval.

7.6.2.4 Tracer tests

Two types of tracer tests can be done, namely point dilution tracer tests and radial convergent tracer tests. From the information obtained from the fracture determination tests, fracture zones can be identified. Tracers will be injected in these areas to determine the transport properties of the fractures including velocities, dispersivities and porosities.

The set-up of the site is as follow:

For the injection borehole, an injection zone will be chosen. The tracer will be injected into a flowcell. The injected tracer will be circulated in this area for the duration of the tracer test. In the abstraction borehole, the pump will be placed below the injection area.

It is very important to conduct radial convergent tests in various directions, due to the fact that transport is anisotropic. During this research, it was found that a tracer substance does not necessarily follow the same flow path when reversed. Tracer solutions can follow different flow paths to move from one point to another. The best injection path must be found to ensure fast and effective injection of the bacteria and nutrients into the aquifer.

The following are additional techniques that may add value:

7.6.2.5 Borehole camera observations

Borehole observations can be done by making use of a borehole camera. Borehole video camera will visually identify the fracture positions in the borehole, and also may show biobarrier formation. Borehole video camera will provide visible indications of apparent apertures, but may not indicate which fractures are transmissive.

7.6.2.6 Measuring the flow rate in the fracture area

The flow rate in the fracture area can be measured by making use of a flowmeter. The flow rates of the fracture can be determined by pumping one of the nearby boreholes at a very low rate. If no borehole is pumped in the vicinity, flow rate determination will be difficult. In the case where two or more fractures are present, the flow between the different fractures will be measured instead of the flow of the individual fracture.

7.6.2.7 Geophysical logging of the boreholes

Geophysical borehole logging can be done to determine the position and orientation of horizontal and vertical fractures, density of rock, resistivity parameters, and borehole diameters etc.

7.6.2.8 Multiple-parameter logging (pH, EC, redox potential and temperature)

Multi-parameter logging is important at these sites to determine the pH EC, redox potential and temperature of the aquifer. Bacteria growth will be affected by temperature and redox potential, salinity (EC) and pH. Salinity can also affect bacterial adhesion.

After site characterisation, enough information should have been gained on the aquifer to determine the most effective manner to implement the biobarrier technology.

Before implementation of the biobarrier on field scale can be done, the isolated bacteria must be evaluated in the laboratory to determine if bacteria will be effective in the environment injected, unless the species chosen already has already been proven to be viable.

7.6.3 Laboratory-scale experiments

With the results of the field characterisation in mind, the bacteria can be tested to determine which one will be applicable in the aquifer to be used.

For the application of biobarriers in porous media, experiments can be done by making use of sand with different grain sizes. It would be best to use sediments or soils from the field site or of the same type.

When choosing bacteria for a field site, the following parameters will play a very important role in the effectiveness of the bacteria in the field:

7.6.3.1 Aerobic or anaerobic bacteria

The choice of bacteria will depend on their purpose. When using aerobic bacteria, the bacteria will use oxygen as an electron acceptor. Saturated aquifers are often low in available oxygen. In the case of bacteria used as a biobarrier and for containment,

oxygen can be pumped into the aquifer by making use of air sparging techniques or injection of an alternative electron acceptor such as nitrate.

When using anaerobic bacteria, the bacteria will be able to survive without oxygen and in many contaminated sites, this may be preferable.

7.6.3.2 Cell size

Bacteria size is a very important parameter for effective transport of the bacteria. The choice of the bacteria size will depend on the aquifer properties of the site. Bacteria must be able to move throughout the surrounding unconsolidated materials or fractures rather than collect at the injection site. In very fine materials, bacteria transport can be inhibited or prevented by filtration as well as bacteria binding to particle surfaces, which will prevent movement. In this case, bacterial starvation might be an option. Starvation will cause changes in bacterial morphology which include reduction in cell size, which may enhance bacteria transport through the aquifer. In intergranular aquifers (sand and gravel), bacteria must be transported through the pores between the grains. In dual porosity aquifers as well as fractured aquifers, the cell size required will depend on the fracture aperture in the area, because bacteria transport will be mainly in the fractures. The rock matrix (sandstone, shale, granite, etc.) is usually too dense to allow bacterial transport.

7.6.3.3 Adhesion

The bacteria used for biobarrier technology must have good adhesion abilities. Adhesion will enable the bacteria to adhere, accumulate and when exposed to nutrients, to start to form biomass.

Adhesion tests must be done on the bacteria to determine their adhesion properties. Adhesion tests can be done as described in DeFlaun *et al.*, 1998.

7.6.3.4 Bacteria transport and distribution

When bacteria are injected into the aquifer, the bacteria must be able to advect in the direction of groundwater flow. For effective biobarrier formation, bacteria must be able to distribute throughout the area. It is important to remember that cell size and adhesion will have an effect on advection of bacteria.

7.6.3.5 Biofilm production

Bacteria must be capable of forming EPS during their growth phase to reduce the free pore space in the formation to reduce the hydraulic conductivity of porous or fractured media.

7.6.3.6 Media used for bacteria cultivation

For the bacteria to grow, applicable nutrient sources must be identified. Cultivation media must consist of electron acceptors (oxygen, nitrates, sulphates, etc.), and electron donors (carbon based sources) to ensure effective growth and multiplication of bacteria.

7.6.4 Column experiments

For the application of biobarrier formation in porous media, for example for intergranular aquifers, it is advised to do column experiments, to determine the transport properties of different tracers and bacteria through the sands. When species of proven viability are used, this will not be necessary.

7.6.4.1 Transport tests

Conservative tracer and bacteria transport tests can be done in columns packed with porous media obtained from the field site. Columns of different dimensions can be used. Sampling along the length is advised. Columns can be packed with different grain size material. For the packing of the columns, coarser material should be packed at the bottom and top to allow even distribution of the tracers through the column. Injection occurred from the bottom. The columns were saturated prior to the experiment. The tracers must be injected as a pulse and then connected to a water source to allow to tracer to flow through the column. The breakthrough of the tracers can be measured by making use of a bromide meter, EC meter, and a spectrophotometer (optical density for bacteria concentration), depending on the tracer.

The transport parameters (velocity and dispersivity) for different conservative tracers, as well as for the bacteria, can be determined in the columns for each sand types or grain size.

The results from the breakthrough curves for each sand and tracer will determine the injection methods used for the bacteria for biobarrier formation. If bacteria have difficulty moving through the sand, starvation of the bacteria becomes an option.

7.6.4.2 Hydraulic reduction tests

In case of very fine material, the starved bacteria will be injected first to ensure equal distribution throughout the area. Media injection occurs after bacteria, to prevent clogging at the beginning. The lag time associated with starvation recovery may increase media penetration through porous media by temporally reducing consumption near the injection site (James *et al.*, 1995).

In case of coarse sand where bacteria do not have transport problems, bacteria and media injection can occur simultaneously.

It is important to allow bacteria and media injection until an even distribution of bacteria is measured in the column. Bacteria distribution can be measured by sampling the side ports and determining the bacteria concentration at each port. The purpose of the hydraulic reduction test is to determine the reduction in hydraulic conductivity obtained using a specific bacterium. The hydraulic conductivity reduction test can be done by applying a constant head to the column and determining the effectiveness of the biobarrier.

For the purpose of testing bacteria and tracer transport as well as biobarrier efficiency in porous sands, upscaling to larger columns is advised.

7.7 APPLICATION OF BIOBARRIER TECHNOLOGY TO FIELD SITUATIONS IN SOUTH AFRICA

All the knowledge obtained during the field characterisation tests as well as the laboratory tests should be used for successful and effective biobarrier formation. Biobarrier formation can be applied in three of the four types of aquifers. (Refer to Chapter 2, section 2.1 and Chapter 7, section 7.6 for the four aquifer types)

Karst aquifers are a special type of fractured rock aquifer (limestone, dolomite or magnetite), in which the water in the fractures dissolves the relatively soft rock, causing

significant increases in the size of the fractures. Groundwater flow in Karst aquifers is more rapid than in the other aquifer types.

The application of biobarrier formation in karst aquifers will not be possible. The flow channels are too large, making biomass formation ineffective. The matrix porosity is too low to transport the bacteria. These aquifers are mainly found in the Karst belt and the Ghaap Plateau in South Africa.

7.7.1 Injection of bacteria and media

The following applies to all aquifers:

The injection depth will depend on the application on the desired depth of the barrier. In the injection borehole, bacteria will be injected in the area of interest. This is determined by the most likely depths of contaminant transport. Prior to injection of the bacteria and media, a pre- injection test must be done to determine the effect of injected volume on the rise of water levels in the area.

To establish and ensure effective barriers, the bacteria must be injected first to ensure equal distribution throughout the area. Nutrient injection will occur after bacteria injection. This will prevent clogging near the injection borehole of the aquifer. The lag time associated with starvation recovery of the bacteria will increase nutrient penetration through porous media by temporarily reducing consumption near the injection site (James *et al.*, 1995). Bacteria and nutrients should be injected via a flowcell. Circulation should be continued to prevent bacteria and media drifting away from the containment area.

Breakthrough curves should be determined for the bacteria transport throughout the aquifer. Abstracted water can be re-injected into the injection borehole to ensure bacteria and nutrients are not wasted.

For the duration of the test, water levels must be monitored to determine possible increases in the water levels due to bacteria growth.

Slug tests, and flowmeter measurements can be taken on a regular basis to determine the reduction in hydraulic conductivity of the aquifer due to biobarrier formation.

Bacteria concentrations can be monitored with Real-Time PCR technology or with spectrophotometry to measure OD.

Preferably, a facultative anaerobic or anaerobic bacterium should be used for biobarrier technology, because oxygen is an absolute requirement (electron acceptor) for aerobes, and oxygen is scarce in the subsurface. Anaerobic bacteria can use NO_3^- , SO_4^{2-} or Fe^{3+} instead of oxygen as electron acceptors.

7.7.2 Intergranular aquifers

The intergranular aquifers mainly consist of unconsolidated sediments (silts, sands and gravels). Primary porosity is dominant in these kinds of aquifers. The groundwater is mainly stored in the pore spaces between loose grains of sediment (high matrix porosity). The implication is that the flow mainly occurs throughout the aquifer media.

Biobarriers may be formed in these aquifers as follows:

During site characterisation (radial convergent tracer tests) the direction of groundwater flow, the hydraulic properties, and the transport characteristics of the unconsolidated sands must be determined. The aim of the barrier will influence the injection depth of the bacteria. If the purpose of the biobarrier is to contain a contaminant plume, the width and depth of plume, flow velocity and hydraulic conductivity must be known. The depth/zones of pollution and expected flow paths must be targeted.

For the purpose of biobarrier formation in unconsolidated materials, bacteria may need to be starved in fine material to ensure the bacteria can be transported through the aquifer rather than collect at the injection site.

Injection of the bacteria and media should be conducted in the same manner as a radial convergent test. In the case of porous media, the injection borehole must be located upstream and the abstraction borehole, downstream.

These aquifers can be remediated by flushing with sodium hypochlorite or left to degrade by not feeding the bacteria.

During laboratory-scale experiments, the effectiveness of biobarrier technology in reducing the hydraulic conductivity of unconsolidated materials (fine and coarse porous

media) was tested. The results show that it is definitely possible to reduce the hydraulic conductivity of porous media. Examples of intergranular aquifers in Southern Africa are alluvium, the Cape Flats.

7.7.3 Dual porosity aquifers and fractured aquifers

The application of biobarriers in dual porosity as well as fractured aquifers can be done on the same principle, because in both aquifers, the majority of the flow will occur in the fractures.

In fractured rock aquifers (dense solid rock granite), groundwater is stored in the fractures, joints, bedding planes and cavities of the rock matrix.

For the dual porosity aquifers, the aquifers consist of solid rock (sandstone and shale). The main storage of water occurs in the intergranular pore spaces, and the main groundwater transmission system is the fracture system in the rock.

7.7.4 Set-up of a field site

The application of biobarriers in the field is done on the same principle as a radial convergent tracer test. The fracture zone identified must be targeted during injection. For the injection borehole, the pump will be placed below the fracture and the recirculation pipe above the fracture. Injection of the bacteria and media will be done by making use of a flowcell.

At the abstraction borehole, the pump will be placed below the fracture area.

Examples of dual porosity aquifers in South Africa are the Table Mountain Group (TMG) and the Karoo Supergroup. Fractured rock aquifers include the West Rand Group and basement sediments.

7.8 SUMMARY

Biobarrier technology was compared to currently used remediation technologies to show the advantages of biobarrier technology.

Physical barriers compared to biobarriers

Current containment methods include sheet pilings and grout curtains, which were compared to biobarrier technology. Biobarriers are likely to be more cost effective and cause less surface disruption than physical barrier technologies.

Biobarriers can be used in funnel and gate systems to isolate contaminant plumes in groundwater and funnel the plumes through *in situ* reactors. Biobarriers are also easier to remove than physical barriers.

Pump-and-treat compared to biobarriers

Conventional pump-and-treat systems are based on the concept of extracting contaminated groundwater for treatment at the surface. *Ex situ* remediation is normally conducted on the abstracted water.

Removal of the contaminated water is often not viable because of the sheer volume of contaminated water to be pumped and treated. Furthermore, contaminants continue to leach out from the sediments, polluting groundwater after the contaminated water has been extracted. Clean-up time varies widely, ranging from years to decades or more.

Biobarriers can be placed in the subsurface to contain the contaminant or decrease the hydraulic conductivity of the aquifer, causing the contaminant migration to slow. The advantage of biobarrier technology over pump-and-treat technology is that biobarriers can be used in conjunction with other remediation technologies to degrade the contaminants *in situ*.

Biobarrier techniques in conjunction with other remediation technologies

A biobarrier can be used as a stand-alone system to reduce the hydraulic conductivity of an aquifer system or in conjunction with bioremediation technologies, to simultaneously degrade a contaminant while hindering its migration.

The use of anaerobes or facultative anaerobe bacteria is an option for *in-situ* bioremediation at contaminated sites. Anaerobes grow in the absence of oxygen and oxidise organic compounds to carbon dioxide, using nitrate, sulphate or Fe³⁺ oxides instead of oxygen as electron acceptors. Bioremediation technologies can be used to

remediate sites contaminated with hydrocarbons, nitrates, metals, and other contaminants.

Implementation of biobarrier techniques in South African aquifers

Biobarrier technology will be viable in three of the four aquifer types in South Africa.

In the intergranular aquifers, the effectiveness of biobarrier formation will depend on the bacteria size and the transport and distribution of the bacteria throughout the aquifer system. Bacteria starvation might be an option. This will enhance the transport of the bacteria throughout the aquifer and reduce the effect of plugging near the injection site. Laboratory experiments show that biobarrier technology for reducing the hydraulic conductivity of a porous media is a viable option.

Laboratory- and field-scale experiments show that biobarrier technology is definitely viable for the reduction of hydraulic conductivity in dual porosity fractured rock aquifers.

The potential of using bacteria injected into the subsurface as a means to contain or reduce the hydraulic conductivity of groundwater is a more cost-effective and conceivable alternative than several other subsurface containment technologies. The full potential for this technology depends on the bacteria used during the investigation. The success of biobarrier technology can also be enhanced by combining it with bioremediation technologies to simultaneously contain and reduce the flow of a contaminant plume, while also degrading it.

8 CONCLUSIONS AND RECOMMENDATIONS

8.1 CONCLUSIONS

The purpose of the research was to test the applicability of biobarriers in South African aquifers.

Site characterisation is a very important aspect of the success of biobarrier implementation. Very thorough site characterisation is necessary prior to the biobarrier field installation to ensure that bacteria transport will occur and at an appropriate rate. It is also essential to understand the aquifer and determine the hydraulic properties, fracture positions, flow directions, flow velocities, dispersivities and other important features.

The results from the radial convergent tests showed that one cannot make assumptions about the transport characteristics of an aquifer. Although boreholes are connected with the same fracture or fractures, the solutes or suspended bacteria can follow different flow paths to migrate from one point to another.

The first step towards efficient biobarrier application is the use of the correct bacterial species. Three bacterial species, namely *R. planticola*, *B. vietnamensis* and *S. marcescens*, were tested and evaluated in the laboratory to determine the one with the most effective biobarrier properties.

8.1.1 Biobarrier formation in porous media

R. planticola

R. planticola clog fine sand 100%, but lack the ability to clog coarse sand due to insufficient adhesion to coarse soil grains. The bacterium could not keep the barrier intact.

B. vietnamensis

B. vietnamensis can be used as a biobarrier as well as for bioremediation application. *B. vietnamensis* has the ability to clog fine and coarse sand 100% over time. Fries *et al.*, (1997) show this species, strain G4, is a very effective trichloroethene (TCE) degrader.

Unfortunately, if the bacterium is to be manufactured or processed for a significant new use, regulators must be notified at least 90 days prior to commencing the process.

S. marcescens

Effective barrier formation (up to 100% reduction in hydraulic conductivity) can be established with cell concentrations of between 10^4 - 10^8 cells/ml and these barriers can withstand increases in the hydraulic gradient. The results showed that *S. marcescens* should be appropriate and that *in-situ* biobarrier formation is feasible in coarse sand with high hydraulic conductivity. This bacterium can also be used to bioremediate several common groundwater contaminants.

8.1.2 Biobarrier formation in fractured media

The effectiveness of *S. marcescens* for reducing the hydraulic conductivity of a laboratory-scale parallel plate fracture with an aperture of 0.8 mm was evaluated. Results showed that it is possible to reduce the hydraulic conductivity of a parallel plate fracture by more than 98%. The results also showed that the barrier has the ability to support hydraulic gradient increases of up to 0.032 without significant failure.

For the removal of biobarrier, the injection of sodium hypochlorite is effective.

Biobarrier technology is definitely a viable method for reducing flow in larger aperture horizontal fractures.

8.1.3 Application of biobarrier formation in a dual porosity fractured rock aquifer

The effectiveness of biobarrier formation for reducing the hydraulic conductivity was tested in a dual porosity fractured rock aquifer.

An 80% reduction in the hydraulic conductivity was measured in the vicinity of the injected borehole. Biobarrier formation was also established over a distance of 20 m. A 60% reduction in the hydraulic conductivity was obtained 10 m from the injection borehole after 16 days and a 40% reduction in a borehole which was 20 m from the injection borehole.

From the results of the field experiment, it can be said with confidence that biobarrier formation is a viable method for decreasing the hydraulic conductivity of a dual porosity fractured rock aquifer.

8.1.4 Advantage of biobarriers over current remediation technologies

Biobarriers can be constructed without excavation and will therefore be economically attractive at many sites. An example of potential application is funnel and gate technology. The biobarrier will act as the funnel, thus containing the contaminant plume. Biobarriers can easily be removed. There is no obvious depth or aquifer type limitation for biobarrier technology. Barriers can be established and removed cost effectively.

Biobarriers can be used as a containment technology (decrease the hydraulic conductivity of the aquifer) and in conjunction with remediation technologies to degrade the contaminants *in situ*. Biobarrier technology with *S. marcescens* can be used to reduce the hydraulic conductivity of a fracture and is effective to contain.

8.1.5 Implementation of biobarrier formation in South African aquifers

Biobarrier technology will be viable in intergranular aquifers, dual porosity fractured rock aquifers and fracture flow aquifers.

The effectiveness of biobarriers in intergranular aquifers will depend on the bacteria size and the transport and distribution of the bacteria throughout the aquifer system. Biobarrier technology is a viable option for reducing the hydraulic conductivity of porous media.

Laboratory- and field-scale experiments show that biobarrier technology is definitely a viable technology for reducing the hydraulic conductivity of a dual porosity fractured rock aquifer.

8.2 RECOMMENDATIONS

Extensive site characterisation must be performed prior to the field application of biobarrier technology. It is important to include fracture positions, hydraulic conductivity, flow velocities, dispersivity values, flow thickness, flow direction, etc.

When building biobarriers, the direction of groundwater flow must always be kept in mind, since the biobarrier will drift in to the direction of groundwater flow. Barriers must be constructed upstream from the target area to build a more effective barrier.

Bacteria and media injection must be conducted according to the radial convergent tracer test methodology. Pumping must be constant and at low rate during the test. This will ensure the containment of biomass and maintenance of aerobic conditions, and minimise the loss of nutrients.

In areas where groundwater is used for domestic purposes, the application of biobarriers must be with care due to the fact that *Serratia* is a opportunistic pathogen which cause infections in immuno-compromised patients. It is important to note that most bacteria used for remediation purposes is opportunistic pathogens.

REFERENCES

- Alexander, M. (1999). Biodegradation and bioremediation. New York: Academic Press.
- Bagley, S.T., Seidler, R.J., and Brenner, D.J. (1981). *Klebsiella planticola* sp. nov: a new species of *Enterobacteriaceae* found primarily in nonclinical environments. *Curr. Microbiol.* 6, pp 105-109.
- Becker, M.W., Shapiro, A.M., (2000). Tracer transport in fractured crystalline rock: evidence of nondiffusive breakthrough tailing. *Water Resour. Res.* 36 (7), pp 1677-1686.
- Becker, M.W. (1996). Tracer tests in a fractured rock and their first passage time mathematical models. Ph.D thesis, University of Texas, Austin, TX.
- Berkowitz, B. (1992). Modelling groundwater flow and pollution in dry regions. Course in Groundwater Modelling, Ben Gurion University of the Negev, Israel.
- Bidlan, R and Manonmani, H.K. (2002). Aerobic degradation of DDT by *Serratia Marcescens*. *Process Biochemistry.* Vol 38. No1. pp 49-56.
- Botha, J.F., Verwey, J.P., Van der Voort, I., Vivier, J.J.P., Buys, J., Colliston, W.P. and Loock, J.C. (1998). Karoo Aquifers. Their geology, geometry and physical properties. Report to the Water Research Commission by the Institute for Groundwater Studies, University of the Free State. WRC report No: pp 487/1/98.
- Camper, A.K., Hayes, J.T., Sturman, P.J., Jones, W. L. and Cunningham, A.B. (1993). Effects of motility and adsorption rate coefficient on transport of bacteria through saturated porous media. *Applied and Environmental Microbiology*, Vol 65: pp 455-3462.
- Chapelle, F.H. (2001). *Ground-water Microbiology and Geochemistry*. New York: Wiley.
- Cliffe, K.A., Gilling, D., Jefferies, N.L., Lineham, T.R. (1993). An experimental study of flow and transport in fractured slate. *J. Contam. Hydrol.* Vol 13, pp 73-90.
- Cunningham, A.B. and Hiebert, R. (2000). Subsurface biofilm barriers (biobarriers) for the containment of contaminated groundwater. *Groundwater Currents*, Issue No 36, June 2000.

DeFlaun, M.F., Fuller, M.E., Zhang, P., Johnson, W.P., Mailloux, B.J., Holben, W.E., Kovacic, W.P., Balkwill, D.L., and Onstott, T.C. (2001). comparison of methods for monitoring bacterial transport in the subsurface. *Journal for Microbiological methods*. Vol 47: pp 219-231.

DeFlaun, M.F., Oppenheimer, S.R., Strenger, S., Condee, C.W., and Fletcher, M. (1998). Alterations in Adhesion, Transport and membrane characteristics in an adhesion-deficient pseudomonad. Envirogen, Inc., Princeton Research Centre, Lawrenceville, New Jersey 08648-4702, and Centre of Marine Biotechnology, University of Maryland Biotechnology Institute, Baltimore.

Dong, H., Rothmel, R., Onstott, T.C., Fuller, M.E., DeFlaun, M.F., Streger, S.H., Dunlap, R. and Fletcher, M. (2002). Simultaneous transport of two bacteria strains in intact cores from Oyster, Virginia: Biological effects and numerical modeling. *Applied and Environmental Microbiology*, vol 68: pp2120-2132.

Dronfield, D.G. and Silliman, S.E. (1993). Velocity dependence of dispersion for transport through a single fracture of variable roughness. *Water Resour. Res.* Vol 29 (10), pp 3477- 3483.

Fetter, C.W. (1999). Contaminant hydrology. Second edition. Prentice Hall, Upper Saddle River, N.J., 500 pp.

Freeze, A.L., and Cherry, J.A. (1979). Groundwater. Prentice-Hill Inc. Englewood Cliffs, New Jersey.

Fries, M.R., Forney, L.J. and Tiedje, J.M. (1997) Phenol- and Toluene-degrading bacterial populations from an aquifer in which successful trichloroethelene cometabolism occurred. *Appl. Environ. Microbiol.* Vol 63: pp 1523-1530.

Fuller, M.E., Dong, H., Mailloux, B.J., Onstott, T.C. and DeFlaun, M.F. (2000). Examining bacteria transport in intact cores from Oyster, Virginia: Effect of sedimentary facies type on bacterial breakthrough and retention. *Water resources research*, Vol 36: pp 2417-2431.

Fu, L., Milliken, K.L. and Sharp, J.M. Jr. (1994). Porosity and permeability variations in fractured and liesegang-banded Breathitt sandstones (Middle Pennsylvanian), eastern

Kentucky: diagenetic controls and implications for modeling dual porosity systems. *J. Hydrol.* 154 (2), pp 351-381.

Gerlach, R., Cunningham, A.B. and Caccavo, F. Jr. (1998). Formation of redox-reactive subsurface barriers using dissimilatory metal-reducing bacteria. Proceedings of the 1998 Conference on Hazardous Waste Research. Centre for Biofilm Engineering, Montana State University.

Grisak, G.E. and Pickens, J.F. (1981). An analytical solution for solute transport through fractured media with matrix diffusion. *J. Hydrol.* Vol 52, pp 47- 57.

Hadermann, J. and Heer, W. (1996). The Grimsel (Switzerland) migration experiment: integrated field experiments, laboratory investigations and modelling. *J. Contam. Hydrol.* Vol 21, pp 87-100.

Hill, D.D. and Sleep, B.E. (2002). Effects of biofilm growth on flow and transport through a glass parallel plate fracture. *Journal of Contaminant Hydrology.* Vol 56. pp 227-246.

Horne, R.N. (1997). *Modern well test analysis: A computer-aided approach*, Petroway Inc., Palo Alto, USA.

ITRC (Interstate Technology & Regulatory Council). (2005). Overview of Groundwater Remediation Technologies for MTBE and TBA. MTBE-1. Washington, D.C.: Interstate Technology & Regulatory Council, MTBE and Other Fuel Oxygenates Team. Available on the Internet at <http://www.itrcweb.org>.

James, G.A., Warwood, B.K., Cunningham, A.B., Sturman, P.J., Hiebert, R. and Costerton, J.W. (1995). "Evaluation of Subsurface Biobarrier Formation and Persistence," In: Proceedings of the 10th Annual Conference on Hazardous Waste Research, Manhattan. May 23-24, 1995, pp 82-91. Abstract 95-052.

James, G.A., Warwood, B.K., Hiebert, R., and Cunningham, A.B. (2000). Bacterial barriers to the Spread of Pollution. In *Bioremediation*. Kluwer Academic pp. 1-14.

Jordan, F.J., Sandrin, S.K., Frye, R.J., Brusseau, M.L., and Maier, R.M. (2004). The influence of system complexity on bacterial transport in saturated porous media. Department of soil, water and environmental science, University of Arizona, USA. *Journal of contaminant hydrology*. Vol 74, pp 19-38.

Kannan A. and Ramteke P.W. (2002). Uptake of Nickel II by *S. Marcescens*. *Environmental Biology*. Vol 23, pp 57-59.

Kinoshita, T., Bales, R.C., Yahya, M.T. and Gerba, C.P. (1993). Bacteria transport in a porous media: retention of *Bacillus* and *Pseudomonas* on silica surfaces. Department of hydrology and water resources, University of Arizona, USA. Vol 27 No. 8 pp 1295-1301.

Komlos, J., Cunningham, A.B., Warwood, B. and James, G. (1998). Biofilm barrier formation and persistence in variable saturated zones. Centre for biofilm engineering, Montana state University. Proceedings of the 1998 conference on hazardous waste research (1998).

Kreisel, I. and Sharp, J.M. Jr. (1996). Fracture skins in the Brushy Canyon Formation. In: DeMis, W.D., Coles, A.G. (Eds.), *The Brushy Canyon Play in Outcrop and Subsurface: Concept and Examples*. SEPM Publ. 96-38. SEPM, Tulsa, OK, pp. 147- 152.

Krishnamurthy, N. S., Kumar, D. Rao, A.V., Jain, S.C. and Ahmed S. (2003). Comparison of surface and sub-surface geophysical investigations in delineating fracture zones. *Curreht science*, vol. 84, pp. 9, 10.

Kruseman, G.P. and De Ridder, N.A. (1991). *Analyses and evaluation of pumping test data*. Second Edition. International Institute for Land Reclamation and Improvement. Publication 47. Wageningen, the Netherlands. 377 pp.

Kunstmann, H. and Kinzelbach, W. (1998). Quantifizierung von Unsicherheiten in Grundwassermodellen. (Quantification of Uncertainty in Groundwater Models). *Mathematische Geology*, 2, June 1998.

Lee, M.D. Odom, R.J. and Buchanan, R.J. (1998). *Ann. Rev. Microbiol.* 52, 423 (Medline).

Madigan, M.T., Martinko, J.M. and Parker, J. (1997). Brock Biology for microorganisms. Eighth edition.

McKay, L.D., Gillham, R.W., and Cherry, J.A. (1993). Field experiments in a fractured clay till: 2. Solute and colloid transport. Water Resour. Res. Vol 29, no.12, pp3879- 3890.

Mills, A.L., Herman, J.S., Hornberger, G.M., and DeJesus, T.H. (1994). Effect of solution ionic strength and iron coating on mineral grains on the sorption of bacterial cells to quartz sand. Applied and Environmental Microbiology. 60:3300-3306.

Montpas,S. Samson, J. Langlois,E. Lei, J. Pich,Y. and Chênevert, R. (1997). Degradation of 2,4,6-trinitrotoluene by *Serratia marcescens*. Biotechnology Letters, Vol 19, no 3, March 1997, pp 291-294.

Moreno, L., Neretnieks, I. and Eriksen, T. (1985). Analysis of some laboratory tracer runs in natural fissures. Water Resour. Res. Vol 21, no. 7, pp 951- 958.

Nelson, M.J., Montgomery, S.O., Mahaffey, W.R. and Pritchard, P.H., (1989). Biodegradation of trichloroethylene and involvement of an aromatic biodegradative pathway. Appl. Environ. Microbiol. Vol 53: pp 949-54.

Neretnieks, I., Eriksen, T. and Tahtinen, P. (1982). Tracer movement in a single fissure in granitic rock: some experimental results and their interpretation. Water Resources Research. Vol 18, no. 4, pp 849- 858.

Novakowski, K.S. (1992). The analysis of tracer experiments conducted in divergent radial flow fields. Water Resources Research, Vol. 28, no. 12, pp 3215-3225.

Novakowski, K.S. and Lapcevic, P.A. (1994). Field measurement of radial solute transport in fractured rock. Water Resources Research. Vol 30, no. 1, pp 37-44.

Novakowski, K.S., Lapcevic, P.A., Voralek, J.W. and Bickerton, G. (1995). Preliminary interpretation of tracer experiments conducted in a discrete rock fracture under conditions of natural flow. Geophysical Research Letters, Vol. 22, no. 11, pp. 1417-1420.

Novakowski, K.S., Lapcevic, P.A. and Voralek, J.W. (1998). A note on a method for measuring the transport properties of a formation using a single well. *Water Resources Research*, Vol. 34, no. 5, pp. 1351-1356.

NRC. (1994). *Alternatives for Ground Water Cleanup*. Washington, D.C.: National Academy Press.

Pietersen, K.C. (2004). A decision-making framework for groundwater management in arid zones (with a case study in Namaqualand). PhD thesis. University of the Western Cape, Bellville, South Africa.

Raven, K.G., Novakowski, K.S. and Lapcevic, P.A. (1988). Interpretation of field tests of a single fracture using a transient solute storage model. *Water Resources. Res.* Vol. 24, no. 12, pp 2019-2032.

Riemann, K. (2002). Aquifer parameters estimation in fractured rock aquifers using a combination of hydraulic and tracer tests. Ph.D thesis. Institute for groundwater studies at the University of the Orange Free State, Bloemfontein, South Africa.

Rowell, D.M. and De Swardt, A.M.J. (1976) Diagenesis in Cape and Karoo sediments, South Africa, and its bearing on their hydrocarbon potential. *Transactions of the Geological Society of South Africa*. Vol 79 no. 1, pp 181-145.

Smith, M. (2005). Prediction, control, and rehabilitation of iron incrustation in water supply boreholes, Western Cape, South Africa: A geological approach. PhD thesis. University of Cape Town.

Smith, L. (2003). Biological clogging of boreholes and aquifer materials in South Africa. The theory behind the biofouling problem and possible solutions. MSc. Thesis. Institute for groundwater studies at the University of the Orange Free State, Bloemfontein, South Africa.

Sonnenborg, T.O., Butts, M.B. and Jengsen, K.H. (1999). Aqueous flow and transport in analog systems of fractures embedded in permeable matrix. *Water Resour. Res.* Vol 35 no. 3, pp 719- 729.

Strietelmeier, B.A., Espinosa, M.L., Jones, M.W., Adams, J.D., Hodge, E.M., Ware, S.D., Leonard, P.A., Longmire, P., Kaszubaland, J.P., and Conca, J.L. (2001). Use of a unique biobarrier to remediate nitrate and perchlorate in groundwater. Conference, February 25-March 1, Tucson, AZ.

Tankard, A.J., Jackson, M.P.A., Eriksson, K.A., Hobday, D.K., Hunter, D.R. and Minter, W.E.L. (1982). Crustal evolution of Southern Africa. Springer-Report, New York.

Truswell, J.F. (1970). Historical geology of South Africa, Purnell, Cape Town.

Tsang, Y.W. (1992). Usage of "equivalent apertures" for rock fractures as derived from hydraulic and tracer tests. Water Resources Research. Vol 28, no. 5, pp 1451-1455.

Vandevivere, P and Beveye, P. (1992). Effect of bacterial extracellular polymers on the saturated hydraulic conductivity of sand columns. Applied and Environmental microbiology, Vol. 58, no. 5, pp 1690-1698.

Van der Voort, I. (2001). Risk based decision tool for managing and protecting groundwater resources. Ph.D. Thesis. Institute for groundwater studies at the University of the Orange Free State, Bloemfontein, South Africa..

Van Heerden, E. (2005). Progress report nr 10. Compiled by the Department of Microbiology and Biotechnology, University of the Free State. Growth studies on bacterium *R. planticola*. Prepared for BHP Billiton.

Van Heerden, E. (2005). Progress report no. 11. Compiled by the Department of Microbiology and Biotechnology, University of the Free State. Growth studies on bacterium *Serratia Marcescens*. Prepared for BHP Billiton.

Van Heerden, E. (2006). Progress report no. 13. Compiled by the Department of Microbiology and Biotechnology, University of the Free State. Quantitative Real time PCR for detection of Biobarrier micro-organism. Prepared for BHP Billiton.

Van Tonder, G.J., Bardenhagen, I., Riemann, K., Van Bosch, J., Dzanga, P. and Xu, Y. (2002). Manual on pumping test analysis in fractured rock aquifers. Final Report, WRC Project, Report nr. 1116/1/02, Pretoria.

Van Tonder, G.J. and Vermeulen, P.D. (2005). The Applicability of Slug Tests in Fractured Rock Formations. Institute for Groundwater Studies, University of the Free State, Bloemfontein. Water SA Vol. 31, no. 2, pp 157-160.

Van Wyk, A.E. (1998). Tracer experiments in fractured rock aquifers. MSc. Thesis. Institute for Groundwater Studies, University of the Free State, Bloemfontein.

Vegter, J.R. (1995). An explanation of a set of National Groundwater Maps. WRC Report TT 74/95. Water Research Commission, Pretoria.

Vereecken, H., Hubbard, S., Binley, A. and Ferre, T. (2004). Hydrogeophysics: An Introduction from the Guest Editors vol. 3. www.vadosezonejournal.org Published in Vadose Zone Journal 3:pp 1060-1062..

Visser, J.N.J. (1984). A review of the Stormberg Group and Drakensberg volcanics in Southern Africa. Palaeont. Afr. Vol 25, pp 5-27.

Vivier, J.J.P., Van Tonder, G.J. and Botha, J.F. (1995). The use of slug tests to predict borehole yields: Correlation between the recession time of slug tests and borehole yields. In Conference proceedings: Groundwater '95: Groundwater recharge and rural water supply, Midrand, South Africa.

Zimmerman, M.D., Bennett, P.C., Sharp, J.M. and Choi, W-J. (2002). Experimental determination of sorption in fracture flow systems. Department of Geological Sciences, Texas, Austin. Journal of Contaminant Hydrology. Vol. 58, pp 51-77.

Web articles

(www.environment-agency.gov.uk). (October 2006)

<http://genome.jgi-psf.org>. (February 2006).

<http://eMedicine.com>. (February 2006).

(Medicinenet.com) <http://www.answers.com/topic/polymerase-chain-reaction>. (October 2006).

(SRS - Savannah River site - Environmental restoration division).

<http://www.srs.gov/general/enviro/erd/technology/Pages/index-i.html>. (September, 2005).

http://en.wikipedia.org/wiki/Water_pollution (September 2006)

APPENDIX A

BURKHOLDERIA VIETNAMENSIS AND SERRATIA MARCESCENS

RESULTS FROM THE EC AND PH - FINE AND COARSE SAND COLUMNS

BURKHOLDERIA VIETNAMENSIS

Results from the EC, pH and cell distribution in columns - Fine sand column

Fine sand column

Electrical conductivity versus time was plotted for the outflow samples of the fine sand column. From the graphs, it can be seen that EC (C/C_0) varies between 0.45 and 0.55 (See Figure 1). The EC of the media was 1053 mS/m. Although constant media injection occurred, the media concentration will vary due to the consumption of nutrients by the bacteria.

For the first two days, the pH was between 5.5 and 6.8. This lower pH-level may result from the interaction of artificial groundwater and quartz mineral before any bacteria or media were injected. Quartz releases very low amounts of H^+ to the solution. After the sixth day, the pH stabilised at a value of 6.8. The pH variation over the ten days is between 5 and 6.8. The pH of the media was 7.06.

See Figure 1 and Figure 2 for EC (C/C_0) and pH vs. time graphs, respectively.

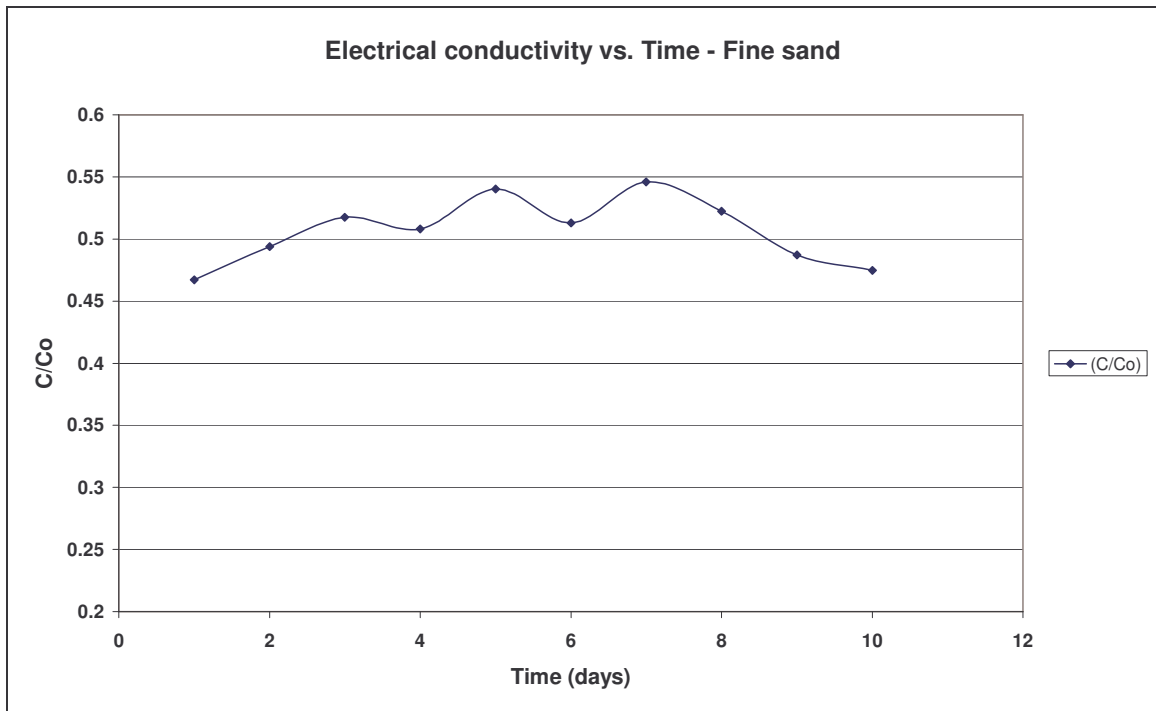


Figure 1 EC vs. time graph for the fine sand column.

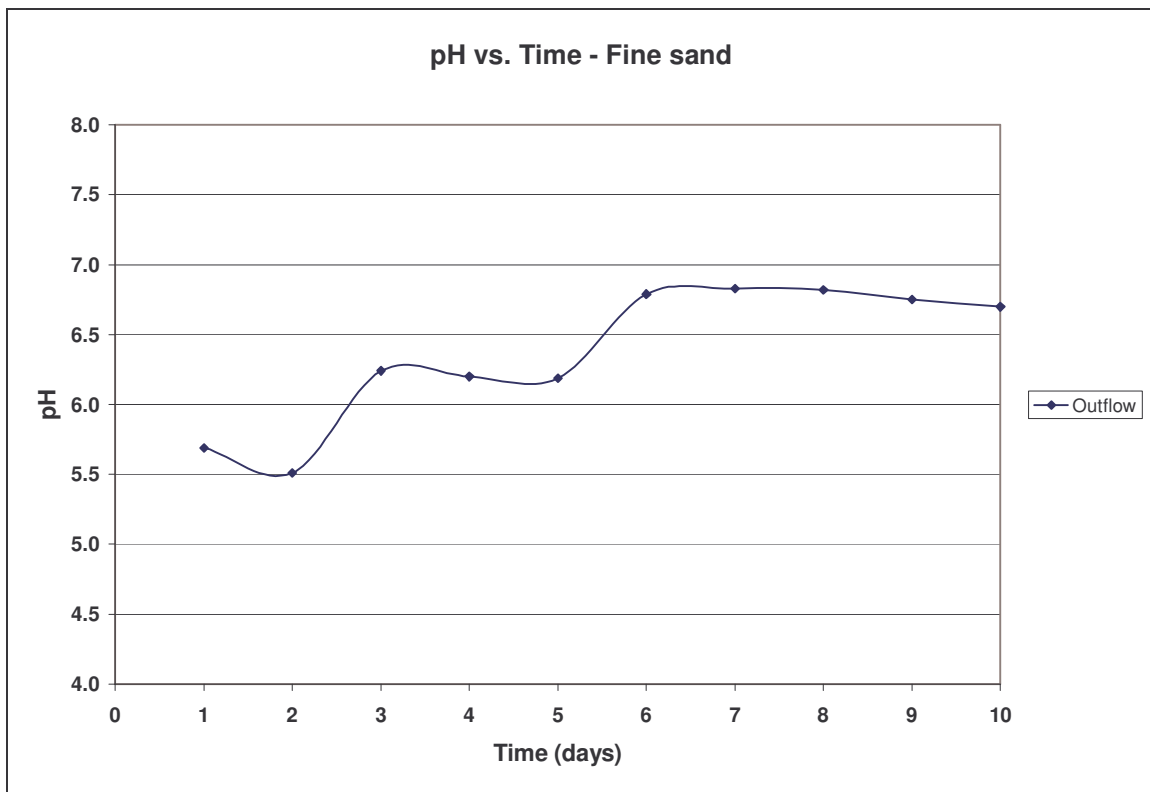


Figure 2 pH vs. time graph for the fine sand column.

Cell distribution in columns

Table 1 Data - Optical density, pH and EC data for the fine sand column.

Time	Optical density						EC (mS/m)	pH
	p1	p2	p3	p4	Outflow 8:00	Outflow 17:00		
							1053.00	
Day 1	0.070	0.008	0.007	0.005	0.001	0.2	492	5.69
Day 2	0.016	0.009	0.020	0.018	0.006	0.03	520	5.51
Day 3	0.207	0.067	0.048	0.047	0.043	0.061	545	6.24
Day 4	0.088	0.050	0.041	0.035	0.019	0.02	535	6.2
Day 5	0.205	0.078	0.042	0.046	0.072	0.056	569	6.19
Day 6	0.170	0.072	0.076	0.120	0.094	0.081	540	6.79
Day 7	0.269	0.196	0.087	0.048	0.036	0.053	575	6.83
Day 8	0.601	0.112	0.056	0.044	0.084	0.069	550	6.82
Day 9	0.642	0.167	0.095	0.109	0.068	0.072	513	6.75
Day 10	0.806	0.225	0.132	0.084	0.084	0.076	500	6.7

Results from the EC and pH - coarse sand column

Coarse sand column

An electrical conductivity versus time graph was plotted for the outflow samples. EC was converted to C/Co. The EC varies between 0.48 and 0.6. The lower EC concentrations over the first two days might be attributed to the presence of artificial groundwater in the column, which causes dilution. The decrease in EC from the seventh day might be attributed to the high media consumption of bacteria.

The pH varies between 5.6 and 6.9. See Figure 3 and Figure 4 for EC and pH versus time graphs.

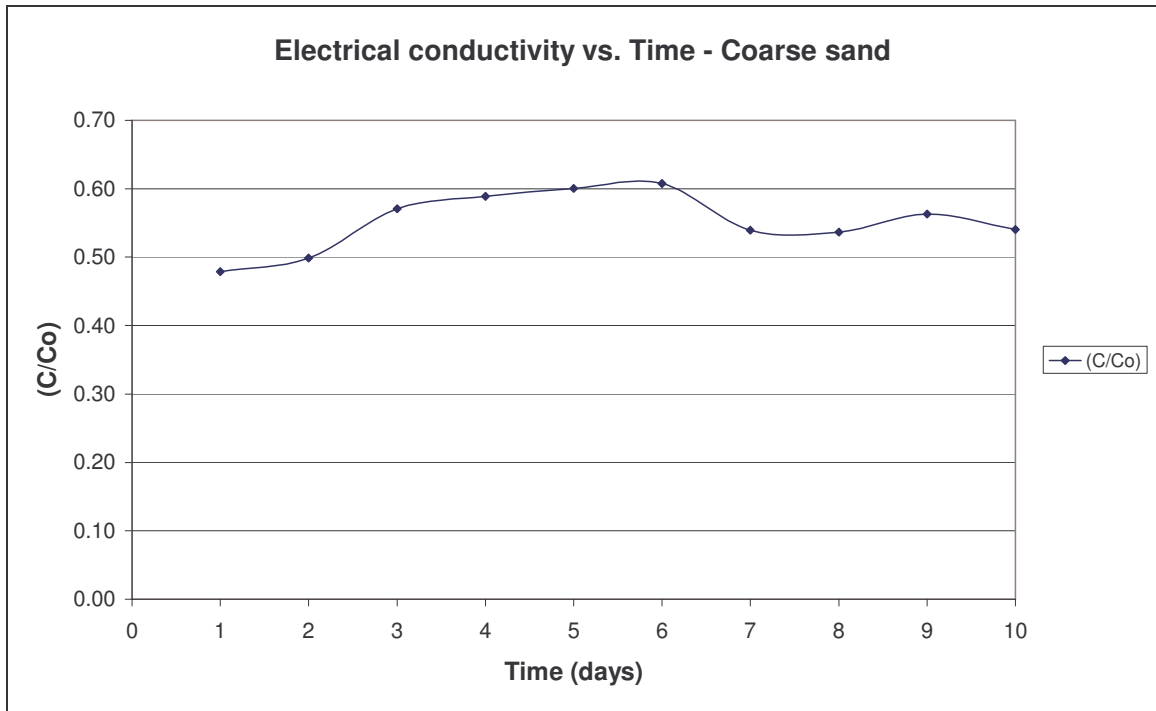


Figure 3. EC vs. time graph for the coarse sand column.

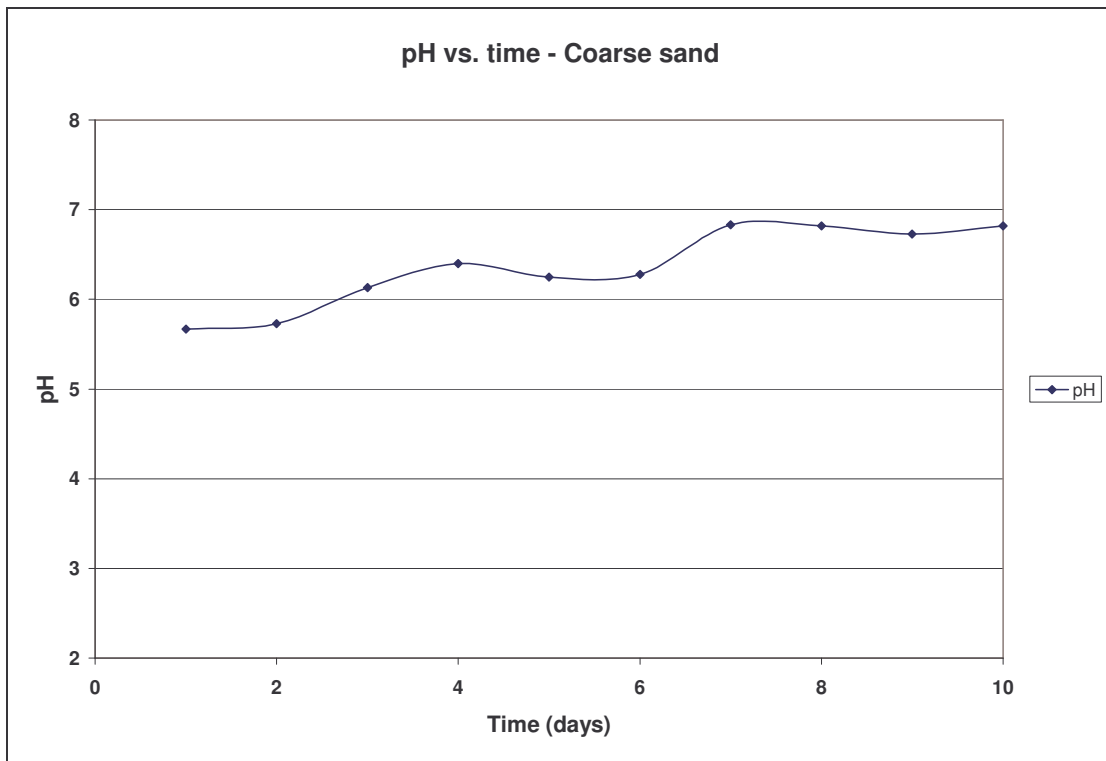


Figure 4 pH vs. time graph for the coarse sand column.

Cell distribution in columns

Table 2 Data - Optical density, pH and EC data for the coarse sand column.

Time	Optical density						EC (mS/m)	pH
	p1	p2	p3	p4	OD-out 8:00	OD-out 17:00		
							1053.0	
1	0.034	0.009	0.005	0.007	0.019	0.012	504	5.7
2	0.080	0.041	0.030	0.007	0.008	0.063	525	5.7
3	0.131	0.057	0.063	0.062	0.076	0.103	601	6.1
4	0.423	0.156	0.083	0.076	0.104	0.248	620	6.4
5	0.658	0.343	0.195	0.144	0.170	0.292	632	6.3
6	0.694	0.340	0.250	0.190	0.282	0.223	640	6.3
7	0.671	0.331	0.246	0.197	0.250	0.246	568	6.8
8	0.659	0.377	0.237	0.211	0.222	0.249	565	6.8
9	0.662	0.365	0.262	0.256	0.196	0.241	593	6.7
10	0.721	0.345	0.249	0.234	0.351	0.217	569	6.8

SERRATIA MARCESCENS

Results from the EC, pH and cell distribution - coarse sand column

Coarse sand column

A large decrease in the pH was measured between Day 1 and 2. This can be attributed to flushing groundwater obtained from the campus test site. For the course of the experiment the pH varied between 5.3 and 6, and can be attributed to simultaneous bacteria and media injection, which causes mixing in the column. The pH of the media was 6.2 and for the bacteria groundwater suspension 5.99. See Figure 5 for the pH vs. time graphs for the 24-hour outflow.

From Figure 6, it can be seen that the EC varies between 400 and 1000 mS/m. The lower EC concentrations over the first two days might be attributed to the presence of artificial groundwater in the column, which causes dilution.

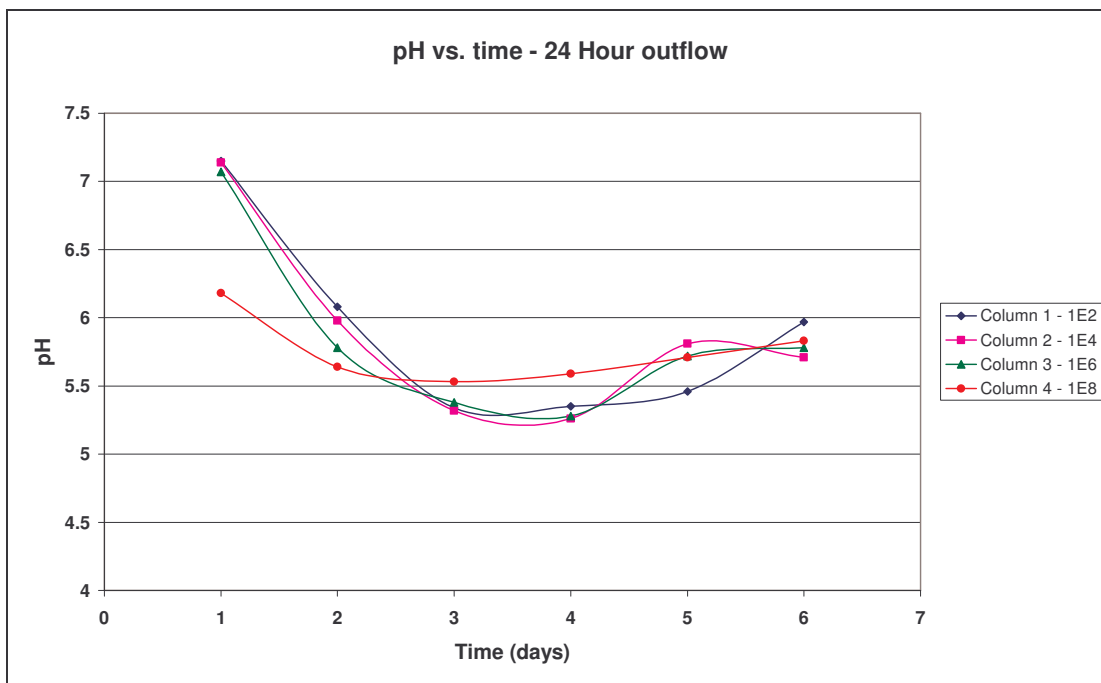


Figure 5 pH vs. time graph for the coarse sand columns. 24-hour outflow.

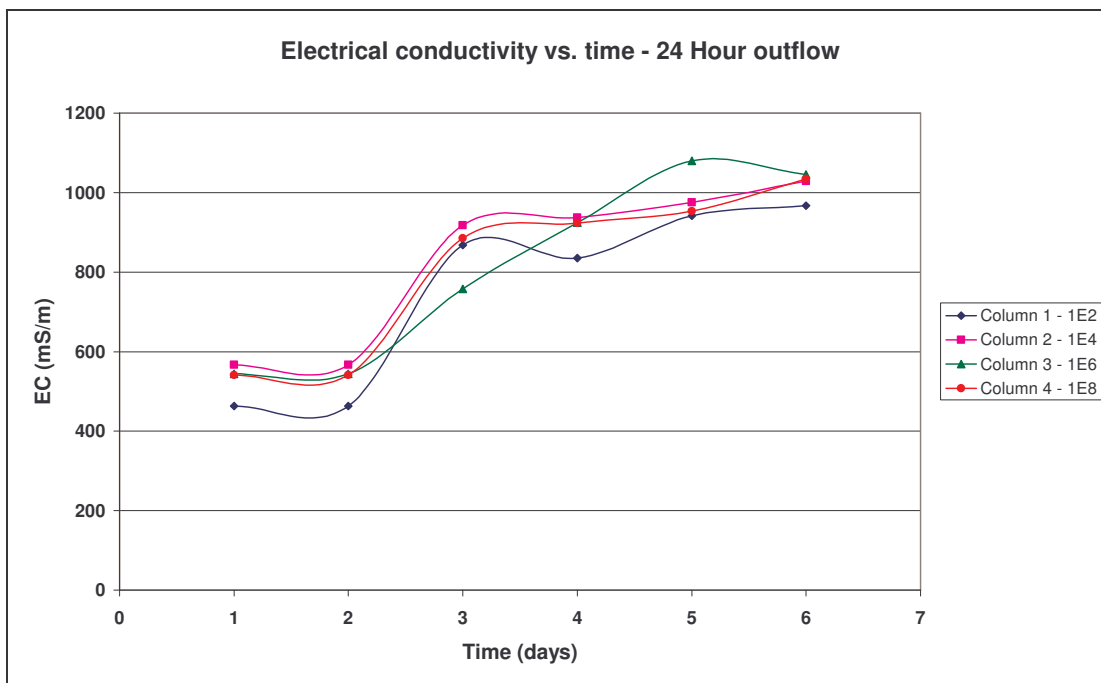
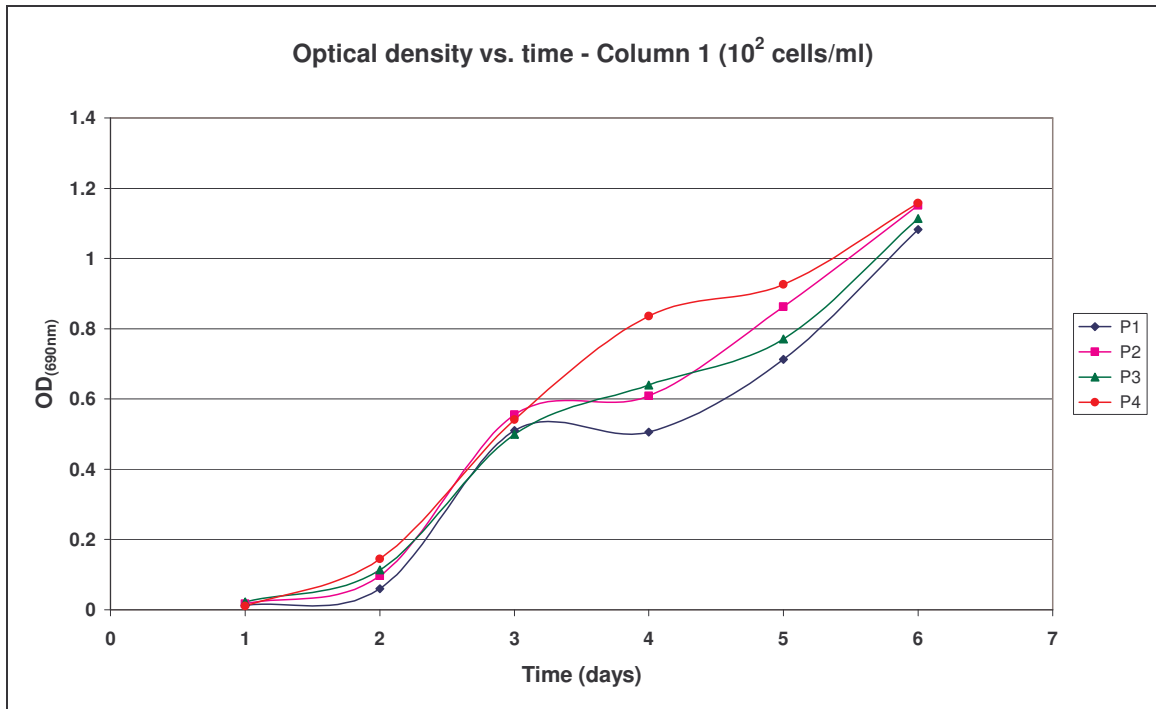
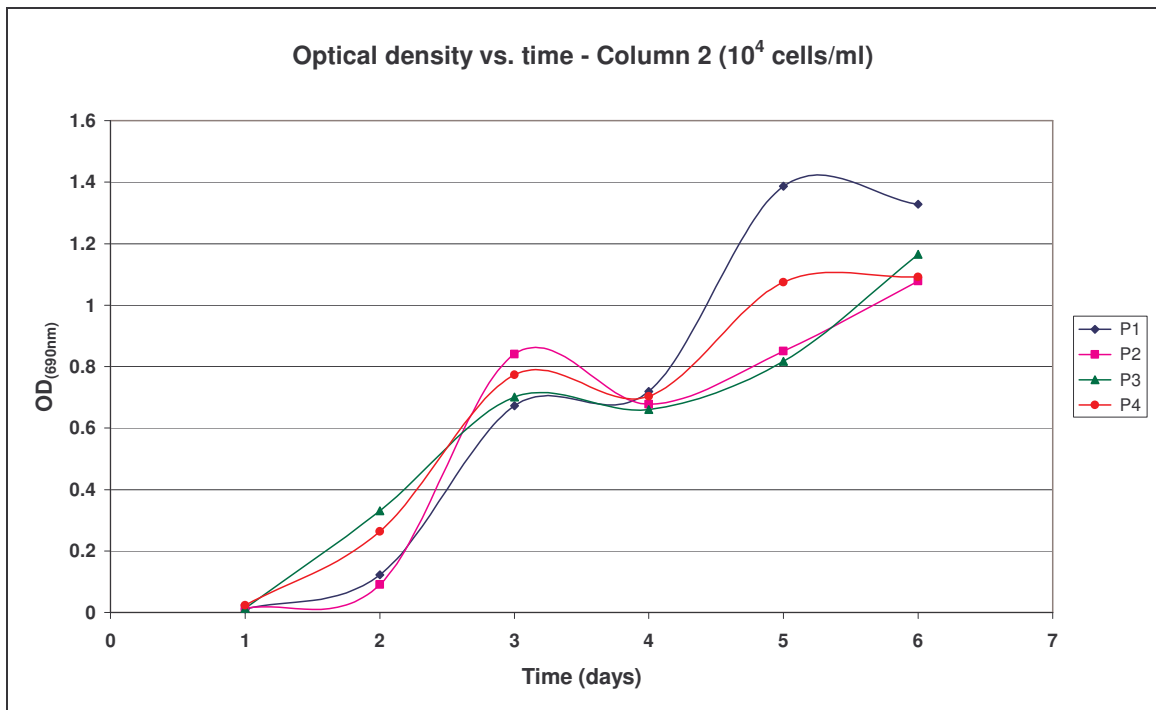


Figure 6 EC vs. time graph for the coarse sand columns. 24-hour outflow.

Cell distribution in columns

See Figure 7 to Figure 10 for the distribution of cells (OD at each port) in the columns.

Figure 7 Cell concentration vs. time -Column 1.(10^2 cells/ml).Figure 8 Cell concentration vs. time -Column 2. (10^4 cells/ml).

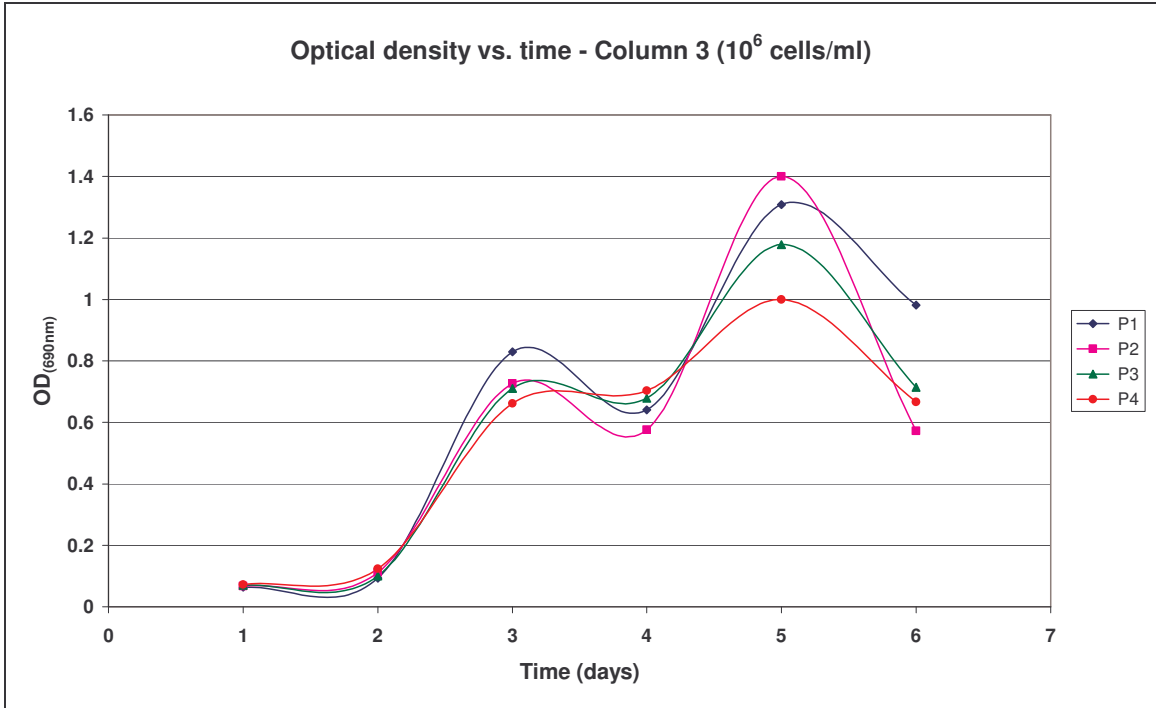


Figure 9 Cell concentration vs. time -Column 3. (10^6 cells/ml).

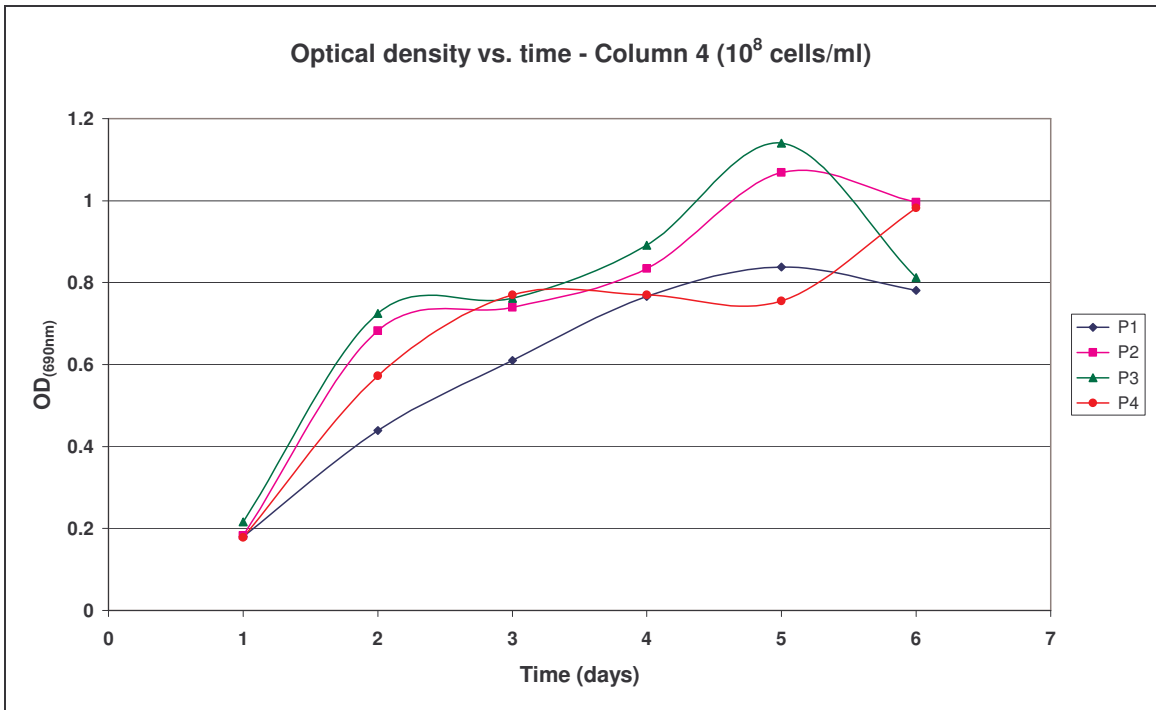


Figure 10 Cell concentration vs. time -Column 4. (10^8 cells/ml).

APPENDIX B

SERRATIA MARCESCENS

TESTING OF BIOBARRIERS IN SMALL DIAMETER PIPES

AND

**BIOBARRIER THROUGH A SANDSTONE PARALLEL PLATE FRACTURE –
EXPERIMENT 1 AND 2**

RESULTS FROM THE EC AND PH MEASUREMENTS

Table 1 Results for Pipe 1.

Pipe 1								
Name	Pipe Length (m)	Vol Out (ml)	Vol Out (g)	Vol per length (ml) (9.4 ml/m)	Adh in pipe (g)	Filter - dry (g)	Bugs on filter (g)	Total cells - dry (g)
FF P1-1	3.96	23.2464	22.7197	37.6191		0.3309	0.0251	0.0251
FF P1-2	4.19	38.5000	38.8500	39.8050		0.1618	0.0043	0.0043
FF P1-3	3.86	31.5819	31.5661	36.6701		0.2149	0.0267	0.0267
Adh P1-1	3.96				14.8994	0.6600	0.0559	0.0559
Adh P1-2	4.19				0.9550	0.0790	0.0092	0.0092
Adh P1-3	3.86				5.1040	0.1545	0.0091	0.0091

FF P1-1	Free flow volume - Pipe 1 - Section 1
Adh P1-1	Adhesive volume - Pipe 1 - Section 1
FF P1-2	Free flow volume - Pipe 1 - Section 2
Adh P1-2	Adhesive volume - Pipe 1 - Section 2
FF P1-3	Free flow volume - Pipe 1 - Section 3
Adh P1-3	Adhesive volume - Pipe 1 - Section 3

Table 2 Results for Pipe 2.

Pipe 2								
Name	Pipe Length (m)	Vol Out (ml)	Vol Out (g)	Vol per length (ml) (9.4 ml/m)	Adh in pipe (ml)	Filter - dry (g)	Bugs on filter (g)	Total cells - dry (g)
FF P2-1	3.96	31	31.5640	37.6200		0.8203	0.0723	0.0723
FF P2-2	4.19	30.5694	30.2797	39.8032		0.2329	0.0114	0.0114
FF P2-3	3.86	32	31.9691	36.6700		0.3190	0.0180	0.0180
Adh P2-1	3.96				6.0560	0.2455	0.0247	0.0247
Adh P2-2	4.19				9.5234	0.2616	0.0083	0.0083
Adh P2-3	3.86				4.7009	0.1332	0.0138	0.0138

FF P2-1	Free flow volume - Pipe 2 - Section 1
Adh P2-1	Adhesive volume - Pipe 2 - Section 1
FF P2-2	Free flow volume - Pipe 2 - Section 2
Adh P2-2	Adhesive volume - Pipe 2 - Section 2
FF P2-3	Free flow volume - Pipe 2 - Section 3
Adh P2-3	Adhesive volume - Pipe 2 - Section 3

BIOBARRIER THROUGH A SANDSTONE PARALLEL PLATE FRACTURE – EXPERIMENT 1

Results from the EC and pH

In Figure 1, the pH was plotted versus time. The pH-values range between 6.2 and 7.2. The pH started of in the order of 6.2 and gradually increased with time.

A large increase in the electrical conductivity was measured on Day 1. This can be attributed to media injection. See Figure 2 for the EC variation measured in the outlet side over a 2 pore volume period.

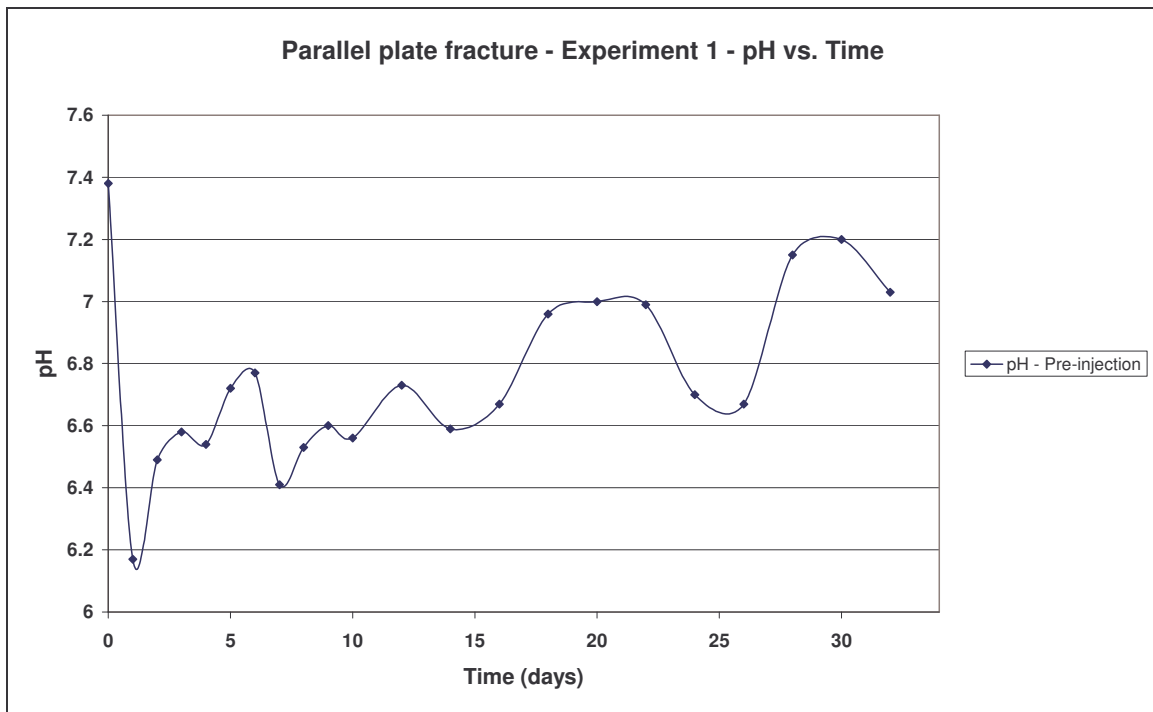


Figure 1 Parallel plate experiment - pH vs. time graph.

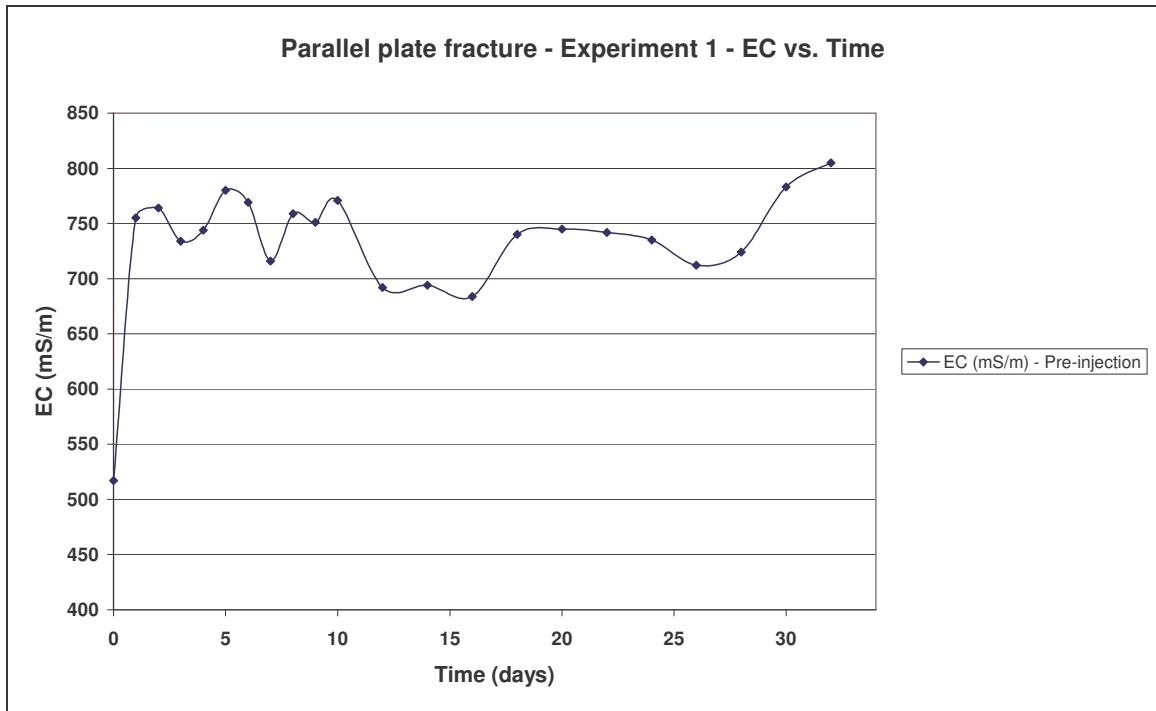


Figure 2 Parallel plate experiment - EC vs. time graph.

BIOBARRIER THROUGH A SANDSTONE PARALLEL PLATE FRACTURE – EXPERIMENT 2

Results from the pH measurements

In Figure 3, a sudden decrease in the pH was measured on Day 1. This can be attributed to the bacteria and media injection. For the rest of the time, the pH-values were very similar and varied between 6.5 and 7.

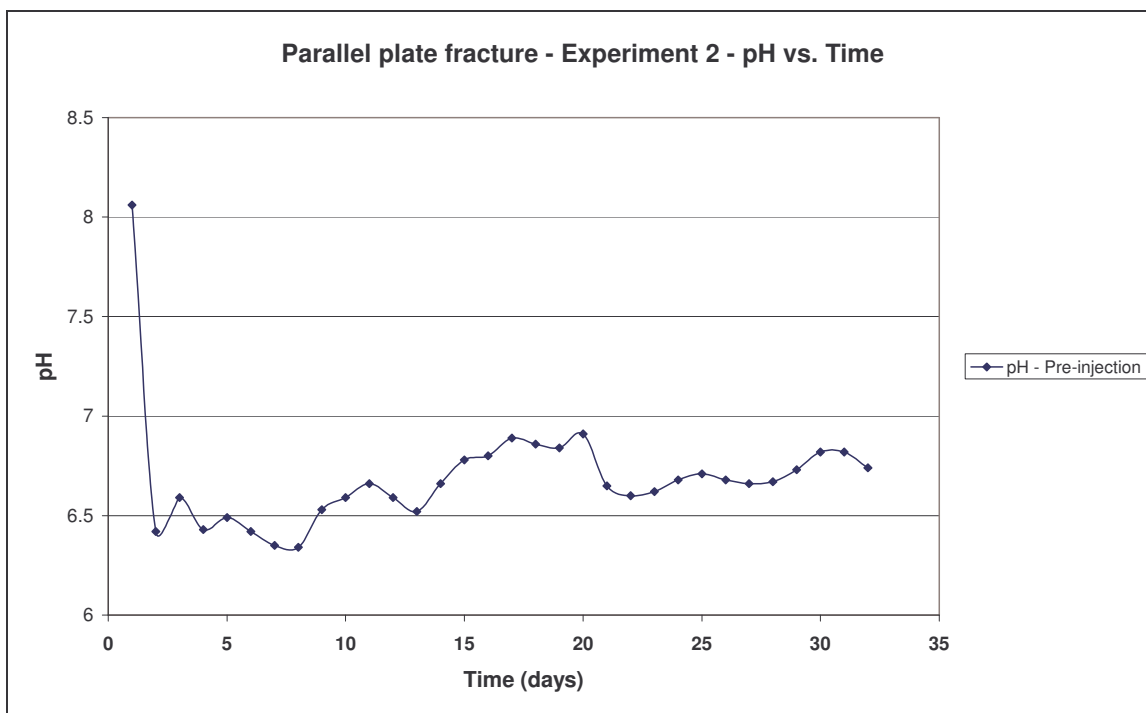


Figure 3 Parallel plate experiment - pH vs. time graph.

APPENDIX C

APPLICATION OF BIOBARRIERS IN THE FIELD

RESULTS FROM AQUIFER HYDRAULICS

Table 1 Summary of the results of the slug tests.

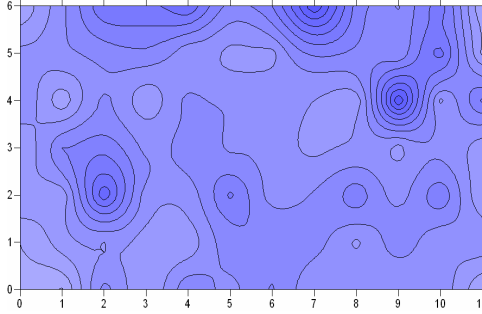
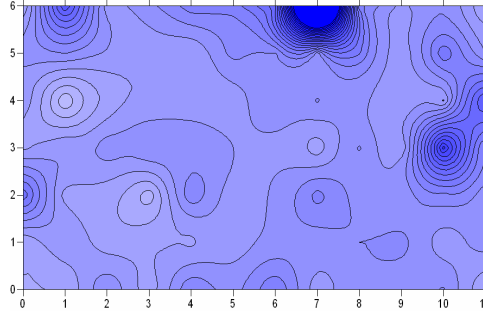
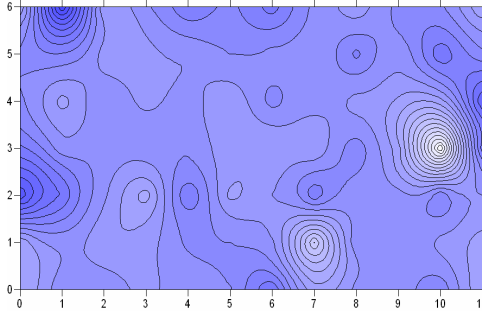
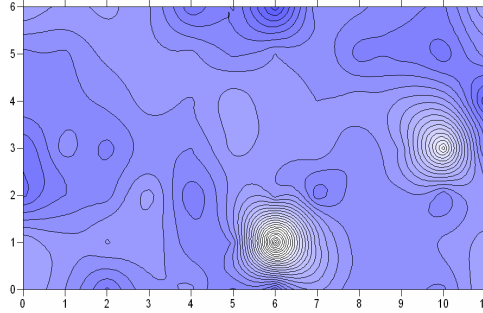
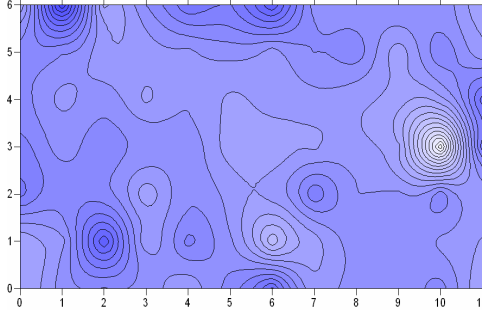
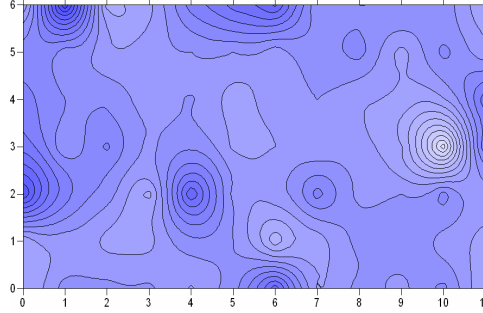
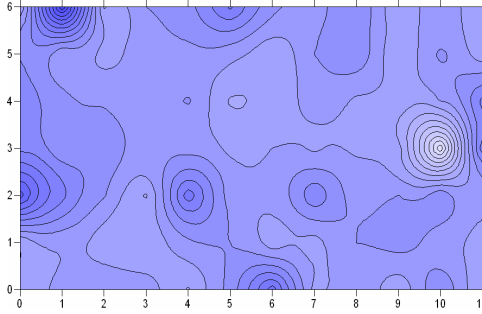
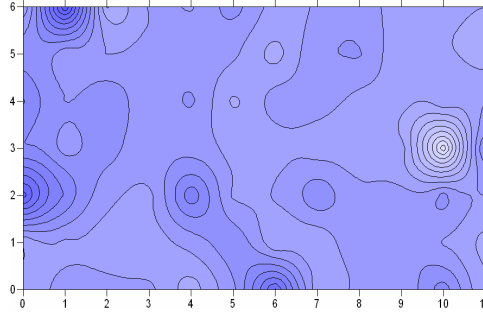
U07		
Days	K value (m/d)	% Reduction in K
Day 0	445.9	
Day 20	70.0	84.3
Day 27	207.0	53.6
Day 30	239.2	46.4
Day 34	259.8	41.7
Day 38	238.4	46.5
Day 40	242.8	45.6
Day 42	248.4	44.3
Day 44	277.7	37.7
Day 48	386.0	13.4
Day 51	399.0	10.5

U020		
Days	K value (m/d)	% Reduction in K
Day 0	590.4	
Day 16	235.0	60.2
Day 20	329.8	44.1
Day 27	392.8	33.5
Day 30	455.0	22.9
Day 34	375.1	36.5
Day 38	476.2	19.3
Day 40	375.1	36.5
Day 42	447.4	24.2
Day 44	462.5	21.7
Day 48	579.0	1.9
Day 51	588.5	0.3

U014		
Days	K value (m/d)	% Reduction in K
Day 0	305.1	
Day 16	181.0	40.7
Day 20	188.0	38.4
Day 27	240.7	21.1
Day 30	262.9	13.8
Day 34	246.1	19.3
Day 38	242.3	20.6
Day 40	230.4	24.5
Day 42	249.4	18.3
Day 44	258.7	15.2
Day 48	278.0	8.9
Day 51	301.7	1.1

APPENDIX D

EFFECT OF INCREASING GRADIENT ON THE GROUNDWATER FLOW PATTERNS

EFFECT OF INCREASING GRADIENT ON THE GROUNDWATER FLOW PATTERNS**Day 4****Day 5****Day 7****Day 8****Day 9****Day 10****Day 11****Day 12****Figure 1 Self potential measurements - Increased gradient flow pattern data (Day 4 to Day 12).**

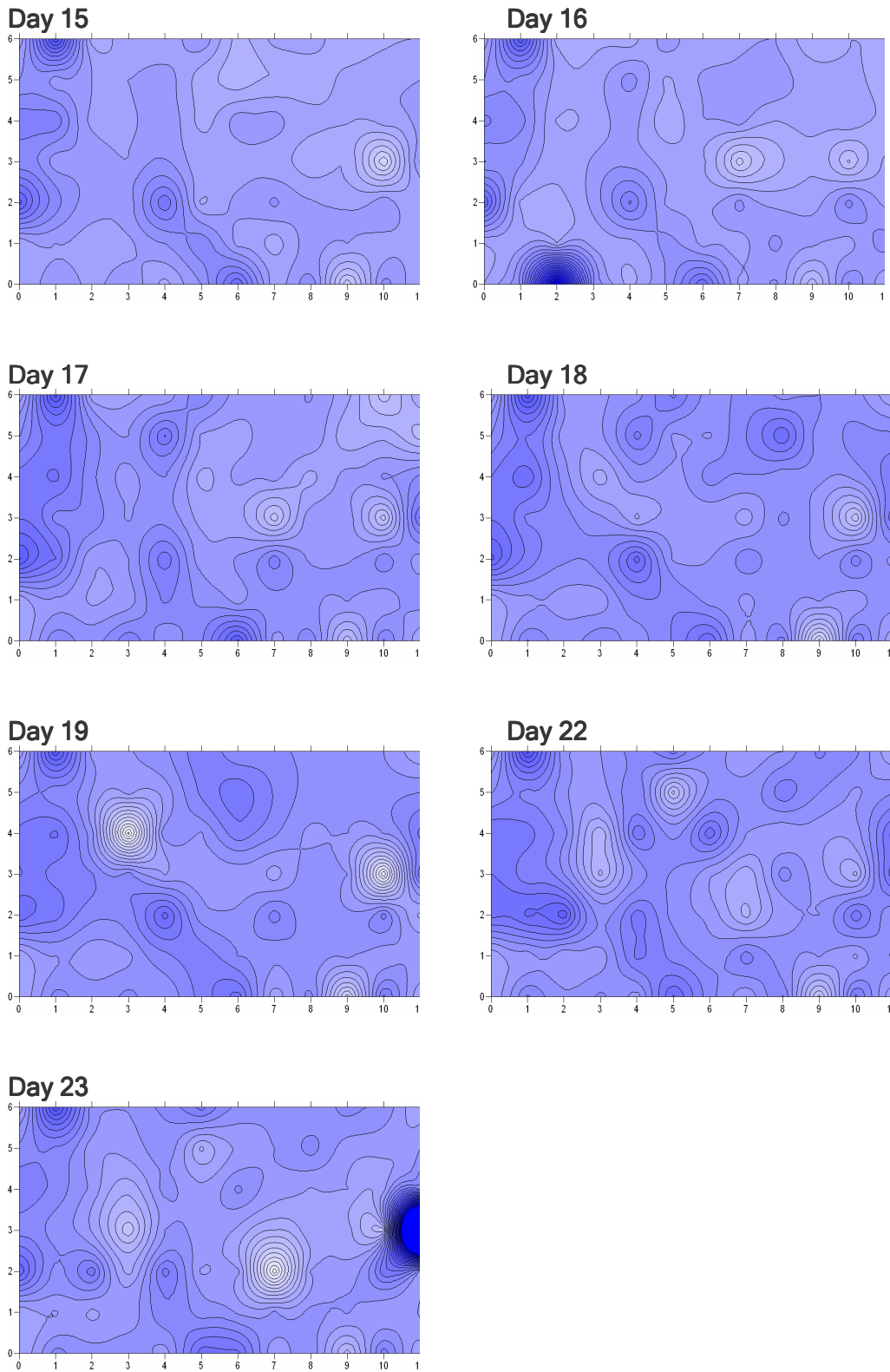


Figure 2 Self potential measurements - Increased gradient flow pattern data (Day 15 to Day 23).

Abstract

Biobarrier formation for hydraulic control in groundwater remediation in South Africa.

PhD thesis, Faculty of Natural Sciences and Agriculture, Institute for Groundwater studies, University of the Free State, Bloemfontein, South Africa.

The aim of this thesis was to determine the transport properties of bacteria through porous media and fractured rock aquifers and to test the effectiveness of biobarrier formation for reducing the hydraulic conductivity of a dual porosity fractured rock aquifer. This was done to determine if biobarriers is a feasible method for subsurface plugging in local aquifers.

Three bacterial species, namely *Raoultella planticola*, *Burkholderia vietnamensis* and *Serratia marcescens*, were tested and evaluated in the laboratory to determine the one with the most effective biobarrier properties.

The effectiveness of biobarriers for reducing the hydraulic conductivity of porous and fractured media was tested in laboratory-scale columns packed with porous sand, and a horizontal parallel plate fracture with an aperture of 0.8 mm. The porous sand and parallel plate fracture were inoculated with a cell suspension of *Serratia marcescens* and a nutrient media to ensure a uniform increase in cell concentrations and a corresponding decrease in hydraulic conductivity.

The results from laboratory experiments in porous and fractured media showed that *Serratia marcescens* have the ability to reduce the hydraulic conductivity of porous sand as well as a parallel plate fracture by more than 90%. Biobarrier technology is thus a viable method for reducing the hydraulic conductivity of porous and fractured media.

The effectiveness of biobarriers for reducing the hydraulic conductivity of a dual porosity fractured rock aquifer was tested on the campus test site at the University of the Free State, South Africa. An 84% reduction in the hydraulic conductivity was measured in the injection borehole after 20 days. A 60% reduction in the hydraulic conductivity was obtained 10 m from injection borehole after 16 days and a 40% reduction in a borehole which was 20 m from the injection borehole.

From the results, it could be seen that biobarriers can be established over a distance. The results showed that it is possible to decrease the hydraulic conductivity of fractures at a distance from the injection borehole. Based on this research, biobarrier formation is a viable method for reducing the hydraulic conductivity of a dual porosity fractured rock aquifer.

When applied to South African aquifers, biobarrier technology will be viable in three of the four aquifer types, namely the unconsolidated aquifers, the dual porosity aquifers and the fractured aquifers. The application of biobarriers in karst aquifers will not be possible.

The potential of using biobarrier technology as a means to contain or reduce the hydraulic conductivity of groundwater is potentially more cost effective and achievable than many other subsurface containment technologies. The full potential for this technology depends on the bacteria used during the investigation and the aquifer conditions. The success of biobarrier technology can also be enhanced by combining it with bioremediation technologies to simultaneously contain and reduce the flow of a contaminant plume, while also degrading it.

Opsomming

Biobarrier formasie vir die beheer en rehabilitasie van grondwater in Suid-Afrika.

PhD tesis, Fakulteit Natuurwetenskappe en Landbou. Instituut vir Grondwater Studies, Universiteit van die Vrystaat, Bloemfontein, Suid-Afrika.

Die doel van die tesis is as volg:

Bepaling van die doeltreffendheid en vervoer eienskappe van bakterieë om deur 'n poreuse matriks asook gefrakteurde akwifere te kan beweeg. Die effektiwiteit van biobarriers is getoets om te bepaal of bakterieë oor die vermoë beskik om die hidroliese geleiding van 'n fraktuur akwifere te verlaag.

Die doel van die navorsing is om te bepaal of biobarrier formasie 'n geskikte metode sal wees om vloei in akwifere te blok.

Vir die doel van die navorsing, is drie tipes bakterieë getoets om vas te stel watter een die mees effektiewe biobarrier eienskappe besit. Die volgende bakterieë is gebruik; *Raoultella planticola*, *Burkholderia vietnamensis* en *Serratia marcescens*.

Laboratorium-skaal eksperimente is gedoen om die effektiwiteit van bakterieë in die hidroliese geleiding van poreuse media en 'n fraktuur te verminder, te toets. Eksperimente sluit die volgende in: kolom eksperimente (kolomme is gepak met poreuse matriks) en 'n horisontale parallele plaat fraktuur eksperiment (fraktuur opening van 0.8 mm).

Bakterium *Serratia marcescens* en nitraatmedia is in beide die kolomme en die parallele plaat fraktuur gepomp. Die doel hiervan was om die eweredige verspreiding van bakterieë in die kolom en parallele plaat fraktuur toe te laat, wat dan tot 'n toename in bakterieë konsentrasies en 'n afname in die hidroliese geleiding van die poreuse matriks en die fraktuur.

Die resultate van die poreuse en gefrakteurde matriks eksperimente het getoon dat bakterium *Serratia marcescens* oor die vermoë beskik om die hidroliese geleiding van poreuse matriks, asook 'n fraktuur, met meer as 90% te verlaag. Die afleiding kan dus

gemaak word dat biobarriers wel 'n effektiewe metode is om die hidroliese geleiding van 'n poreuse en gefrakteerde media te verlaag.

Die effektiwiteit van biobarriers is ook in 'n fraktuur akwifere getoets. Die toetsreël is geleë op die kampus van die Universiteit van die Vrystaat, in Suid-Afrika.

'n 84% afname in die hidroliese geleiding is na 16 dae gemeet in die inpomp boorgat. 'n 60% afname is in 'n boorgat 10 meter vanaf die inpomp boorgat gemeet en 'n 40% afname in 'n boorgat 20 meter vanaf die inpomp gat.

Die resultate het getoon dat biobarrier formasie effektief oor 'n afstand gevestig kan word en dat die hidroliese geleiding oor 'n afstand geaffekteer kan word. Gebaseer op die navorsing, kan die afleiding gemaak word dat biobarrier formasie 'n goeie metode is om die hidroliese geleiding van 'n fraktuur akwifere te kan verlaag.

Biobarriers sal effektief werk in drie van die vier akwifertipes in Suid-Afrika naamlik die unconsolidated akwifere, die dual porosity akwifere en die fractured akwifere. Biobarriers sal nie effektief wees in karst akwifere nie.

Biobarriers vir die doel van afbakening en afname in die hidroliese geleiding van grondwater sal potensieel a meer koste effektiewe metode wees as die meeste van die metodes huidiglik in gebruik.

Die effektiwiteit van die tegnologie sal afhang van die tipe bakterieë wat gebruik word, asook die akwifertoestande.

Biobarriers kan nog meer suksesvol wees as dit met bioremediasiemetodes gekombineer word. Die doel sal dus wees om bioremediasie toe te pas terwyl die besoedelingspluim afgebaken word.

List of abbreviations

- α_L - Dispersivity in direction of flow (longitudinal).
- α_T - Dispersivity normal to direction of flow (transversal).
- AGW - Artificial groundwater.
- A - Cross-sectional area of the column.
- c - Concentration of dissolved solids.
- C - Solute concentration.
- C/Co - The total number of cells measured in optical density in a sample divided by the total number of cells.
- cells/ml - Cells per millilitre.
- cm - Centimetre.
- D - Aquifer thickness (or effective thickness of fracture zone).
- D* - Effective molecular diffusion coefficient.
- dC/dx- Concentration gradient.
- D_d - Diffusion coefficient.
- dh/dl - Piezometric gradient.
- D_L - Longitudinal dispersion coefficient (m^2/s).
- DO - Dissolved oxygen (mg).
- D_T - Transversal hydrodynamic dispersion coefficient.
- ε - Kinematic porosity.
- EC - Electrical conductivity.
- ECP - Extra-cellular polymers.
- EPS - Exopolysaccharides.
- F - Mass flux of solute per unit area per unit time.
- FWS - Full wave sonic.
- g - Gram.
- g/l - Gram per litre.
- K - Hydraulic conductivity (m/d).
- L - Depth.
- l - Litre.
- l/s - Litres per second.
- M - Injected mass of tracer (kg).

- m - Metre.
- m/d - Metre per day.
- m²/d - Square metres per day.
- m³/d - Cubic metres per day.
- mamsl - Metres above main sea level.
- mbgl - Metres below ground level.
- mg/l - Milligrams per litre.
- min - Minutes.
- ml - Millilitre.
- ml/min - Millilitre per minute.
- ml/hour - Millilitre per hour.
- mS/m - Milli-Siemens per metre.
- NaCl - Sodium Chloride.
- NaBr - Sodium Bromide.
- NaOCl - Sodium Hypochlorite.
- n_e - Effective porosity.
- N-N - Neutron-Neutron probe.
- OD - Optical density.
- PCR - Polymerase chain reaction.
- POT - Rotation.
- PV - Pore volume.
- Q - Flow-rate.
- Rpm - Rate per minute.
- RT-PCR - Real-time Polymerase chain reaction.
- SP - Self potential.
- SRB - Sulphate-reducing bacteria.
- TCE - Trichloroethene.
- TMG - Table Mountain Group.
- v - Groundwater velocity under natural gradient (m/s).
- V_i - Averaged linear velocity.
- v_x - Average linear velocity.
- x - Distance (m) between the column inlet and outlet in x-direction (direction of groundwater flow).